INFORMATION TO USERS

This manuscript has been reproduced from the microfilm master. UMI films the text directly from the original or copy submitted. Thus, some thesis and dissertation copies are in typewriter face, while others may be from any type of computer printer.

The quality of this reproduction is dependent upon the quality of the copy submitted. Broken or indistinct print, colored or poor quality illustrations and photographs, print bleedthrough, substandard margins, and improper alignment can adversely affect reproduction.

In the unlikely event that the author did not send UMI a complete manuscript and there are missing pages, these will be noted. Also, if unauthorized copyright material had to be removed, a note will indicate the deletion.

Oversize materials (e.g., maps, drawings, charts) are reproduced by sectioning the original, beginning at the upper left-hand corner and continuing from left to right in equal sections with small overlaps. Each original is also photographed in one exposure and is included in reduced form at the back of the book.

Photographs included in the original manuscript have been reproduced xerographically in this copy. Higher quality 6" x 9" black and white photographic prints are available for any photographs or illustrations appearing in this copy for an additional charge. Contact UMI directly to order.

UMI

A Bell & Howell Information Company
300 North Zeeb Road, Ann Arbor MI 48106-1345 USA
313/761-4700   800/521-0600

University of Alberta

C-H Bond Activation and C-C Bond Formation at Adjacent Metals

by

Jeffrey Robert Torkelson   Ⓒ

A thesis submitted to the Faculty of Graduate Studies and Research in partial fulfillment of the requirements for the degree of Doctor of Philosophy

Department of Chemistry

Edmonton, Alberta
Fall, 1998

The author has granted a non-exclusive licence allowing the National Library of Canada to reproduce, loan, distribute or sell copies of this thesis in microform, paper or electronic formats.

The author retains ownership of the copyright in this thesis. Neither the thesis nor substantial extracts from it may be printed or otherwise reproduced without the author's permission.

L'auteur a accordé une licence non exclusive permettant à la Bibliothèque nationale du Canada de reproduire, prêter, distribuer ou vendre des copies de cette thèse sous la forme de microfiche/film, de reproduction sur papier ou sur format électronique.

L'auteur conserve la propriété du droit d'auteur qui protège cette thèse. Ni la thèse ni des extraits substantiels de celle-ci ne doivent être imprimés ou autrement reproduits sans son autorisation.
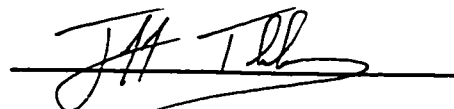
0-612-34848-2

Canada

University of Alberta

Library Release Form

Name of Author: Jeffrey Robert Torkelson

Title of Thesis: C-H Bond Activation and C-C Bond Formation at Adjacent Metals

Degree: Doctor of Philosophy

Year Degree Granted: 1998

Jeffrey Robert Torkelson

21 Forest Place
Regina, Saskatchewan
S4S 4M2
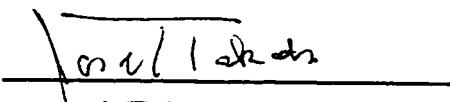
Date June 18, 1998

University of Alberta
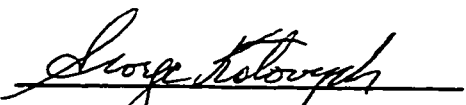
Faculty of Graduate Studies and Research
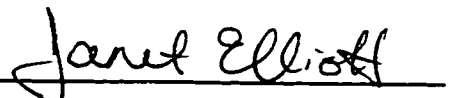
The undersigned certify that they have read, and recommend to the Faculty of Graduate Studies and Research for acceptance, a thesis entitled **C-H Bond Activation and C-C Bond Formation at Adjacent Metals** submitted by Jeffrey Robert Torkelson in partial fulfillment of the requirements for the degree of Doctor of Philosophy.

M. Cowie (supervisor)

J. Takats

S. H. Bergens

G. Kotovych

J. A. W. Elliott

D. M. Heinekey
(external examiner)

Date____ June 17, 1998

Abstract

Reaction of the methylene hydride compound $[Ir_2(H)(CO)_3(\mu\text{-}CH_2)$-$(dppm)_2][CF_3SO_3]$ (1) with Me_3NO removes a carbonyl, generating the fluxional methyl complex $[Ir_2(CH_3)(CO)(\mu\text{-}CO)(dppm)_2][CF_3SO_3]$ (2), the reactivity of which forms the basis of much of this thesis. Reaction of 2 with small molecules (L = CO, SO_2, PR_3, ^tBuNC) yields the methylene hydride products $[Ir_2(H)(CO)_2L$-$(\mu\text{-}CH_2)(dppm)_2][CF_3SO_3]$ (1, 3-7) by C-H activation of the methyl ligand.
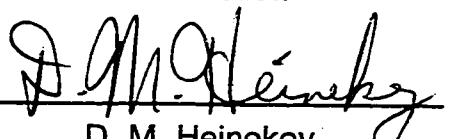
Addition of activated alkynes or olefins to 2, yields the cis dimetallated products $[Ir_2(CH_3)(CO)_2(\mu\text{-}RCCR')(dppm)_2][CF_3SO_3]$ (R = R' = CO_2Me (9); R = R' = CF_3 (12); R = H, R' = CO_2Me (13); R = R' = F_2 (31)). Compound 2 reacts at low temperature with non-activated 1-alkynes to initially yield the acetylide hydride complexes $[Ir_2(CH_3)(H)(CO)_2(\mu\text{-}C\equiv CR)(dppm)_2][CF_3SO_3]$ (R = Me (14), Ph (17), H (20)). Upon warming, 14 and 17 transform into the bridging alkyne complexes $[Ir_2(CH_3)(CO)_2(\mu\text{-}HC\equiv CR)(dppm)_2][CF_3SO_3]$ (R = Me (15), Ph (18)), before eliminating methane at room temperature to yield the bridging acetylide species, $[Ir_2(CO)_2(\mu\text{-}C\equiv CR)(dppm)_2][CF_3SO_3]$ (R = Me (16), Ph (19)). Compound 20 transforms into the vinylidene/methyl complex $[Ir_2(CH_3)(CO)_2(\mu\text{-}C=CH_2)$-$(dppm)_2][CF_3SO_3]$ (21), which upon reaction with CO generates the methylvinylidene/hydride, $[Ir_2(H)(CO)_3(\mu\text{-}C=C(H)Me)(dppm)_2][CF_3SO_3]$ (22).

Reaction of 2 with internal, non-activated alkynes, allene and methylallene initially yields the kinetic products in which the organic group

bridges the metals cis to the methyl ligand. The allene adducts form rare μ-η^1:η^3-allene compounds. These products transform into the vinylcarbene compounds of formula $[Ir_2(H)(CO)_2(\mu$-η^1:η^3-CHCR=CR'H)(dppm)_2][CF_3SO_3]$ (25-29, 36). Isotopic labelling shows one route for the production of the vinylcarbenes from the bridging alkyne precursors and two routes for the generation from the allene and methylallene adducts. The relevance of these transformations to the Fischer-Tropsch mechanism has been discussed.

The substituted methyl complex $[Ir_2(CH_2OCH_3)(I)(CO)(\mu$-CO$)(dppm)_2]$ (40), was prepared by oxidative addition of iodomethyl methyl ether to $[Ir_2(CO)_3(dppm)_2]$. Compound 40 reacts with trimethylsilyl triflate and trimethylsilyl iodide to yield the methylene bridged species $[Ir_2(CO)_2(\mu$-CH$_2)(\mu$-I)- (dppm)_2][CF_3SO_3]$ (41) and $[Ir_2(I)_2(CO)_2(\mu$-CH$_2)(dppm)_2]$ (42a, b), respectively. Reaction of 40 with methyl triflate generates the methoxycarbyne $[Ir_2(H)_2(CO)_2(COCH_3)(dppm)_2][CF_3SO_3]$ (43) by removal of iodide ion and double C-H activation of the methoxymethyl ligand.

To Fawn and Kaylyn

Acknowledgments

My supervisor, Marty Cowie deserves the first nod for his support, encouragement and "enlightening commentary" on everything from my writing to marriage and life in general.

The Cowie group, always a source of laughs, should be thanked. Steve, nobody's laughing but thanks for the incessant joking anyways and all the coffee breaks, the stories better not end. Todd, stop trying all your Kung Fu moves on us. Thanks for your friendship and teaching me about how a real synthetic chemist does things. Darren, the guy who could never let you forget about government insufficiencies; that's where the mad-bomber mentality starts. Maria for providing a foreign look to things and Oke and John, you guys need to make more noise. Past members also deserve some thanks. Brian, for making everyone else I know look cheerful; Fred, for leaving me with the methyl compound and all its exciting chemistry; and Oliver and Angela for providing many fun times.

Other people in the department, who were always friendly and helpful and made my stay here that much better also deserve acknowledgment. Above all, the NMR staff: Tom Nakishima, Tom Brisbane, Gerdy Aarts, Glen Bigam and Lai Kong, are thanked for the many hours spent on the machines. The staff of the spectral services and elemental analysis labs are acknowledged for their input. Selina in the mailroom for the millions of photocopies, stamps and faxes; Jeanette and Ilona in the general office who always had a smile and Jackie for your assistance with word-processing and the scholarship applications. I would

also like to thank Bob McDonald who solved most of my crystal structures and Joe Takats who is a real role model when it comes to showing passion and dedication for teaching.

My friends and family were always a source of inspiration and recreation. Jeff Kearns for the many nights of Sega because of a shortage of funds to do anything else. My brother Joel, who was my never ending squash partner, thanks for being a friend, good luck at vet school. The Jordes, thanks for the encouragement, making me feel like part of the family and letting me steal your youngest daughter/sister. Mom and Dad, for the unending support in whatever I did, thanks for always being there and Ryan, for giving me someone to pick on.

Most important of all, without whom none of this would have happened, my wife Fawn, thanks for your love and support.

Table of Contents

Chapter 2   C-H Activation of a Methyl Group by an Adjacent

    Metal:Reaction of [Ir$_2$(CH$_3$)(CO)(μ-CO)(dppm)$_2$][CF$_3$SO$_3$]

    with Small Molecules.

Chapter 3   C-H Activation and C-C Bond Formation in the Reactions

    of [Ir$_2$(CH$_3$)(CO)(μ-CO)(dppm)$_2$][CF$_3$SO$_3$] with Alkynes.

Chapter 4   C-H Activation and C-C Bond Formation in the Reactions of [Ir$_2$(CH$_3$)(CO)(μ-CO)(dppm)$_2$][CF$_3$SO$_3$] with Olefins.

Chapter 5   Methoxymethyl Complexes as Precursors to Methylene- and Methyne-bridged Species.

List of Tables

List of Figures and Schemes

Chapter 1

Chapter 2

List of Abbreviations and Symbols

anal.	analysis
approx.	approximately
ca.	circa (approximately)
calcd	calculated
DMAD	dimethylacetylenedicarboxylate
dppm	bis(diphenylphosphinomethane)
equiv	equivalent
Et	ethyl
h	hour(s)
HFB	hexafluro-2-butyne
IR	infrared
Me	methyl
MeOH	methanol
mg	milligrams
min	minute(s)
mL	millilitres
mmol	millimoles
MHz	megahertz
NMR	nuclear magnetic resonance
*n*Pr	normal propal
Ph	phenyl, C_6H_5-
THF	tetrahydrofuran
^{t}Bu	tertiary butyl
μL	microlitres

Crystallographic Abbreviations and Symbols

a, b, c	lengths of the x, y, and z axes, respectively, of the unit cell
deg (or °)	degrees
F_c	calculated structure factor
F_o	observed structure factor
GOF(S)	goodness of fit
h, k, l	Millar indices defining lattice planes, where the plane intersects the unit cell axes at 1/h, 1/k 1/l of the respective lengths a, b, and c.
R_1	residual index (a measure of agreement between calculated and observed structure factors)
wR_2	weighted residual index
V	unit cell volume
w	weighting factor applied to structure factor
Z	number of molecules per unit cell
Å	Angstrom(s) ($1\text{Å} = 10^{-10}$ metres)
α, β, γ	angles between b and c, a and c, and a and b axes, respectively, of unit cell
λ	wavelength
ρ	density
σ	standard deviation

Chapter 1

Introduction

Effective utilization of available energy and material resources is one of the vital goals of modern catalytic research. One important goal of this research is the design of catalysts that can more effectively transform the available resources into the desired products. The vast majority of industrial catalysts are heterogeneous, owing to advantages in the ease of catalyst preparation and separation, and in robustness.[1] In spite of these advantages, heterogeneous catalysts are notoriously difficult to study,[2] leaving the catalytic processes generally poorly understood. With the difficulty inherent in studying heterogeneous systems at the molecular level, in an effort to understand the catalytic steps, homogeneous systems can serve as models that are more amenable to study through the use of a battery of spectroscopic techniques. These model systems can yield vital information about reactive intermediates proposed for the heterogeneous system and about the individual catalytic steps in the process of interest. With a more detailed understanding of the catalytic process the catalyst can be tailored to optimize specificity and yield, thereby effectively utilizing raw materials to their utmost potential.

Monometallic complexes are commonly used in the modelling of chemistry that is thought to occur on metal surfaces (heterogeneous systems),[3]

and many of the transformations that have been proposed to occur on metal surfaces can be duplicated with mononuclear systems.[3,4] However, one disadvantage in the metal-surface/mononuclear complex comparison is that a metal surface differs substantially from a mononuclear complex, in having a number of metals in close proximity which can significantly change the chemistry of the metal-substrate interaction when compared to a mononuclear system. Thus, metal clusters have become prominent in the modelling of heterogeneous systems, owing to the presence of adjacent metal centers.[5] It has been suggested that metal clusters can be considered tiny pieces of metal with chemisorbed species on the periphery.[5a] The "cluster/surface" analogy, developed by Muetterties,[5] has driven much of the work in the area of polymetallic homogeneous catalytic research.

In metal clusters, the metals are held in close proximity by metal-metal bonds or bridging ligands and can therefore supply multisite interactions for the substrate molecules, similar to metal surfaces and which are not available in mononuclear systems. The presence of adjacent metal sites provides the opportunity for a number of substrate molecules to interact at one time as well as supplying differing reaction pathways and bonding modes for the substrate molecules. Cluster complexes more closely resemble the active sites of the surfaces of heterogeneous catalysts than do mononuclear complexes, so it is conceivable that the study of clusters under homogeneous conditions could more closely parallel the chemistry of surfaces.

An important difference between mononuclear and polynuclear reactivity is shown in the behaviour of alkyl groups in the two systems.[6] With late-metal mononuclear alkyl complexes, a common reactivity is β-hydrogen elimination, whereas with polynuclear alkyls, α-hydrogen elimination is common.[7] In the mononuclear case the β-hydrogens of the alkyl group are geometrically disposed to form an agostic M-C-H interaction to the metal as outlined in **A**, leading to C-H bond cleavage. In a polymetallic system the presence of a second metal allows a favorable interaction between itself and the α-hydrogen atoms, outlined in **B**, leading to the agostic bond formation that ultimately can
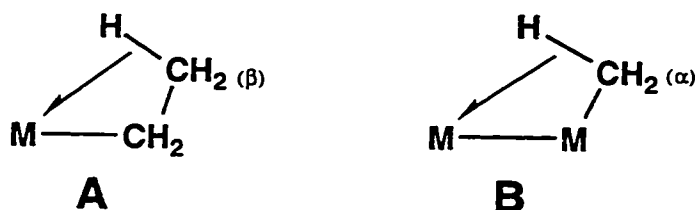
lead to cleavage of the α C-H bond. This reaction is not common for mononuclear late-metal complexes[8] but is common in clusters and on metal surfaces.[4]

The Fischer-Tropsch (FT) reaction is a potentially important heterogeneously catalyzed reaction because it allows for the formation of valuable chemicals from inexpensive feedstocks. In this reaction, CO and H_2 react in the presence of a catalyst to form long chain hydrocarbons and other organic products. C_1 fragments derived from CO have been postulated to be important species in FT and other surface catalyzed reactions, and as a result,

the chemistry of C_1 fragments is of interest in the modelling of heterogeneously catalyzed reactions. The C_1 units: carbide (C), methyne (CH), methylene (CH_2) and methyl (CH_3) which are known to be present on metal surfaces in a number of heterogeneous processes including Fischer-Tropsch synthesis, have also been prepared and characterized in cluster chemistry. Examples[9-12] are shown below (**C-G**). These species clearly demonstrate bonding modes different than
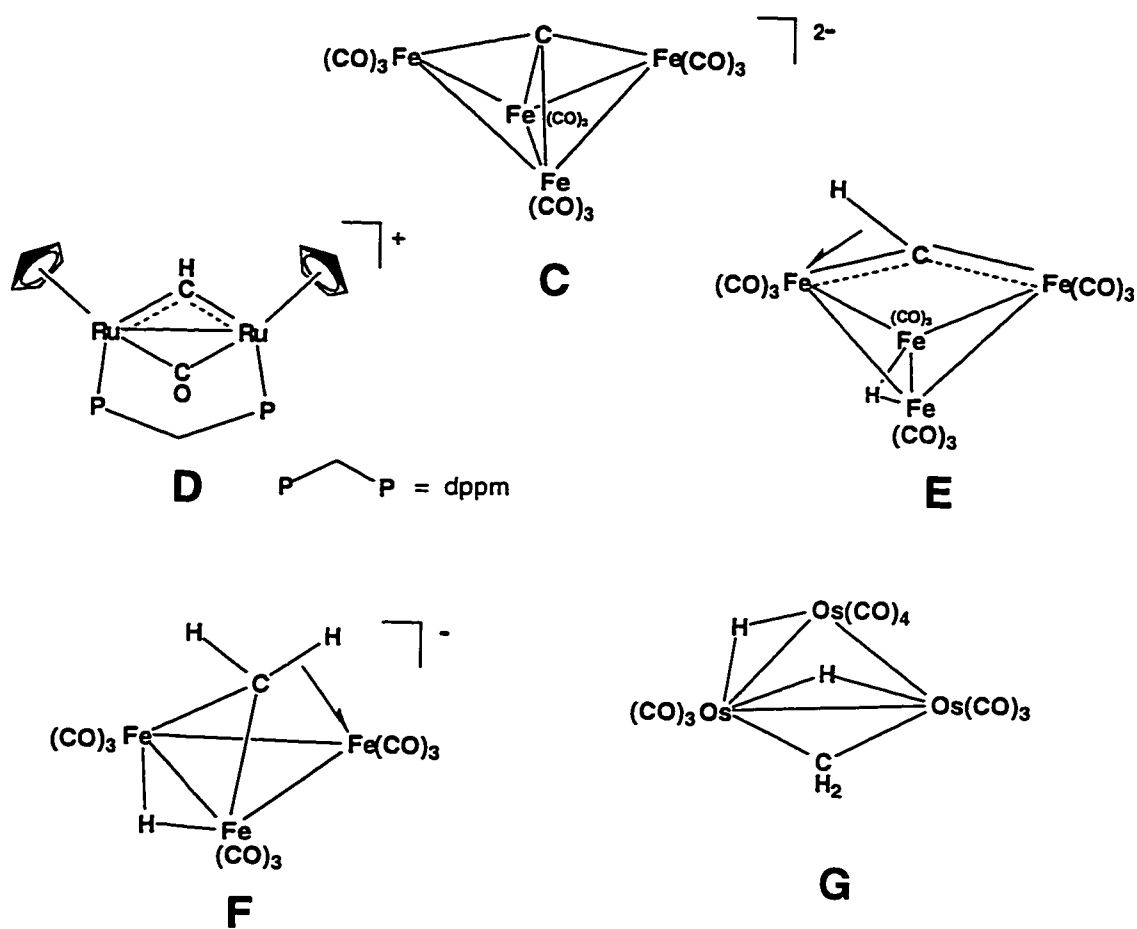
those observed in mononuclear chemistry, and in some instances make evident the increased capacity of multimetal systems to bind through a C-H bond rather

than just the metal-carbon σ-bonds.[12,13] The capacity for the different binding modes for clusters and, by analogy, metal surfaces, allows stabilization of otherwise highly reactive fragments. The isolation and reactivity of the iron-carbide cluster (C) clearly demonstrates the stabilization of a highly reactive species.[9] The chemistry displayed by this carbide fragment is thought to be similar to that proposed for the bare carbon atoms assumed to be present on Fischer-Tropsch catalyst surfaces.[9b]

Facile interconversion between methyl, methylene and methyne groups has been observed in a number of complexes and is outlined for a diiron system in Scheme 1.1.[14]

Scheme 1.1
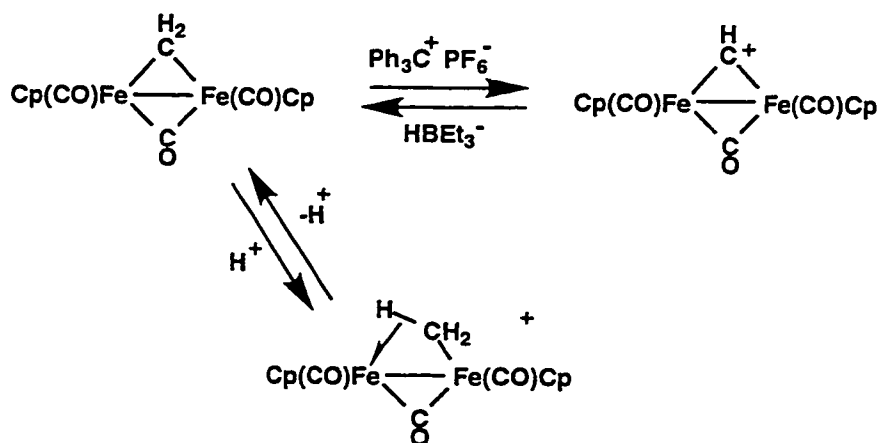
The facile reactivity observed on clusters implies that C_1 fragments can easily interconvert on metal surfaces. This proposal is supported by studies of

surface-bound alkyl groups[15] which have demonstrated extensive interconversion between the C_1 fragments through reversible dehydrogenation and hydrogenation steps. The activation barrier for the dehydrogenation of the surface bound alkyls on a platinum surface was found to involve energies of about 6-8 kcal/mol, indicating a very facile process. Thus one relationship between the chemistry demonstrated with homogeneous cluster complexes and on metal surfaces is clearly established.

Bimetallic systems are the simplest examples of polymetallic clusters able to display metal-metal cooperativity effects. Clusters that contain a large number of metals typically also have a large number of ligands which makes characterization of reaction pathways and intermediates difficult. Bimetallic species on the other hand have the advantage of a smaller number of ligands and are therefore easier to characterize by spectroscopic techniques. Our interest in bimetallic complexes arises from our desire to model the involvement of adjacent metals in simple organic substrate transformations thought to occur in heterogeneous systems.

We have chosen the diphosphine-bridged diiridium framework (shown below) for our studies because of its ease of synthesis, its stability, and the wide
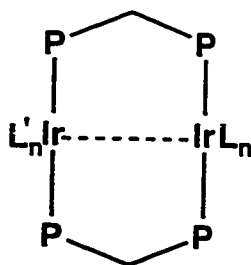
use of group 9 metals in catalytic applications.[16] Bis(diphenylphosphino)-methane (dppm) was used as the bridging ligand for two main reasons. First, it is a good ligand for holding the metals at an appropriate separation to allow the reversible formation of metal-metal bonds.[17] With the metals held in close proximity, the potential of metal-metal cooperativity is possible. Second, the NMR active, 100% abundant ^{31}P nuclei and methylene protons provide good NMR handles with which to characterize compounds. We chose to investigate the reactivity of possibly the simplest organic fragment, the methyl group, in the presence of the adjacent metals. Late-transition metal-alkyl complexes are known to be involved as key intermediates in catalytic processes, including olefin hydrogenation and hydroformylation,[18] methanol carbonylation[19] and Fischer-Tropsch chemistry.[20] Although work on mononuclear alkyl complexes has resulted in an improved understanding of the involvement of mono-metal alkyl species in catalysis,[21] very little has been reported on alkyl complexes involving more than one metal,[22] in spite of the fact that many catalytic processes involve adjacent metals, either in heterogeneous processes or in homogeneous catalysis by metal clusters.[23]

In late-metal binuclear systems the alkyl ligand can display a number of bonding modes that make it dissimilar to the mononuclear case. In structure H, shown below, the methyl group is terminally bound to one metal and approximates a mononuclear alkyl species. In addition to the terminal binding mode, two bridging modes are common, in which the alkyl group symmetrically bridges the metals in a 3-center M-C-M interaction (I), or in which it bridges in

terminal

H

symmetric

I

asymmetric (agostic)

J
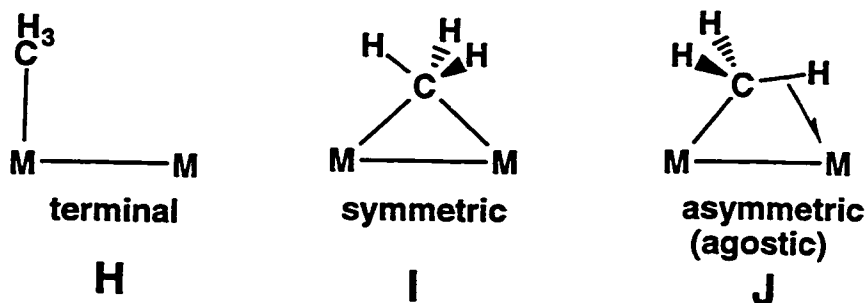
an unsymmetrical manner (**J**), σ-bound to one metal through carbon and interacting with the second metal in an agostic 2-electron donation from a C-H bond. The agostic interaction can be viewed as an important intermediate in the activation of an alkyl C-H bond[13] to form a methylene-hydride (**K**), exemplifying how the presence of more than one metal has activated the organic substrate in a manner typically not observed in a mononuclear species. There are examples of α-hydrogen elimination in monometallic species, but

methylene-hydride

K
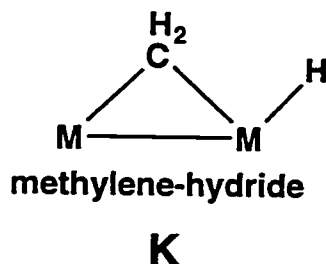
these systems usually involve electrophilic early-metals[24] or more recently, high valent late-metals.[25] The progression in metal-alkyl interactions (from **H** to **J** to **K**) suggests how a methyl ligand on a surface can undergo transformation into methylene and hydride fragments or conversely how the methylene and hydride fragments can combine (**K** to **J** to **H**) on adjacent metals yielding a methyl group.

Examples of the different types of bimetallic alkyl (methyl) bonding modes are pictured below. The terminal coordination mode is displayed for Eisenberg's dirhodium complex (L).[26]

L
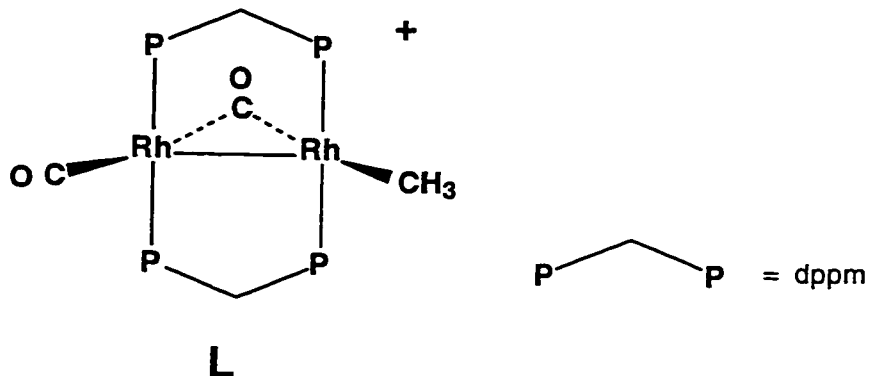
The symmetrical bridging case is rare for late metals but has been observed with the dinickel[27] (M) and diiridium[28] (N) complexes shown below.

M

N

= dmpm
= bis(dimethyl-phosphino) methane
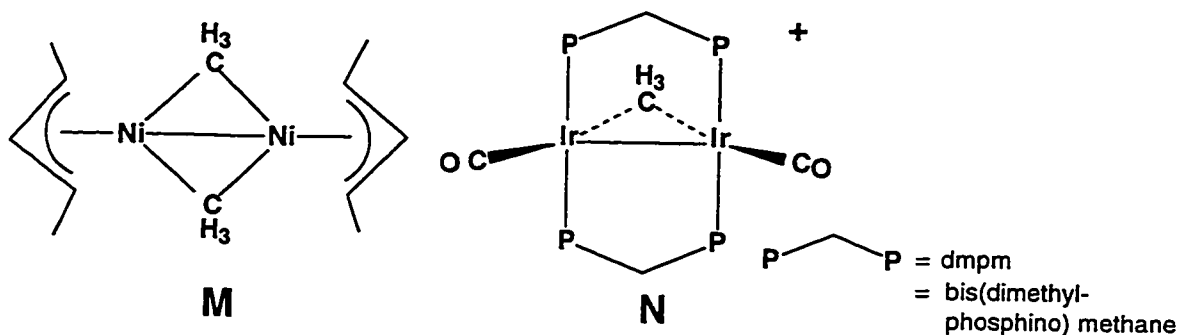
The first agostic interaction to be crystallographically established was for the diiron complex (O).[29] The asymmetric interaction is illustrated by the different

O
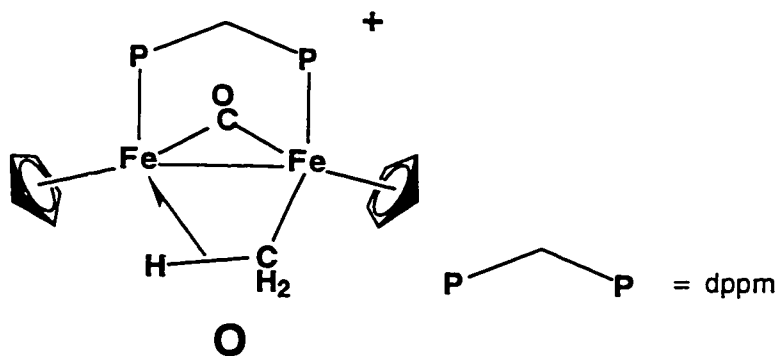
Fe-C(methyl) bond lengths (2.008(4) Å, 2.108(3) Å) and a short Fe-H distance of 1.64(4) Å.

Our interest in modelling surface-bound methyl groups applies directly to the Fischer-Tropsch (FT) reaction, in which hydrogenation of carbon monoxide over a late metal catalyst occurs, producing a range of hydrocarbons for subsequent use as chemical feedstocks. The use of this process has been gaining in popularity due to decreased processing costs with advancing technology, and recently Shell,[30] Exxon,[31] Texaco[32] and other companies[33] have either brought online, or have plans to bring online, FT plants to produce commodity chemicals. Because of the heterogeneous nature of the process, little is presently understood about the reactions occurring on the catalyst surface, and studies using organometallic model complexes that contain the organic fragments similar to those thought to exist on the FT catalyst surface are therefore of interest in order to gain an understanding of the individual steps in the C-C bond-formation process. By understanding how C-C bond formation occurs, it is hoped that the rational design of catalysts can be undertaken that will improve the selectivity of the process.

Numerous studies have been performed with late-metal organometallic systems in an effort to model the chemistry thought to occur on FT surfaces.[34] In the 1980's, Brady and Pettit[22] proposed a scheme for C-C bond formation (outlined in Scheme 1.2), that involved the initial formation of methyl and methylene fragments on the surface by dissociation of CO and hydrogenation of the carbide fragment. Insertion of methylene units into a growing alkyl chain

Scheme 1.2
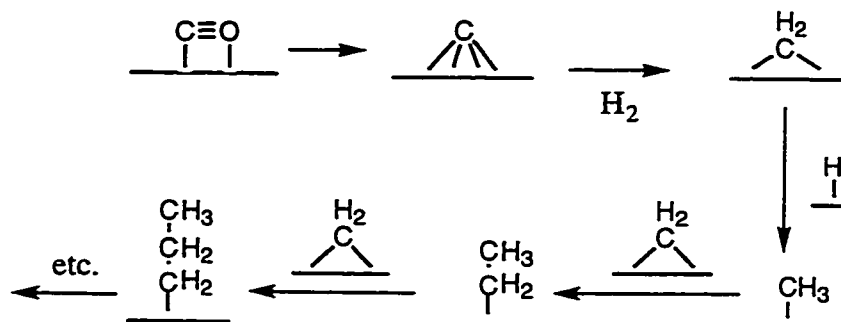
was proposed to yield long-chain hydrocarbons. This mechanism is in doubt however, because more recent studies[34a,35] show that α-olefins are the primary product of FT synthesis and the Brady-Petitt proposal does not accurately account for product distribution or explain how a β-elimination step to yield an α-olefin from a long chain alkyl would be favored on a metal surface covered in hydride ligands.

More recently, Maitlis has proposed a mechanism based on model studies carried out with the dirhodium compounds **i** and **ii**, shown below,[36] which contain fragments (methyl, methylene, vinyl) that are thought to be present on the surface of FT catalysts. Thermolysis of compound **i** resulted
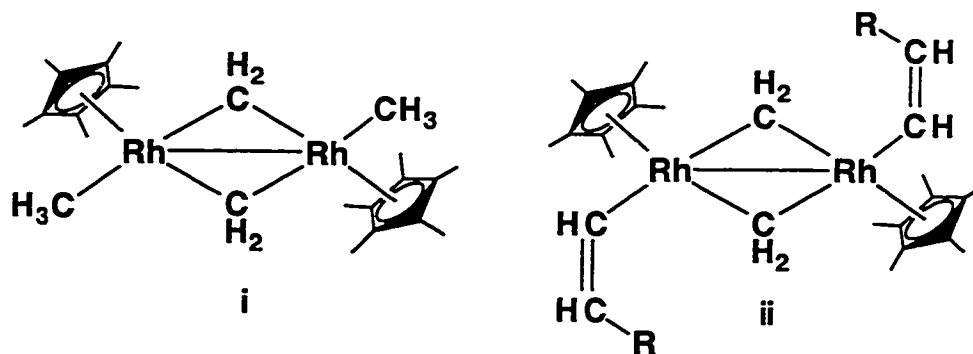
in C-C bond formation, generating the C_3 fragment $CH_2=CHCH_3$, however isotopic labelling experiments argued against a direct methyl to methylene migration as the primary C-C chain growth step. Instead, a vinyl intermediate was proposed to be the initator, yielding an allyl ligand that reductively eliminated to produce $CH_2=CHCH_3$. Compound ii offered further support for the proposed mechanism, showing facile vinyl to methylene migration. The Maitlis alkenyl mechanism is outlined in Scheme 1.3.[35,36d,37] Initially carbon monoxide

Scheme 1.3
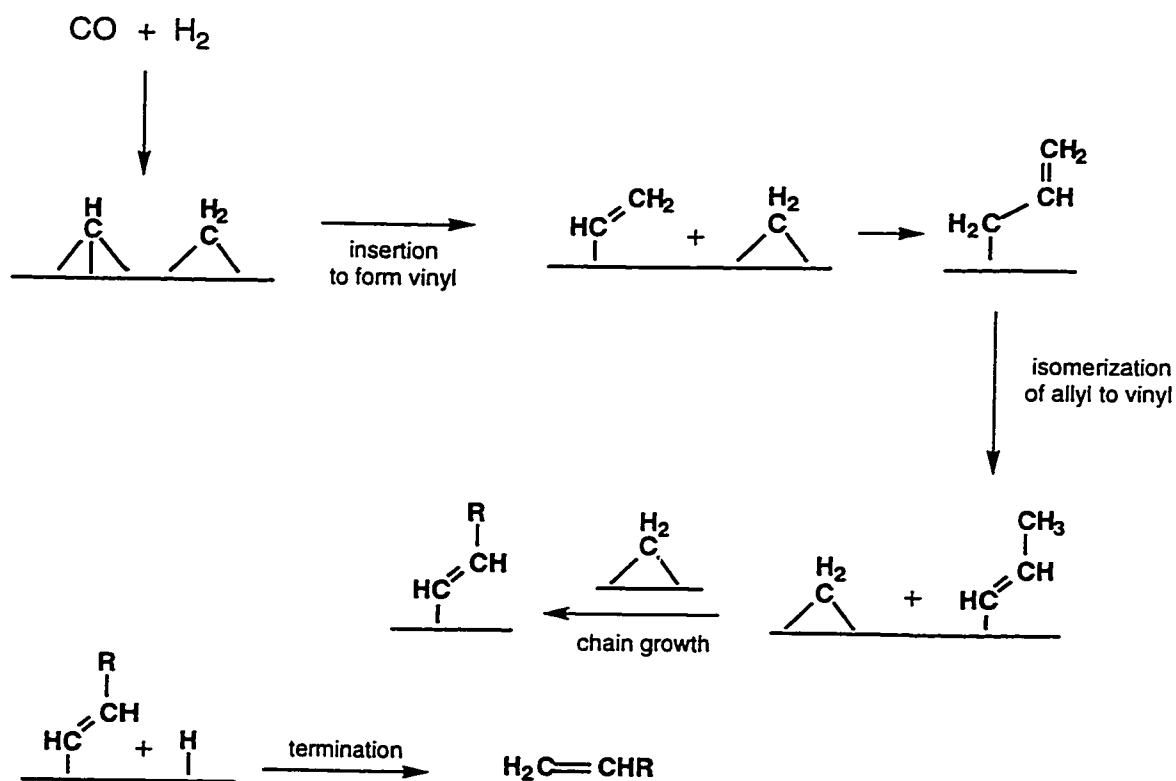
dissociation and hydrogenation generates surface-bound methyne and methylene groups. Combination of the methylene and methyne groups yields a vinyl species, which is thought to be the key species involved in the catalytic

cycle. Vinyl to methylene migration yields an η^1-bound allyl that isomerizes by transfer of an α-hydrogen to the γ-carbon, yielding a substituted vinyl species. Sequential vinyl-to-methylene migration steps result in the propagation of the hydrocarbon chain. Termination of the cycle occurs by reductive elimination of the vinyl with a surface bound hydride ligand, producing an α-olefin.

The inclusion of methylene species in both the proposed FT mechanisms (Scheme 1.2 and 1.3), and the facile interconversion of C_1 fragments observed in both cluster and heterogeneous studies, makes the study of methyl and methylene complexes attractive for modelling the FT reaction.

Goal

The goal of this thesis was to investigate the influence of adjacent metals on alkyl groups. We hoped to model the possible chemistry of a surface-bound methyl group specifically looking at factors that effected the reversible C-H bond cleavage/formation that occurs on metal surfaces. Subsequent chemistry of a binuclear alkyl species will be investigated in order to generate other organic fragments to gain an understanding of C-C bond formation processes in the presence of adjacent metals.

A second goal of this thesis was the production of a substituted methyl compound to study what effect a change in the steric or electronic influence of the methyl subtituents might have on the C-H bond cleavage and C-C bond formation reactions such a ligand could undergo. As part of the second goal, a

substituted methyl ligand could be used as a precursor to bridging methylene groups which are pivotal fragments in FT chemistry.

References

1. (a) Satterfield, C. N. *Heterogeneous Catalysis in Practice*; McGraw-Hill: New York, 1980. (b) Bond, G. C. *Heterogeneous Catalysis*; Clarendon: Oxford, 1987. (c) Davis, B. H.; Hettinger, W. P. Jr., eds., *Heterogeneous Catalysis*; American Chemical Society: Washington, DC, 1983.

2. (a) Niemantsverdriet, J. W. *Catalysis*; Moulijin, J. A.; van Leeuwen, P. W. N. M.; Santen, R. A., eds.; Elsevier: Netherlands, 1993, Chapter 10. (b) Campbell, I. M. *Catalysis at Surfaces*; Chapman and Hall: New York, 1988, Chapter 4.

3. (a) Marks, T. J. *Acc. Chem. Res.* **1992**, *25*, 57. (b) Suss-Fink, G.; Meister, G. *Adv. Organomet. Chem.* **1993**, *35*, 41.

4. Zaera, F. *Chem Rev.* **1995**, *95*, 2651.

5. (a) Muetterties, E. L. *Science* **1977**, *196*, 839. (b) Muetterties, E. L. *Chem. Soc. Rev.* **1982**, *11*, 283. (c) Mutterties, E. L. *Pure Appl. Chem.* **1982**, *54*, 83. (d) Muetterties, E. L.; Rhodin, T. N.; Band, E.; Brucker, C. F.; Pretzer, W. R. *Chem. Rev.* **1979**, *79*, 91.

6. Crabtree, R. H. *The Organometallic Chemistry of the Transition Metals*; Wiley: New York, 1988, p327.

7. (a) Calvert, R. B.; Shapley, J. R. *J. Am. Chem. Soc.* **1977**, *99*, 5225. (b) Cree-Uchiyama, M.; Shapley, J. R.; St. George, G. M. *J. Am. Chem. Soc.* **1986**, *108*, 1316.

8. (a) Luecke, H. F.; Arndtsen, B. A.; Burger, P.; Bergman, R. G. *J. Am. Chem. Soc.* **1996**, *118*, 2517. (b) Boutry, O.; Gutierrez, E.; Monge, A.;

Nicasio, M. C.; Perez, P. J.; Carmona, E. *J. Am. Chem. Soc.* **1992**, *114*, 7288.

9. (a) Tachikawa, M.; Muetterties, E. L. *J. Am. Chem. Soc.* **1980**, *102*, 4541.

(b) Beno, M. A.; Williams, J. M.; Tachikawa, M.; Muetterties, E. L. *J. Am. Chem. Soc.* **1980**, *102*, 4542

10. Davies, D. L.; Gracey, B. P.; Guerchais, V.; Knox, S. A. R.; Orpen, A. G. *J. Chem. Soc., Chem. Commun.* **1984**, 841.

11. (a) Vites, J. C.; Jacobsen, G.; Dutta, T. K.; Fehlner, T. P. *J. Am. Chem. Soc.* **1985**, *107*, 5563. (b) Dutta, T. K. Vites, J. C.; Jacobsen, G. B.; Fehlner, T. P. *Organometallics* **1987**, *6*, 842.

12. Calvert, R. B.; Shapley, J. R. *J. Am. Chem. Soc.* **1978**, *100*, 7726.

13. (a) Brookhart, M.; Green, M. L. H.; Wong, L-L. *Prog. Inorg. Chem.* **1988**, *36*, 1. (b) Crabtree, R. H.; Hamilton, D. G. *Adv. Organomet. Chem.* **1988**, *28*, 299.

14. Casey, C. P.; Fagan, P. J.; Miles, W. H. *J. Am. Chem. Soc.* **1982**, *104*, 1134.

15. Zaera, F. *Acc. Chem. Res.* **1992**, *25*, 260.

16. Dickson, R. S. *Homogeneous Catalysis with Compounds of Rhodium and Iridium*; Reidel: Boston, 1985.

17. (a) Puddephatt, R. J. *Chem. Soc. Rev.* **1983**, *12*, 99. (b) Chaudret, B.; Delvaux, B.; Poilblanc, R. *Coord. Chem. Rev.* **1988**, *86*, 191.

18. Foster, D. *Adv. Organomet. Chem.* **1979**, *17*, 255.

19. (a) James, B. R. *Adv. Organomet. Chem.* **1979**, *17*, 319. (b) Pruet, R. L. *Adv. Organomet. Chem.* **1979**, *17*, 1. (c) Masters, C. Homogeneous Transition-Metal Catalysis: A Gentle Art; Chapman and Hall: London, 1980. (d) Speier, J. L. *Adv. Organomet. Chem.* **1979**, *17*, 407.

20. (a) Brady, R. C.; Pettit, R. *J. Am. Chem. Soc.* **1980**, *102*, 6181. (b) Brady, R. C.; Pettit, R. *J. Am. Chem. Soc.* **1981**, *103*, 1297.

21. (a) Parshall, G. W.; Mrowca, J. J. *Adv. Organomet. Chem.* **1969**, *7*, 157. (b) Atwood, J. D. *Coord. Chem. Rev.* **1988**, *83*, 93.

22. (a) Calvert, R. B.; Shapley, J. R. *J. Am. Chem. Soc.* **1978**, *100*, 7726. (b) Casey, C. P.; Fagan, P. J.; Miles, W. H. *J. Am. Chem. Soc.* **1982**, *104*, 1134. (c) Schmidt, G. F.; Muetterties, E. L.; Bena, M. A.; Williams, J. M. *Proc. Natl. Acad. Sci.* **1981**, *78*, 1318. (d) Hursthouse, M. B.; Jones, R. A.; Abdul-Malik, K. M.; Wilkinson, G. *J. Am. Chem. Soc.* **1979**, *101*, 4128. (e) Davies, D. L.; Gracey, B. P.; Guerchais, V.; Knox, S. A. R.; Orpen, A. G. *J. Chem. Soc., Chem. Commun.* **1984**, 841.

23. (a) Balch, A. L. In *Homogeneous Catalysis with Metal Phosphine Complexes*; Pignolet, L. H., Ed.; Plenum: New York, 1983. (b) Brown, M. P.; Fisher, J. R.; Franklin, S. J. ; Puddephatt, R. J.; Thomson, M. A. In *Catalytic Aspects of Metal Phosphine Complexs*; Alyea, E. C., Meek, D. W., Eds.; Advances in Chemistry Series196; American Chemical Society: Washington, DC, 1982; p 231. (c) Poilblanc, R. *Inorg. Chim. Acta.* **1982**, *62*, 75. (d) Muetterties, E. L.; Krause, M. J. *Angew. Chem., Int. Ed. Engl.* **1983**, *22*, 135. (e) Ertl, G. In *Metal Clusters in Catalysis*; Gates, B. C.,

Guczi, L., Knozinger, H., Eds.; Elsevier: New York, 1986; Chapter 11. (f) Levigne, G.; Kaesz, H. D. In ref 23e, Chapter 4. (g) Marko, L.; Vizi-Orosz, A. In ref 23e, Chapter 5. (h) Herrmann, W. A. *Angew. Chem., Int. Ed. Engl.* **1982**, *21*, 117. (i) Garland, C. S.; Giles, M. F.; Sunley, J. G. (BP Chemicals Ltd.) Eur. Pat. Appl. EP 643, 034. (j) Collman, J.P.; Hegedus, L.S.; Norton, J.R.; Finke, R.G. *Principles and Applications of Organotransition Metal Chemistry*; University Science Books: Mill Valley, California, 1987, pp. 412-415 and 581-590.

24. Schrock, R. R. *Acc. Chem. Res.* **1979**, *12*, 98 and references therein.

25. Luecke, H. F.; Arndtsen, B. A.; Burger, P.; Bergman, R. G. *J. Am. Chem. Soc.* **1996**, *118*, 2517.

26. Shafiq, F.; Kramarz, K. W.; Eisenberg, R. *Inorg. Chim. Acta.* **1993**, *213*, 111.

27. Kruger, C.; Sckutowski, J. C.; Berke, H.; Hoffman, R. *Naturforsch* **1978**, *336*, 1110.

28. Reinking, M. K.; Fanwick, P.E.; Kubiak, C.P. *Angew. Chem. Int. Ed. Engl.* **1989**, *28*, 1377.

29. Dawkins, G. M.; Green, M.; Orpen, A. G.; Stone, F. G. A. *J. Chem. Soc., Chem. Commun.* **1982**, 41.

30. Freemantle, M. *Chem. and Eng. News* 1996, August 12, p31.

31. Henry, C. Manager, Imperial Oil Products and Chemicals Division. Personal communication.

32. *Chem. and Eng. News* 1997, December 15, p14.

33. Morse, P. M. *Chem. and Eng. News* 1998, March 23, p17.

34. (a) Herrmann, W. *Angew. Chem. Int. Ed.* Engl. **1982**, *21*, 117. (b) Gladysz, J. A. *Adv. Organomet. Chem.* **1982**, *20*, 1. (c) Rofer-DePoorter, C. K. *Chem. Rev.* **1981**, *81*, 447.

35. Maitlis, P. M.; Long, H. C.; Quyoum, R.; Turner, M. L.; Wang, Z-Q. *Chem. Commun.* **1996**, 1.

36. (a) Martinez, J.; Gill, J. B.; Adams, H.; Bailey, N. A.; Saez, I, M.; Maitlis, P. M. *Can. J. Chem.* **1989**, *67*, 1698. (b) Martinez, J.; Gill, J. B.; Adams, H.; Bailey, N. A.; Saez, I. M.; Sunley, G. J.; Maitlis, P. M. *J. Organomet. Chem.* **1990**, *394*, 583. (c) Martinez, J. M.; Adams, H.; Bailey, N. A.; Maitlis, P. M. *J. Chem. Soc., Chem. Commun.* **1989**, 286. (d) Maitlis, P. M. *J. Organomet. Chem.* **1995**, *500*, 239 and references therein.

37. (a) Turner, M. L.; Long, H. C.; Shenton, A.; Byers, P. K. Maitlis, P. M. *Chem. Eur. J.* **1995**, *1*, 549. (b) Maitlis, P. M.; Saez, I. M.; Meanwell, N. J.; Isobe, K.; Nutton, A.; Vaquez de Miguel, A.; Bruce, D. W.; Okeya, S.; Bailey, P. M.; Andrews, D. G.; Ashton, P. R.; Johnstone, I. R. *New J. Chem.*, **1989**, *13*, 419.

Chapter 2

C-H Activation of a Methyl Group by an Adjacent Metal: Reaction of $[Ir_2(CH_3)(CO)(\mu\text{-}CO)(dppm)_2][CF_3SO_3]$ with Small Molecules.

Introduction

Binuclear complexes are the smallest and simplest cluster systems that are capable of demonstrating metal-metal cooperativity effects. Understanding the mobility and the activation of simple ligands on bimetallic complexes may help in developing an understanding of key aspects of ligand interactions on metal surfaces thereby extending our knowledge of surface reactivity. As part of an ongoing interest in the reactivity of binuclear alkyl complexes with a variety of metal combinations,[1] we undertook a study of the "Ir_2" core. This thesis will be concerned primarily with the reactivity of the methyl complex $[Ir_2(CH_3)(CO)(\mu\text{-}CO)(dppm)_2][CF_3SO_3]$ (2). In this chapter we begin by studies of the reactivity of 2 with a number of simple ligands such as CO, SO_2, CN^{t}Bu and phosphines in order to determine factors that may influence the bonding modes of the methyl group and its subsequent chemistry. Of specific interest in the reactivity of compound 2 is the possibility of migratory insertion reactions and C-H activation of the methyl group, with the aim of possibly modeling the transformations of surface-bound methyl groups on metal surfaces.

Experimental Section

General Comments. All solvents were dried (using appropriate drying agents), distilled prior to use, and stored under nitrogen. Deuterated solvents used for NMR experiments were degassed and stored under argon over molecular sieves. Reactions were carried out at room temperature (unless otherwise stated) using standard Schlenk procedures, and compounds, which were isolated as solids, were purified by recrystallization. A flow rate of ca 0.2 mLs^{-1} was employed for all reactions that involved purging a solution with a gas. Carbon monoxide and sulphur dioxide were purchased from Matheson. Carbon-13 enriched CO (99%) was supplied by Isotec Inc. All gases were used as received. Ammonium hexachloroiridate(IV) was purchased from Vancouver Island Precious Metals, and the chemicals, methyl triflate, d^3-methyl triflate, ^{13}C-methyl triflate, tert-butyl isocyanide, 2,2,6,6-tetramethylpiperidine, all phosphines and triphenylphosphite were purchased from Aldrich. The compound [Ir$_2$(H)(CO)$_3$(μ-CH$_2$)(dppm)$_2$][CF$_3$SO$_3$] (1), was prepared as previously reported.[1f,g]

Standard NMR spectra were recorded on a Bruker AM-400 spectrometer operating at 400.1 MHz for ^{1}H, 161.9 MHz for ^{31}P and 100.6 MHz for ^{13}C spectra. The solid-state ^{13}C{^{1}H} NMR spectrum was recorded on a Bruker AMR-300 spectrometer (with MAS accessory) operating at 75.5 MHz. The ^{13}C{^{1}H}{^{31}P} NMR spectra were obtained on a Bruker WH-200 spectrometer operating at 50.32 MHz. All ^{13}C NMR spectra were obtained using ^{13}CO- or ^{13}CH$_3$- enriched

samples (the latter obtained from ^{13}C-methyl triflate). Infrared spectra were obtained on a Nicolet Magna 750 FTIR spectrometer, as solids either in Nujol or as CH_2Cl_2 casts on KBr plates or as solutions in KCl cells with 0.5 mm-window pathlengths. Carbonyl stretches reported are for isotopically non-enriched samples. The elemental analyses were performed by the microanalytical service within the department. Spectroscopic data for all compounds are given in Table 2.1.

Preparation of Compounds.

(a) $[Ir_2(CH_3)(CO)(\mu-CO)(dppm)_2][CF_3SO_3]$ (2). Compound 1 (80 mg, 0.057 mmol) was dissolved in 5 mL of CH_2Cl_2. One equiv of anhydrous Me_3NO (4.3 mg, 0.057 mmol), dissolved in 5 mL of CH_2Cl_2, was added dropwise through a cannula to the solution of 1 over 15 min, while maintaining a slow stream of argon over the solution. The mixture was stirred for 45 min, resulting in a color change from light orange to dark red, and the solvent was removed under vacuum. The solid was then recrystallized from CH_2Cl_2/Et_2O, dried under argon, and then in vacuo. Yield 78%. Anal. Calcd for $Ir_2SP_4F_3O_5C_{54}H_{47}$: C, 47.23; H, 3.45. Found: C, 46.81; H, 3.24.

(b) $[Ir_2(H)(CO)_2(PMe_3)(\mu-CH_2)(dppm)_2][CF_3SO_3]$ (3). To a solution of compound 2 (30 mg, 0.022 mmol) in 5 mL of CH_2Cl_2 was added 1 equiv (2.3 μL, 0.022 mmol) of PMe_3 leading to an immediate color change to bright yellow. After stirring for 1/2 h the solution was concentrated to ca. 2 mL and a bright yellow powder was obtained by addition of 10 mL of Et_2O. The powder

Table 2.1 Spectroscopic Data for the Compounds

Compound[a,b]	δ(³¹P{¹H})[c]	δ(¹H)[d,e]	δ(¹³C{¹H})[d]	IR, cm⁻¹[h,i]
[Ir₂(CH₃)(CO)(μ-CO)(dppm)₂][CF₃SO₃] (2)	22.1 (s)	4.45 (m, 2H), 3.78 (m, 2H), 0.58 (q, ³J_{P-H} = 4.1 Hz, 3H, ¹J_{C-H} = 127 Hz)[f]	171.4 (b, 2C), 17.5 (q, ²J_{C-P} = 3.9 Hz,1C)	1964 (s), 1886 (w)[j]
			187.8 (m, 1C)[g], 167.0 (m, 1C)[g]	1974 (vs), 1832 (s)
[Ir₂(H)(CO)₂(PMe₃)(μ-CH₂)(dppm)₂][CF₃SO₃] (3)	-7.7 (m), -11.3 (m), -79.2 (b)	4.05 (m, 2H), 3.45 (m, 2H), 3.05 (m, 2H), 0.75 (d, 9H), -12.35 (dm, ³J_{P-H} = 21.2, 4.8, ²J_{P-H} = 13.5Hz, 1H)	183.0 (t, 1C), 180.1 (b, 1C)	1961 (vs), 1950 (vs)
[Ir₂(H)(CO)₂(PMe₂Ph)(μ-CH₂)(dppm)₂][CF₃SO₃] (4)	-5.7 (m), -12.1 (m), -71.6 (b)	3.82 (m, 2H), 3.35 (m, 2H), 3.30 (m, 2H), 1.12 (d, 6H), -12.2 (dm, ³J_{P-H} = 21.6 Hz, 1H)	182.6 (t, 1C), 180.6 (b, 1C)	1963 (vs), 1952 (s)
[Ir₂(H)(CO)₂(PPh₃)(μ-CH₂)(dppm)₂][CF₃SO₃] (5)	-4.1 (m), -13.7 (m), -33.9 (b)	3.84 (m, 2H), 3.71 (m, 2H), 3.13 (m, 2H), -13.25 (dm, ³J_{P-H} = 22.3 Hz, 1H)	183.4 (t, 1C), 180.5 (b, 1C)	1975 (vs), 1948 (vs)
[Ir₂(H)(CO)₂(P(OPh)₃)(μ-CH₂)(dppm)₂][CF₃SO₃] (6a)	43.9 (m), -4.1 (m), -12.6 (m)	5.2-3.7 (m), -12.69 (dm, ³J_{P-H} = 37.3 Hz, 1H)	180.4 (b, 1C), 179.7 (t, 1C), 167.1 (dt, 1C)	1985 (vs), 1975 (vs), 1951 (s)
[Ir₂(H)(CO)₂(P(OPh)₃)(μ-CH₂)(dppm)₂][CF₃SO₃] (6b)	82.7 (t), -5.6 (m), -8.1 (m)	5.2 - 3.7 (m), -11.71 (dt, ²J_{P-H} = 17.7 Hz, 1H)		

Table 2.1 cont.

Compound^{a,b}	$\delta(^{31}P\{^1H\})^c$	$\delta(^1H)^{d,e}$	$\delta(^{13}C\{^1H\})^d$	IR, cm$^{-1 h,i}$
[Ir₂(H)(CO)₂(μ-CH₂)(μ-SO₂)(dppm)₂][CF₃SO₃] (7)	-1.0 (s)	4.50 (m, 2H), 3.94 (m, 2H), -2.15 (b, $^1J_{C-H}$ = 98 Hz, 3H)^j	170.8 (t, 2C), 36.1 (q, $^2J_{C-P}$= 4.6 Hz, 1C)	2044 (vs), 1997 (vs)
[Ir₂(CO)₂(μ-CH₂)(μ-SO₂)(dppm)₂] (8)	2.7 (s)	3.78 (m, 2H), 3.50 (m, 2H), 2.93 (q, $^3J_{P-H}$ = 12 Hz, 2H)	—	2013 (w), 1951 (s)

^{a} NMR abbreviations: s = singlet, d = doublet, t = triplet, m = multiplet, q = quintet, dm = doublet of multiplets, b = broad. ^{b} NMR data at 25°C in CD₂Cl₂ unless otherwise stated. ^{c} ^{31}P{^{1}H} chemical shifts are referenced vs external 85% H₃PO₄. ^{d} ^{1}H and ^{13}C vs external TMS. ^{e} Chemical shifts for the phenyl hydrogens are not given in the ^{1}H NMR data. ^{f} $^1J_{C-H}$ coupling values for ^{13}C labelled compounds. ^{g} Solid state NMR ^{h} IR abbreviations (ν(CO) unless otherwise stated): vs = very strong, s = strong, m = medium, w = weak, sh = shoulder, b = broad. ^{i} Nujol mull or CH₂Cl₂ cast unless otherwise stated. ^{j} CH₂Cl₂ solution.

was washed (2 x 10 mL) with Et_2O, dried under argon and then under vacuo. Yield 77%. Anal. Calcd for $Ir_2SP_5F_3O_5C_{57}H_{56}$: C, 47.23; H, 3.89. Found: C, 47.12; H, 4.12.

(c) **$[Ir_2(H)(CO)_2(PMe_2Ph)(\mu-CH_2)(dppm)_2][CF_3SO_3]$ (4).** To a solution of compound **2** (30 mg, 0.022 mmol) in 0.6 mL of CD_2Cl_2, in an NMR tube capped with a rubber septum, was added 1 equiv (3.1 µL, 0.022 mmol) of PMe_2Ph leading to an immediate color change to yellow. The NMR spectra showed that the product was compound **4**, based on comparison with the spectra of compound **3**. Yield is quantitative by NMR.

(d) **$[Ir_2(H)(CO)_2(PPh_3)(\mu-CH_2)(dppm)_2][CF_3SO_3]$ (5).** Compound **2** (20 mg, 0.015 mmol) and PPh_3 (4.3 mg 0.016 mmol) were placed in an NMR tube to which 0.6 mL of CD_2Cl_2 was added resulting in an immediate color change to orange. The NMR spectra showed that the product was compound **5**, based on comparison with the spectra of compound **3**. Yield is quantitative by NMR.

(e) **$[Ir_2(H)(CO)_2(P(OPh)_3)(\mu-CH_2)(dppm)_2][CF_3SO_3]$ (6a & 6b).** The procedure was the same as that described for **3** except that $P(OPh)_3$ (97%) was used instead of PMe_3, and the mixture was stirred for 1 h instead of 1/2 h. Two isomers were formed (see Results and Discussion). Yield 60% total for both isomers. Anal. Calcd for $Ir_2SP_5F_3O_8C_{72}H_{62}$: C, 51.36; H, 3.71. Found: C, 51.40; H, 3.82.

(f) **[Ir$_2$(H)(CO)$_2$(μ-CH$_2$)(μ-SO$_2$)(dppm)$_2$][CF$_3$SO$_3$] (7).** Sulphur dioxide gas was passed through a solution of compound **2** (60 mg, 0.044 mmol) in 5 mL of CH$_2$Cl$_2$ for 1 min, leading to an immediate color change of the solution from red to dark red. After stirring for 10 min, the solution was concentrated to about 2 mL under an argon stream and the dark red-brown solid was precipitated by addition of Et$_2$O and washed twice with Et$_2$O. The solid was dried under an argon stream and then under vacuum. Yield 72%. Anal. Calcd for Ir$_2$S$_2$P$_4$F$_3$O$_7$C$_{54}$H$_{47}$: C, 45.12; H, 3.30; S, 4.46. Found: C, 45.40; H, 3.16; S, 4.19.

(g) **[Ir$_2$(CO)$_2$(μ-CH$_2$)(μ-SO$_2$)(dppm)$_2$] (8).** Compound **2** (30 mg, 0.022 mmol) was dissolved in 5 mL of THF, and sulphur dioxide was bubbled through the solution for 1 min, causing formation of compound **7**. This solution was stirred for 10 min under the SO$_2$ atmosphere after which the flask was purged with argon. Four μL (0.024 mmol) of 2,2,6,6-tetramethylpiperidine was added and the solution was stirred for 1 h after which the solvent was removed under vacuum. The residue was then dissolved in CH$_2$Cl$_2$, precipitated by addition of Et$_2$O, and washed (3 X 10 mL) with Et$_2$O. Microanalysis was not done since **8** was always contaminated with the piperidinium-triflate salt. Attempts at separation by fractional crystallization, washing the product with water or by chromatography proved unsuccessful. Approx. yield 68%.

Reaction of Compound 2 with CO. To a solution of compound **2** (30 mg, 0.022 mmol) in 0.6 mL of CD$_2$Cl$_2$, in an NMR tube capped with a rubber septum, was added 2 mL of CO, by means of a gas-tight syringe, leading to an

immediate color change from red to yellow. The NMR spectra showed that the reaction mixture contained the previously characterized compounds $[Ir_2(CH_3)(CO)_4(dppm)_2][CF_3SO_3]$ and $[Ir_2(COCH_3)(CO)_4(dppm)_2][CF_3SO_3]$ in a typical ratio of about 1.0 : 0.2.[1f,g] However, the products were not isolated as solids, because they revert to compound **1** in the absence of a CO atmosphere.

Reaction of Compound 2 with ᵗBuNC. The procedure was similar to the reaction of **2** with CO but one equivalent of ᵗBuNC was added. The product was the previously characterized $[Ir_2(H)(CO)_2(^tBuNC)(\mu\text{-}CH_2)(dppm)_2][CF_3SO_3]$.[1f,g] Yield is quantitative by NMR.

Reaction of Compound 7 with CO. The procedure was the same as the reaction of compound **2** with CO. The NMR spectrum of the reaction mixture showed that it contained only the previously characterized compounds $[Ir_2(CH_3)(CO)_3(\mu\text{-}SO_2)(dppm)_2][CF_3SO_3]$ and $[Ir_2(CH_3CO)(CO)_3(\mu\text{-}SO_2)(dppm)_2]$-$[CF_3SO_3]$, in a typical ratio of 3:1.[1f,g]

X-ray Data Collection. For each of compounds **2, 3** and **7**, crystals suitable for X-ray diffraction were grown via slow diffusion of diethyl ether into a concentrated CH_2Cl_2 solution of the compound. Crystals were mounted and flame-sealed in glass capillaries under solvent vapor to minimize decomposition or deterioration due to solvent loss. Data were collected at -50°C on an Enraf-Nonius CAD4 diffractometer using graphite-monochromated Mo Kα radiation. Unit-cell parameters and space group assignments were obtained as described below. For each compound, three reflections were

chosen as intensity standards and were remeasured every 120 min of X-ray exposure time; in no case was decay evident. Absorption corrections were applied to the data as described below. Crystal parameters and final agreement factors are summarized in Table 2.2.

Unit cell parameters for compounds **2**, **3** and **7** were obtained from a least-squares refinement of 24 reflections in the approximate range $20°<2\theta<24°$. For compounds **2** and **7** the cell parameters and the systematic absences defined the space groups as $P2_1/n$ and $P2_1/c$, respectively, whereas for **3** the cell parameters, the lack of absences and the diffraction symmetry suggested the space group $P1$ or $P\bar{1}$, the latter of which was established by successful refinement of the structure. Absorption corrections to **2** and **3** were applied by the method of Walker and Stuart,[2a] while for **7** the crystal faces were indexed and measured, and a Gaussian integration carried out.

Structure Solution and Refinement. For each structure, the positions of the iridium and phosphorus atoms were found using the direct-methods program *SHELXS-86*;[2b] the remaining atoms were found using a succession of least-squares and difference Fourier maps. Refinement of each structure proceeded using the program *SHELXL-93*.[2c] Hydrogen atom positions (except for hydride ligands as noted below) were calculated by assuming idealized sp^2 or sp^3 geometries about their attached carbon atoms (as appropriate), and were given thermal parameters 120% of the equivalent isotropic displacement parameters of their attached carbons. Further details of structure refinement (other than described below) and final residual indices

Table 2.2 Crystallographic Data for Compounds 2, 3 & 7.

A. Crystal Data

compd	$[Ir_2(CH_3)(CO)(\mu\text{-}CO)(dppm)_2]$-$[CF_3SO_3]$ (2)	$[Ir_2(H)(PMe_3)(CO)_2(\mu\text{-}CH_2)(dppm)_2]$-$[CF_3SO_3]$ (3)·$2CH_2Cl_2$	$[Ir_2(H)(CO)_2(\mu\text{-}CH_2)(\mu\text{-}SO_2)(dppm)_2]$-$[CF_3SO_3]$ (7)·CH_2Cl_2[a]
formula	$C_{54}H_{47}F_3Ir_2O_6P_4S$	$C_{59}H_{60}Cl_4F_3Ir_2O_5P_5S$	$C_{54.875}H_{48.625}Cl_{2.125}F_3Ir_2O_7P_4S_2$[a]
formula wt	1373.26	1619.18	1524.79
crystal dimensions (mm)	0.38 × 0.22 × 0.16	0.46 × 0.30 × 0.10	0.42 × 0.20 × 0.13
color	dark red	yellow	dark red
crystal system	monoclinic	triclinic	monoclinic
space group	$P2_1/n$ (an alternate setting of $P2_1/c$ [No. 14])	$P\bar{1}$ (No. 2)	$P2_1/c$ (No. 14)
unit cell parameters[b,c,d]			
a(Å)	13.8372 (14)	11.910 (2)	13.974 (2)
b(Å)	15.569 (2)	12.8934 (15)	18.422 (3)
c(Å)	23.629 (2)	20.532 (3)	22.264 (3)
α(deg)	90.0	91.256 (10)	90.0
β(deg)	96.413 (9)	95.308 (13)	105.25 (1)
γ(deg)	90.0	102.601 (12)	90.0
V(Å³)	5058.5 (10)	3060.9 (8)	5532.6 (12)

Table 2.2 cont.

Z	4	2	4
ρcalcd (g cm^{-3})	1.803	1.757	1.831
μ (mm^{-1})	5.483	4.739	5.161

B. Data Collection and Refinement Conditions

diffractometer[e]	Enraf-Nonius CAD4	Enraf-Nonius CAD4	Enraf-Nonius CAD4
radiation (λ [Å])	Mo Kα (0.71073)	Mo Kα (0.71073)	Mo Kα (0.71073)
temperature (°C)	–50	–50	–50
scan type	θ–2θ	θ–2θ	θ–2θ
data collection 2θ limit (deg)	50.0	50.0	50.0
total data collected	9106 (-16 $\leq h \leq$ 16, 0 $\leq k \leq$ 18, 0 $\leq l \leq$ 28)	11073 (-14 $\leq h \leq$ 14, -15 $\leq k \leq$ 15, 0 $\leq l \leq$ 24)	9986 (-16 $\leq h \leq$ 16, 0 $\leq k \leq$ 21, 0 $\leq l \leq$ 26)
independent reflections	8874	10737	9716
number of observations (NO)	5528 ($F_o^2 \geq 2\sigma(F_o^2)$)	8535 ($F_o^2 \geq 2\sigma(F_o^2)$)	5646 ($F_o^2 \geq 2\sigma(F_o^2)$)
structure solution method	direct methods (SHELXS–86[f])	direct methods (SHELXS–86[f])	direct methods (SHELXS–86[f])
refinement method	full-matrix least-squares on F^2 (SHELXL–93[g])	full-matrix least-squares on F^2 (SHELXL–93[g])	full-matrix least-squares on F^2 (SHELXL–93[g])
absorption correction method	DIFABS[h]	DIFABS[h]	empirical (face-indexed)

Table 2.2 cont.

range of absorption correction factors	1.074–0.895	1.348–0.263	0.5448–0.3396
data/restraints/parameters	8873 $[F_o^2 \geq -3\sigma(F_o^2)]$/0/616	11072 $[F_o^2 \geq -3\sigma(F_o^2)]$/1/716	9716 $[F_o^2 \geq -3\sigma(F_o^2)]$/5/685
largest difference peak and hole	0.896 and –0.957 e Å^{-3}	2.724 and –3.147 e Å^{-3}	1.371 and –1.839 e Å^{-3}
final R indices^k $F_o^2 > 2\sigma(F_o^2)$	R_1 = 0.0405, wR_2 = 0.0669	R_1 = 0.0598, wR_2 = 0.1640	R_1 = 0.0505, wR_2 = 0.1042
all data	R_1 = 0.1167, wR_2 = 0.0815	R_1 = 0.0807, wR_2 = 0.1798	R_1 = 0.1441, wR_2 = 0.1298
GOF(S)^j	1.003 $[F_o^2 \geq -3\sigma(F_o^2)]$	1.082 $[F_o^2 \geq -3\sigma(F_o^2)]$	0.993 $[F_o^2 \geq -3\sigma(F_o^2)]$

^{a}The sample crystallized as a mixture of 87.5% of compound 7 and 12.5% of [Ir$_2$(CO)$_2$(μ-Cl)(μ-SO$_2$)(dppm)$_2$][CF$_3$SO$_3$]·CH$_2$Cl$_2$.

^{b}For 2, obtained from least-squares refinement of 24 reflections with 21.0° < 2θ < 24.0°.

^{c}For 3, obtained from least-squares refinement of 24 reflections with 20.1° < 2θ < 23.7°.

^{d}For 7, obtained from least-squares refinement of 24 reflections with 19.9° < 2θ < 23.8°.

^{e}Programs for diffractometer operation, data collection and data processing were those supplied by Enraf-Nonius.

^{f}Sheldrick, G. M. *Acta Crystallogr.* **1990**, *A46*, 467–473.

^{g}Sheldrick, G. M. *SHELXL-93*. Program for crystal structure determination. University of Göttingen, Germany, 1993. Refinement on F_o^2 for all reflections except for 1 with very negative F^2. Weighted R-factors wR_2 and all goodnesses of fit S are based on F^2; conventional R-factors R_1 are based on F_o, with F_o set to zero for negative F_o^2. The observed criterion of $F_o^2 > 2\sigma(F_o^2)$ is used only for calculating R_1, and is not relevant to the choice of reflections for refinement. R-factors based on F_o^2 are

Table 2.2 cont.

statistically about twice as large as those based on F_o, and R- factors based on ALL data will be even larger.

[h]Walker, N.; Stuart, D. *Acta Crystallogr.* **1983**, *A39*, 158–166.

[i]The Ir(2)–H(2) distance was constrained to be 1.70 ± 0.01 Å.

[j]The Ir(1)–H(1) distance was fixed at 1.70(1) Å, and the nonbonded P(1)···H(1) and P(3)···H(1) distances were constrained to be equal (within 0.01 Å). Distances involving the minor-constituent carbonyl C(1')O(1') were also fixed (d(C(1')–O(1')) = 1.15(1) Å, d(Ir(1)–C(1')) = 1.85(1) Å and d(Ir(1)···O(1')) = 3.00(1) Å).

[k]$R_1 = \Sigma||F_o| - |F_c||/\Sigma|F_o|$; $wR_2 = [\Sigma w(F_o^2 - F_c^2)^2/\Sigma w(F_o^4)]^{1/2}$.

[l]$S = [\Sigma w(F_o^2 - F_c^2)^2/(n-p)]^{1/2}$ (n = number of data; p = number of parameters varied; $w = [\sigma^2(F_o^2) + (a_1 P)^2 + a_o P]^{-1}$ where $P = [Max(F_o^2, 0) + 2F_c^2]/3)$. a_o and a_1 are suggested by the least-squares program for each structure (for **2**, a_o = 0.0216, a_1 = 2.2944; for **3**, a_o = 0.1278, a_1 = 10.1840; for **7**, a_o = 0.0554, a_1 = 0).

may be found in Table 2.2.

For [Ir$_2$(CH$_3$)(CO)(μ-CO)(dppm)$_2$][CF$_3$SO$_3$] (2), electron density maps in the equatorial plane, essentially perpendicular to the Ir-P vectors, indicated similar coordination environments for both iridium atoms. Although the bridging carbonyl group was well behaved, each Ir apparently also had a terminal CO in which the peaks corresponding to the oxygens were of low intensity. This suggested a disorder involving superposition of the terminal carbonyl and methyl ligands, resulting from the two orientations of the complex as diagrammed below (dppm groups , above and below the plane of the paper, omitted for clarity).
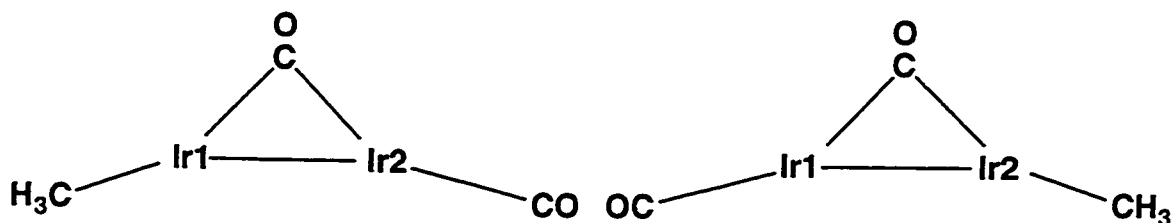
Subsequent difference Fourier maps showed that the disordered carbonyl and methyl carbons were not exactly superimposed but were slightly offset from each other, and these two half-occupancy positions on each Ir refined well. The atoms corresponding to the disordered CO and CH$_3$ groups were refined isotropically with an occupancy factor of 0.5.

Location of all atoms in [Ir$_2$(H)(CO)$_2$(PMe$_3$)(μ-CH$_2$)(dppm)$_2$][CF$_3$SO$_3$]·2CH$_2$Cl$_2$ (3) proceeded smoothly and even the hydride ligand H(2) was located and refined with a fixed Ir(2)–H(2) distance of 1.70(1) Å.

Although all of the non-hydrogen atoms of $[Ir_2(H)(CO)_2(\mu\text{-}CH_2)(\mu\text{-}SO_2)$-$(dppm)_2][CF_3SO_3]\cdot CH_2Cl_2$ (7) were located, the carbon atom of the bridging methylene group (C(3)) did not behave well in least squares refinements. A difference Fourier map at this stage located another peak near C(3) in the Ir(1)Ir(2)C(3) plane, but at approximately 2.5 Å from each metal. A $^{31}P\{^1H\}$ NMR spectrum obtained on a few of the single crystals showed about 10-15% of the previously characterized $[Ir_2(CO)_2(\mu\text{-}Cl)(\mu\text{-}SO_2)(dppm)_2][CF_3SO_3]$,[3] which had apparently resulted from reaction of 7 with the chlorinated solvent. All subsequent attempts to obtain suitable crystals of 7 without the chloro-bridged impurity failed; attempts to grow crystals in non-chlorinated solvents gave poor quality crystals. Inclusion of a chlorine atom (Cl(1)) in the least-squares refinement with an occupancy factor of 0.125 (and concomitant reduction of the occupancy factor for C(3) to 0.875) yielded the most satisfactory results. The hydride ligand H(1) was not located from a difference Fourier map, but its position was idealized at 1.70 Å from Ir(1) in a position that minimized contacts with the surrounding ortho-hydrogen atoms of the dppm groups. Unfortunately, owing to the disorder in which the fractional Cl atom was essentially superimposed on the CH_2 group, the methylene hydrogens could not be located. Disorder of the carbonyl group attached to Ir(1) was suggested by an extreme elongation of the thermal ellipsoids of C(1) and O(1) in a direction perpendicular to the Ir(1)-C(1) bond axis. In addition, the Ir(2)-Ir(1)-C(1) angle observed for 7 (ca. 144° prior to correcting for the disorder) was substantially different from that previously determined for the chloro-bridged complex (ca.

167°) indicating that these carbonyl groups for the two disordered molecules would not be superimposed. This carbonyl group was therefore disordered over two sites having occupancy factors of 0.875 and 0.125, corresponding to those of the bridging methylene and chloro groups, respectively. Correcting for the disorder substantially reduced the thermal parameters for the carbonyl group. The placement of C(1')O(1') was initially set at the coordinates previously found for the pure chloro-bridged species, and was refined as a rigid group having Ir(1)-C(1'), C(1')-O(1') and Ir(1)-O(1') distances approximating those within the Ir(2)-C(2)-O(2) unit. Atom C(1') was given a fixed isotropic thermal parameter roughly equal to U_{eq} for C(2) while O(1') was refined isotropically. Carbonyl C(1)O(1) having the major occupancy was refined anisotropically without restriction. A drawing of the equatorial plane of the disordered structure (dppm groups omitted) is shown in Figure 2.1. Atoms Ir(1), Ir(2), C(2), O(2), S(1), O(3) and O(4) are common to both disordered molecules with C(1'), O(1') and Cl(1) corresponding to the chloro-bridged species and C(3)H₂, C(1), O(1) and H(1) belonging to the methylene-bridged complex (7). Superposition of the atom positions of complex 7 with the pure chloro-bridged species shows that, apart from the atoms involved in the disorder, all atoms superimpose almost exactly.

Dr. Bob McDonald is acknowledged for X-ray data collection and solution for compounds **2, 3** and **7**.

Measurement of Exchange in Compound 7. A variable temperature line shape analysis was done on compound **7** to calculate the activation parameters
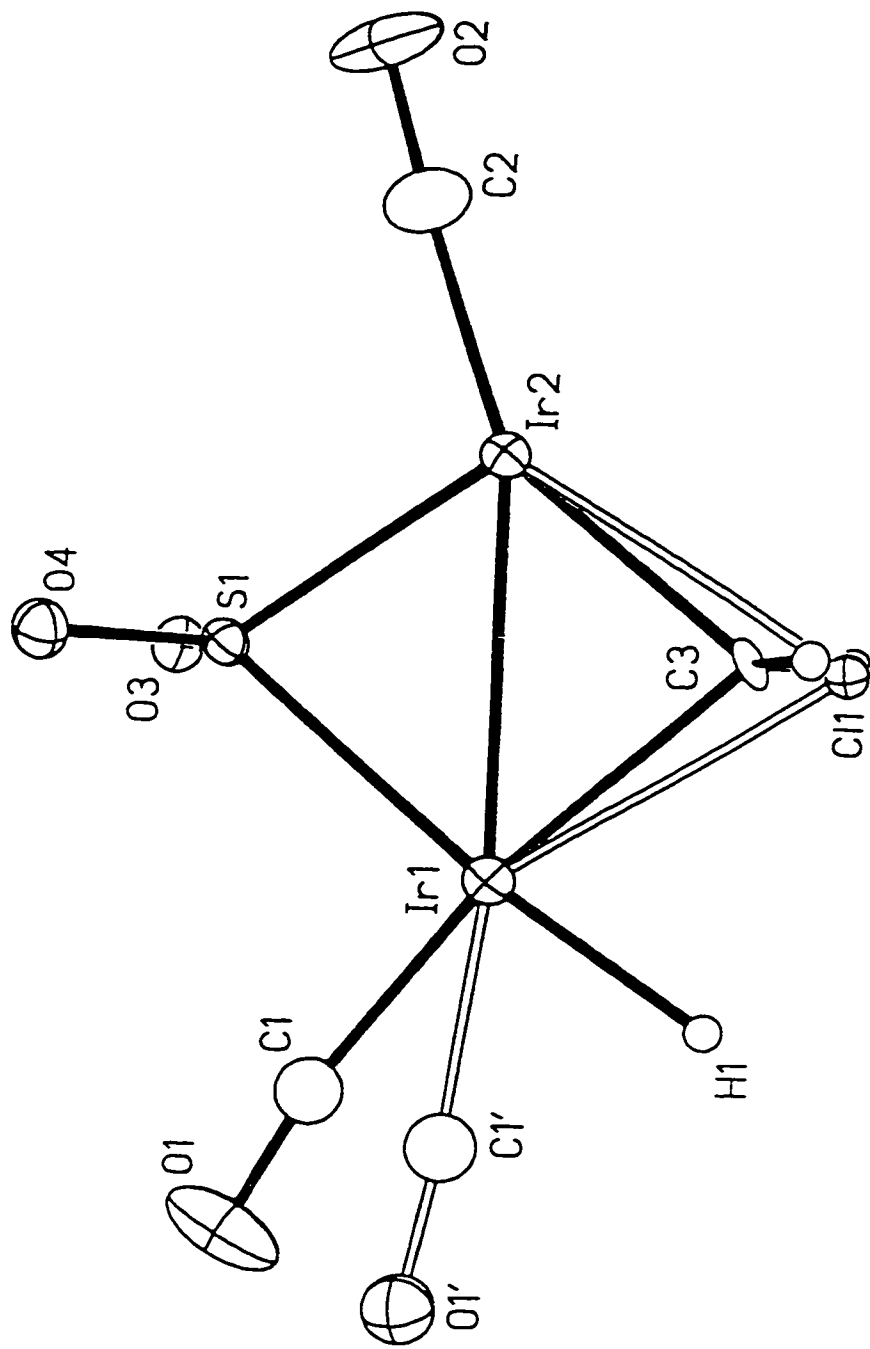
Figure 2.1 View of the equatorial plane containing the disordered ligands of $[Ir_2(H)(CO)_2(\mu\text{-}CH_2)(\mu\text{-}SO_2)(dppm)_2]^+$ (7) (major constituent) and $[Ir_2(CO)_2(\mu\text{-}Cl)(\mu\text{-}SO_2)(dppm)_2]^+$ (minor). The carbonyl group C(1)O(1), hydride ligand H(1), and bridging methylene group containing C(3) were refined with an occupancy factor of 0.875, while the carbonyl group C(1')O(1') and bridging chloride Cl(1) were refined with an occupancy factor of 0.125. Open bonds show the connectivity within the minor constituent, together with the SO_2 group and C(2)O(2).

for the exchange between the hydride and methylene ligands. NMR probe temperatures were measured with an independently calibrated thermocouple immersed in the appropriate volume of toluene in an NMR tube before and after the experiments (Mrs. G. Aarts is acknowledged for her assistance in running these experiments). An error value of ±5 K should be assumed for the temperatures measured. Spectra were then visually fit to spectra generated by a computer program written by Dr. R. E. D. McClung. Refer to Table 2.3 for results.

Results and Compound Characterization

Earlier work in this research group and by Eisenberg and coworkers had shown that protonation of the complexes $[Ir_2(CO)_3(dppm)_2]$, $[Rh_2(CO)_3(dppm)_2]$ and their heterobinuclear analogue, $[RhIr(CO)_3(dppm)_2]$, yielded the respective hydrido-bridged complexes, $[Ir_2(CO)_2(\mu\text{-}H)(\mu\text{-}CO)(dppm)_2][BF_4]$,[4] $[Rh_2(CO)_2(\mu\text{-}H)(\mu\text{-}CO)(dppm)_2][BF_4]$[5] and $[RhIr(CO)_3(\mu\text{-}H)(dppm)_2][BF_4]$,[6] by apparent electrophilic attack at the metal-metal bond. An obvious extension of these protonations was to substitute H^+ by CH_3^+ (in the form of methyl triflate (MeOTf)) in attempts to obtain methyl-bridged analogues. This expectation has not been realized for the Rh-containing complexes, for which an acyl-bridged species was obtained for dirhodium[7] and a product containing a methyl group terminally bound to Ir was obtained in the RhIr case.[1f,g] The reaction with the diiridium precursor also did not proceed strictly according to expectation.[1f,g] Instead of the anticipated methyl-bridged product,

Table 2.3 Data for Variable Temperature Line-Shape Analysis for

Methylene-Hydride Exchange in Compound **7**.

Temperature (K)	Observed Rate Constant (sec⁻¹)	Calculated Rate Constant (sec⁻¹)
298.3	1.20×10^7	8.95×10^6
282.3	4.00×10^6	4.73×10^6
274.4	3.10×10^6	3.36×10^6
263.7	2.11×10^6	2.05×10^6
251.0	1.10×10^6	1.08×10^6
240.2	6.60×10^5	6.00×10^5
227.9	3.00×10^5	2.80×10^5
217.7	1.95×10^5	1.40×10^5
173.7	2.80×10^3	3.20×10^3
171.2	2.70×10^3	2.40×10^3

Using the modified Eyring equation,

$$\ln(k/T) = \ln(\kappa/h) - \Delta H^{\ddagger}/RT + \Delta S^{\ddagger}/R$$

where   R = gas constant
κ = Boltzmann's constant
h = Planck's constant
T = temperature in K

a plot of ln(k/T) vs. 1/T gives a straight line with a slope equal to - $\Delta H^{\ddagger}/R$ and an

intercept equal to $\Delta S^{\ddagger}/R$. Error limits are based on the standard deviations of

the calculated slope and intercept of a least-square fit to the Eyring plot.*

Calculated Parameters: $\Delta H^{\ddagger}$ = 6.11 ± 0.33 kcal/mol
$\Delta S^{\ddagger}$ = -6.24 ± 1.50 cal/mol K

* Dr. R. E. D. McClung is acknowledged for carrying out these calculations.

the methylene-bridged hydrido species $[Ir_2(H)(CO)_3(\mu\text{-}CH_2)(dppm)_2][CF_3SO_3]$ (1)

results from C-H bond cleavage of the methyl group; a representation of **1** is

shown in Scheme 2.1. This result parallels an earlier study in which methyl

triflate addition to $[Cp^*Ir(\mu\text{-}CO)]_2$ yielded the methylene-bridged hydride

$[Cp^*_2Ir_2(CO)_2(\mu\text{-}CH_2)(\mu\text{-}H)][CF_3SO_3]$.[8]

Compound **1** bears an interesting relationship to two *dicarbonyl* methyl

compounds previously reported; in $[Rh_2(CH_3)(CO)(\mu\text{-}CO)(dppm)_2][CF_3SO_3]$[7] the

methyl group is *terminally* bound to one rhodium center, whereas in

$[Ir_2(CO)_2(\mu\text{-}CH_3)(dmpm)_2][CF_3SO_3]$[9] (dmpm = $Me_2PCH_2PMe_2$) the methyl group

bridges the metals in a symmetrical arrangement. The existence of these

dicarbonyl, methyl complexes suggested that CO removal from **1** may *reverse*

the C-H bond cleavage step, regenerating a related methyl product. If this were

the case, the further question arose as to whether the methyl group would be

terminally bound to one metal, as in the above dppm-bridged dirhodium

complex, or bridging, as in the dmpm-bridged diiridium complex. The answer to

the first suggestion is affirmative; one carbonyl is readily removed from **1** by

reaction with Me_3NO, generating the methyl complex $[Ir_2(CH_3)(CO)_2(dppm)_2]$-

$[CF_3SO_3]$ (2). This species is highly fluxional, so at ambient temperature all

spectral parameters suggest a symmetrical species having a bridging methyl

group. The $^{31}P\{^1H\}$ NMR spectrum at this temperature shows a singlet at δ 22.1,

the ^1H NMR spectrum displays the methyl signal as a quintet at δ 0.58,

displaying equal coupling to all four ^{31}P nuclei, and the $^{13}C\{^1H\}$ NMR spectrum

Scheme 2.1
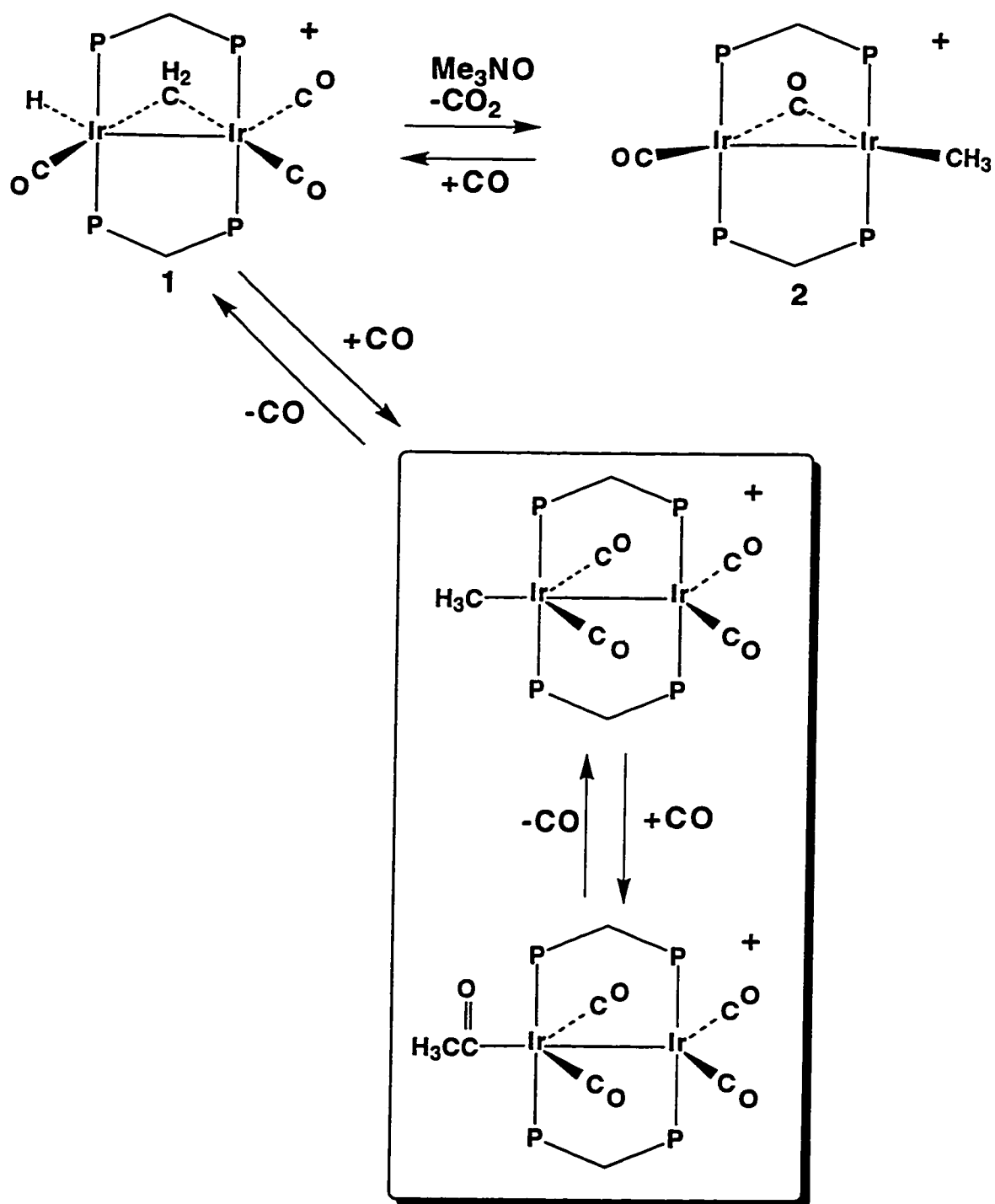
Species in box have been previously characterized[1f,g]

shows one singlet carbonyl resonance at δ 171.4 and a sharp quintet at δ 17.5

($^2J_{P-C}$ = 4.5 Hz) for the methyl group. However, at low temperatures the spectral parameters are more in keeping with an unsymmetrical species having a terminally bound methyl group. Therefore at -80 °C the $^{31}P\{^1H\}$ NMR spectrum shows two resonances for the two chemically distinct phosphorus environments (by virtue of the chemically inequivalent metal centers), and the $^{13}C\{^1H\}$ NMR spectrum displays two carbonyl resonances at δ 182.5 and 162.1. In the solid-state ^{13}C NMR spectrum the carbonyl resonances (δ 187.8 and 167.0) are close to those observed in solution at -80 °C, while the IR spectrum (Nujol mull) shows carbonyl bands at 1974 and 1832 cm^{-1}, suggesting one terminal and one bridging carbonyl group. Compound **2** is therefore formulated as $[Ir_2(CH_3)(CO)(\mu-CO)(dppm)_2][CF_3SO_3]$ in the solid state, having a structure much like that of Eisenberg's Rh_2 analogue.[7]

In solution, the structure of **2** must be subtly different than that in the solid, as judged by the essential disappearance of the IR stretch correspoding to the bridging carbonyl. We suggest therefore that in solution, the bridging carbonyl of **2** has moved to a terminal site as shown in **2a**. Although a structure of this type has not, to our knowledge, previously been observed in dppm-bridged complexes of Rh or Ir, analogous structures have been observed or proposed for a closely related PNP-bridged complex of rhodium (PNP = $(RO)_2PN(Et)P(OR)_2)$[10] and dppm complexes of platinum and palladium.[11] In addition, Density Functional Theory calculations have shown that for the

2a
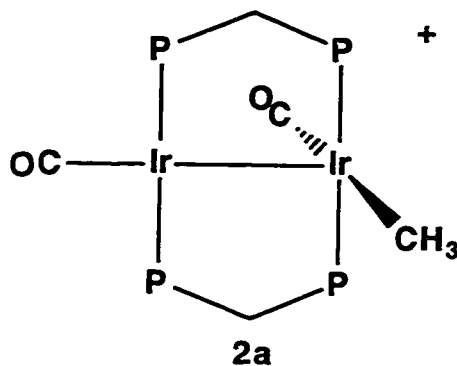
isolated cation, structure **2a** is the stable conformation.[12] In any case, in all subsequent schemes, compound **2** will be shown having the structure established in the solid state (vide infra).

The fluxionality of **2**, which gives rise to time-averaged equivalence of both metals, results from transfer of the methyl group from one metal to the other (presumably via a methyl-bridged intermediate) accompanied by slight movement of the carbonyls from opposite the Ir-Ir bond to opposite the methyl group, and vice versa. A full turnstile-type motion of these ligands around the Ir_2 core is ruled out since this would give rise to a time-averaged symmetry on either side of the Ir_2P_4 plane, leading to only one resonance for the dppm methylene hydrogens; at ambient temperature two resonances are observed indicating different environments on either side of the Ir_2P_4 plane.

Confirmation of the proposed structure for **2** in the solid state comes from the X-ray structure determination, as shown in Figure 2.2, with selected distances and angles given in Table 2.4. Compound **2** has an unsymmetrical A-frame structure in which one carbonyl group is bridging, while the other carbonyl and the methyl group occupy a terminal position on each metal. These terminal ligands are not opposite the bridging carbonyl, but are in a

Figure 2.2 Perspective view of the [Ir₂(CH₃)(CO)(μ-CO)(dppm)₂]⁺ cation of compound **2**. Thermal ellipsoids are shown at the 20% probability level except for hydrogens which are shown arbitrarily small. Phenyl hydrogens have been omitted.

Table 2.4 Selected Interatomic Distances and Angles for Compound 2.

(a) Distances (Å)

Atom1	Atom2	Distance	Atom1	Atom2	Distance
Ir(1)	Ir(2)	2.7775(5)	Ir(2)	C(2)	2.089(9)
Ir(1)	P(1)	2.307(2)	Ir(2)	C(3)	2.16(2)
Ir(1)	P(3)	2.308(2)	P(1)	C(4)	1.816(8)
Ir(1)	C(1)	1.77(2)	P(2)	C(4)	1.828(8)
Ir(1)	C(2)	2.110(8)	P(3)	C(5)	1.837(8)
Ir(1)	C(3′)	2.15(2)	P(4)	C(5)	1.825(8)
Ir(2)	P(2)	2.315(2)	O(1)	C(1)	1.19(2)
Ir(2)	P(4)	2.313(2)	O(1′)	C(1′)	1.15(2)
Ir(2)	C(1′)	1.76(2)	O(2)	C(2)	1.095(9)

(b) Angles (deg)

Atom1	Atom2	Atom3	Angle	Atom1	Atom2	Atom3	Angle
Ir(2)	Ir(1)	C(1)	176.4(6)	P(2)	Ir(2)	P(4)	173.46(8)
Ir(2)	Ir(1)	C(2)	48.3(2)	C(1′)	Ir(2)	C(2)	134.5(7)
Ir(2)	Ir(1)	C(3′)	166.0(5)	C(2)	Ir(2)	C(3)	148.5(6)
P(1)	Ir(1)	P(3)	170.96(8)	Ir(1)	C(1)	O(1)	177.6(16)
C(1)	Ir(1)	C(2)	128.2(7)	Ir(2)	C(1′)	O(1′)	175.8(20)
C(2)	Ir(1)	C(3′)	145.7(6)	Ir(1)	C(2)	Ir(2)	82.8(3)
Ir(1)	Ir(2)	C(1′)	176.6(6)	Ir(1)	C(2)	O(2)	137.9(8)
Ir(1)	Ir(2)	C(2)	48.9(2)	Ir(2)	C(2)	O(2)	138.8(7)
Ir(1)	Ir(2)	C(3)	162.4(5)				

"flattened A-frame" arrangement being almost trans to the Ir-Ir bond (C(1)-Ir(1)-Ir(2) = 176.4(6)°, Ir(1)-Ir(2)-C(3) = 162.4(5)°). This arrangement results in somewhat different angles between the bridging carbonyl and the different terminal groups (C(1)-Ir(1)-C(2) = 128.2(7)° and C(2)-Ir(2)-C(3) = 148.5(6)°). The geometry observed for **2** is reminiscent of that observed in the isoelectronic species [Rh$_2$(X)$_2$(μ-CO)(dppm)$_2$] (X = Br, Cl).[13] The Ir-Ir separation of 2.7775(5) Å is consistent with a single bond and is shorter than the Rh-Rh separation of 2.811(2) Å in the dirhodium analogue;[7] otherwise the two structures are closely comparable. Although the disorder in the equatorial ligand positions (see Experimental section) was satisfactorily resolved, the almost superposition of the terminal methyl and carbonyl groups does result in an uncertainty in their exact positions precluding an in-depth discussion of the structural parameters.

Reaction of **2** with 1 equiv of carbon monoxide regenerates the tricarbonyl complex **1**, accompanied by C-H bond cleavage of the methyl group and formation of the bridging methylene and terminal hydrido groups. This is, of course, essentially the reverse of the conversion of **1** to **2** upon reaction with Me$_3$NO. Under excess CO compound **2** transforms into a mixture of two tetracarbonyl species, the methyl complex [Ir$_2$(CH$_3$)(CO)$_4$(dppm)$_2$][CF$_3$SO$_3$] and the related acyl product [Ir$_2$(C(O)CH$_3$)(CO)$_4$(dppm)$_2$][CF$_3$SO$_3$], both of which have been previously characterized,[1f,g] in varying ratios depending upon the CO pressure (see Scheme 2.1).

The conversion of a hydrido methylene species (**1**) into a methyl complex (**2**) upon removal of a carbonyl group, and the reverse process, C-H bond

activation of a methyl group upon addition of a carbonyl ligand, is a fascinating transformation. Usually C-H bond activation in low-valent, late transition-metal complexes is induced by *ligand loss* to generate the required coordinative unsaturation.[14] We know of only one other example of ligand addition resulting in C-H bond activation, in which phosphine addition to a diruthenium complex resulted in cleavage of an agostic C-H bond.[15] It was therefore of interest to determine the scope of the present oxidative addition reaction by reacting compound **2** with a number of ligands having a range in electronic properties. In preliminary studies[1f,9] compound **1** was used as precursor, but the outcome was invariably the same (in the reactions discussed here) as the reactions with **2**, with substitution of a carbonyl by the added ligand in the former case.

Reaction of **2** with various phosphines and triphenylphosphite also results in methyl C-H bond cleavage, yielding the methylene-bridged, hydride products $[Ir_2(H)(CO)_2(PR_3)(\mu\text{-}CH_2)(dppm)_2][CF_3SO_3]$ (PR_3 = PMe_3 (**3**), PMe_2Ph (**4**), PPh_3 (**5**), $P(OPh)_3$ (**6**)) as shown in Scheme 2.2. For compound **3** the $^{31}P\{^1H\}$ NMR spectrum shows three resonances at δ -7.7, -11.3 and -79.2 (intensity 2:2:1) with the high-field signal being attributed to the trimethylphosphine ligand. The ^1H NMR spectrum shows a hydride signal at δ -12.35 as a doublet of multiplets, and selective ^{31}P decoupling shows that this signal is actually a doublet of triplets of triplets with the largest coupling ($^3J_{P\text{-}H}$ = 21.2 Hz) to the trimethylphosphine.

In all PR_3 adducts the hydride resonance is complex, displaying the largest coupling to the PR_3 group (*ca.* 22Hz) and secondary coupling (*ca.* 13

Scheme 2.2

2

PR$_3$ →

3 - 6a

PR$_3$ = PMe$_3$ (3), PMe$_2$Ph (4),
PPh$_3$ (5), P(OPh)$_3$ (6a)

2

^{t}BuNC →
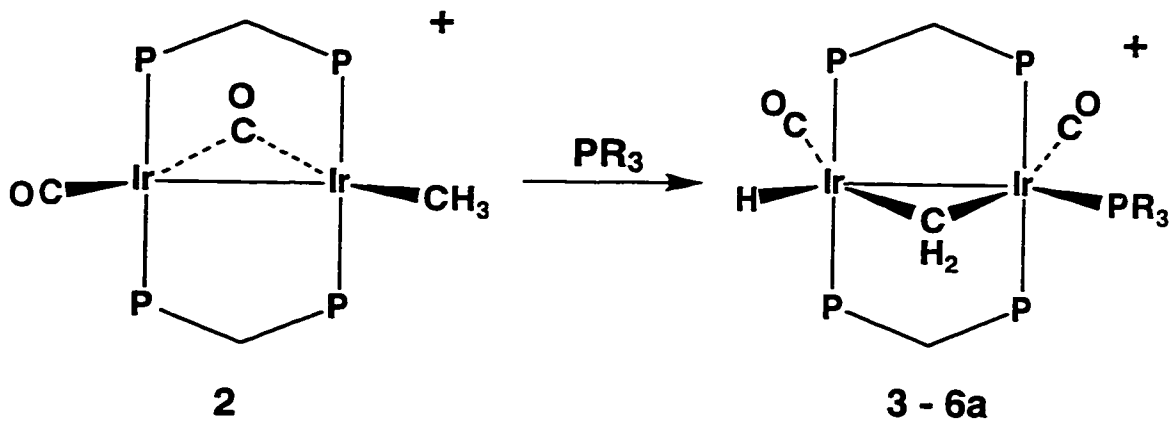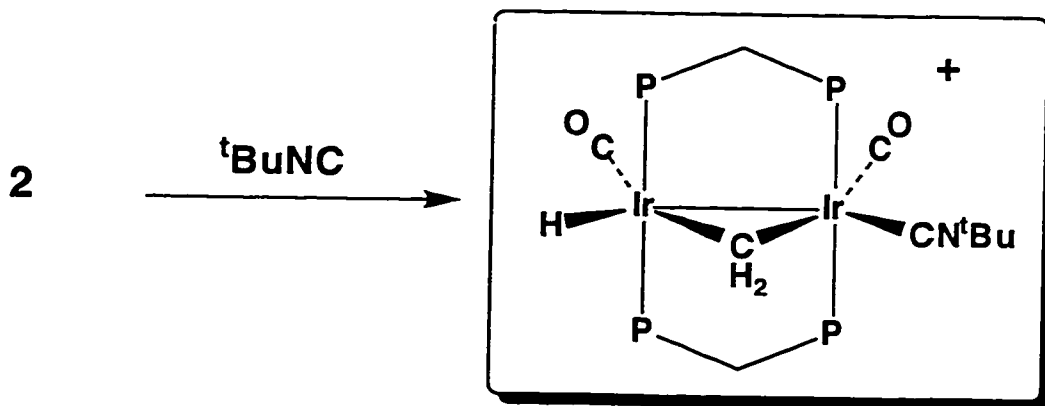
Species in box has been previously
characterized.[1f,g]

Hz) to one pair of dppm phosphorus nuclei and *ca.* 5 Hz to the other pair. In spite of the large coupling between the hydride and the PR$_3$ group, selective ^{1}H{^{31}P} and ^{13}C{^{31}P} NMR experiments on compound **3** suggest that the trimethylphosphine is **not** on the same metal as the hydride ligand and the two carbonyl ligands are on different metals. The larger three-bond coupling ($^3J_{P-H}$ = 21.2 Hz) between the hydride and the PMe$_3$ group compared to the two-bond coupling ($^2J_{P-H}$ = 13.5 Hz) between the hydride and the adjacent dppm groups may result from an approximately linear arrangement of the hydride and PMe$_3$ groups in solution, with respect to the Ir-Ir bond. Strong coupling through the metal-metal bond has previously been observed in such systems.[16] The proposed structure for **3** and its analogues (**4, 5, 6a**) is supported by the X-ray structure determination of **3**, a representation of which is shown in Figure 2.3. A compilation of important bond lengths and angles is given in Table 2.5. This structure confirms the methylene-bridged, hydride formulation and also displays the arrangement of carbonyl, hydride and PMe$_3$ groups proposed on the basis of the spectral results. The overall geometry is that of an A-frame structure having the carbonyls essentially opposite the bridging methylene group, with the PMe$_3$ and hydride ligands on the outside of the A-frame, almost bisecting the angles between the respective μ-CH$_2$ and terminal carbonyl groups. Both ends of the diphosphine ligands are bent significantly from a trans alignment owing to repulsions involving the PMe$_3$ group, (P(1)-Ir(1)-P(3) = 163.16(9)° and P(2)-Ir(2)-P(4) = 154.79(8)°). These repulsions may also be responsible for larger Ir-P (dppm) distances at the more crowded Ir(1) center (2.330(2),
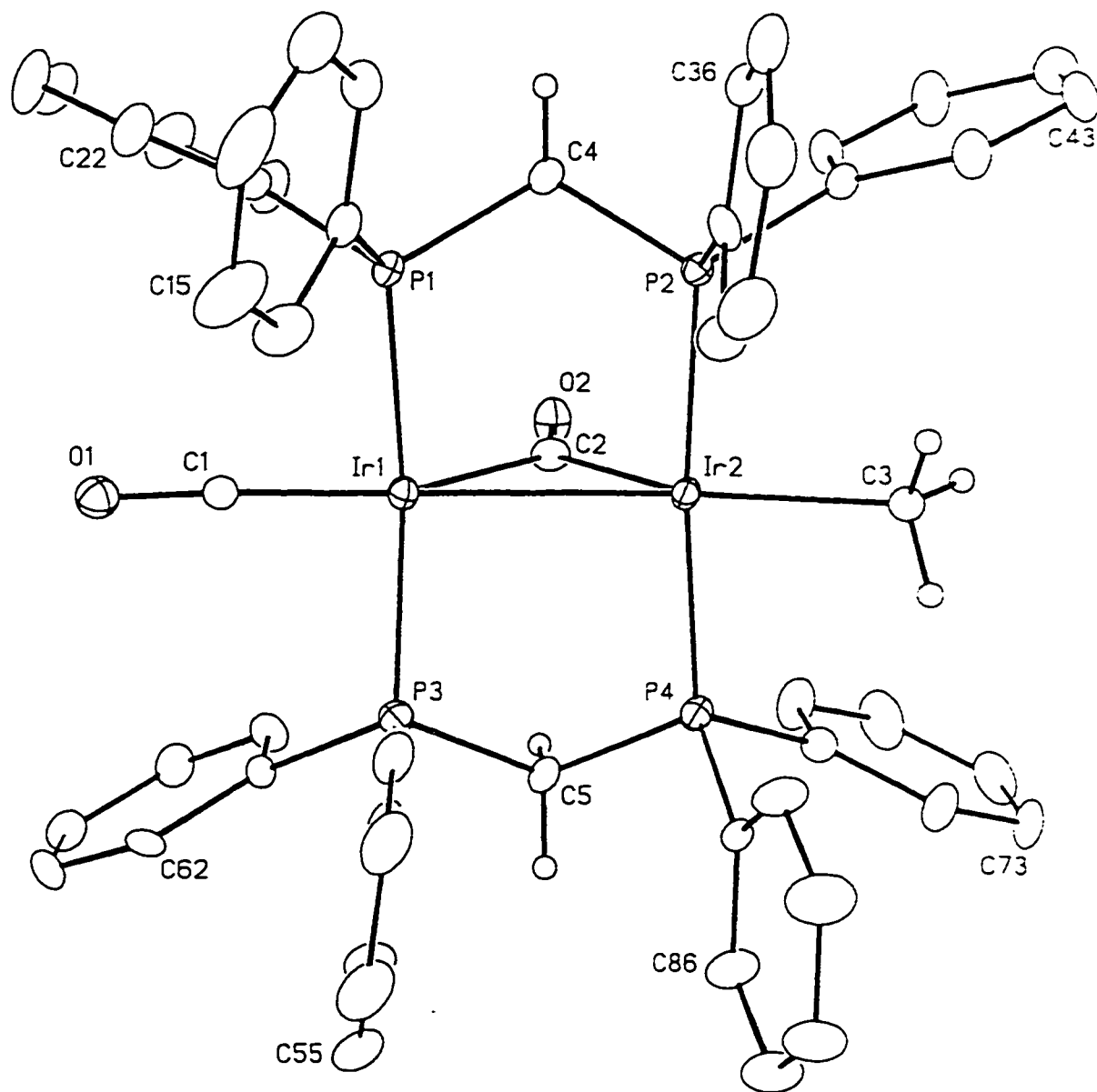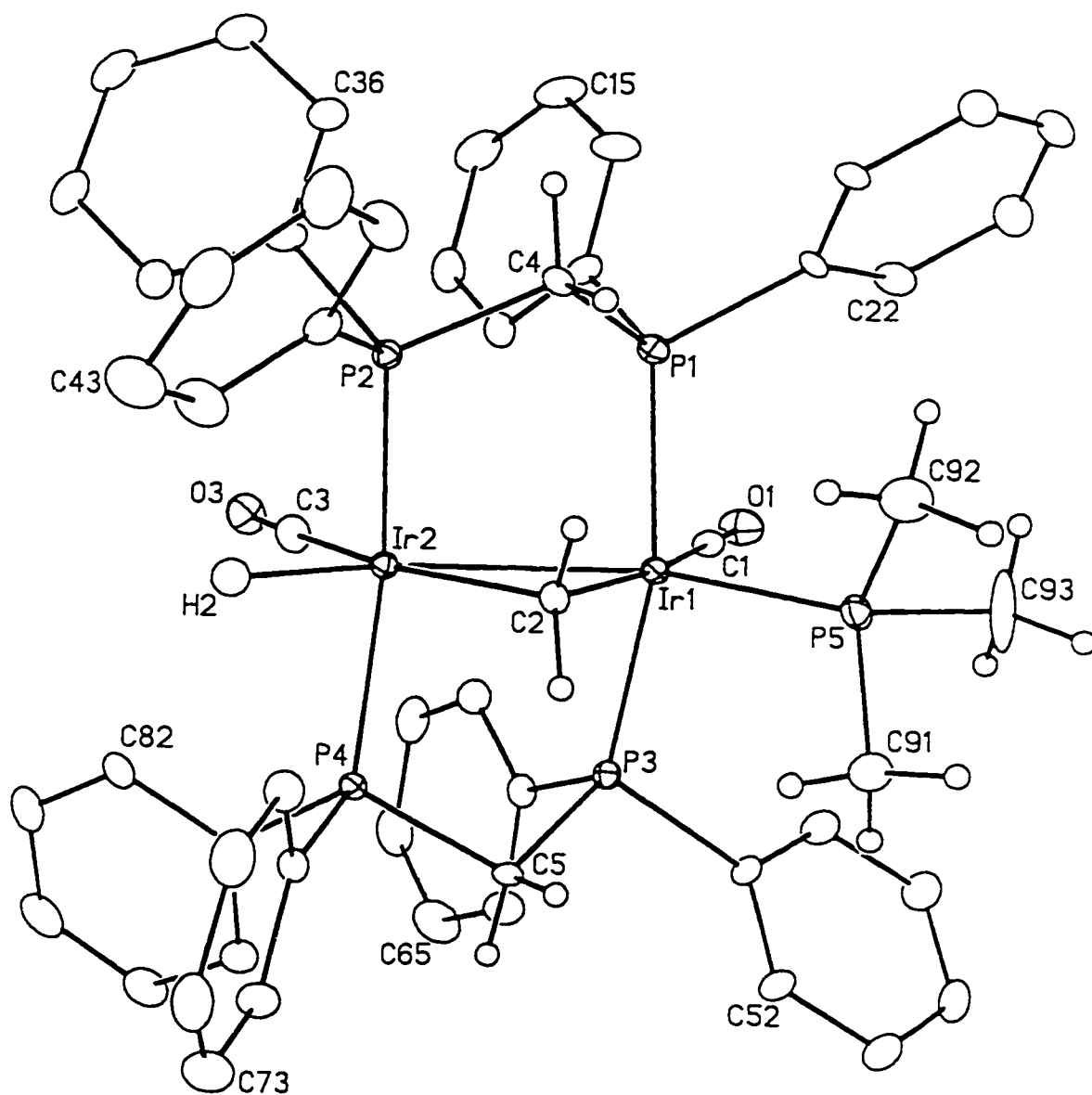
Figure 2.3 Perspective view of the [Ir₂(CO)₂(H)(PMe₃)(μ-CH₂)(dppm)₂]⁺ cation of compound **3**. Thermal ellipsoids are shown at the 20% probability level except for hydrogens which are shown arbitrarily small. Phenyl hydrogens have been omitted.

Table 2.5 Selected Interatomic Distances and Angles for Compound **3**.

(a) Distances (Å)

Atom1	Atom2	Distance	Atom1	Atom2	Distance
Ir1	Ir2	2.8308(6)	Ir2	C3	1.909(9)
Ir1	P1	2.332(2)	Ir2	H2	1.71
Ir1	P3	2.330(2)	P1	C4	1.819(9)
Ir1	P5	2.359(3)	P2	C4	1.830(9)
Ir1	C1	1.887(9)	P3	C5	1.818(9)
Ir1	C2	2.172(9)	P4	C5	1.850(9)
Ir2	P2	2.304(2)	O1	C1	1.141(11)
Ir2	P4	2.305(2)	O3	C3	1.117(12)
Ir2	C2	2.098(9)			

(b) Angles (deg)

Atom1	Atom2	Atom3	Angle	Atom1	Atom2	Atom3	Angle
Ir2	Ir1	P5	131.72(7)	C2	Ir2	C3	157.9(4)
Ir2	Ir1	C1	123.3(3)	Ir1	P5	C91	116.7(4)
Ir2	Ir1	C2	47.4(2)	Ir1	P5	C92	116.9(5)
P1	Ir1	P3	163.16(9)	Ir1	P5	C93	115.5(4)
P5	Ir1	C1	104.9(3)	C91	P5	C92	99.5(6)
P5	Ir1	C2	84.4(2)	C91	P5	C93	102.6(7)
C1	Ir1	C2	170.7(4)	C92	P5	C93	103.2(8)
Ir1	Ir2	C3	108.3(3)	Ir1	C1	O1	178.5(9)
Ir1	Ir2	C2	49.6(2)	Ir1	C2	Ir2	83.0(3)
P2	Ir2	P4	154.79(8)	Ir2	C3	O3	177.4(9)

2.332(2)Å) than at Ir(2) (2.304(2), 2.305(2)Å), as well as the larger Ir(1)-C(2) distance (2.172(9)Å) compared to Ir(2)-C(2) (2.098(9)Å) involving the methylene group. The angle at the methylene carbon (83.0(3)°) is typical of such a group when bridging a metal-metal bond (2.8308(6)Å).[17]

Compounds **3-5** all have very similar spectral parameters, apart from the $^{31}P\{^1H\}$ resonances for the monodentate phosphine groups, and also spectrally resemble compound **1** in which a PR_3 group is replaced by CO; therefore all are assumed to have similar structures. The reaction of **2** with $P(OPh)_3$ actually yields two isomers (**6a** and **6b**). Isomer **6a** has spectral parameters closely resembling those of compounds **3-5** so is assumed to have an analogous structure, whereas the structure of **6b** could not be conclusively established using NMR spectroscopy. The two structures shown below (as **A** and **B**) for isomer **6b** are suggested on the basis of the two carbonyl resonances, one of which is in the region of those in **6a**, suggesting it is opposite the μ-CH_2 group,
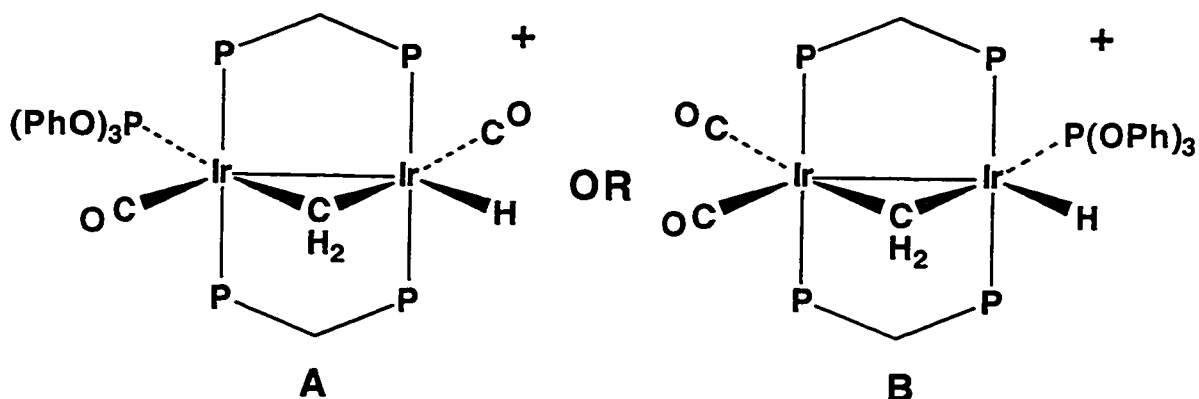
and one of which is clearly in a different environment. Although we favor structure **A** shown for **6b**, on the basis that both dppm ^{31}P resonances are at similar chemical shifts, suggesting similar environments with one carbonyl on

each metal, we could not carry out a selective ^{31}P-decoupling experiment to conclusively rule out an alternate structure (**B**) in which both carbonyls are on one metal, with the hydride and phosphite on the other.

Compound **2** also reacts with tBuNC to give the previously characterized isocyanide adduct $[Ir_2(H)(CO)_2(^tBuNC)(\mu-CH_2)(dppm)_2][CF_3SO_3]^{1f,g}$ with a structure analogous to **3**, as shown in Scheme 2.2.

The reaction of compound **2** with SO_2 appears to be somewhat analogous to the reactions with CO, phosphines and ^tBuNC, producing a methylene-bridged, hydrido complex $[Ir_2(H)(CO)_2(\mu-CH_2)(\mu-SO_2)(dppm)_2]$-$[CF_3SO_3]$ (**7**) as shown in Scheme 2.3. Like the CO adduct (**1**), compound **7** is fluxional, undergoing facile exchange of the hydride ligand and the methylene hydrogens, but is in contrast to compounds **3-6**, for which the exchange of hydrogens is not observed. The extremely facile exchange process in **7** caused some initial uncertainty about its formulation, since it was necessary to rule out a species, $[Ir_2(CO)_2(\mu-\eta^1,\eta^2-CH_3)(\mu-SO_2)(dppm)_2][CF_3SO_3]$, containing an asymmetrically bridging methyl group, in which the carbon was σ-bound to one metal with one of the C-H bonds involved in an agostic interaction with the adjacent metal. In this case, facile hydrogen exchange would occur by rotation about the $Ir-CH_3$ bond, interchanging the agostic interaction between the three C-H bonds. At ambient temperature the $^{31}P\{^1H\}$ NMR spectrum appears as a singlet at δ -1.0, consistent with the chemical equivalence of all four phosphorus nuclei. In the ^1H NMR spectrum the three hydrogens of the methyl group appear

Scheme 2.3
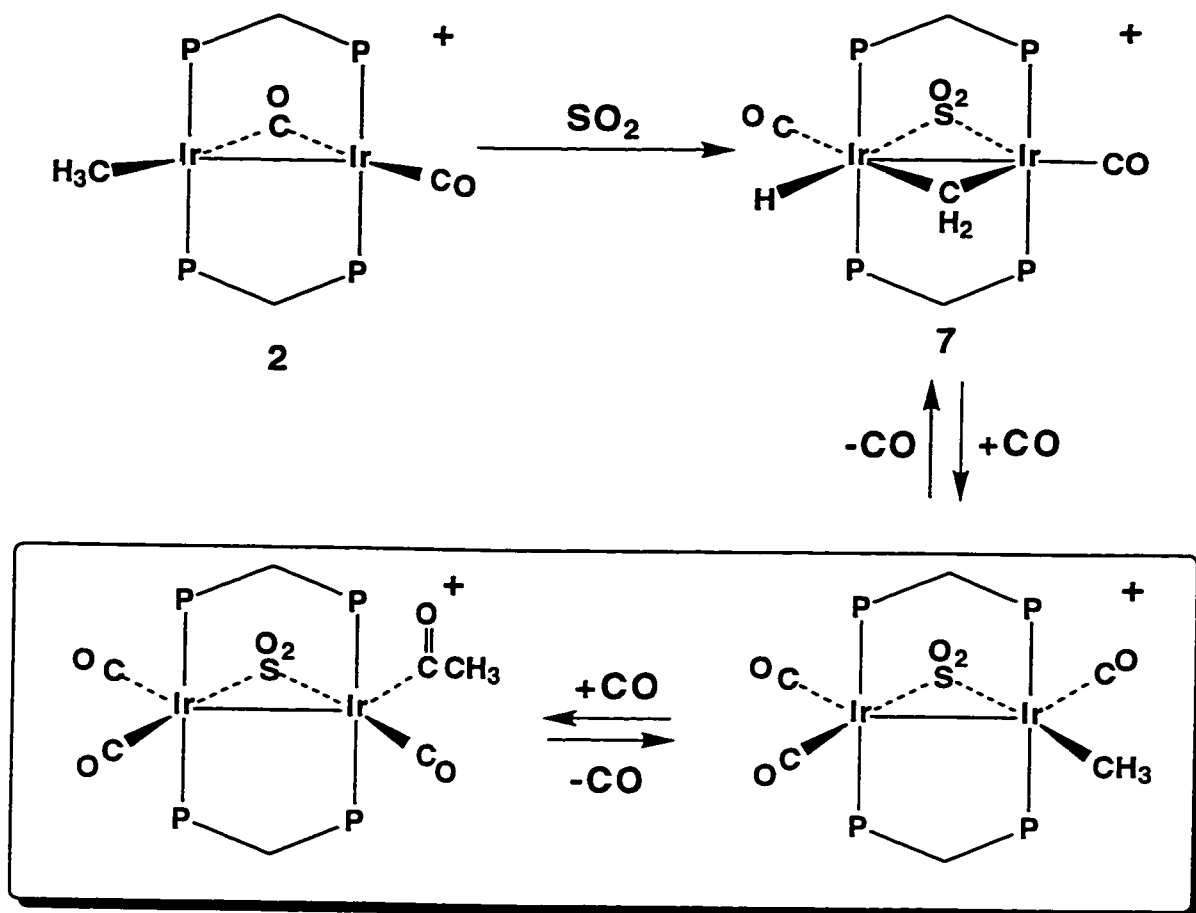
Species in box have been previously characterized.[1f,g]
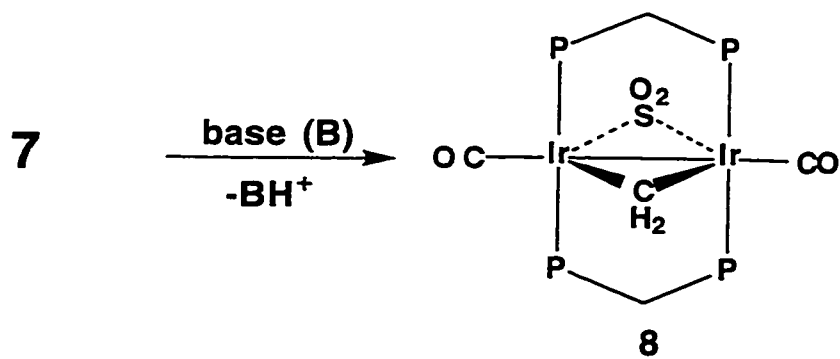
as a broad singlet at δ -2.15, with coupling of 98 Hz observed to carbon when $^{13}CH_3$ is used. At 50 °C this "CH_3 signal" appears as a well resolved quintet, coupling equivalently to all four phosphorus nuclei. The high-field shift of this resonance and the small average C-H coupling constant are consistent with a fluxional process involving either the methylene-hydride or the agostic methyl formulations, although the average value of $^1J_{C-H}$ is slightly lower than has previously been suggested for asymmetrically bridged methyl groups.[18] At ambient temperature the ^{13}C NMR spectra add additional support for the symmetric time-averaged structure with only one signal (at δ 170.8) for both carbonyls and a sharp quartet at δ 36.8 for the methyl carbon, showing equivalent coupling to the **three** hydrogens.

Lowering the temperature causes the methyl resonance in the ^1H NMR spectrum to broaden until at -60 °C the signal has fully collapsed into the baseline. At -110 °C a **very** broad methylene signal at *ca.* δ 4.2 and an equally broad hydride signal at *ca.* δ -14.6 start to appear, but are only barely discernible above baseline. Support for the exchange process was shown by irradiating the methylene region at -110 °C and observing that the hydride signal disappeared (although the barely discernible signal at this temperature makes such a conclusion equivocal). The activation parameters for this exchange process ($\Delta H^{\neq} = 6.11 \pm 0.33$ kcal/mol and $\Delta S^{\neq} = -6.24 \pm 1.50$ cal/mol K) were obtained from a line-shape analysis on variable-temperature ^1H NMR spectra (see Experimental Section). The activation energy for this exchange

process is very low, close to half the activation energy determined for a similar exchange process in compound **1** ($\Delta H^{\neq} = 10.3 \pm 0.4$ kcal/mol and $\Delta S^{\neq} = -11.2 \pm 1.5$ cal/mol K)[19] and substantially smaller than that calculated for a similar process in the compound $[Cp_2TaPt(H)(\mu\text{-}CH_2)_2(PMe_3)]$ ($\Delta H^{\neq} = 18.2 \pm 0.4$ kcal/mol and $\Delta S^{\neq} = -0.1 \pm 1.1$ cal/mol K).[19] Suprisingly, the values given for **7** (which yield $\Delta G^{\neq} = 7.6$ kcal/mol at T = -40°C) are even smaller than the activation energy ($\Delta G^{\neq} = 9.8$ kcal/mol at T = -40°C) observed for exchange of the methyl hydrogens in a bridging agostic methyl interaction in $[Cp_2TiRh(COD)\text{-}(\mu\text{-}CH_2)(\mu\text{-}CH_3)]$, by rotation about the metal-carbon bond.[20a]

Attempts to prepare compound **7** with d^3-methyl triflate resulted in partial hydrogen incorporation (presumably from solvent) such that the desired product was contaminated with small, but significant amounts of the CHD_2, CH_2D and CH_3 isotopomers.[21] This inadvertent result presented us with the opportunity to investigate the effects of isotopic perturbation of resonance (IPR) in compound **7**. Although first described by Saunders[22] in studies of carbocations, this effect was later used (first by Shapley[23] and subsequently by others[18,24]) to help establish the presence of agostic interactions involving methyl groups. Owing to the greater zero-point energy difference between a C-H and a C-D bond in a terminal rather than an agostic interaction, structures having terminal C-D bonds and agostic C-H interactions are thermodynamically favored over those having the opposite arrangement. This results in differences in ^1H chemical shift between CH_3, CH_2D and CHD_2 groups involved in agostic interactions.

Whereas the ^{1}H chemical shift of the agostic CH_3 group is given by $1/3(2\delta_t + \delta_b)$ (δ_t, δ_b = chemical shifts for terminal and bridging (agostic) hydrogens), owing to the equivalence of the three contributing structures, the inequivalence of structures **C** and **D** in the CH_2D analogue results in a greater population of **C** resulting in an upfield shift of the ^{1}H resonance. For similar reasons the ^{1}H resonance for the CHD_2 analogue is shifted to even higher field. Partial deuteration also results in a temperature dependence of the ^{1}H chemical
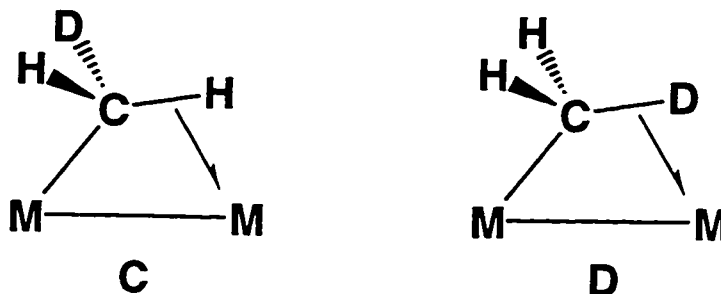
shift that is not observed in the non-deuterated analogue; this dependence is an order of magnitude larger than the secondary isotope shifts associated with methyl groups in organic compounds.[25] For compounds containing an agostic CH_3 group the three structures are degenerate, so lowering the temperature does not change the population of each structure, and the ^{1}H chemical shift is essentially temperature independent. However, for the CH_2D and CHD_2 groups, lower temperatures will result in higher population of the more stable state, resulting in upfield shifts with decreasing temperature.

The ^{1}H NMR spectrum in the methyl region for compound **7**, which was prepared from d^3-methyl triflate is shown in Figure 2.4, and the temperature

variation of the chemical shifts is presented in Table 2.6. These results clearly demonstrate the IPR phenomenon, consistent with hydrogen exchange between structures such as **C** and **D**. However, it has been pointed out that this effect will also be demonstrated by a system in which facile exchange occurs between a hydrido ligand and methylene hydrogens.[18,24a] In such a system the structures analogous to those of **C** and **D** are shown in **E** and **F**, respectively.

```
         HD                              H2
          C              H                C              D
         / \            /                / \            /
        /   \          /                /   \          /
   M————————M                      M————————M
          E                                F
```
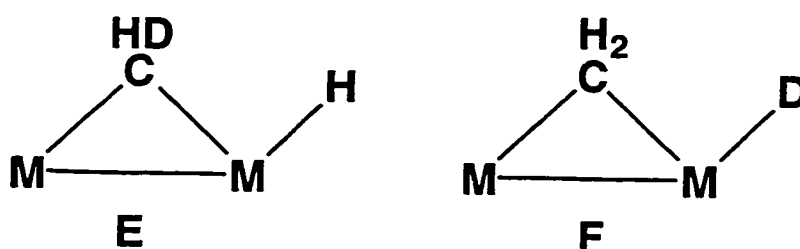
Again, zero-point energy considerations dictate that **E** is more stable than **F**, so in the monodeuterated species structure **E** is more probable, resulting in an upfield shift of the weighted average ^1H resonance, exactly as was the case for the agostic methyl interaction.

From the IPR data, the chemical shifts for the two different hydrogen environments can be calculated.[26] In the agostic methyl case these correspond to δ_t and δ_b, defined earlier, whereas in the methylene-hydride structure these correspond to the methylene and hydride resonances. It is encouraging that the calculated chemical shifts, δ 4.13 and -14.47, are in very close agreement with the positions of the very broad resonances that are beginning to appear in the ^1H NMR spectrum at -110 °C. Furthermore, the chemical shift of the lowfield signal is more consistent with a methylene group than a methyl group. This
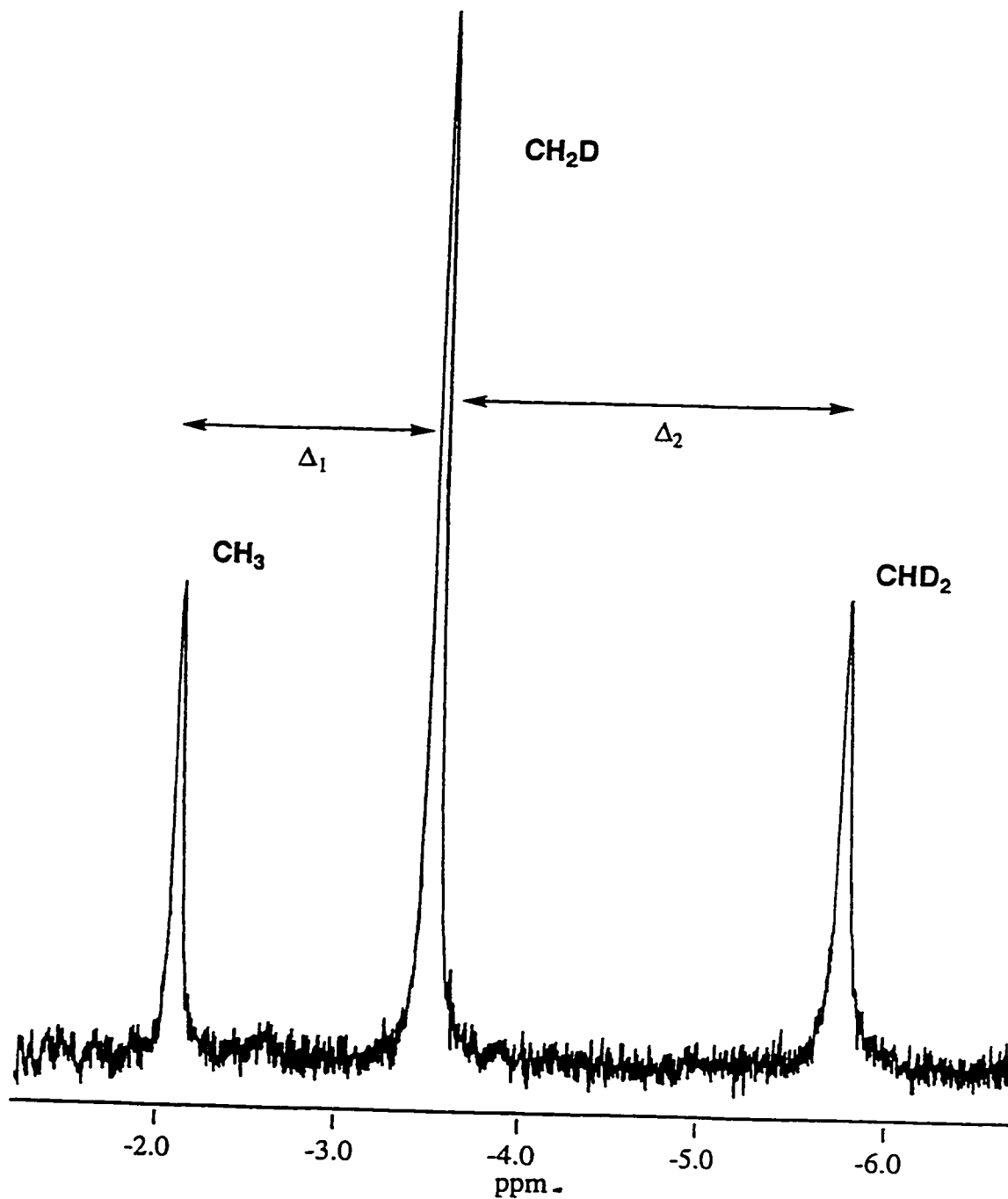
Figure 2.4 ^{1}H NMR spectrum of compound **7** in the methyl region, showing chemical shift differences for deuterium labelling in the methyl position.

Table 2.6 Temperature Variation of Methyl Signal for Deuterium Labelled Compound **7**.

Temp (°C)	$\delta(CH_3)$	$\delta(CH_2D)$	$\delta(CHD_2)$	Δ_1[a]	Δ_2[a]
25	-2.07	-3.48	-5.72	1.41	2.24
10	-2.05	-3.52	-5.90	1.47	2.38
0	-2.05	-3.56	-6.02	1.51	2.46
-20	-2.02	-3.62	-6.40	1.60	2.78

[a] See Figure 2.4 for the definitions of Δ_1 and Δ_2.

conclusion is supported by the low average value of $^1J_{C-H}$ (98 Hz), which would then result from averaging of the two one-bond coupling constants of $^1J_{C-H} \approx 147$ Hz with a three-bond coupling (between the methylene carbon and the hydride ligand) of $^3J_{C-H} \approx 0$ Hz. Our ability to observe what appears to be the two different hydrogen resonances (albeit at very low temperature) also argues against an agostic methyl species since we know of only two cases in which the two resonances have been observed in such a bimetallic species;[20] in all other cases the very low barrier to rotation about the M-CH$_3$ bond were too low to enable the low-temperature limiting spectrum to be obtained.

In hopes of establishing conclusively (at least in the solid state) whether compound **7** contained an agostic methyl group or methylene and hydride groups, the X-ray structure determination of **7** was undertaken. Unfortunately, here also the conclusions are equivocal. Our only successful attempts to obtain suitable crystals were from CH_2Cl_2 solvent, from which the desired crystals were always found to be contaminated by varying amounts of $[Ir_2(CO)_2(\mu\text{-Cl})\text{-}(\mu\text{-SO}_2)(dppm)_2][CF_3SO_3]$, which has resulted from replacement of the methyl group by a chlorine atom (crystals of compound **7** and this chloro-bridged species are isomorphous). When crystallization attempts were carried out under conditions designed to minimize radical formation, which presumably results in transformation of **7** into the chloro species, (eg. in the dark, with radical scavengers or from 1,2-dichloroethane or non-chlorinated solvents) crystals were not obtained. It is our assertion that the successful crystallization of **7** is initiated by seeding due to the chloro species which apparently

crystallizes better. In the crystal on which data were collected the ratios of **7** to the chloro species was 87.5 : 12.5, as determined by NMR studies on the bulk sample and on refinement of the occupancy factors of the disordered atoms in the X-ray study. This sample had the most favorable ratio of the several recrystallizations attempted. The placement of the fractional occupancy chloro ligand on top of the CH_3 or CH_2 group prevents location of the attached hydrogens, however the metrical parameters of the complex (*vide infra*) are consistent with the methylene-hydride formulation suggested by the NMR study.

An ORTEP diagram for compound **7** is shown in Figure 2.5 with important bond lengths and angles given in Table 2.7. Compound **7** has the SO_2 group in a bridging arrangement with the carbonyl ligands bound terminally, one on each metal. Although the hydrogen atoms originating on the methyl group of the precursor (**2**) could not be located, C(3) is assumed to be associated with a methylene group which bridges the metals on the face opposite the SO_2 group; the hydride ligand has been idealized in the position shown. Excluding the metal-metal bond the geometry around the metals is best described as octahedral at Ir(1) and trigonal bipyramidal at Ir(2), with both diphosphine groups in the expected trans arrangements (P(1)-Ir(1)-P(3) = 170.6(1)° and P(2)-Ir(2)-P(4) = 161.9(1)°). The SO_2 group bridges in an asymmetric manner with the Ir(1)-S bond length (2.447(3)Å) longer than the Ir(2)-S bond length (2.273(3)Å); this difference is consistent with the high trans influence of the hydride ligand which is opposite S(1) on Ir(1).

Although the crystallographic data do not unambiguously differentiate
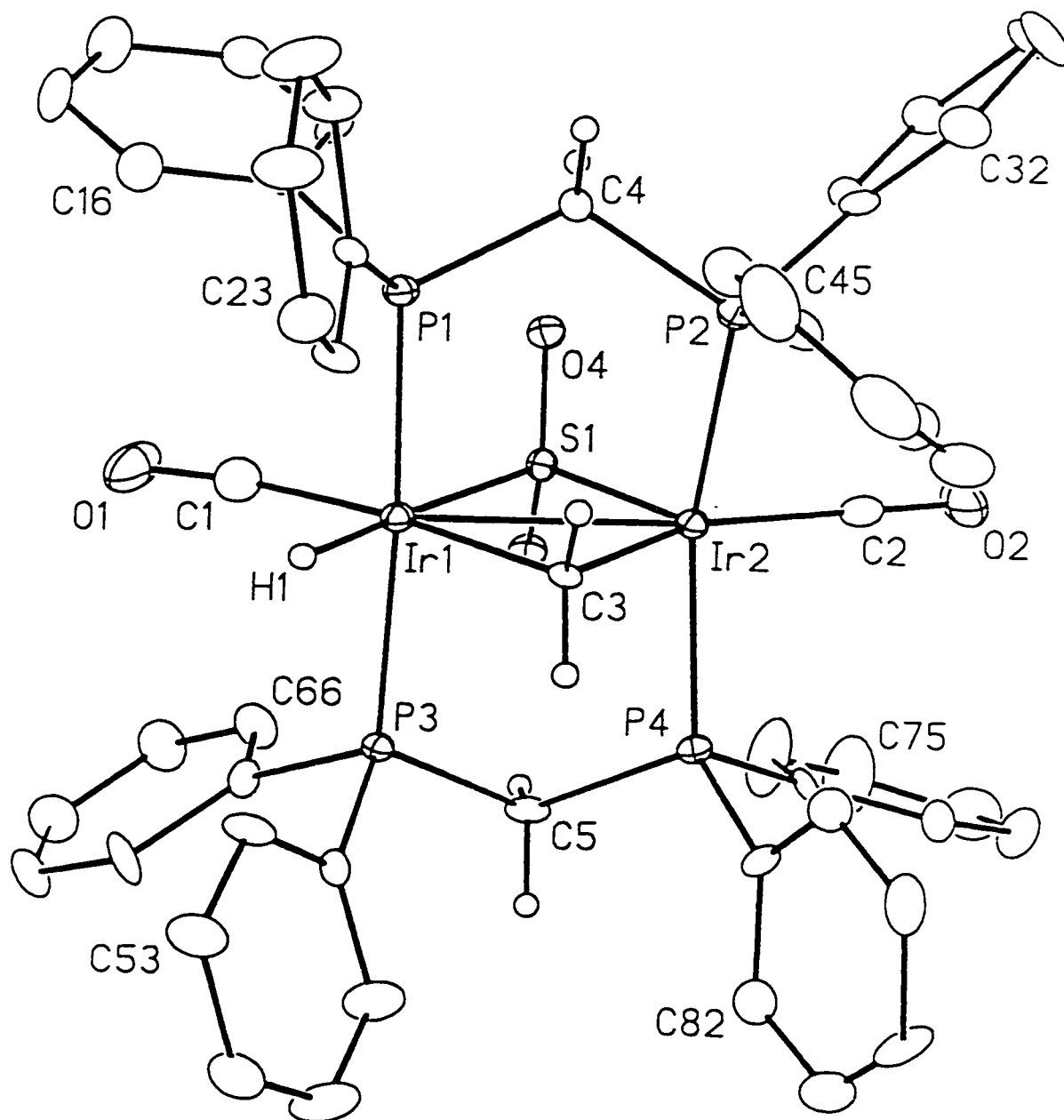
Figure 2.5 Perspective view of the [Ir₂(H)(CO)₂(μ-CH₂)(μ-SO₂)(dppm)₂]⁺ cation of compound **7**. Thermal ellipsoids are shown at the 20% probability level except for hydrogens which are shown arbitrarily small. Phenyl hydrogens have been omitted. H(1) has been placed in idealized position, 1.70 Å from Ir(1).

Table 2.7 Selected Interatomic Distances and Angles for Compound 7.

(a) Distances (Å)

Atom1	Atom2	Distance	Atom1	Atom2	Distance
Ir(1)	Ir(2)	2.8534(7)	Ir(2)	C(2)	1.85(2)
Ir(1)	Cl(1)	2.66(2)	Ir(2)	C(3)	2.123(14)
Ir(1)	S(1)	2.449(3)	S(1)	O(3)	1.459(8)
Ir(1)	C(1)	1.88(2)	S(1)	O(4)	1.450(8)
Ir(1)	C(1')	1.85^a	O(1)	C(1)	1.16(2)
Ir(1)	C(3)	2.190(12)	O(1')	C(1')	1.15^a
Ir(2)	Cl(1)	2.68(2)	O(2)	C(2)	1.14(2)
Ir(2)	S(1)	2.273(3)	Ir(2)	P(2)	2.337(3)
Ir(1)	P(1)	2.353(3)	Ir(2)	P(4)	2.330(3)
Ir(1)	P(3)	2.364(3)	Ir(1)	H(1)	1.70 ^{a}

^{a}distance fixed (within 0.01 Å of this value) during refinement

(b) Angles (deg)

Atom1	Atom2	Atom3	Angle	Atom1	Atom2	Atom3	Angle
Ir(2)	Ir(1)	S(1)	50.06(7)	Ir(1)	Ir(2)	C(3)	49.6(3)
Ir(2)	Ir(1)	C(1)	141.6(5)	Cl(1)	Ir(2)	C(2)	141.3(7)
Ir(2)	Ir(1)	C(1')	170.3(32)	S(1)	Ir(2)	C(2)	105.6(5)
Ir(2)	Ir(1)	C(3)	47.6(4)	S(1)	Ir(2)	C(3)	105.3(3)
Cl(1)	Ir(1)	C(1')	130.7(32)	P(2)	Ir(2)	P(4)	161.90(11)
S(1)	Ir(1)	C(1)	91.6(5)	C(2)	Ir(2)	C(3)	149.1(6)
S(1)	Ir(1)	C(1')	120.9(33)	Ir(1)	Cl(1)	Ir(2)	64.6(5)
S(1)	Ir(1)	C(3)	97.6(4)	Ir(1)	S(1)	Ir(2)	74.24(8)
P(1)	Ir(1)	P(3)	170.60(10)	Ir(1)	C(1)	O(1)	172.3(17)
C(1)	Ir(1)	C(3)	170.7(6)	Ir(1)	C(1')	O(1')	175.7(77)
Ir(1)	Ir(2)	Cl(1)	57.4(5)	Ir(2)	C(2)	O(2)	177.4(16)
Ir(1)	Ir(2)	S(1)	55.70(8)	Ir(1)	C(3)	Ir(2)	82.8(5)
Ir(1)	Ir(2)	C(2)	161.3(5)				

between an asymmetrically bridged methyl group and a methylene-bridged hydride structure, the structural parameters are more supportive of the latter assignment. It is clear that carbonyl group C(1)O(1) is bent back towards the μ-SO$_2$ group compared to C(2)O(2) (compare: Ir(2)-Ir(1)-C(1) = 141.6(5)°, Ir(1)-Ir(2)-C(2) = 161.3(5)°), leaving a vacant coordination site on Ir(1) for the hydride ligand. This bending back of C(1)O(1) gives rise to a larger C(1)-Ir(1)-C(3) angle (170.7(6)°) compared to the C(2)-Ir(2)-C(3) angle of 149.1(6)°, suggesting the location of the hydride ligand as shown in Figure 2.5. All spectroscopic and crystallographic data together support the methylene-bridged, hydride structure for compound 7.

Reaction of compound 7 with CO parallels that of the methyl species (2), yielding the previously characterized SO$_2$-bridged tricarbonyl methyl species, [Ir$_2$(CH$_3$)(CO)$_3$(μ-SO$_2$)(dppm)$_2$][CF$_3$SO$_3$],[19] in which the methyl group is now terminally bound to one of the metals. Although the relative positions of the methyl and μ-SO$_2$ groups are not known, the geometry shown in Scheme 2.3 is based on the assumption that hydride transfer from Ir to the methylene group, yielding a methyl group σ-bound to the adjacent metal, would leave coordinative unsaturation at the first metal, which would be alleviated by CO coordination. This SO$_2$-bridged, tricarbonyl methyl compound reacts further with CO to produce the acyl compound [Ir$_2$(CH$_3$CO)(CO)$_3$(μ-SO$_2$)(dppm)$_2$]-[CF$_3$SO$_3$].[19] Again the geometry shown for the acyl species is not known but is

based on the migration of the methyl group to the adjacent carbonyl on the same metal.

Reaction of compound **7** with a strong nitrogen base such as 2,2,6,6-tetramethylpiperidine or DBU (1,8-diazabicyclo[5.4.0]undec-7-ene) resulted in deprotonation to give the methylene-bridged product $[Ir_2(CO)_2(\mu\text{-}CH_2)(\mu\text{-}SO_2)(dppm)_2]$ (**8**) as shown in Scheme 2.3. The $^{31}P\{^1H\}$ NMR spectrum shows a singlet at $\delta\,2.7$ indicating the equivalence of the phosphorus nuclei, and the ^1H NMR spectrum shows the dppm methylenes as multiplets at δ 3.78 and 3.50 with the Ir_2-bridging methylene as a quintet at δ 2.93. The IR spectrum shows two CO bands at 2013 cm^{-1} and 1951 cm^{-1} indicating that both CO's are terminal. The facile deprotonation of **7** to give **8** offers further support for the hydride formulation, since we would not expect facile deprotonation of an agostic methyl group. For reasons that we do not understand, attempts to deprotonate compound **1** along the same lines as deprotonating compound **7** have so far been unsuccessful.

Discussion

A comparison of the reaction of the electrophile, CH_3^+, with the homo- and heterobimetallic complexes $[Rh_2(CO)_3(dppm)_2]$, $[RhIr(CO)_3(dppm)_2]$ and $[Ir_2(CO)_3(dppm)_2]$ shows three different products. With the dirhodium analogue CH_3^+ addition resulted in an acyl species $[Rh_2(\mu\text{-}COCH_3)(CO)_2(dppm)_2][CF_3SO_3]$,[7] while the mixed RhIr system yielded $[RhIr(CH_3)(CO)_3(dppm)_2]$-

$[CF_3SO_3]$, in which the methyl group is terminally bound to iridium.[1f,g] With the diiridium species, described in this chapter, electrophilic attack by CH_3^+ resulted in addition to the metals and subsequent C-H activation yielding the methylene hydride $[Ir_2(H)(CO)_3(\mu\text{-}CH_2)(dppm)_2][CF_3SO_3]$ (**1**).[1f,g] The dirhodium system illustrates the greater tendency of Rh alkyls to undergo migratory insertion compared to Ir alkyls, while in the mixed RhIr analogue, terminal coordination to Ir is observed, reflecting the greater strength of the Ir-C bond compared the Rh-C bond. For the Ir_2 system, the added methyl group undergoes facile and reversible C-H bond cleavage. The facile C-H activation of this species compared to the Rh_2 compound is as expected for the greater basicity of Ir, and again may be a result of stronger metal-H and metal-C bonds of Ir compared to Rh.

Removing a carbonyl from the methylene hydride compound (**1**), reverses the C-H bond cleavage step, yielding $[Ir_2(CH_3)(CO)(\mu\text{-}CO)(dppm)_2]$-$[CF_3SO_3]$ (**2**), having an intact methyl group, terminally bound to one metal. The fluxionality displayed by compound **2**, in which there is facile methyl migration between the metal centers, presumably occurs via a methyl-bridged intermediate, not unlike the type of species originally targetted in the methyl triflate addition.

The X-ray structure determined for compound **2**, is analogous to that of the previously characterized $[Rh_2(CH_3)(CO)_2(dppm)_2][CF_3SO_3]$[7] with the only major difference arising from the different M-M separations. In both structures the methyl group is terminally bound to one metal. In contrast, the closely

related compound $[Ir_2(CO)_2(\mu\text{-}CH_3)(dmpm)_2][CF_3SO_3]$ (dmpm = bis(dimethyl-phosphino)methane),[9] has the methyl group symmetrically bridging the two iridium centers. The solution structure of **2** and the calculated structure by DeKock[12] (i.e. **2a**) suggests that the differences observed in the solid state do not reflect electronic stabilization of the different geometries by the different phosphines, but more likely result from subtle non-bonded contacts in the solid.

The reaction of compound **2** with small molecules (CO, SO_2, ^tBuNC, PR_3) has in each case resulted in C-H activation of the methyl group producing the corresponding methylene-hydride products. The SO_2 adduct differs slightly from the other adducts in having this ligand *opposite* the methylene group rather than in a cis position. We suggest that these differences can be explained on the basis of the favored sites of substrate attack. It should be recalled that in solution, **2** is highly fluxional, so establishing the geometry of the reactive species, and therefore the site of attack seems highly unlikely. However, previous studies[27] in which SO_2 apparently had a different site of attack from other ligands in A-frame species suggests one possibility. The fluxionality of **2** suggests the involvement of a methyl-bridged species in transferring the methyl ligand from metal to metal. One possible geometry for such an intermediate is an A-frame intermediate like that shown in Scheme 2.4, having an agostic methyl interaction. DFT calculations by DeKock have shown that this structure is only about 5 kcal/mole higher in energy than that of **2a**.[12] Previous studies on A-frame complexes have shown that SO_2 attack occurs in the A-frame pocket, between the metals, whereas attack by other ligands

Scheme 2.4
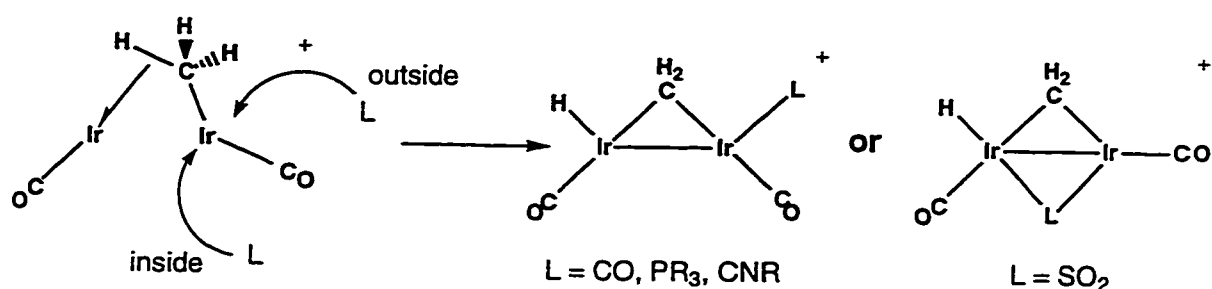
occurs on the outside of the complex as shown above (dppm ligands above and below the plane of the drawing are omitted).[27] Such a proposal offers a rationalization for the different structure types obtained with SO_2 and other ligands. This does not, however, offer a rationalization for why ligand attack at one metal should promote C-H bond cleavage at the *adjacent* metal. With outside attack an electronic influence must be transmitted via the metal-metal framework since the added ligand is not in a position to interact directly with the adjacent metal. Attack in this instance would give rise to an 18e center which can form a dative Ir-Ir bond that supplies the additional electron density at the adjacent metal, leading to C-H bond cleavage (as outlined below). SO_2 attack
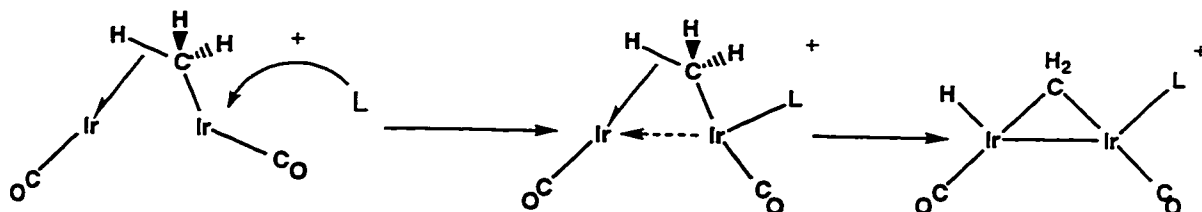
from within the pocket, would yield a species as diagrammed below in **G**; the

G
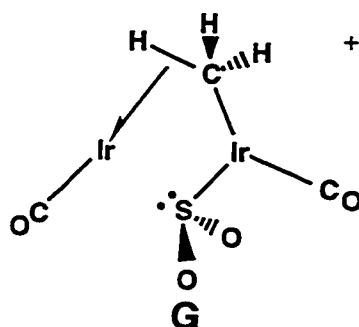
metal on the right would have a geometry that is reminiscent of that on the SO_2

adduct of Vaska's compound.[28] Presumably movement of the SO_2 towards the

adjacent metal results in donation of the lone pair, increasing the electron

density, favoring the C-H activated product. In support of this proposal, such an

intermediate has been identified in the DFT calculations by DeKock[12] as that

which preceeds C-H activation.

It may also be that compound **2** (structure **2a** in solution) is in equilibrium

with undetectable amounts of the reactive methylene hydride species (**H**), as

shown below, which again reacts in either of the two sites shown to yield the

2a   **H**
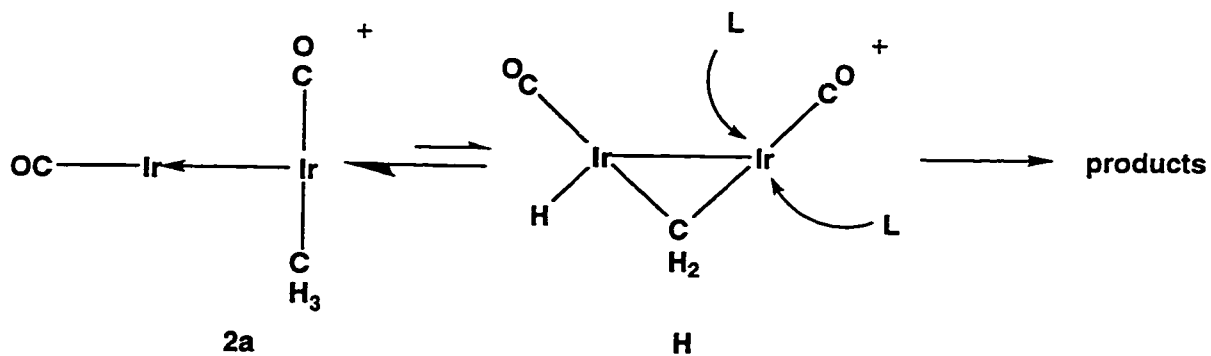
observed products.

The activation energy ($\Delta H^{\neq}$ = 6.11 kcal/mole) for the exchange of the methylene hydrogens and hydride ligand of compound **7** was determined and was shown to be comparable to simple M-CH$_3$ rotation in an agostic methyl complex. The small value for this exchange indicates that the difference between the ground state configuration (methylene-hydride) and transition state (assumed to be an agostic bridging methyl species) is very small. Fehlner recently wrote,[29] "...reaction paths depend on small energy differences that can induce large changes in rates. The sequence of reactions occurring on a catalyst is driven by small perturbations between states of nearly equal energy....if one wants to model catalytic reactivity with cluster chemistry, small barrier processes must be understood." Recent work on platinum surface bound alkyls has shown the activation energies for interconversion between methyl and methylene species to be on the order of 6 to 8 kcal/mol.[30] The small barrier for the exchange process observed in the SO$_2$-bridged methylene-hydride offers further support that these simple binuclear complexes can function as useful models for surfaces, and that metal-metal cooperativity effects can be of comparable magnitude in the two systems.

Conclusions

Ligand attack on the fluxional methyl complex [Ir$_2$(CH$_3$)(CO)(μ-CO)-(dppm)$_2$][CF$_3$SO$_3$] (**2**) results in facile and (with CO and SO$_2$) reversible C-H activation of the methyl group, producing the methylene-hydride products

$[Ir_2(H)(CO)_2(L)(\mu\text{-}CH_2)(dppm)_2][CF_3SO_3]$ (L = CO, PR_3, SO_2, ^tBuNC). Such reactivity for the addition of strong π-acid ligands is unprecedented, and shows another important way in which adjacent metals may be important in the cooperative activation of bound ligands. The facile and reversible conversion of a methyl group to methylene and hydride moieties is reminiscent of processes occurring on metal-surfaces and suggests that **2** may function as a useful model for the reactivity of methyl groups on surfaces. In the work that follows, the reaction of **2** with unsaturated organic substrates will be investigated to further probe the involvement of the adjacent metals in methyl group activation and in subsequent C-C bond formation.

References

1. (a) Antwi-Nsiah, F.H.; Oke, O.; Cowie, M. *Organometallics* **1996**, *15*, 506.

   (b) Antwi-Nsiah, F.H.; Oke, O.; Cowie, M. *Organometallics* **1996**, *15*,

   1042. (c) Sterenberg, B. T.; Hilts, R. W.; Moro, G.; McDonald, R.; Cowie,

   M. *J. Am. Chem. Soc.* **1995**, *117*, 245. (d) Wang, L.-S., Cowie, M. *Can.*

   J. Chem. **1995**, *73*, 1058. (e) Wang, L-S.; Cowie, M. *Organometallics*

   1995, *14*, 2374. (f) Antwi-Nsiah, F.; Cowie, M. *Organometallics* **1992**,

   11, 3157. (g) Antwi-Nsiah, F. Ph.D. Thesis, University of Alberta,

   Edmonton, Alberta, 1994. (h) Antonelli, D. M.; Cowie, M. *Organometallics*

   1991, *10*, 2550. (i) Graham, T.; Van Gastel, F.; Cowie, M., manuscript in

   preparation.

2. (a) Walker, N.; Stuart, D. *Acta Crystallogr.* **1983**, *A39*, 158–166. (b)

   Sheldrick, G. M. *Acta Crystallogr.* **1990**, *A46*, 467–473. (c) Sheldrick, G.

   M. *SHELXL-93*. Program for crystal structure determination. University

   of Göttingen, Germany, 1993.

3. Torkelson, J. R.; Cowie, M. unpublished results.

4. Sutherland, B. R.; Cowie, M. *Organometallics* **1985**, *4*, 1637.

5. (a) Kubiak, C.P.; Woodcock, C.; Eisenberg, R. *Inorg. Chem.* **1982**, *21*,

   2119. (b) Kubiak, C. P.; Eisenberg, R. *J. Am. Chem. Soc.* **1980**, *102*,

   3637.

6. McDonald, R.; Cowie, M. *Inorg. Chem.* **1990**, *29*, 1564.

7. Shafiq, F.; Kramarz, K. W.; Eisenberg, R. *Inorg. Chim. Acta.* **1993**, *213*,

   111.

8. Heinekey, D. M.; Michel, S. T.; Schulte, G. K. *Organometallics* **1989**, *8*, 1241.

9. Reinking, M. K.; Fanwick, P.E.; Kubiak, C.P. *Angew. Chem. Int. Ed. Engl.* **1989**, *28*, 1377.

10. Haines, R. J.; Meintjies, E.; Laing, M. *Inorg. Chim. Acta* **1979**, *36*, L403.

11. (a) Brown, M. P.; Cooper, S. J.; Frew, A. A.; Manojlovic-Muir, L.; Muir, K. W.; Puddephatt, R. J.; Seddon, K. R.; Thomson, M. A. *Inorg. Chem.* **1981**, *20*, 1500. (b) Hill, R. H.; Puddephatt, R. J. *J. Am. Chem. Soc.* **1983**, *105*, 5797. (c) Xu, C.; Anderson, G. K. *Organometallics* **1996**, *15*, 1760.

12. (a) DeKock, R. personal communication. (b) All DFT calculations had the diphosphine ligand $H_2PCH_2PH_2$ in place of either dppm or dmpm.

13. (a) Cowie, M. Dwight, S. K. *Inorg. Chem.* **1980**, *19*, 2508. (b) Gelmini, L.; Stephan, D. W.; Loeb, S. J. *Inorg. Chim. Acta* **1985**, *98*, L3.

14. (a) Janowicz, A. H.; Bergman, R. G. *J. Am. Chem. Soc.* **1982**, *104*, 352. (b) Hoyano, J. K.; Graham, W. A. G. *J. Am. Chem. Soc.* **1982**, *104*, 3723. (c) Jones, W. D.; Feher, F. J. *J. Am. Chem. Soc.* **1982**, *104*, 4240. (d) Collman, J.P.; Hegedus, L.S.; Norton, J.R.; Finke, R.G. *Principles and Applications of Organotransition Metal Chemistry*; University Science Books: Mill Valley, California, 1987, p 298-304. (e) See all articles in *J. Organomet. Chem.* **1995**, *504*, 1-155.

15. Kuhlman, R.; Folting, K.; Caulton, K. G. *Organometallics* **1995**, *14*, 3188.

16. a) Brown, M. P; Fisher, J. R.; Hill, R. H.; Puddephatt, R. J.; Seddon, K. R. *Inorg. Chem.* **1981**, *20*, 3516. b) Wang, L-S; Cowie, M. *Organometallics* **1995**, *14*, 3040.

17. Herrmann, W. A. *Adv. Organomet. Chem.* **1982**, *20*, 159.

18. (a) Brookhart, M.; Green, M. L. H.; Wong, L-L. *Prog. Inorg. Chem.* **1988**, *36*, 1. (b) Tolman, C. A.; Faller, J. W. in *Homogeneous Catalysis with Metal Phosphine Complexes*; Pignolet, L. H., Ed.; Plenum Press: New York and London, 1983. p 30-34.

19. Jacobsen, E. N.; Goldberg, K. I.; Bergman, R. G. *J. Am. Chem. Soc.* **1988**, *110*, 3706.

20. (a) Park, J. W.; Mackenzie, P. B.; Schaefer, W. P.; Grubbs, R. H. *J. Am.Chem. Soc.* **1986**, *108*, 6402. (b) Ozawa, F.; Park, J. W.; Mackenzie, P. B.; Schaefer, W. P.; Henling, L. M.; Grubbs, R. H. *J. Am. Chem. Soc.* **1989**, *111*, 1319.

21. [Ir$_2$(CD$_3$)(CO)(μ-CO)(dppm)$_2$][CF$_3$SO$_3$] could not be prepared without losing all of the deuterium label, presumably in exchange with H$_2$O, and therefore deutero compound **7** was prepared by reacting D$_3$-compound **1** with SO$_2$ and then decarbonylating.

22. Saunders, M.; Jaffe, M. H.; Vogel, P. *J. Am. Chem. Soc.* **1971**, *93*, 2558.

23. Calvert, R. B.; Shapley, J. R. *J. Am. Chem. Soc.* **1978**, *100*, 7726.

24. (a) Crabtree, R. H.; Hamilton, D. G. *Adv. Organomet Chem.* **1988**, *28*, 299 and references therein. (b) Green, M. L. H.; Hughes, A. K.; Popham, N. A.; Stephans, A. H. H.; Wong, L. L. *J. Chem. Soc., Dalton Trans.* **1992**,

3077. (c) Dutta, T. K.; Vites, J. C.; Jacobsen, G. B.; Fehlner, T. P. *Organometallics* **1987**, *6*, 842. (d) Hursthouse, M. B.; Jones, R. A.; Abdul-Malik, K. M.; Wilkinson, G. *J. Am. Chem. Soc.* **1979**, *101*, 4128. (e) Dawkins, G. M.; Green, M.; Orpen, A. G.; Stone, F. G. A. *J. Chem. Soc., Chem. Commun.* **1982**, 41. (f) Casey, C. P.; Fagan, P. J.; Miles, W. H. *J. Am. Chem. Soc.* **1982**, *104*, 1134.

25. Harrison, P. E. *Annu. Rep. NMR Spectrosc.* **1983**, *15*, 105.

26. $\delta_t = 4.13$ ppm, $\delta_b = -14.47$ ppm. See ref. 18a and 23 for calculations.

27. (a) Cowie, M. *Inorg. Chem.* **1979**, *18*, 286. (b) Cowie, M.; Dwight, S. K. *Inorg. Chem.* **1979**, *18*, 2700. (c) George, D. S. A.; McDonald, R.; Cowie, M. Submitted to Organometallics.

28. Muir, K. W.; Ibers, J. A. *Inorg. Chem.* **1969**, *8*, 1921.

29. Dutta, T. K.; Vites, J. C.; Jacobsen, G. B.; Fehlner, T. P. *Organometallics* **1987**, *6*, 842.

30. Zaera, F. *Acc. Chem. Res.* **1992**, *25*, 260.

Chapter 3

C-H Activation and C-C Bond Formation

in the Reactions of

$[Ir_2(CH_3)(CO)(\mu\text{-}CO)(dppm)_2][CF_3SO_3]$ with Alkynes.

Introduction

Alkynes are extremely versatile ligands on transition metals.[1] Not only can alkynes display simple changes in coordination modes and electron donation in mono- and polymetallic complexes,[1,2] but they also display interesting chemical transformations into acetylides[3] and vinylidenes[4] as well as the many examples of migratory insertions[5-7] and condensation reactions.[8] With the wealth of chemical transformations displayed by alkyne transition metal complexes our group has an ongoing interest in alkyne reactivity with binuclear species.[9]

In Chapter 2, it was shown that the binuclear methyl complex, $[Ir_2(CH_3)\text{-}(CO)(\mu\text{-}CO)(dppm)_2][CF_3SO_3]$ (2), undergoes C-H bond cleavage of the methyl group upon reaction with a number of small molecules (eg. CO, SO_2, CNR, PR_3). Our interests in using complexes such as 2 as models for adjacent metal involvement in heterogeneously catalyzed processes such as Fischer-Tropsch chemistry, suggested that the reaction of 2 with unsaturated organic substrates could yield valuable information about C-C bond formation in multimetal

systems. Two obvious substrate types to be investigated were alkynes and olefins. In this chapter the reactivity of **2** with a variety of alkynes (electrophilic or activated alkynes, non-activated 1-alkynes and internal, non-activated alkynes) will be described.

Experimental Section

General Comments. Acetylene was obtained from Matheson, ^{13}C-labelled acetylene was purchased from Cambridge Isotopes and ^{13}CO (99%) was supplied by Isotec Inc. Propyne and hexafluoro-2-butyne (HFB) were purchased from Farchan Laboratories Ltd.; all other alkynes, and trimethylphosphine were purchased from Aldrich. Two-dimensional NMR experiments were performed on a Varian Unity 500 MHz spectrometer. All ^{13}C{^{1}H} NMR spectra were obtained using ^{13}CO-, ^{13}C-acetylene or ^{13}CH$_3$- enriched samples (the latter obtained from ^{13}C-methyl triflate) unless otherwise stated. The ^{31}P{^{1}H} and ^{1}H NMR, and IR spectroscopic data for all compounds are given in Table 3.1, while selected ^{13}C{^{1}H} and ^{19}F NMR data are given, where appropriate, with the details on the preparation of the compounds.

Preparation of Compounds.

(a) **[Ir$_2$(CH$_3$)(CO)$_2$(μ-DMAD)(dppm)$_2$][CF$_3$SO$_3$] (9).** The compound [Ir$_2$(CH$_3$)(CO)(μ-CO)(dppm)$_2$][CF$_3$SO$_3$] (**2**) (40mg, 0.029 mmol) was dissolved in 5 mL of CH$_2$Cl$_2$, and DMAD (3.65 μL, 0.029 mmol) was added by syringe. The

Table 3.1 Spectroscopic Data for the Compounds

Compound	IR cm⁻¹ [a,b]	δ ¹H [e]	δ ³¹P{¹H} [e,f,i]
[Ir₂(CH₃)(CO)₂(μ-DMAD)(dppm)₂][CF₃SO₃] (9)	2009 s 1980 m 1702 m, b[c] 1682 m, b[c]	4.28 (m, 2H), 3.37 (m, 2H), 2.91 (s, 3H), 2.27 (s, 3H), 0.65 (t, 3H)	7.7 (m), -9.3 (m)
[Ir₂(CH₃)(CO)₃(μ-DMAD)(dppm)₂][CF₃SO₃] (10)	2041 s, 1995 vs 1967 s 1709 s[c] 1682 m[c]	4.87 (m, 2H), 4.08 (m, 2H), 3.55 (s, 3H), 2.22 (s, 3H), -0.39 (t, 3H)	-11.2 (m), -28.9 (m)
[Ir₂(CH₃)(CO)₂(PMe₃)(μ-DMAD)(dppm)₂][CF₃SO₃] (11)	1986 vs 1967 vs 1695 vs[c]	5.03 (bm, 2H), 4.55 (bm, 2H), 3.56 (bs,3H), 1.87 (bs, 3H), 0.71 (bs, 3H), 0.40 (d, ²J_{H-P} = 9 Hz, 9H)	-22.6 (b, 2P), -24.3 (b, 2P), -89.3 (b, 1P)
[Ir₂(CH₃)(CO)₂(μ-HFB)(dppm)₂][CF₃SO₃] (12)	2018 vs 1992 vs 1547 w[d]	4.12 (m, 2H), 3.64 (m, 2H), 0.98 (tm, 3H)	5.9 (m), -15.5 (m)
[Ir₂(CH₃)(CO)₂(μ-HC≡CC(O)OMe)(dppm)₂][CF₃SO₃] (13)	2002 vs 1982 sh 1678 s[c]	9.9 (tt, ³J_{H-P} = 4.7 Hz, ⁴J_{H-P} = 2.5 Hz, 1H), 3.89 (m, 2H), 3.19 (m, 2H), 2.31 (s, 3H), 0.45 (t, 3H)	12.3 (m), -11.7 (m)
[Ir₂(H)(CH₃)(CO)₂(μ-C≡CMe)(dppm)₂][CF₃SO₃] (14)[k]	—	3.62 (m, 2H), 3.01 (m, 2H), 0.62 (s, 3H), 0.19 (t, 3H), -9.52 (t, 1H)	2.1 (m), -10.4 (m)
[Ir₂(CH₃)(CO)₂(μ-HC≡CMe)(dppm)₂][CF₃SO₃] (15)[l]	—	5.79 (m, 1H), 4.51 (m, 2H), 2.95 (m, 2H), 1.73 (t, 3H), 0.95 (b, 3H)	24.8 (m), -6.7 (m)
[Ir₂(CO)₂(μ-C≡CMe)(dppm)₂][CF₃SO₃] (16)	1971 s 1945 vs	4.28 (m, 2H), 3.99 (m, 2H), 1.02 (q, ⁴J_{H-P} = 1.5 Hz, 3H)	8.3 (s)

Table 3.1 cont.

Compound	IR cm$^{-1,a,b}$	δ ^{1}H^{e,i}	δ ^{31}P{^{1}H}^{e,i,l}
[Ir$_2$(H)(CH$_3$)(CO)$_2$(μ-C≡CPh)(dppm)$_2$][CF$_3$SO$_3$] (17)^k	—	6.71 (m, 3H), 6.12 (m, 2H), 3.73 (m, 2H), 2.94 (m, 2H), 0.26 (bt, 3H), -9.17 (t, 1H)	-0.9 (m), -12.4 (m)
[Ir$_2$(CH$_3$)(CO)$_2$(μ-HC≡CPh)(dppm)$_2$][CF$_3$SO$_3$] (18)^l	—	3.61 (m, 2H), 2.96 (m, 2H), 1.74 (t, 3H)	23.0 (m), -10.6 (m)
[Ir$_2$(CO)$_2$(μ-C≡CPh)(dppm)$_2$][CF$_3$SO$_3$] (19)	1970 sh 1953 vs, b	4.21 (m, 2H), 3.92 (m, 2H)	7.9 (s)
[Ir$_2$(H)(CH$_3$)(CO)$_2$(μ-C≡CH)(dppm)$_2$][CF$_3$SO$_3$] (20)^k	—	4.39 (m, 2H), 4.15 (s, 1H), 3.40 (m, 2H), 0.68 (t, 3H), -10.06 (t, 1H)	-16.1 (s)
[Ir$_2$(CH$_3$)(CO)$_2$(μ-C=CH$_2$)(dppm)$_2$][CF$_3$SO$_3$] (21)^m	—	6.26(s, $^1J_{C-H}$ = 160 Hz, 1H), 6.24(s, $^1J_{C-H}$ = 160 Hz, 1H), 4.42 (m, 2H), 2.99 (m, 2H), -0.20 (t, 3H)	13.3 (m), 3.7 (m)
[Ir$_2$(H)(CO)$_3$(μ-C=CHMe)(dppm)$_2$][CF$_3$SO$_3$] (22)	2045 s 1992 vs 1963 sh	6.50 (b, $^1J_{C-H}$ = 155 Hz, 1H), 4.08 (m, 2H), 3.59 (m, 2H), 0.84 (b, $^1J_{C-H}$ = 126 Hz, 3H), -10.62 (t, 1H)	-7.8 (m), -14.3 (m)
[Ir$_2$(CH$_3$)(C≡CH)(CO)$_2$(μ-H)(μ-C=CH$_2$)(dppm)$_2$]-[CF$_3$SO$_3$] (23)	2064 s 2000 vs 1574 m^n	6.23(s, $^1J_{C-H}$ = 156 Hz, 1H), 6.21(s, $^1J_{C-H}$ = 156 Hz, 1H), 4.12 (m, 2H), 3.10 (m, 2H), 1.87 (t, $^3J_{H-P}$ = 1.9 Hz, $^1J_{H-C}$ = 228 Hz, 1H), -0.35 (t, 3H), -14.01 (tt, $^2J_{H-P}$ = 10 Hz, 5 Hz, 1H)	-7.99 (m), -24.58 (m)
[Ir$_2$(CH$_3$)(CO)$_2$(μ-CH$_3$C≡CCH$_3$)(dppm)$_2$][CF$_3$SO$_3$] (24)	1982 b, vs 1959 b, vs	3.91 (m, 2H), 3.24 (m, 2H), 1.33 (b, 3H), 0.76 (b, 3H), 0.47 (t, 3H)	10.4 (m), -9.4 (m)
[Ir$_2$(H)(CO)$_2$(μ-η^1-η^3-HCC(Me)=CHMe)(dppm)$_2$]-[CF$_3$SO$_3$] (25)	1969 b, s	8.79 (m, 1H), 7.12 (m, 1H), 5.83 (m, 1H), 4.60 (m, 1H), 3.78 (m, 1H), 3.29 (m, 1H), 2.72 (d, 3H), 1.42 (bm, 3H), -11.25 (m, 1H)	-5.8 (m), -6.0 (m), -34.3 (m), -37.8 (m)

Table 3.1 cont.

Compound	IR cm⁻¹ a,b	δ ¹H e,i	δ ³¹P{¹H} e,i,j
[Ir₂(H)(CO)₂(μ-η¹-η³-HCC(Et)=CHEt)(dppm)₂]-[CF₃SO₃] (26)	1980 s, sh 1964 vs	8.83 (m, 1H), 5.83 (m, 1H), 4.52 (m, 1H), 3.68 (bm, 1H), 3.23 (m, 1H), 2.97 (m, 1H), 2.56 (m, 1H), 1.88 (b, 1H), 1.43 (t, 3H), 1.32 (b, 1H), 0.89 (t, 3H), -11.2 (m, 1H)	-5.4 (m), -7.7 (m), -35.1 (m), -38.4 (m)
[Ir₂(H)(CO)₂(μ-η¹-η³-HCC(Me)=CHEt)(dppm)₂]-[CF₃SO₃] (27a, 27b)	1971 b, s	8.80 (m, 1H), -11.2 (m, 1H)	-5.7 (m), -6.8 (m), -34.7 (m), -38.4 (m)
[Ir₂(H)(CO)₂(μ-η¹-η³-HCC(Me)=CHPh)(dppm)₂]-[CF₃SO₃] (28a)	1972 b, vs	8.91 (m, 1H), -11.10 (b)	-5.7 (m, 2P), -32.7 (m), -38.0 (m)
[Ir₂(H)(CO)₂(μ-η¹-η³-HCC(Ph)=CHMe)(dppm)₂]-[CF₃SO₃] (28b)		9.22 (m, 1H), -11.10 (b)	0.1 (m), -8.4 (m), -33.7 (m), -43.2 (m)
[Ir₂(H)(CO)₂(μ-η¹-η³-HCC(nPr)=CHnPr)(dppm)₂]-[CF₃SO₃] (29)	1968 s, b	8.78 (m, 1H), -11.19 (m, 1H)	-5.0 (m), -7.4 (m), -34.8 (m), -38.1 (m)

[a] IR abbreviations (ν(CO)) unless otherwise stated); vs = very strong, s = strong, m = medium, w = weak, sh = shoulder, b = broad. [b]Nujol mull or CH₂Cl₂ cast unless otherwise stated. [c] ν(C=O ester) [d] ν(C≡C) [e] NMR abbreviations: s = singlet, d = doublet, t = triplet, m = multiplet, q = quintet, dm = doublet of multiplets, b = broad. [f]NMR data at 25°C in CD₂Cl₂ unless otherwise stated. [g] ¹J_C-H coupling values for ¹³C labelled compounds. [h] Chemical shifts for the phenyl hydrogens are not given in the ¹H NMR data. [i] ³J_P-H triplet coupling for methyl protons is typically 5-7 Hz [j] ³¹P{¹H} chemical shifts are referenced vs external 85% H₃PO₄. [k]NMR data at -80°C. [l] NMR data at -20°C. [m] NMR data at 0°C. [n]ν(C=C)

solution was stirred for 1h by which time the color had changed from red to dark red. The solvent was evaporated to *ca.* 2 mL and the product was precipitated and washed with Et$_2$O (2 × 10 mL) and dried under vacuum, yielding a brown powder in 79% yield. Anal. Calcd for Ir$_2$SP$_4$F$_3$O$_9$C$_{60}$H$_{53}$: C, 47.55; H, 3.53. Found: C, 47.16; H, 3.26.

(b) [Ir$_2$(CH$_3$)(CO)$_3$(μ-DMAD)(dppm)$_2$][CF$_3$SO$_3$] (10).

Compound **9** (50 mg, 0.033 mmol) was dissolved in 5 mL of CH$_2$Cl$_2$. Carbon monoxide gas was passed over the dark red solution for 30 s producing a color change to yellow and then the solution was stirred under a static atmosphere of the gas for 5 min. The bright yellow solution was worked up in the same manner as described for compound **9**, yielding a yellow powder in 78% yield. Anal. Calcd for Ir$_2$SP$_4$F$_3$O$_{10}$C$_{61}$H$_{53}$: C, 47.46; H, 3.47. Found: C, 46.99; H, 3.22.

(c) [Ir$_2$(CH$_3$)(CO)$_2$(PMe$_3$)(μ-DMAD)(dppm)$_2$][CF$_3$SO$_3$] (11).

Compound **9** (50 mg, 0.033 mmol) was dissolved in 5 mL of CH$_2$Cl$_2$ and trimethylphosphine (3.7 μL, 0.033 mmol) was added immediately giving a bright yellow solution. The solution was stirred for 1h and then worked up the same as described for compound **9**, yielding a bright yellow powder in 91 % yield. Anal. Calcd for Ir$_2$ClSP$_5$F$_3$O$_9$C$_{63.5}$H$_{63}$: C, 46.67; H, 3.89. Found: C, 46.70; H, 3.63. The compound was crystallized as the hemi-solvate **11**•1/2CH$_2$Cl$_2$ as was shown by the X-ray structure determination (*vide infra*).

(d) [Ir$_2$(CH$_3$)(CO)$_2$(μ-HFB)(dppm)$_2$][CF$_3$SO$_3$] (12).

Compound **2** (34 mg, 0.025 mmol) was dissolved in 5 mL of CH$_2$Cl$_2$ and HFB was passed over

the solution for 30 s resulting in an immediate color change from red to orange. The solution was stirred under a static atmosphere of the gas for 10 min and then worked up as described for compound **9**, yielding a light orange powder in 95% yield. Anal. Calcd for $Ir_2SP_4F_9O_5C_{58}H_{47}$: C, 45.37; H, 3.09. Found: C, 45.55; H, 3.06. ^{19}F NMR: δ -44.4 (q, $^5J_{F-F} = 14$ Hz, 3F), -50.9 (q, 3F).

(e) $[Ir_2(CH_3)(CO)_2(\mu\text{-}HC\equiv CC(O)OMe)(dppm)_2][CF_3SO_3]$ (13).
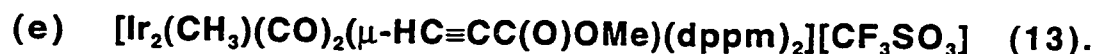
Compound **2** (34 mg, 0.025 mmol) was dissolved in 5 mL of CH_2Cl_2 and cooled to -78 °C. Methyl propiolate (2.2 μL, 0.026 mmol) was added, producing a yellow solution that was stirred at -78 °C for 1h. The solution was then warmed to room temperature and worked up the same way as described for compound **9**, yielding a yellow powder in 89% yield. Anal. Calcd for $Ir_2SP_4F_3O_7C_{58}H_{51}$: C, 47.80; H, 3.53. Found: C, 47.57; H, 3.35.

(f) $[Ir_2(CO)_2(\mu\text{-}C\equiv CMe)(dppm)_2][CF_3SO_3]$ (16).   Compound **2** (30 mg 0.022 mmol) was dissolved in 5 mL of CH_2Cl_2 and cooled to -78 °C. Propyne (1mL) was added via a gas tight syringe causing a color change from red to yellow and the solution was stirred at -78 °C for 1h. Upon slowly warming, the solution darkened to a light brown at *ca.* -20 °C. After stirring at room temperature for 1h the solvent was evaporated to *ca.* 2mL and a light brown powder was precipitated and washed with Et_2O (2 × 10 mL), followed by drying under vacuum. Low temperature intermediates in the reaction, $[Ir_2(H)(CH_3)(CO)_2(\mu\text{-}C\equiv CMe)(dppm)_2][CF_3SO_3]$ (14) and $[Ir_2(CH_3)(CO)_2\text{-}$

(μ-HC≡CMe)(dppm)$_2$][CF$_3$SO$_3$] (15) were characterized by NMR spectroscopy, as described later.

(g) [Ir$_2$(CO)$_2$(μ-C≡CPh)(dppm)$_2$][CF$_3$SO$_3$] (19). The procedure used was the same as that used for the preparation of compound 16 except that one equivalent of phenyl acetylene was used, yield 83%. Anal. Calcd for Ir$_2$SP$_4$F$_3$O$_5$C$_{61}$H$_{49}$: C, 50.20; H, 3.39. Found: C, 50.10; H, 3.28. Low temperature intermediates in the reaction, [Ir$_2$(H)(CH$_3$)(CO)$_2$(μ-C≡CPh)(dppm)$_2$] [CF$_3$SO$_3$] (17) and [Ir$_2$(CH$_3$)(CO)$_2$(μ-HC≡CPh)(dppm)$_2$][CF$_3$SO$_3$] (18) were characterized by NMR spectroscopy, as described later.

(h) **Low temperature reaction of Compound 2 with one equivalent of acetylene.** The procedure used is as described below for the characterization of low temperature intermediates. The compound [Ir$_2$(H)(CH$_3$)(C≡CH)(CO)$_2$(dppm)$_2$][CF$_3$SO$_3$] (20) was formed at -78 °C by addition of ca. one equivalent of acetylene by gas tight syringe to compound 2, and persisted in solution until ca. 0 °C. ^{13}C{^{1}H} NMR for (20): δ 124.0 (dt, $^1J_{C-C}$ = 78 Hz, C≡CH), 77.2 (d, C≡CH). Upon warming 20 to ca. 0 °C compound [Ir$_2$(CH$_3$)(μ-C=CH$_2$)(CO)$_2$(dppm)$_2$][CF$_3$SO$_3$] (21) began to appear and persisted in solution until room temperature along with other uncharacterized products. ^{13}C{^{1}H} NMR for (21): δ 218.2 (dq, $^1J_{C-C}$ = 63 Hz, μ-C=CH$_2$), 120.0 (d, μ-C=CH$_2$). After stirring at room temperature for 1 day, CO gas was added to the mixture of compound 21 and uncharacterized products, and the solution

was stirred for 2 h, after which, NMR spectra on the complex reaction mixture showed production of compound $[Ir_2(H)(\mu\text{-}C=CHCH_3)(CO)_3(dppm)_2]\text{-}[CF_3SO_3]$ (22) in *ca.* 35% yield. $^{13}C\{^1H\}$ NMR for (22): δ 192.0 (dq, $^1J_{C\text{-}C}$ = 64 Hz, $\mu\text{-}C=CHCH_3$), 137.1 (dd, $\mu\text{-}C=CHCH_3$), 24.5 (d, $^1J_{C\text{-}C}$ = 42 Hz, $\mu\text{-}C=CHCH_3$).

(i) $[Ir_2(CH_3)(C\equiv CH)(CO)_2(\mu\text{-}H)(\mu\text{-}C=CH_2)(dppm)_2][CF_3SO_3]$ (23).

Compound 2 (30 mg, 0.022 mmol) was dissolved in 5 mL of CH_2Cl_2. Acetylene was passed through the solution for 10 min causing a color change from red to orange and then to yellow. The solution was stirred under a static atmosphere of the gas for 1 h and then worked up as described for compound 9, giving a yellow powder in 83% yield. Anal. Calcd for $Ir_2Cl_{0.566}SP_4F_3O_5C_{58.283}H_{51.566}$: C, 48.29; H, 3.59. Found: C, 48.18; H, 3.34. The amount of CH_2Cl_2 present (0.283 moles/mole complex) in the elemental analysis was obtained from an NMR spectrum run in $CDCl_3$. $^{13}C\{^1H\}$ NMR: δ 193.6 (dm, $^1J_{C\text{-}C}$ = 69.9 Hz, $C=CH_2$), 173.8 (t, CO), 166.6 (m, CO), 120.2 (d, $C=CH_2$), 103.7 (d, $^1J_{C\text{-}C}$ = 119.1 Hz, $C\equiv CH$), 61.6 (ddt, $^2J_{C\text{-}P}$ = 15.1 Hz, $^2J_{C\text{-}C}$ = 15 Hz, $C\equiv CH$), -5.2 (t, CH_3).

(j) $[Ir_2(CH_3)(CO)_2(\mu\text{-}CH_3C\equiv CCH_3)(dppm)_2][CF_3SO_3]$ (24).

Compound 2 (40 mg, 0.029 mmol) was dissolved in 5 mL of CH_2Cl_2. Excess 2-butyne (3.5 µL, 0.045 mmol) was added causing an immediate color change from red to dark red. The solution was stirred for 1h and then worked up in a similar manner to that described for compound 9, giving a reddish brown

powder in 86% yield. Anal. Calcd for $Ir_2SP_4F_3O_5C_{58}H_{53}$: C, 48.80; H, 3.75. Found: C, 49.02; H, 3.74.

(k) [Ir$_2$(H)(CO)$_2$(μ-η^1:η^3-HCC(CH$_3$)=CHCH$_3$)(dppm)$_2$][CF$_3$SO$_3$]

(25). Compound **24** was prepared in situ as above and stirred for a period of 24 h during which time the color changed from dark red to yellow. The solvent was evaporated to *ca.* 2 mL and a yellow powder was precipitated and washed with Et$_2$O (2 × 10 mL) and then dried under vacuum, yield 84%. Anal. Calcd for $Ir_2SP_4F_3O_5C_{59}H_{58}$: C, 48.80; H, 3.75. Found: C, 48.30; H, 3.58. $^{13}C\{^1H\}$ NMR (natural abundance): δ 170.9 (m, *CO*), 168.2 (b, *CO*), 138.4 (t, $^2J_{C\text{-}P}$ = 63.5 Hz, μ-η^1:η^3-H*C*C(CH$_3$)=CHCH$_3$), 110.2 (s, μ-η^1:η^3-HC*C*(CH$_3$)=CHCH$_3$), 64.1 (t, Ph$_2$P*C*H$_2$PPh$_2$), 56.2 (m, μ-η^1:η^3-HCC(CH$_3$)=*C*HCH$_3$), 42.3 (t, Ph$_2$P*C*H$_2$PPh$_2$), 23.4 (s, μ-η^1:η^3-HCC(*C*H$_3$)=CHCH$_3$), 18.1 (s, μ-η^1:η^3-HCC(CH$_3$)=CH*C*H$_3$).

(l) - (o) [Ir$_2$(H)(CO)$_2$(μ-η^1:η^3-HCC(R)=CHR´)(dppm)$_2$][CF$_3$SO$_3$] (R = R´ = Et (26); R = Me, R´ = Et (27); R = Me, R´ = Ph (28); R = R´ = nPr (29)). Compounds **26-29** were prepared by adding 1.1 equivalents of the appropriate alkyne (3-hexyne **(26)**, 2-pentyne **(27)**, 1-phenyl-2-propyne **(28)**, 4-octyne **(29)**), to a CH$_2$Cl$_2$ solution of compound **2**, stirring for 24 h and then working up the same as was done with compound **25** except that pentane was used for precipitation and washing. In each case the color of the solution changed from red to dark upon addition of the alkyne and then over 24 h changed to yellow. Typical yields were between 75 - 85%. For **26** Anal. Calcd for $Ir_2SP_4F_3O_5C_{59}H_{57}$: C, 49.51; H, 3.96. Found: C, 49.66; H, 3.55. For **27** Anal.

Calcd for $Ir_2SP_4F_3O_5C_{58}H_{55}$: C, 49.16; H, 3.85. Found: C, 48.89; H, 3.38. Satisfactory elemental analyses were not obained for compounds **28** and **29** and characterization is based on $^{31}P\{^1H\}$ and ^1H NMR data (see Table 3.1).

General Procedure for Characterization of Low Temp. Intermediates. Compound **2** (*ca.* 20 mg, 0.015 mmol) was dissolved in 0.6 mL of CD_2Cl_2 in an NMR tube, capped with a rubber septum, and cooled to -78°C. Approximately one equivalent of the appropriate alkyne was added to the NMR tube via gas tight syringe, and NMR spectra of the reaction mixture were obtained at temperatures starting from -80 °C to +25 °C by warming the probe to the desired temperature, with the sample in place, and allowing the sample to stand at that temperature for 20 min before recording the spectra.

X-ray Data Collection. For compounds **11**, and **23**, crystals suitable for X-ray diffraction were grown via slow diffusion of diethyl ether into a concentrated CH_2Cl_2 solution of the compound. For compound **26**, crystals were grown by diffusing Et_2O into a concentrated 1:1 CH_3Cl/toluene solution of **26**. Crystals of each compound were mounted and flame-sealed in glass capillaries under solvent vapor to minimize decomposition or deterioration due to solvent loss. Data were collected at -50 °C on an Enraf-Nonius CAD4 diffractometer for compounds **11** and **26** using graphite-monochromated Mo Kα radiation and for compound **23** at -60 °C on a Siemens P4RA diffractometer using graphite-monochromated Cu Kα radiation. Unit-cell parameters and space group assignments were obtained as described below. For each compound, three reflections were chosen as intensity standards and were

remeasured every 120 min of X-ray exposure time; in no case was decay evident. Absorption corrections were applied to the data as described below. Crystal parameters and details of data collection are summarized in Table 3.2.

Unit cell parameters for compounds **11** and **26** were obtained from a least-squares refinement of 24 reflections in the approximate range $20°<2\theta<24°$. Unit cell parameters for compound **23** were obtained from a least-squares refinement of 46 reflections in the range $57.0°<2\theta<58.9°$. For compounds **11** and **23** the cell parameters and the systematic absences defined the space groups as $P2_1/c$, whereas for **26** the cell parameters, the lack of absences and the diffraction symmetry suggested the space group $P1$ or $P\bar{1}$, the latter of which was established by successful refinement of the structure. Absorption corrections to **26** were applied by the method of Walker and Stuart,[11a] while for **11** and **23** the crystal faces were indexed and measured, with absorption corrections being carried out using Gaussian integration.

Structure Solution and Refinement. For each structure, the positions of the iridium and phosphorus atoms were found using the direct-methods program *SHELXS-86*;[11b] the remaining atoms were found using a succession of least-squares and difference Fourier maps. Refinement of each structure proceeded using the program *SHELXL-93*.[11c] Hydrogen atom positions (except for hydride ligands as noted below) were calculated by assuming idealized sp^2 or sp^3 geometries about their attached carbon atoms (as appropriate), and were

Table 3.2 Crystallographic Data for Compounds 11, 23 & 26

A. Crystal Data

	[Ir$_2$(CH$_3$)(CO)$_2$(PMe$_3$)(μ-DMAD)(dppm)$_2$][CF$_3$SO$_3$] (11)•3/4CH$_2$Cl$_2$•H$_2$O	[Ir$_2$(CH$_3$)(C≡CH)(CO)$_2$(μ-C=CH$_2$)(μ-H)(dppm)$_2$][CF$_3$SO$_3$](23)•CH$_2$Cl$_2$	[Ir$_2$H(CO)$_2$(μ-η^2:η^1-HCCEtCHEt)(dppm)$_2$][CF$_3$SO$_3$] (26)•2PhMe
compd			
formula	C$_{63.75}$H$_{65.5}$Cl$_{1.5}$F$_3$Ir$_2$O$_{10}$P$_5$S	C$_{59}$H$_{53}$Cl$_2$F$_3$Ir$_2$O$_5$P$_4$S	C$_{74}$H$_{73}$F$_3$Ir$_2$O$_5$P$_4$S
formula wt	1673.15	1510.25	1639.66
crystal dimensions (mm) color	0.40 × 0.15 × 0.05 dark red	0.42 × 0.24 × 0.08 yellow	0.43 × 0.19 × 0.08 yellow
crystal system	monoclinic	monoclinic	triclinic
space group	P2$_1$/c (No. 14)	P2$_1$/c (No. 14)	P$\bar{1}$ (No. 2)
unit cell parameters a,b,c			
a(Å)	12.9605 (15)	12.5041 (9)	12.599 (2)
b(Å)	39.912 (6)	21.7598 (15)	14.284 (3)
c(Å)	13.224 (2)	21.5316 (15)	18.871 (4)
α(deg)	90.0	90.0	88.50 (2)
β(deg)	109.610 (10)	99.522 (5)	84.946 (15)
γ(deg)	90.0	90.0	89.16 (2)
V(Å^3)	6444.0 (15)	5777.7 (7)	3381.4 (12)
Z	4	4	2

Table 3.2 cont

ρ_{calcd} (g cm^{-3})	1.725	1.736	1.610
μ (mm^{-1})	4.410	11.50	4.116

B. Data Collection and Refinement Conditions

diffractometer	Enraf-Nonius CAD4[d]	Siemens P4A rotating anode [e]	Enraf-Nonius CAD4[d]
radiation (λ [Å])	graphite-monochromated Mo Kα (0.71073)	graphite-monochromated Cu Kα (1.54178)	graphite-monochromated Mo Kα (0.71073)
temperature (°C)	-50	-60	-50
scan type	ω	θ–2θ	θ–2θ
data collection 2θ limit (deg)	50.0	113.50	50.0
total data collected	7137 (-15 $\leq h \leq$ 14, 0 $\leq k \leq$ 34, 0 $\leq l \leq$ 15)	8144 (0$\leq h \leq$13, 0$\leq k \leq$23, -23$\leq l \leq$23)	12231 (-14 $\leq h \leq$ 14, -16 $\leq k \leq$ 16, 0 $\leq l \leq$ 22)
independent reflections	6801	7730	11827
number of observations (NO)	3394 ($F_o{}^2 \geq 2\sigma(F_o{}^2)$)	5472 ($F_o{}^2 \geq 2\sigma(F_o{}^2)$)	8426 ($F_o{}^2 \geq 2\sigma(F_o{}^2)$)
structure solution method	direct methods (*SHELXS–86*[f])	direct methods (*SHELXS–86*[f])	direct methods (*SHELXS–86*[f])
refinement method	full-matrix least-squares on F^2 (*SHELXL–93*[g])	full-matrix least-squares on F^2 (*SHELXL–93*[g])	full-matrix least-squares on F^2 (*SHELXL–93*[g])
absorption correction method	Gaussian integration (face indexed)	Gaussian integration (face indexed)	*DIFABS*[h]

Table 3.2 cont

range of absorption correction factors	0.7996–0.3593	0.1714 - 0.4240	1.223–0.892
data/restraints/parameters	6784 $[F_o^2 \geq -3\sigma(F_o^2)]$/24/446	7716 $[F_o^2 \geq -3\sigma(F_o^2)]$/24/663	11827 $[F_o^2 \geq -3\sigma(F_o^2)]$/4/808
largest difference peak and hole	1.268 and -1.277 e Å^{-3}	2.179 and -1.202 e Å^{-3}	1.290 and -1.362 e Å^{-3}
final R indices[i] $F_o^2 > 2\sigma(F_o^2)$	$R_1 = 0.0627$, $wR_2 = 0.1153$	$R_1 = 0.0640$, $wR_2 = 0.1495$	$R_1 = 0.0364$, $wR_2 = 0.0841$
all data	$R_1 = 0.2002$, $wR_2 = 0.1579$	$R_1 = 0.0971$, $wR_2 = 0.1755$	$R_1 = 0.0777$, $wR_2 = 0.0958^2$
GOF(S)[j]	1.002 $[F_o^2 \geq -3\sigma(F_o^2)]$	1.041 $[F_o^2 \geq -3\sigma(F_o^2)]$	1.050 $[F_o^2 \geq -3\sigma(F_o^2)]$

[a]Obtained from least-squares refinement of 24 reflections with 19.9° < 2θ < 23.6°.

[b]Obtained from least-squares refinement of 46 reflections with 57.0° ≤ 2θ ≤ 58.9°.

[c]Obtained from least-squares refinement of 24 reflections with 20.9° < 2θ < 23.9°.

[d]Programs for diffractometer operation, data collection and processing were those supplied by Enraf-Nonius.

[e]Programs for diffractometer operation, data collection and data processing were those of the XSCANS system supplied by Siemens.

[f]Sheldrick, G. M. *Acta Crystallogr.* **1990**, *A46*, 467.

[g]Sheldrick, G. M. *SHELXL-93*. Program for crystal structure determination. University of Göttingen, Germany, 1993. Refinement on F_o^2 for all reflections (all of these having $F_o^2 \geq -3\sigma(F_o^2)$) except for compound **11**, refinement on F^2 for ALL reflections except for 17 with very negative F^2 and for compound **23**, refinement on F^2 for ALL reflections except for 14 with very negative F^2. Weighted R-factors wR_2 and all goodnesses of fit S are based on F_o^2; conventional R-factors R_1 are based on F_o^2. The observed criterion of

Table 3.2 cont

$F_o^2 > 2\sigma(F_o^2)$ is used only for calculating R_1, and is not relevant to the choice of reflections for refinement. R-factors based on F_o^2 are statistically about twice as large as those based on F_o, and R-factors based on ALL data will be even larger.

[h]Walker, N.; Stuart, D. *Acta Crystallogr.* **1983**, *A39*, 158–166.

[i]$R_1 = \Sigma||F_o| - |F_c||/\Sigma|F_o|$; $wR_2 = [\Sigma w(F_o^2 - F_c^2)^2/\Sigma w(F_o^4)]^{1/2}$.

[j]$S = [\Sigma w(F_o^2 - F_c^2)^2/(n-p)]^{1/2}$ (n = number of data; p = number of parameters varied; $w = [\sigma^2(F_o^2) + (a_0 P)^2 + a_1 P]^{-1}$ where $P = [Max(F_o^2, 0) + 2F_c^2]/3$). For compound **11** $a_o = 0.0507$, $a_1 = 34.2392$; for compound **23** $a_o = 0.0725$, $a_1 = 101.6339$; for compound **26** $a_o = 0.0481$, $a_1 = 0.0$.

given thermal parameters 120% of the equivalent isotropic displacement parameters of their attached carbons. For compound **26** the hydride ligand (H(2)) was located and refined with a fixed Ir(2)–H(2) distance of 1.70(1) Å and position to minimize nonbonded contacts. Further details of structure refinement (other than described below) and final residual indices may be found in Table 3.2. Interatomic distances and angles have also been tabulated for each compound (Table 3.3 for **11**, Table 3.4 for **23** and Table 3.5 for **26**).

Location of all atoms in $[Ir_2(CH_3)(CO)_2(PMe_3)(\mu\text{-DMAD})(dppm)_2][CF_3SO_3]$ (**11**)•3/4CH_2Cl_2•H_2O proceeded smoothly, however the triflate ion and the water molecule did not behave well so bond distances were constrained. The following distance restraints were applied to enforce an idealized geometry upon the triflate ion: d(S–C(98)) = 1.80(1) Å; d(S–O(91)) = d(S–O(92)) = d(S–O(93)) = 1.45(1) Å; d(F(91)–C(98)) = d(F(92)–C(98)) = d(F(93)–C(98)) = 1.35(1) Å; d(F(91)···F(92)) = d(F(91)···F(93)) = d(F(92)···F(93)) = 2.20(1) Å; d(O(91)···O(92)) = d(O(91)···O(93)) = d(O(92)···O(93)) = 2.37(1) Å; d(F(91)···O(92)) = d(F(91)···O(93)) = d(F(92)···O(91)) = d(F(92)···O(93)) = d(F(93)···O(91)) = d(F(93)···O(92)) = 3.04(1) Å) and to the hydrogen atoms of the water molecule (d(O(99)–H(99C)) = d(O(99)–H(99D)) = 1.00(1) Å; d(H(99C)···H(99D)) = 1.00(1) Å; d(O(91)···H(99C)) = d(O(3)···H(99D)) = 1.86(2) Å). All atoms were refined isotropically except the iridium and phosphorus atoms which were refined anisotropically.

For the compound [Ir$_2$(CH$_3$)(C≡CH)(CO)$_2$(μ-C=CH$_2$)(μ-H)(dppm)$_2$]-[CF$_3$SO$_3$] (**23**)•CH$_2$Cl$_2$ all nonhydrogen atoms were located. The hydride ligand (H(1)) was not located from a difference Fourier map so based on spectroscopic data was placed in an idealized position bridging the two metals. The triflate anion and the dichloromethane solvent molecule were not well behaved so were constrained to idealized geometries by fixing the bond distances. The same distance restraints were applied to the triflate ion as for compound **11**, and the following restraints were applied to enforce an idealized geometry upon the dichloromethane solvent molecule: d(C(99)–Cl(1)) = d(C(99)–Cl(2)) = 1.80(1) Å; d(Cl(1)–Cl(2)) = 2.90(1) Å.

For the compound [Ir$_2$H(CO)$_2$(μ-η^1:η^3-HCC(Et)C(H)Et)(dppm)$_2$][CF$_3$SO$_3$] (**26**)•2PhMe all nonhydrogen atoms were located; even the hydride ligand (H(2)) was located on a difference Fourier map and refined with a fixed Ir(2)–H(2) distance of 1.70(1) Å and position to minimize nonbonded contacts with the carbonyl carbon (C(2)), the vinyl carbene hydrogen (H(7)) and the dppm phenyl hydrogen (H(46)). The restraints are as follows: H2⋯H7, H2⋯H46 (both not less than 2.0 Å) and H2⋯C2 (not less than 2.2 Å).

Dr. Bob McDonald is acknowledged for X-ray data collection for compound **23** and data collection and solution for compounds **11** and **26**.

Results and Characterization of Compounds

Previous work, described in Chapter 2, with the methyl compound $[Ir_2(CH_3)(CO)(\mu\text{-}CO)(dppm)_2][CF_3SO_3]$ (2) showed that upon addition of a variety of ligands that were either σ-donors (eg. PR_3) or π-acceptors (eg. CO, SO_2), C-H activation of the methyl group occurred producing the adducts in which conversion of the methyl group to methylene hydride moieties had occurred. In this chapter we extend this study to include alkynes as the added substrate, with the goal of obtaining a better understanding of the factors that induce carbon-carbon bond formation in such binuclear species.

A previous study done on the related tricarbonyl species, $[Ir_2(H)(CO)_3$-$(\mu\text{-}CH_2)(dppm)_2][CF_3SO_3]$ (1), had shown that the activated alkyne dimethyl acetylenedicarboxylate (DMAD) inserted into the iridium-methyl bond (presumably formed by hydride-to-methylene migration) to produce the vinylic species $[Ir_2(CR=C(Me)R)(CO)_3(dppm)_2][CF_3SO_3]$ (R = CO_2Me).[9h,10] It was of obvious interest to determine whether compound 2 would react similarly to give vinylic products resulting from migratory insertion of the methyl group, or whether reactivity analogous to SO_2, PR_3 and CO attack, to give a methylene-bridged hydride would result. In the event that the latter occurred, two other transformations were of interest, involving the possibility of alkyne migratory insertion with the methylene or hydride fragments.

Compound 2 reacts with dimethyl acetylenedicarboxylate (DMAD) to produce the alkyne-bridged product $[Ir_2(CH_3)(CO)_2(\mu\text{-}DMAD)(dppm)_2][CF_3SO_3]$

(9), as outlined in Scheme 3.1. This product is similar to other alkyne-bridged products characterized in this group and elsewhere.[13] The ^{1}H NMR resonance for the Ir-bound methyl group in **9** is a triplet at δ 0.65; the coupling ($^3J_{P-H}$ = 5 Hz) to two adjacent phosphorus nuclei demonstrates that this group has remained terminal on one metal. The failure of the alkyne ligand and the methyl group to undergo migratory insertion is suprising in light of the insertion observed in the tricarbonyl analogue. Even addition of CO to the alkyne-bridged **9** to give a compound having the same stoichiometry as the inserted product[9h,10] did not result in migratory insertion but instead yielded the simple carbonyl adduct, [Ir$_2$(CH$_3$)(CO)$_3$(μ-DMAD)(dppm)$_2$][CF$_3$SO$_3$] (**10**). Similarly phosphine addition did not induce migration but yielded the phosphine adduct [Ir$_2$(CH$_3$)(CO)$_2$-(PMe$_3$)(μ-DMAD)(dppm)$_2$][CF$_3$SO$_3$] (**11**). In order to determine whether the alkyne and methyl groups were mutually cis and therefore capable of migratory insertion without significant rearrangement, the X-ray structure of **11** was determined. A representation of the molecule is shown in Figure 3.1, with selected distances and angles given in Table 3.3. The structure confirms the bridging-alkyne formulation with the methyl ligand bound terminally to Ir(2) cis to one end of the alkyne. The overall geometry is best described as octahedral at each metal having the carbonyls essentially opposite the bridging-alkyne group, with the PMe$_3$ and methyl ligands trans to each other across the metal-metal bond, almost bisecting the angles between the respective μ-DMAD and terminal carbonyl groups. The metal-metal separation of 3.022(2) Å is long for

Scheme 3.1

9: R = R' = C(O)OCH₃
12: R = R' = CF₃
13: R = H , R' = C(O)OCH₃

R = C(O)OCH₃
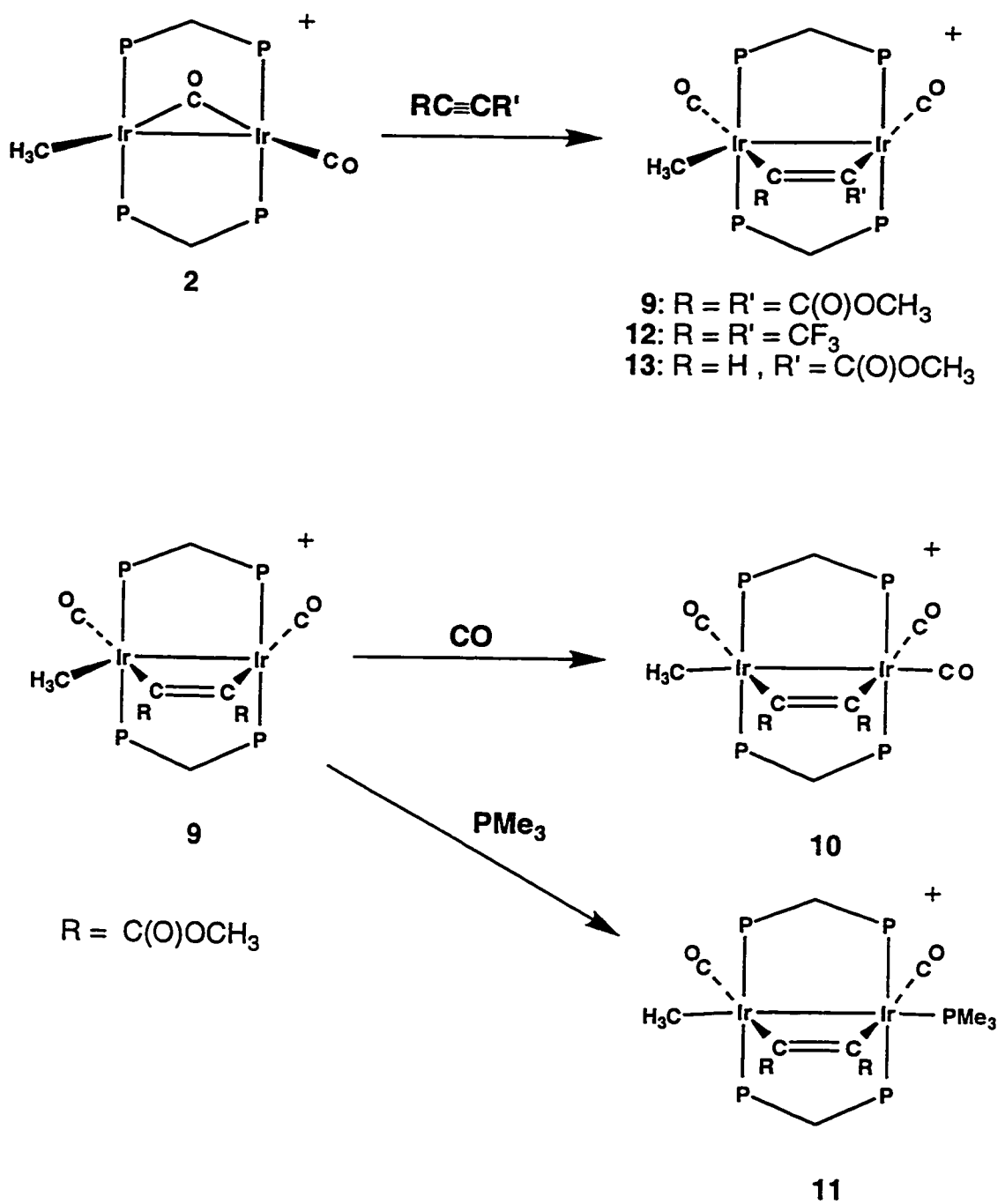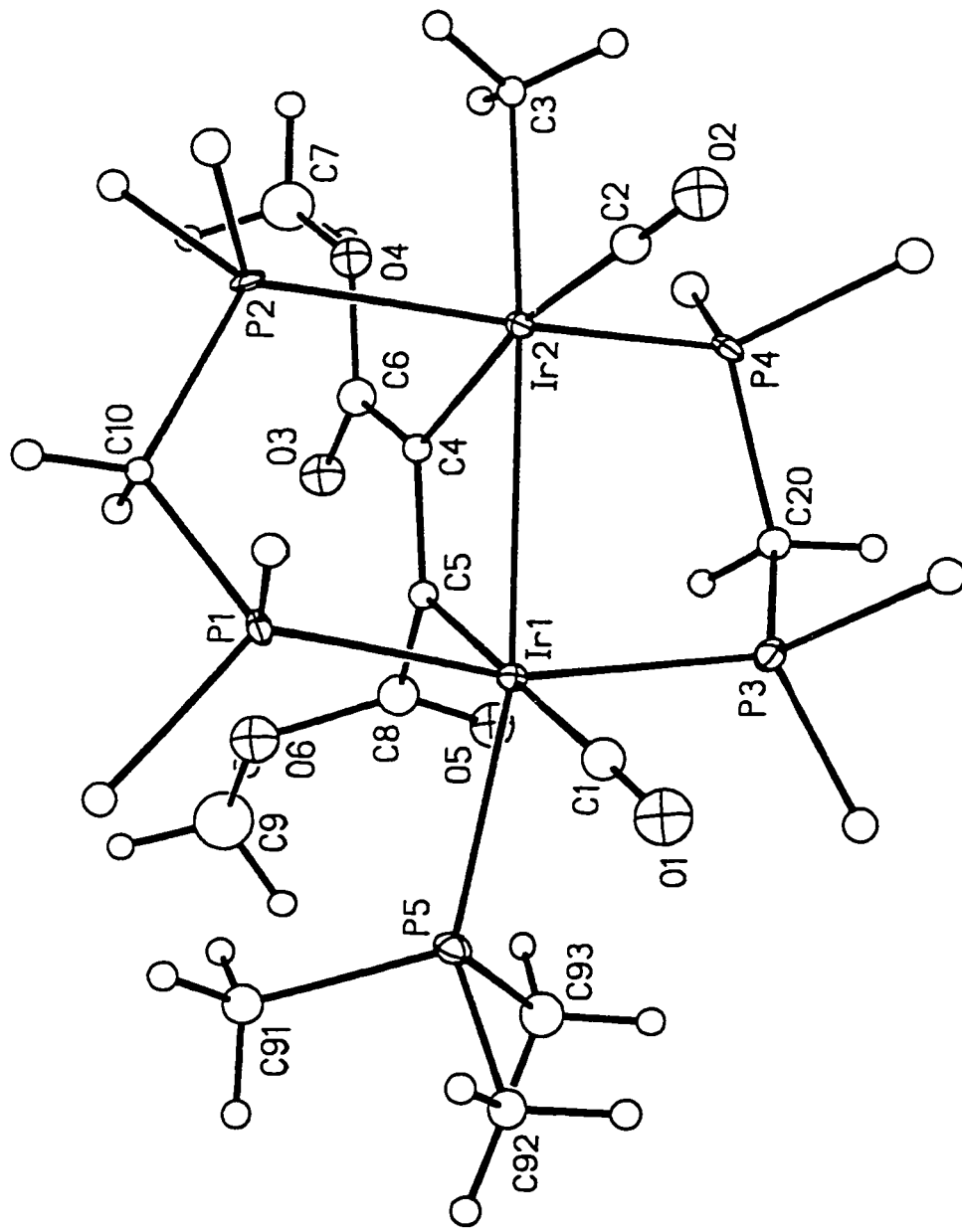
Figure 3.1 Perspective view of the $[Ir_2(CH_3)(CO)_2(PMe_3)(\mu\text{-DMAD})(dppm)_2]^+$ cation of compound **9**. Thermal ellipsoids are shown at the 20% probability level except for hydrogens which are shown arbitrarily small. Only the ipso carbons of the dppm phenyl rings are shown.

Table 3.3 Selected Interatomic Distances and Angles for Compound **11**.

(a) Distances (Å)

Atom1	Atom2	Distance	Atom1	Atom2	Distance
Ir(1)	Ir(2)	3.022(2)	O(1)	C(1)	1.10(4)
Ir(1)	P(5)	2.453(11)	O(2)	C(2)	1.14(4)
Ir(1)	P(1)	2.348(9)	O(3)	C(6)	1.21(4)
Ir(1)	P(3)	2.342(9)	O(4)	C(6)	1.32(4)
Ir(2)	P(2)	2.336(9)	O(4)	C(7)	1.46(4)
Ir(2)	P(4)	2.357(10)	O(5)	C(8)	1.22(4)
Ir(1)	C(1)	1.91(4)	O(6)	C(8)	1.32(4)
Ir(1)	C(5)	2.14(3)	O(6)	C(9)	1.46(5)
Ir(2)	C(2)	1.87(4)	C(4)	C(5)	1.33(4)
Ir(2)	C(3)	2.16(3)	C(4)	C(6)	1.49(5)
Ir(2)	C(4)	2.11(3)	C(5)	C(8)	1.49(5)

(b) Angles (deg)

Atom1	Atom2	Atom3	Angle	Atom1	Atom2	Atom3	Angle
Ir(2)	Ir(1)	P(5)	156.6(3)	C(6)	O(4)	C(7)	118.1(31)
Ir(2)	Ir(1)	C(1)	115.5(12)	C(8)	O(6)	C(9)	115.9(33)
Ir(2)	Ir(1)	C(5)	64.1(10)	Ir(1)	C(1)	O(1)	177.0(39)
P(1)	Ir(1)	P(3)	161.2(4)	Ir(2)	C(2)	O(2)	176.1(34)
P(1)	Ir(1)	P(5)	97.2(3)	Ir(2)	C(4)	C(5)	109.1(27)
P(3)	Ir(1)	P(5)	100.3(4)	Ir(2)	C(4)	C(6)	130.8(30)
P(5)	Ir(1)	C(1)	87.8(12)	C(5)	C(4)	C(6)	120.0(36)
P(5)	Ir(1)	C(5)	92.6(10)	Ir(1)	C(5)	C(4)	117.6(28)
C(1)	Ir(1)	C(5)	179.3(15)	Ir(1)	C(5)	C(8)	121.6(27)
Ir(1)	Ir(2)	C(2)	99.5(12)	C(4)	C(5)	C(8)	120.0(35)
Ir(1)	Ir(2)	C(3)	171.5(9)	O(3)	C(6)	O(4)	122.5(39)
Ir(1)	Ir(2)	C(4)	69.0(11)	O(3)	C(6)	C(4)	123.5(42)
P(2)	Ir(2)	P(4)	160.5(4)	O(4)	C(6)	C(4)	113.9(35)
C(2)	Ir(2)	C(3)	89.0(15)	O(5)	C(8)	O(6)	125.1(39)
C(2)	Ir(2)	C(4)	168.4(17)	O(5)	C(8)	C(5)	123.0(35)
C(3)	Ir(2)	C(4)	102.5(14)	O(6)	C(8)	C(5)	111.9(33)

an iridium-iridium single bond but electron counting necessitates that a metal-metal bond be included to give each metal an 18-electron configuration. Without the metal-metal bond each Ir-center would have a 17-electron configuration, and consequently be paramagnetic, for which there is no evidence. Other examples of long M-M single bonds with bis-dppm bridged dirhodium or diiridium complexes have been observed in which a similar octahedral coordination about each metal is observed. In these structures strong ligand-ligand repulsions produced by the eclipsed octahedra may be responsible for the long M-M bond.[14] Both ends of the diphosphine ligands are bent significantly from a trans alignment owing to repulsions involving the PMe_3 group and the large alkyne substituents, (P(1)-Ir(1)-P(3) = 161.2(4)° and P(2)-Ir(2)-P(4) = 160.5(4)°). As noted earlier, the alkyne is bound parallel to the metal-metal axis in a cis-dimetalated olefin geometry. The C(4)-C(5) distance of 1.33(4) Å is consistent with a carbon-carbon double bond. The Ir(2)-C(4) and Ir(1)-C(5) distances (2.11(3) Å and 2.14(3) Å) are not significantly different than the Ir(2)-C(3) distance of 2.16(3) Å, even though the former pair involve sp^2 carbons, while the latter involves an sp^3 carbon. The Ir-P distances for the dppm ligands are all quite consistent (2.348(9) Å, 2.342(9) Å, 2.336(9) Å, 2.357(10) Å), however the Ir(1)-P(5) distance (2.453(11) Å) involving the PMe_3 group, is ca. 0.1 Å longer, possibly owing to the trans influence, noted previously, for a metal-metal bond.[15]

The reaction of compound **2** with other activated alkynes such as hexafluorobutyne (HFB) and methylpropiolate gave the products

$[Ir_2(CH_3)(CO)_2(\mu\text{-HFB})(dppm)_2][CF_3SO_3]$ **(12)** and $[Ir_2(CH_3)(CO)_2\text{-}$

$(\mu\text{-HC}{\equiv}CC(O)OMe)(dppm)_2][CF_3SO_3]$ **(13)**, respectively, which, on the basis of

the similarity of their spectral parameters with those of **9**, are assigned similar

structures (see Scheme 3.1). For compound **13**, the ^{1}H NMR spectrum with

selective phosphorus decoupling shows that the terminal acetylenic carbon

having the small hydrogen substituent, is bound to the more crowded iridium

center, bearing the methyl ligand, as expected based on steric arguments.

Compound **2** also reacts with non-activated 1-alkynes. However, the

simple alkyne adducts are not observed; instead, the products result from

oxidative addition of the acetylenic C-H bond. The reaction of **2** with propyne

proceeds at -78°C to initially form the acetylide-hydride methyl compound

$[Ir_2(H)(CH_3)(CO)_2(\mu\text{-C}{\equiv}CMe)(dppm)_2][CF_3SO_3]$ **(14)**, (see Scheme 3.2) which

has resulted from C-H activation of the terminal alkyne. The ^{1}H NMR spectrum

of compound **14** obtained at -80°C shows the acetylide methyl protons as a

singlet at δ 0.62, the Ir-bound methyl resonance as a triplet at δ 0.19 and the

terminal hydride signal as a triplet at δ -9.52. ^{1}H NMR experiments with

selective ^{31}P decoupling indicate that the methyl and hydride ligands are

terminally bound to the same metal. On the basis that methane elimination is

not observed from **14**, the compound is assumed to have the structure shown in

Scheme 3.2 in which the hydride and methyl ligands are separated by a

carbonyl. Upon warming compound **14** to -20°C, a new isomer, **15** begins to

appear, in which the hydride signal in the ^{1}H NMR spectrum has disappeared.

Scheme 3.2

14: R = CH$_3$
17: R = C$_6$H$_5$

HC≡CR
−80°C

−20°C

−CH$_4$
RT

16: R = CH$_3$
19: R = C$_6$H$_5$

15: R = CH$_3$
18: R = C$_6$H$_5$

2
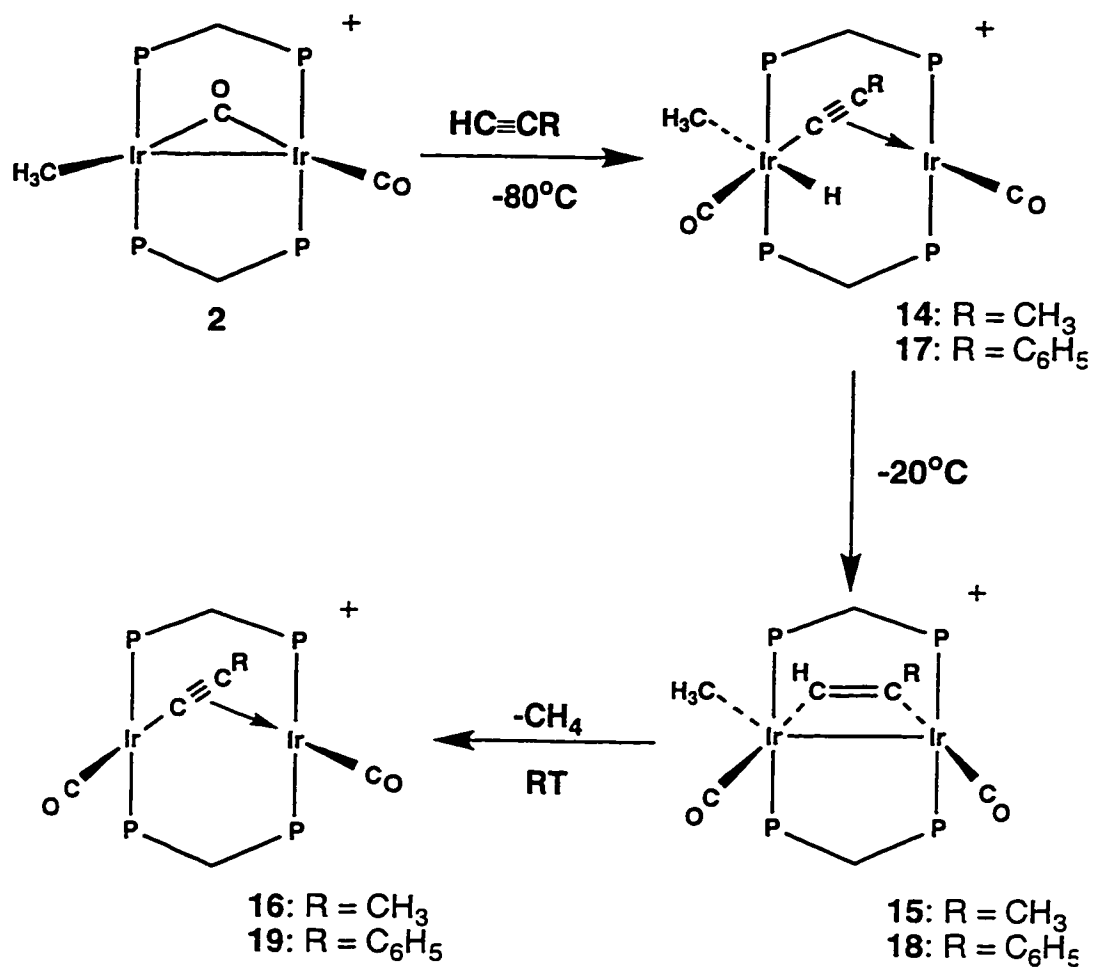
Based upon this observation two structures seem possible for compound **15**, having either a bridging-alkyne or a bridging vinylidene functionality. We favor the alkyne-bridged formulation [Ir$_2$(CH$_3$)(CO)$_2$(μ-HC$\equiv$CMe)(dppm)$_2$][CF$_3$SO$_3$], based on a comparison of the reaction of the related methylene hydride species [Ir$_2$(H)(CO)$_3$(μ-CH$_2$)(dppm)$_2$][CF$_3$SO$_3$] (**1**) with acetylene and phenyl acetylene that shows a similar product with a bridging alkyne.[9h] In addition, low temperature, natural abundance ^{13}C{^{1}H} NMR experiments did not show a resonance in the region typical for the α-carbon of a bridging vinylidene. This last result is equivocal however, because the reaction mixture containing **1 4** and **15**, contained numerous carbon signals that could not be positively identified. The orientation of the bridging-alkyne (i.e. with the methyl substituent towards or away from the metal-bound methyl group) could not be established so the proposed structure, shown in Scheme 3.2, is based upon steric considerations, putting the smaller acetylinic hydrogen adjacent to the Ir-bound methyl group. A resonance assigned to a bridging-alkyne proton appears as a broad multiplet at δ 5.79, with the alkyne-bound methyl group appearing as a broad signal at δ 0.95. The Ir-bound terminal methyl group appears as a triplet at δ 1.73. Upon further warming of compound **15**, reductive elimination of methane occurs (implied by the loss of the methyl resonance) with concomitant formation of the bridging acetylide species, [Ir$_2$(CO)$_2$(μ-C$\equiv$CMe)-(dppm)$_2$][CF$_3$SO$_3$] (**16**). Methane was not directly observed in the ^{1}H NMR spectrum of the reaction mixture due to the number and complexity of the

signals. The σ-, π-bridging mode proposed for the acetylide group in compound 16 is common.[16] The $^{31}P\{^1H\}$ NMR spectrum for 16, run at room temperature, shows a singlet at δ 8.3, indicative of a symmetrical species. However this can also be explained by a fluxional windshield wiper motion of the acetylide ligand in which it transfers back and forth between the two metals. This type of fluxionality is common in homobimetallic complexes with bridging acetylide ligands.[17] As is common to these type of homobimetallic bridging acetylides,[17] the low temperature limiting spectrum was not obtained, even at -80°C. The ^1H NMR spectrum of 16 shows the acetylide methyl protons at δ 1.02 as a quintet ($^4J_{H-P}$ = 1.5 Hz) coupling equally to all four phosphorus nuclei. If the acetylide were bridging the two metals in a symmetric fashion with no fluxional movement, we would not expect the methyl protons to show 5-bond coupling to the phosphorus nuclei. With the acetylide bound in an η^2 fashion to each metal in turn, the coupling is through four bonds.

Compound 2 reacts with phenyl acetylene in an analogous manner to the reaction with propyne, as outlined in Scheme 3.2, first yielding an acetylide-hydride species $[Ir_2(H)(CH_3)(CO)_2(\mu\text{-}C\equiv CPh)(dppm)_2][CF_3SO_3]$ (17) at low temperature, which upon warming transforms into a bridging-alkyne $[Ir_2(CH_3)(CO)_2(\mu\text{-}HC\equiv CPh)(dppm)_2][CF_3SO_3]$ (18) and finally at room temperature eliminates methane and produces a bridging acetylide $[Ir_2(CO)_2\text{-}(\mu\text{-}C\equiv CPh)(dppm)_2][CF_3SO_3]$ (19). The $^{31}P\{^1H\}$ NMR spectra for the three compounds 17, 18 and 19 are very similar to the analogous compounds

produced in the reaction of **2** with propyne (**14, 15, 16**), and by analogy are assumed to have the same structures. The ^{1}H NMR spectrum of **17** shows the acetylide phenyl protons at δ 6.71 and 6.12, separated from the dppm phenyl protons which are at slightly lower field. The Ir-bound methyl resonance appears as a broad triplet at δ 0.26 and the terminal hydride appears as a triplet at δ -9.17. For compound **18**, the methyl protons appear at δ 1.74 as a triplet in the ^{1}H NMR spectrum and the hydride resonance has disappeared suggesting conversion to a bridging-alkyne (see characterization of compound **15**). The characterization of compound **19** as a bridging acetylide is based upon the singlet in the ^{31}P{^{1}H} NMR spectrum indicative of a fluxional compound as was discussed for compound **16**, and the loss of the methyl resonance corresponding to the elimination of methane.

The low temperature reaction of compound **2** with one equivalent of acetylene proceeds in a similar manner as the reaction of **2** with propyne or phenylacetylene producing an acetylide-hydride species, [Ir$_2$(H)(CH$_3$)(CO)$_2$-(μ-C≡CH)(dppm)$_2$][CF$_3$SO$_3$] (**20**), as outlined in Scheme 3.3. Although the ^{31}P{^{1}H} NMR spectrum shows a singlet at -80°C, there is actually a coincidental overlap of two signals that upon warming begin to separate indicating that compound **20** has left-right asymmetry. The ^{1}H NMR spectrum of **20** at -80°C shows the bridging-acetylide proton as a singlet at δ 4.15 and the terminal methyl and hydride signals as triplets at δ 0.68 and -10.06, respectively. Selective ^{31}P decoupling experiments could not be done on this compound

Scheme 3.3
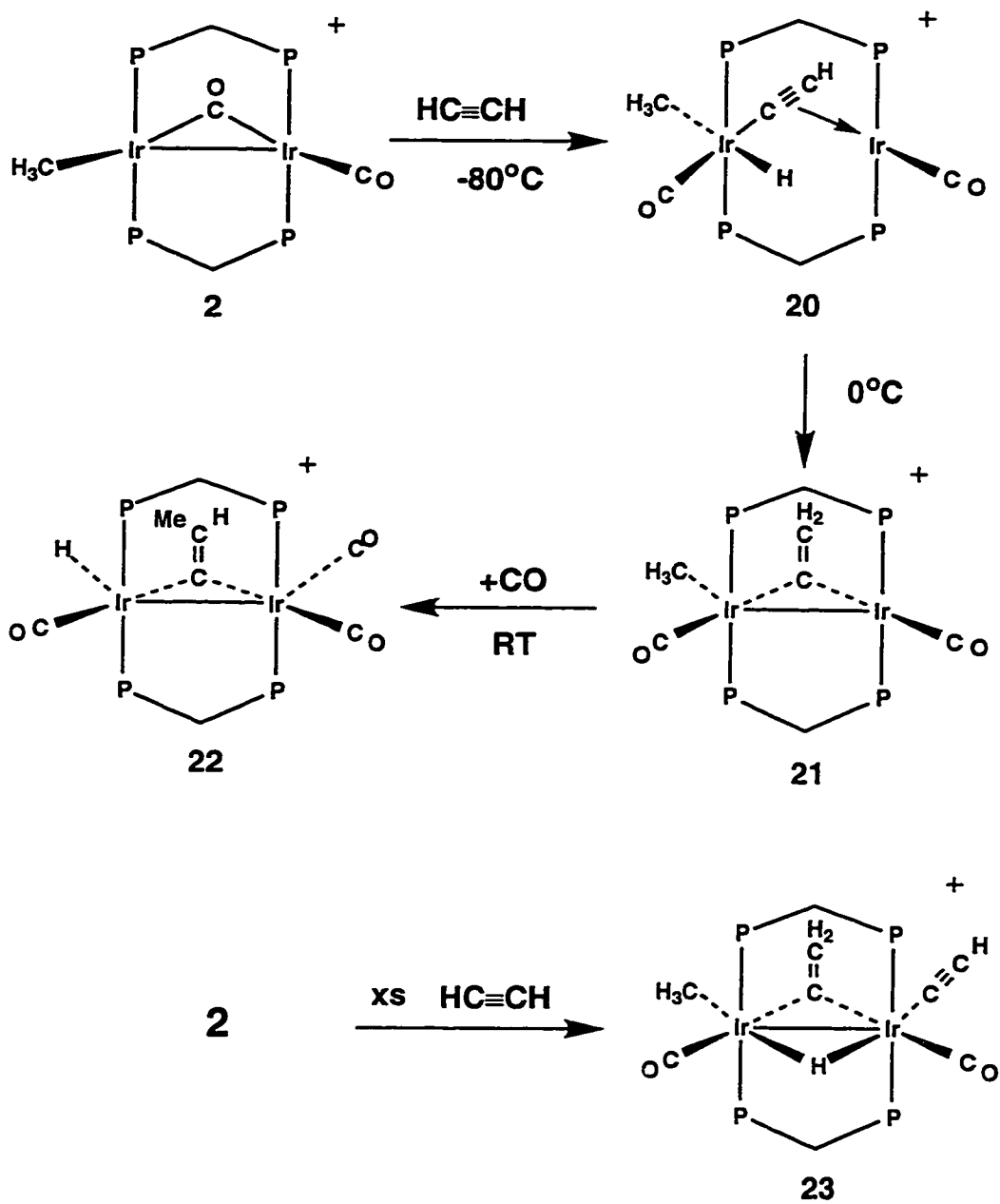
because of the close proximity of the phosphorus resonances, but the proposed trans arrangement of the hydride and methyl ligands is based on similarities between the spectral data of compounds **14** and **17** as well as the previously characterized tricarbonyl species $[Ir_2(CH_3)(H)(CO)_3(\mu\text{-}C\equiv CH)(dppm)_2][CF_3SO_3]$ that was prepared by the low temperature reaction of $[Ir_2(H)(CO)_3(\mu\text{-}CH_2)\text{-}(dppm)_2][CF_3SO_3]$ with acetylene.[9h,10] The $^{13}C\{^1H\}$ NMR spectrum obtained for a sample of **20**, prepared using ^{13}C-enriched acetylene,[19] shows the acetylide α-carbon as a doublet of triplets at δ 124 with $^1J_{C\text{-}C} = 78$ Hz, typical for bridging-acetylide α-carbons,[9h,20] with the β-carbon appearing as a doublet at δ 77. The triplet coupling of the α-carbon to one set of phosphorus nuclei, the lack of phosphorus coupling to the β-carbon and the relatively large carbon-carbon coupling indicates that the acetylide is primarily σ-bound to one iridium center. The weak bridging interaction with the second metal is proposed based on differences in the chemical shifts for bridging vs. terminal acetylides (see characterization of compound **23** *vide infra*). Upon warming to 0°C the vinylidene compound $[Ir_2(CH_3)(CO)_2(\mu\text{-}C=CH_2)(dppm)_2][CF_3SO_3]$ (**21**) begins to appear in solution. The ^1H NMR spectrum of compound **21** shows the vinylidene protons at δ 6.26 and 6.24 as broad signals with the Ir-bound methyl protons appearing at δ -0.20 as a triplet. When compound **21** is prepared with ^{13}C-enriched acetylene the protons of the vinylidene group show coupling of 160 Hz to the β-carbon, consistent with one-bond C-H coupling of an sp^2

hybridized carbon.[21] The $^{13}C\{^1H\}$ NMR spectrum shows the vinylidene α-carbon as a doublet of quintets at δ 218 with $^1J_{C-C}$ = 63 Hz, and the β-carbon as a doublet at δ 124. The quintet coupling of the α-carbon indicates that the vinylidene bridges the two metals with approximately equal coupling to the two different sets of inequivalent phosphorus nuclei. Compound 21 decomposes after a period of 3 days in solution. In an attempt to stop this decomposition process, compound 21 and the mixture of uncharacterized products was allowed to stand for a period of 24 h after which it was reacted with CO, producing the methylvinylidene compound $[Ir_2(H)(CO)_3(\mu\text{-}C=CHMe)(dppm)_2]$-$[CF_3SO_3]$ (22) in about 35% yield as determined by NMR spectroscopy. The many other products remain uncharacterized. Compound 22 is an interesting product of carbon-carbon bond formation in which the methyl group and one of the vinylidene hydrogens have exchanged positions. NMR spectra were gathered on a sample of compound 22 prepared from ^{13}C-methyl labelled compound 2 reacted with ^{13}C-enriched acetylene and purified by recrystallization. The ^1H NMR spectrum shows the vinylidene proton as a broad signal at δ 6.50 with the typical one-bond C-H coupling of 155 Hz.[21] The methyl protons appear as a broad signal at δ 0.84 showing one-bond C-H coupling of 126 Hz, consistent for a sp^3 hybridized carbon[21] when generated from ^{13}C-methyl labelled compound 2, and the terminal hydride appears as a triplet at δ -10.6. In the $^{13}C\{^1H\}$ NMR spectrum the α-carbon of the vinylidene appears as a doublet of quintets at δ 192 showing coupling to the β-carbon and the four

phosphorus nuclei. The β-carbon appears as a doublet of doublets at δ 137 and the methyl substituent of the vinylidene appears as a doublet at δ 24 showing coupling of 42 Hz to the β-carbon.

If compound **2** is reacted with a large excess of acetylene at room temperature, two equivalents of acetylene are incorporated producing the compound $[Ir_2(CH_3)(C≡CH)(CO)_2(\mu-H)(\mu-C=CH_2)(dppm)_2][CF_3SO_3]$ **(23)**, as shown in Scheme 3.3. The bridging vinylidene protons appear as singlets in the ^1H NMR at δ 6.23 and 6.21 showing the typical $^1J_{C-H}$ values for a vinylidene when prepared using ^{13}C-enriched acetylene. The terminal acetylide proton resonance appears at δ 1.87 as a triplet with 1.9 Hz coupling to one set of phosphorus nuclei and 228 Hz coupling to the β-carbon for the ^{13}C-enriched sample. The infrared spectrum displays a stretch at 1574 cm^{-1} for the bridging vinylidene and stretches at 2064 and 2000 cm^{-1} that are assigned to the terminal acetylide and carbonyl groups, respectively. A labelling experiment using a ^{13}CO-enriched sample of compound **23** confirmed the correct assignment for the acetylide and carbonyl bands, showing a lowering of the carbonyl stretch to 1956 cm^{-1} with no change in the acetylide band. The terminal Ir-bound methyl resonance appears as a triplet at δ -0.35 and the bridging hydride appears at δ -14.01 as an apparent septet which upon selective phosphorus decoupling is better described as a triplet of triplets showing 5 and 10 Hz coupling to the two differerent sets of phosphorus nuclei.

In the $^{13}C\{^1H\}$ NMR spectrum the α-carbon of the bridging vinylidene appears as a broad doublet at δ 193.6 and the β-carbon as a doublet at δ 120.2. The acetylide α-carbon appears at δ 61.6 as a doublet of doublets of triplets coupling to the β-carbon, the vinylidene α-carbon and the dppm phosphines, with the β-acetylide carbon appearing at δ 103.7 as a doublet.[18] The iridium-bound methyl carbon appears at δ -5.2 as a triplet. Selective ^{31}P decoupling experiments showed that the methyl and acetylide ligands are on different metals, and the fact that compound **23** did not reductively eliminate methane suggested that a carbonyl separates the methyl and the bridging hydride ligands. The structure proposed in Scheme 3.3 with the methyl, acetylide and vinylidene ligands all on the same face of the complex is supported by the X-ray structure determination, a representation of which is shown in Figure 3.2. A compilation of important bond lengths and angles is given in Table 3.4. The diphosphine groups are oriented approximately trans to each other about the metal centers [P(1)-Ir(1)-P(3) = 176.2(1)°, and P(2)-Ir(2)-P(4) = 176.7(1)°] and are cis to the other ligands. The geometry about each metal is best described as octahedral if we ignore the metal-metal bond. The metal-metal bond length of 2.9460(9) Å is longer than typically observed for an Ir-Ir single bond, but this lengthening is in line with the presence of a bridging hydride ligand.[22] The hydride ligand was not located but was fixed in the bridging position shown, based upon ^1H NMR data. The carbonyl ligands are both terminal, opposite the bridging vinylidene group, with the methyl and acetylide ligands
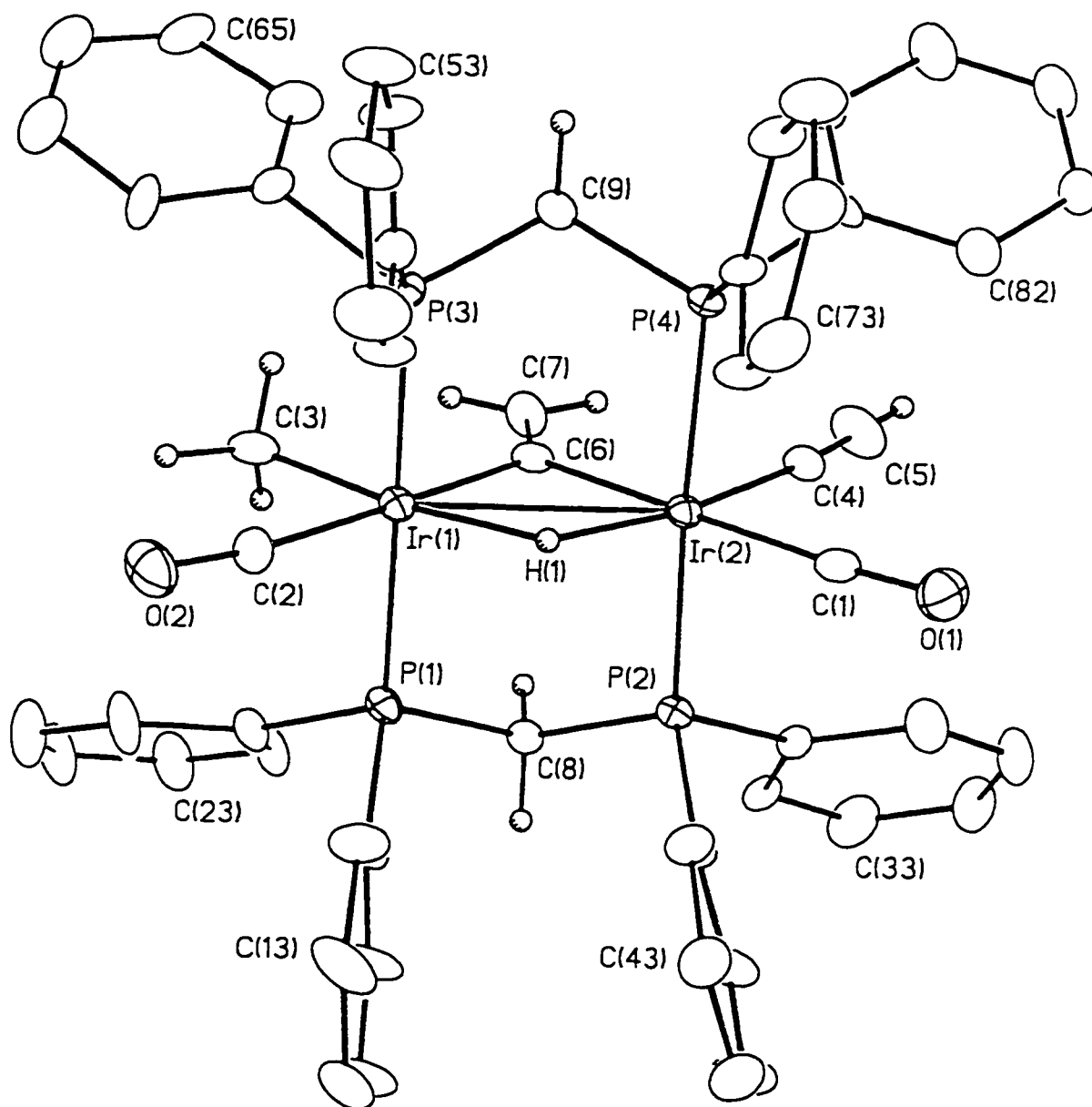
Figure 3.2 Perspective view of the $[Ir_2(CH_3)(C\equiv CH)(CO)_2(\mu\text{-}H)(\mu\text{-}C=CH_2)$ $(dppm)_2]^+$ cation of compound **23**. Thermal ellipsoids are shown at the 20% probability level except for hydrogens which are shown arbitrarily small. Phenyl hydrogens have been omitted.

Table 3.4 Selected Interatomic Distances and Angles for Compound **23**.

(a) Distances (Å)

Atom1	Atom2	Distance	Atom1	Atom2	Distance
Ir1	Ir2	2.9460(9)	Ir2	C6	2.09(1)
Ir1	C2	1.90(2)	Ir2	P2	2.340(4)
Ir1	C3	2.13(2)	Ir2	P4	2.337(4)
Ir1	P1	2.354(4)	O1	C1	1.15(2)
Ir1	P3	2.345(4)	O2	C2	1.14(2)
Ir1	C6	2.07(2)	C4	C5	1.13(2)
Ir2	C1	1.94(2)	C6	C7	1.31(2)
Ir2	C4	2.01(2)			

(b) Angles (deg)

Atom1	Atom2	Atom3	Angle	Atom1	Atom2	Atom3	Angle
Ir2	Ir1	C2	137.0(5)	P2	Ir2	P4	176.7(1)
Ir2	Ir1	C3	132.2(5)	C1	Ir2	C4	93.7(7)
Ir2	Ir1	C6	45.4(4)	C1	Ir2	C6	178.7(6)
P1	Ir1	P3	176.2(1)	C4	Ir2	C6	87.6(6)
C2	Ir1	C3	90.8(7)	Ir2	C1	O1	170.7(15)
C2	Ir1	C6	177.5(7)	Ir1	C2	O2	167.8(17)
C3	Ir1	C6	86.8(6)	Ir2	C4	C5	174.1(18)
Ir1	Ir2	C1	134.1(5)	Ir1	C6	Ir2	90.0(6)
Ir1	Ir2	C4	132.2(5)	Ir1	C6	C7	135.0(13)
Ir1	Ir2	C6	44.6(4)	Ir2	C6	C7	135.0(13)

on the opposite face, trans to the bridging hydride. The metal-ligand bond lengths and angles compare well with those seen in structures with similar ligands. The vinylidene symmetrically bridges the two metals with Ir-C(6) distances of 2.07(2) Å and 2.09(1) Å, and an Ir(1)-C(6)-Ir(2) angle of 90.0(6)° in good agreement with the parameters observed in the bridging vinylidene ligands in $[Ir_2I_2(CO)_2(\mu\text{-}CCH_2)(dppm)_2]$ and $[Ir_2I_2(CO)_2\text{-}(\mu\text{-}CC(H)Ph)(dppm)_2]$.[9e] The C(6)-C(7) bond distance of 1.31(2) Å corresponds to a normal double bond in an olefinic unit.[23] The methyl ligand has an iridium-carbon bond length of 2.13(2) Å, similar to those observed in the structure of compound **11** and in the structures of $[Ir_2(CH_3)(CO)(\mu\text{-}CO)(dppm)_2][CF_3SO_3]$ (**2**) (2.15(2) Å), $[Ir_2(CH_3)\text{-}(CO)_3(\mu\text{-}F_2C{=}CF_2)(dppm)_2][CF_3SO_3]$ (**32**) (2.17(2) Å) and $[Ir_2(CH_3)\text{-}(CO)_2(\mu\text{-}\eta^1\text{-}\eta^3H_2CCCH_2)(dppm)_2][CF_3SO_3]$ (**36**) (2.19(1) Å). The acetylide ligand is σ-bound to Ir(2) with a metal-carbon bond length of 2.01(2) Å, similar to the distance seen for the terminal acetylide in $[RhIr(C{\equiv}CPh)(CO)_2(\mu\text{-}H)\text{-}(\mu\text{-}C{\equiv}CPh)(dppm)_2][CF_3SO_3]$.[9h] The difference observed in the carbon-carbon distances for the vinylidene (C(6)-C(7) = 1.31(2) Å) and acetylide (C(4)-C(5) = 1.13(2) Å) ligands is consistent with the double and triple bond orders, respectively. Since the structural parameters involving the carbonyl and acetylide groups do not easily distinguish the two; Ir(2)-C(1) = 1.94(2) Å, Ir(2)-C(4) = 2.01(2) Å, C(4)-C(5) = 1.13(2) Å, C(1)-O(1) = 1.15(2) Å, Ir(2)-C(4)-C(5) = 174.1(18)°, Ir(2)-C(1)-O(1) =170.7(15)°, there was some doubt about the formulation shown in Figure 3.2. Two other solutions seemed possible: (1) the

carbonyl (C(1)O(1)) and the acetylide group could be disordered, i.e. two isomers could be present; or (2) these groups could be completely interchanged such that the carbonyl could be misidentified as the acetylide group. $^{31}P\{^1H\}$ and ^1H NMR spectra obtained from the crystals used for the X-ray study indicated that only one isomer was present discounting the possibility of the disordered model. Switching the positions of the acetylide C(5) and carbonyl O(1) atoms (giving the C(4)O(1) carbonyl and C(1)C(5) acetylide) resulted in poor refinement of the β-carbon and oxygen thermal parameters such that the the acetylide β-carbon thermal parameter became abnormally small and the oxygen thermal parameter became abnormally large. It was therefore concluded that the acetylide and carbonyl ligands were in the correct positions as shown, with no disorder. Although the bridging-hydride ligand was not located crystallographically, its position is assigned on the basis of ^1H NMR spectroscopic data and the geometry of the other ligands present in the compound.

So far the reactions of 2 with alkynes proceed differently than described in Chapter 2 for compound 2 with other small molecules, in that the alkyne reactions left the methyl group intact and did not give rise to C-H bond cleavage of this group. Furthermore, in only one case, the reaction with acetylene, did the targetted C-C bond formation occur. Reactions with internal, non-activated alkynes exhibited the desired C-C bond formation as described below.

Reaction of 2-butyne with 2 occurred much as those described for HFB and DMAD, initially giving a product $[Ir_2(CH_3)(CO)_2(\mu\text{-}CH_3C\equiv CCH_3)(dppm)_2]\text{-}$

[CF$_3$SO$_3$] (**24**), (see Scheme 3.4) in which the alkyne group bridges the two metals as was observed for compounds **9-13**. The assignment of the structure of compound **24** as a bridging-alkyne is based upon similarities with the ^{31}P{^{1}H} and ^{1}H NMR data for compound **9**. However, upon stirring for 24h at ambient temperature, compound **24** transforms into the unusual vinylcarbene compound [Ir$_2$(H)(CO)$_2$(μ-η^1:η^3-HCC(Me)=CHMe)(dppm)$_2$][CF$_3$SO$_3$] (**25**). The ^{31}P{^{1}H} NMR spectrum shows a complex pattern with four individual resonances at δ -5.8, -6.0, -34.3, -37.8, indicating an ABCD spin system. Figure 3.3 shows the ^{31}P{^{1}H} NMR spectra for compounds **24** and **25** for comparison. The ^{1}H NMR spectrum of **25** shows the bridgehead or carbene proton as a multiplet at δ 8.79,[24] with the methyl groups on the vinyl substituent appearing as a doublet and a broad multiplet at δ 2.72 and 1.42, respectively, and the hydride resonance appearing as a complex multiplet at δ -11.25. Two dimensional ^{1}H-^{13}C correlation NMR data help in determining the dppm methylene proton resonances at δ 7.12, 5.83, 4.60 and 3.78 with the vinyllic hydrogen resonance appearing at δ 3.29. The ^{13}C{^{1}H} NMR spectrum shows two terminal carbonyl resonances as a multiplet at δ 170.9 and a broad singlet at δ 168.2. The carbene carbon appears at δ 138.4[24] as a triplet with the vinyl resonances appearing as a singlet at δ 110.2 for the α-carbon and as a multiplet at δ 56.2 for the β-carbon. The α and β methyl-substituents on the vinyl appear as singlets at δ 23.4 and 18.1, respectively. The ^{13}C{^{1}H} NMR spectrum of a sample of

Scheme 3.4
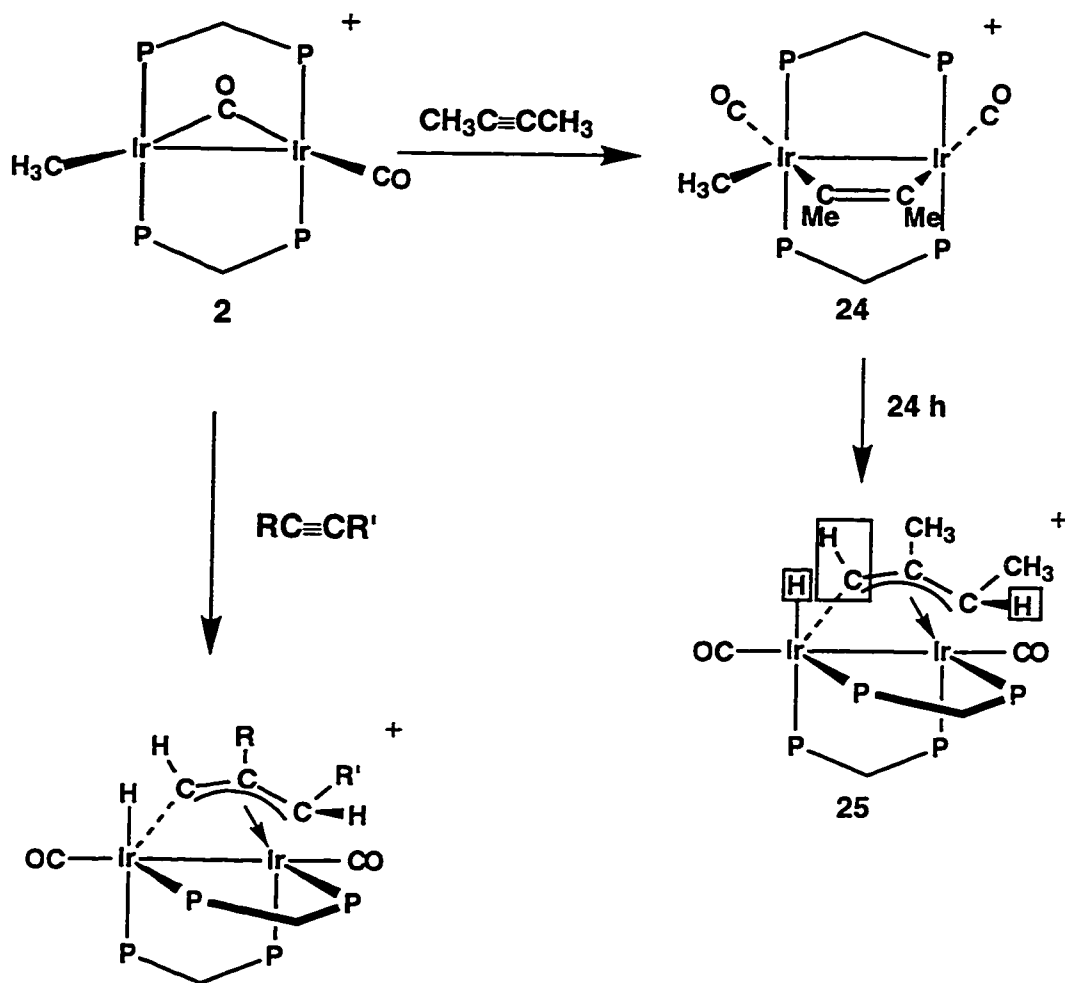
26: R = R' = Et
27a: R = CH₃, R' = CH₂CH₃
27b: R = CH₂CH₃, R' = CH₃
28a: R = CH₃, R' = C₆H₅
28b: R = C₆H₅, R' = CH₃
29: R = R' = nPr

Scheme 3.4

26: $R = R' = Et$
27a: $R = CH_3$, $R' = CH_2CH_3$
27b: $R = CH_2CH_3$, $R' = CH_3$
28a: $R = CH_3$, $R' = C_6H_5$
28b: $R = C_6H_5$, $R' = CH_3$
29: $R = R' = nPr$

^{31} P NMR spectrum
for compound **24**

^{31} P NMR spectrum
for compound **25**
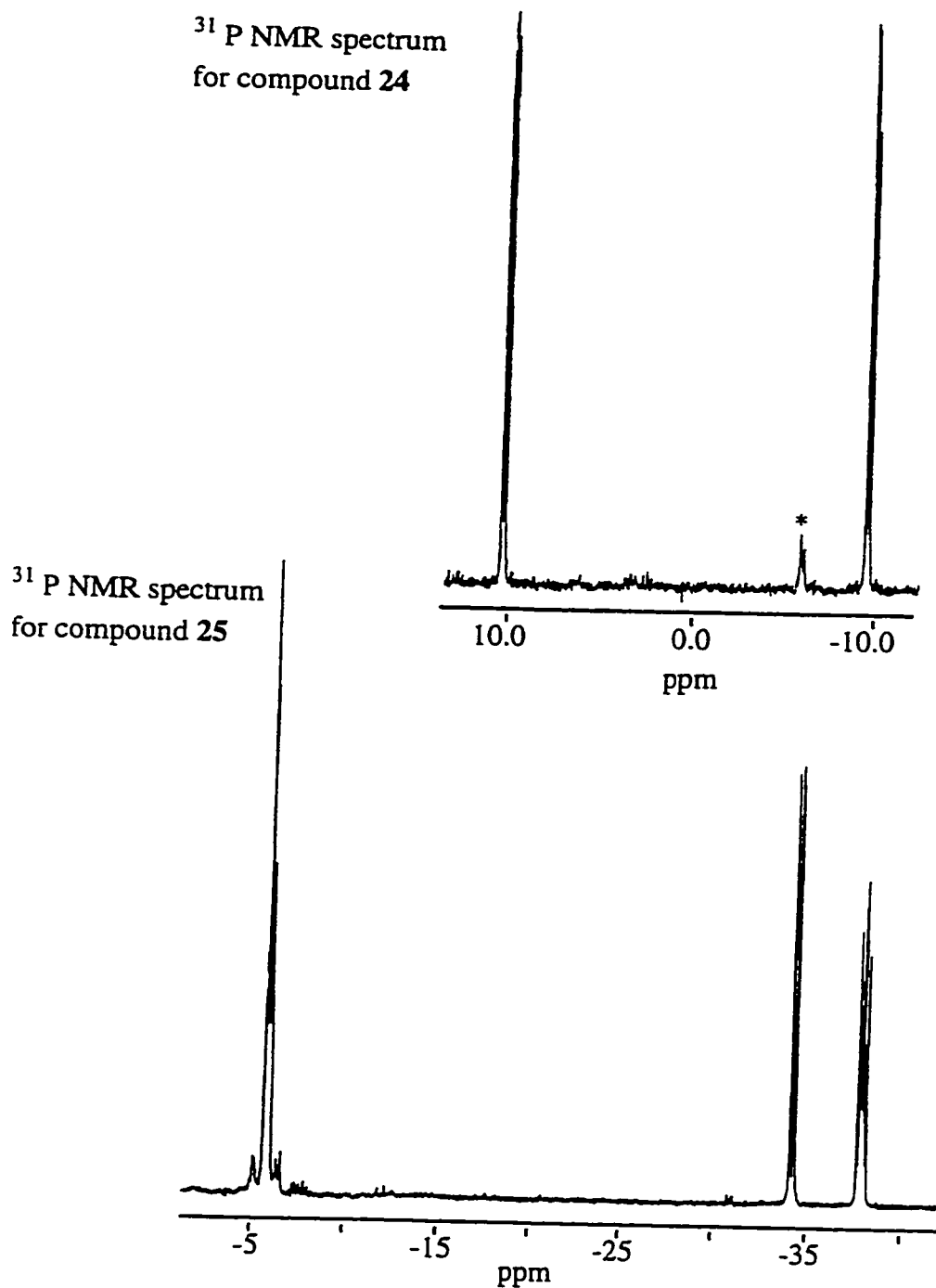
Figure 3.3 ^{31}P{^{1}H} NMR spectra for the compounds [Ir$_2$(CH$_3$)(CO)$_2$-
(μ-CH$_3$C≡CCH$_3$)(dppm)$_2$][CF$_3$SO$_3$] (**24**) (top) and
[Ir$_2$(H)(CO)$_2$(μ-η$_1$:η$_3$-HCC(Me)=CHMe)(dppm)$_2$][CF$_3$SO$_3$] (**25**)
(bottom), illustrating the difference between the typical AA'BB' pattern
observed when the phosphines are trans (**24**) and the ABCD pattern
observed when the phosphines are cis (**25**). * denotes impurity.

compound **25** prepared using ^{13}C-methyl labelled compound **2** shows that the methyl carbon is incorporated only into the carbene or bridgehead position. The fragments of the original Ir-bound methyl group are shown in boxes in Scheme 3.4.

Compound **2** reacts similarly with other internal alkynes producing the vinylcarbene compounds **26-29** $[Ir_2(H)(CO)_2(\mu-\eta^1:\eta^3-HCC(R)=CHR')(dppm)_2]$-$[CF_3SO_3]$ (R = R' = Et (**26**); R = Me, R' = Et (**27**); R = Me, R' = Ph (**28**); R = R' = nPr (**29**)) (outlined in Scheme 3.4). The characterization of each of these compounds is based on similarities with the spectral data of compound **25**. They all show similar ABCD patterns in the $^{31}P\{^1H\}$ NMR spectra and have a characteristic downfield shift in the ^1H NMR spectra between δ 8.79 to 9.22 for the proton on the bridgehead carbon. Positive assignment of all the other ^1H NMR resonances proved to be very difficult due to the number, overlap and complexity of the signals, and so is incomplete. Compounds **27** and **28**, prepared using unsymmetrical alkynes added an increased difficulty in that isomers were produced depending on which substituent was on the α- or β-carbon of the resulting vinyl portion of the ligand. The isomers of compound **27** were produced in a 1:1 ratio while those of **28** appeared in a 4:1 ratio. The ratio for the isomers of **27** could not be determined from the $^{31}P\{^1H\}$ NMR spectra because of the coincidental overlap of the signals and instead was determined by ^1H NMR experiments with ^{31}P broadband decoupling. Upon decoupling, the carbene proton signal collapsed to two singlets instead of one

singlet, which would be expected if there were only one isomer. In addition, two of the dppm methylene signals collapsed upon ^{31}P broadband decoupling to pseudo triplets instead of the expected doublets, indicating the overlap of signals. The ^{31}P{^{1}H} NMR spectrum for compound **28** gave signals that were separated enough to determine the ratio of the isomers as 4:1. In addition, in the ^{1}H NMR spectrum the carbene proton resonances are separated enough to distinguish between the two species but the hydride signal is broad and featureless, indicative of overlap for two signals.

The proposed structure for **26** and its analogues **(25,27-29)** is supported by the X-ray structure determination of **26**, a representation of which is shown in Figure 3.4, with an alternate view, in which only the ipso carbons of the phenyl groups appear, represented in Figure 3.4.1. A compilation of important bond lengths and angles is given in Table 3.4. This structure confirms the vinylcarbene-bridged, hydride formulation. The diphosphine groups are in a cis position with angles of 96.79 (6)° and 98.39 (6)° for P(1)-Ir(1)-P(3), and P(2)-Ir(2)-P(4), respectively, and the Ir-Ir distance of 2.7623 (7) Å is typical of a metal-metal bond.[25] The carbonyls are terminally bound to each metal and the vinylcarbene moiety asymmetrically bridges the metals; η^1-bound to Ir(2) (Ir(2)-C(3) = 2.064(7)Å) and η^3-bound to Ir(1) (Ir(1)-C distances: 2.207(6), 2.233(6), 2.220(7)Å). The C(3)-C(6) and C(6)-C(7) bonds of the resulting fragment (1.440(10), 1.431(9)Å) are typical of an η^3-bound allyl group.[26] In this geometry the vinylcarbene unit can equally well be considered as a metallaallyl moiety, and both formulations have previously been considered.[27]
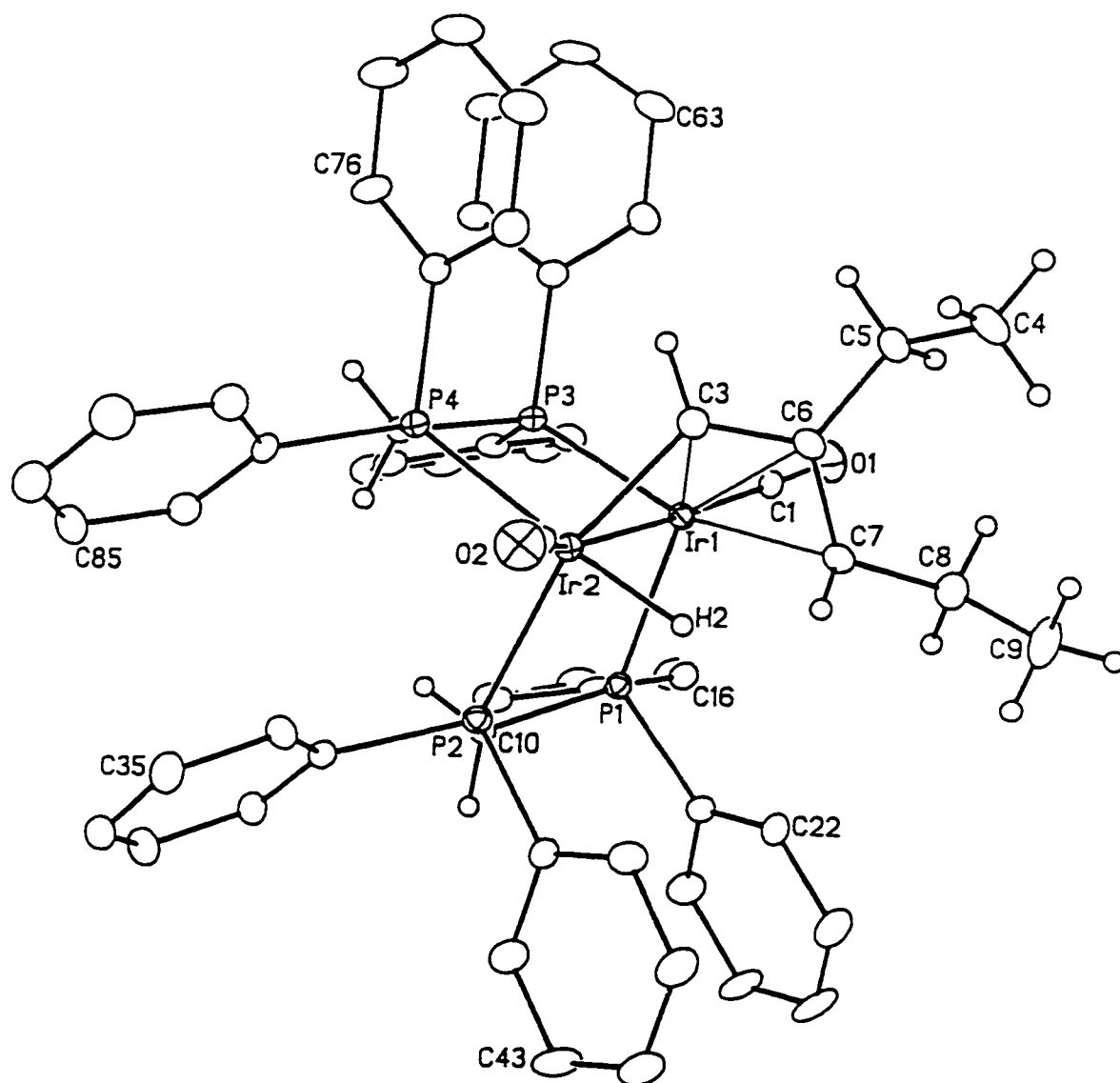
Figure 3.4 Perspective view of the [Ir₂H(CO)₂(μ-η³:η¹-HCCEtCHEt)(dppm)₂]⁺ cation of compound **26**. Thermal ellipsoids are shown at the 20% probability level except for hydrogens which are shown arbitrarily small. Phenyl hydrogens have been omitted.
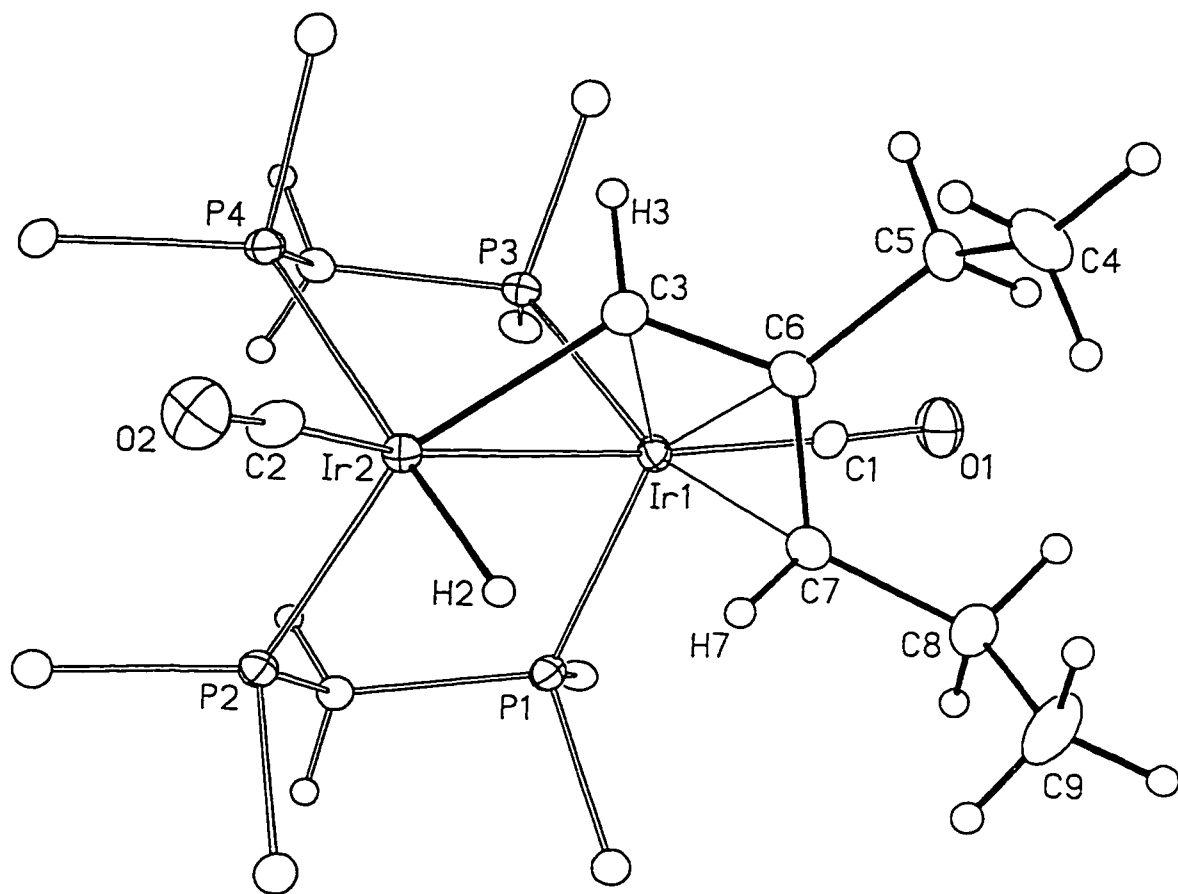
Figure 3.4.1 Alternate view of the [Ir₂H(CO)₂(μ-η³:η¹-HCCEtCHEt)-(dppm)₂]⁺ cation of compound **26**. Only the ipso carbons of the dppm phenyl rings are shown.

Table 3.5 Selected Interatomic Distances and Angles for Compound **26**.

(a) Distances (Å)

Atom1	Atom2	Distance	Atom1	Atom2	Distance
Ir1	Ir2	2.7623(7)	Ir2	C3	2.064(7)
Ir1	P1	2.329(2)	O1	C1	1.164(8)
Ir1	P3	2.361(2)	O2	C2	1.141(8)
Ir1	C1	1.864(7)	C3	C6	1.440(10)
Ir1	C3	2.207(6)	C4	C5	1.505(10)
Ir1	C6	2.233(6)	C5	C6	1.520(9)
Ir1	C7	2.220(7)	C6	C7	1.431(9)
Ir2	P2	2.322(2)	C7	C8	1.497(10)
Ir2	P4	2.372(2)	C8	C9	1.503(11)
Ir2	C2	1.869(7)			

(b) Angles (deg)

Atom1	Atom2	Atom3	Angle	Atom1	Atom2	Atom3	Angle
Ir2	Ir1	C1	168.8(2)	Ir2	C2	O2	175.5(7)
Ir2	Ir1	C3	47.5(2)	Ir1	C3	Ir2	80.5(2)
Ir2	Ir1	C6	76.9(2)	Ir1	C3	C6	72.1(4)
Ir2	Ir1	C7	83.1(2)	Ir2	C3	C6	126.0(5)
P1	Ir1	P3	96.79(6)	C4	C5	C6	111.6(6)
C1	Ir1	C3	122.3(3)	Ir1	C6	C3	70.1(4)
C1	Ir1	C6	91.9(3)	Ir1	C6	C5	127.5(5)
C1	Ir1	C7	88.3(3)	Ir1	C6	C7	70.7(4)
C3	Ir1	C6	37.9(2)	C3	C6	C5	119.8(6)
C3	Ir1	C7	67.1(2)	C3	C6	C7	116.9(6)
C6	Ir1	C7	37.5(2)	C5	C6	C7	123.3(6)
Ir1	Ir2	C2	159.6(2)	Ir1	C7	C6	71.8(4)
Ir1	Ir2	C3	52.0(2)	Ir1	C7	C8	123.9(5)
P2	Ir2	P4	98.39(6)	C6	C7	C8	124.2(6)
C2	Ir2	C3	109.3(3)	C7	C8	C9	112.6(7)
Ir1	C1	O1	175.8(6)				

Discussion

With the activated alkynes (DMAD, HFB, and methyl propiolate), one type of product was observed in the reactions with compound **2**, in which reaction at the alkyne triple bond yields the alkyne-bridged products $[Ir_2(CH_3)(CO)_2\text{-}(\mu\text{-}RC{\equiv}CR')(dppm)_2][CF_3SO_3]$ **(9,12,13)**. Suprisingly, migratory insertion involving the alkyne and the methyl group, as was observed in the analogous reaction of the tricarbonyl species **(1)** with DMAD, was not observed for the dicarbonyl compound **2**. It appears that once these alkynes, having strong electron-withdrawing substituents, adopt a position bridging the metals, subsequent migratory insertion is inhibited. The inertness of the alkyne when bound as a cis-dimetallated olefin has previously been reported,[13j,k,28] and is presumably caused by the strong $Ir\text{-}C_{alkyne}$ bonds that result. As a comparison it should be recalled that alkyl groups having electron withdrawing substituents (cf. CF_3) are much more inert to migratory insertion than the unsubstituted alkyls.[29]

It was thought that additional reaction of the DMAD adduct with simple Lewis bases like CO or PMe_3 might induce migratory insertion, since the tricarbonyl species **1** had given the migratory insertion product. Furthermore, the additional crowding about the metals, particularly upon addition of PMe_3 would tend to favor the migratory insertion product, by movement of the methyl from the metal to the alkyne, and concommitant movement of the resulting vinyl moiety to a single metal.[9h] In reactions with both CO and PMe_3 the simple adducts were obtained with the added ligand occupying the vacant

coordination site. Further conversion was not observed in either case, even under reflux.

The difference in reactivity of electrophilic alkynes observed for compound **2** compared to **1** is presumably due to the extra steric crowding of **1** that imparts either a different initial site of attack of the alkyne or a different initial coordination mode (presumably terminal η^2), not allowing the bridging-alkyne mode to be obtained.

The reactions of compound **2** with nonactivated 1-alkynes at low temperature all initially yield an intermediate in which the 1-alkyne has undergone C-H bond cleavage producing an acetylide hydride product $[Ir_2(CH_3)(H)(CO)_2(\mu-C\equiv CR)(dppm)_2][CF_3SO_3]$ (R = Me (**14**), Ph (**17**), H (**20**)). Upon warming, the methyl- and phenylacetylide compounds, **14** and **17**, transform into the alkyne-bridged compounds $[Ir_2(CH_3)(CO)_2(\mu-HC\equiv CR)-(dppm)_2][CF_3SO_3]$ (R = (Me) **15**, (Ph) **18**), respectively, via H-transfer from the metal back to the acetylide α-carbon.

There is a further transformation of **15** and **18** upon warming to ambient conditions, into the bridging acetylide complexes $[Ir_2(CO)_2(\mu-C\equiv CR)(dppm)_2]-[CF_3SO_3]$ (R = Me (**16**), Ph (**19**)) with loss of methane (implied by the loss of the methyl signal displaying ^{31}P coupling and no appearance of a hydride signal). These bridging acetylides are similar to compounds produced in other studies.[9h,10,17] The loss of methane is assumed to go through an undetected methyl acetylide hydride intermediate similar to compounds **14** and **17** but with

124 of the hydride ligand from one face of the

a cis orientation of the methyl and hydride ligands that would facilitate the reductive elimination of methane.

Compound **20**, having an unsubstituted acetylide, is initially formed as for the methyl- and phenylacetylide reactions. However, hydrogen transfer in this case yields a bridging vinylidene product (**21**) instead of an acetylene-bridged product. The transformation of a 1-alkyne into a vinylidene group is well documented[4] and has been shown to occur readily in the presence of adjacent metal centers,[30] probably because of the mobility of the acetylide and hydride ligands around the metal core. Two pivotal transformations that allow the acetylide/hydride-to-vinylidene transformation to occur are the "windshield wiper" motion of the acetylide ligand in which it transforms from σ-bound to one metal and π-bound to the other to the opposite arrangement, as shown below,

$$
\begin{array}{ccc}
\underset{\text{M}}{\diagup}\overset{\text{R}}{\underset{\text{C}\equiv\text{C}}{}}\searrow_{\text{M}}
& \rightleftharpoons &
\underset{\text{M}}{\diagup}\overset{\overset{\text{R}}{\underset{\text{C}}{\|}}}{\underset{\text{C}}{}}\searrow_{\text{M}}
& \rightleftharpoons &
\underset{\text{M}}{\diagup}\overset{\text{R}}{\underset{\text{C}\equiv\text{C}}{}}\searrow_{\text{M}}
\end{array}
$$
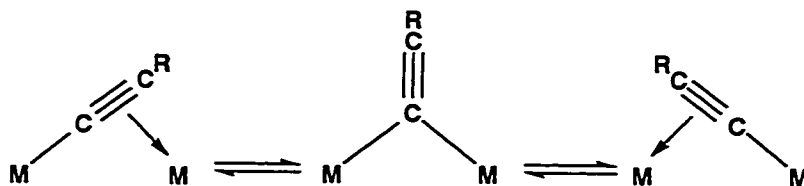
and the facile migration of the hydride ligand from one face of the M_2P_4 unit to the other by "tunneling" between the metals, a number of examples of which are known.[31] Together these two processes allow a rationalization of the acetylide/hydride-to-vinylidene transformation as outlined below.[32] Rotation of the acetylide-hydride unit on one metal about the P-Ir-P axis can transform the acetylide from a bridging interaction to a terminal mode while the terminal hydride alleviates the loss of electron density at the other metal by forming a

bridging interaction (i to ii). The hydride can then 'tunnel' between the metals to the opposite face of the compound (iii). Again this merely involves twisting about the P-Ir-P axis, and results in no substantial change in bonding within the Ir-H-Ir moiety. A reversal of the first step occurs, in which clockwise rotation about the metal on the left forces the bridging hydride into a terminal position and the terminal acetylide reforms the bridging interaction, bringing the hydride
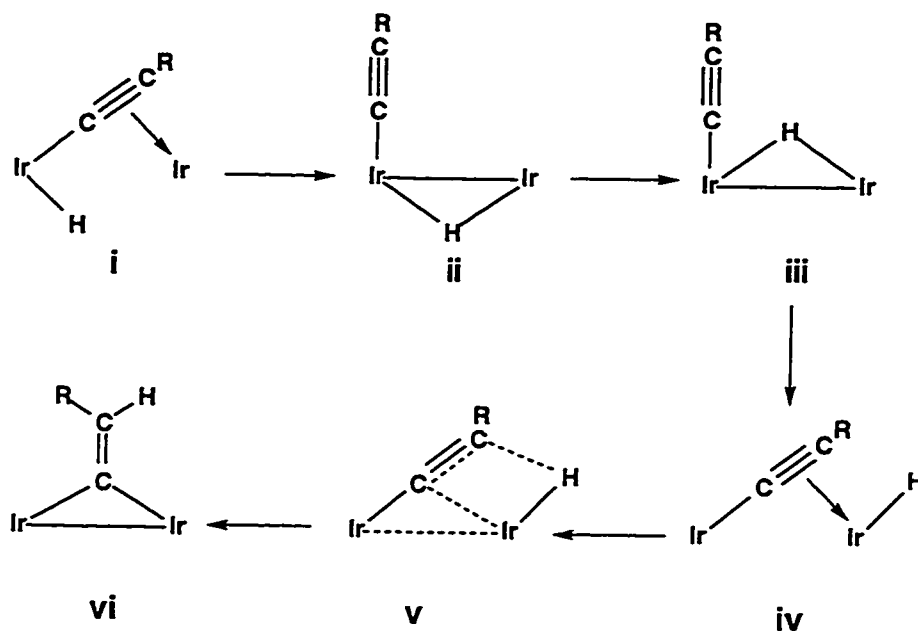
and β-carbon of the acetylide into close proximity (iv), allowing facile ligand transfer of the hydride to the acetylide to yield the vinylidene (v to vi). It must be pointed out that the ancillary ligands, not shown in the generic scheme, can also migrate from metal to metal, maintaining appropriate valence electron counts.

For the vinylidene methyl species (**21**), there was no loss of methane as is observed in the propyne and phenylacetylene reactions. Instead, compound

21 was found to transform slowly over several days into numerous uncharacterizable products. Presumably this decomposition was facilitated by the open coordination site on one of the metal centers. In a previous study[9h] the analogous phenylvinylidene species $[Ir_2(CH_3)(CO)_3(\mu\text{-}C=C(H)Ph)(dppm)_2]$-$[CF_3SO_3]$ was found to be stable for prolonged periods of time, presumably due to the coordinative saturation. In an attempt to stabilize compound 21, CO was added to the reaction mixture at room temperature, 24 h after compound 21 was prepared, giving ample time for conversion of 20 to 21. Suprisingly, CO addition did not merely generate the vinylidene-bridged, tricarbonyl species but instead yielded 22, in which exchange of the methyl group and one of the vinylidene hydrogens has occurred. A proposal accounting for this transformation is shown in Scheme 3.5. Initially migration of the methyl ligand to the α-carbon of the vinylidene can occur producing a vinyl species, which may then undergo C-H activation producing a propyne-hydride. The transformation of a 1-alkyne to a vinylidene is well known and can occur producing the vinylidene-hydride product. The open coordination site is then taken by the carbonyl ligand. Although we have no direct evidence for this proposal, a complicated broad resonance in the $^{13}C\{^1H\}$ NMR spectrum at δ 170, obtained on a sample of compound 21 in which the acetylene and methyl ligands were ^{13}C-enriched may be consistent with the α-carbon of a vinyl species, similar to the one shown in Scheme 3.5.

Scheme 3.5
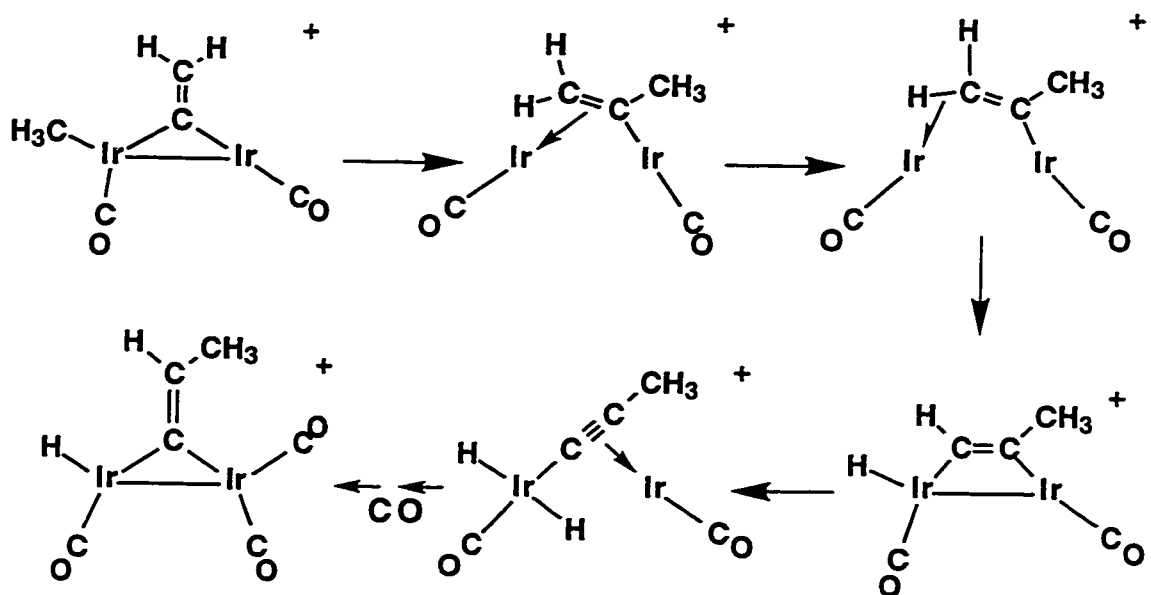
It is not known why different rearrangements were observed for the methyl-and phenylacetylide species (**14**, **17**) compared to the unsubstituted acetylide (**20**). Presumably steric interactions for the hydrogen substituent of **20** are less demanding than for the methyl or phenyl groups of **14** and **17**, allowing the vinylidene production from the unsubstituted acetylide.

When compound **2** is reacted with an excess of acetylene we see incorporation of two equivalents of acetylene in the form of a vinylidene, an acetylide and a hydride ligand to form compound **23** as shown in Scheme 3.3. With all three organic fragments on one face of the complex, it appears to be a prime candidate for C-C bond formation. However, this is not observed, even under reflux conditions. This lack of further reactivity is presumably due to the coordinative saturation at the metal centers.

In the reaction of compound **2** with nonactivated, internal-alkynes, the first products observed are the kinetic products having the alkyne bridging the the metals. These species are spectroscopically similar to the DMAD and HFB adducts with a terminal methyl group and $^{31}P\{^1H\}$ NMR signals in similar regions. Presumably the activated alkynes bind too strongly and are stable as such. However, with the non-activated alkynes, the initial products transform to thermodynamic products, which have arisen from formal activation of two C-H bonds of the methyl group, C-C bond formation between the resulting methyne carbon and one of the acetylenic carbons, and H transfer to the other acetylenic carbon. This conversion occurs for a number of internal alkynes, and although characterization of their products is not complete, 2-pentyne, 1-phenylpropyne and 4-octyne each reacts in a similar manner with **2**, proceeding through an uncharacterized red intermediate to a yellow product, having NMR spectral parameters much like those of **25** and **26**, except that the two unsymmetrical alkynes yield two isomers. The isomers observed for compounds **27** and **28** presumably arise from C-C bond formation through one end of the alkyne or the other. For compound **27** the steric difference between the ethyl and methyl portions is apparently inconsequential and we therefore see a 1:1 ratio for the isomers produced, but in the reaction of 1-phenylpropyne and compound **2**, the phenyl group exerts a steric influence substantially different from the methyl group favoring one structure over the other as is shown by the isomer ratio of 4:1. It is not known which isomer of **28** is more abundant, the one with the phenyl substituent on the β-carbon of the vinylcarbene (shown in **A** below) or

the one with the methyl substituent on the β-carbon of the vinylcarbene (**B**) but based on steric arguments if the initial insertion (see later) exhibits some steric control then we would expect **B** to be preferentially formed.
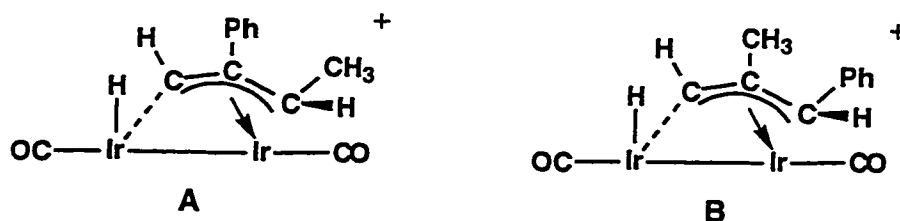
dppm ommitted for clarity

Vinylcarbene compounds, analogous to compounds **25-29** are well known,[26,32] and are typically generated by addition of alkynes to bridging methylene compounds. Their generation from a methyl complex and alkynes is unprecedented and deserves comment. A unified proposal for the formation of these vinylcarbene products, that is also consistent with the results in the reactions of **2** with CO, SO_2 and other groups, in which there is C-H bond cleavage of the methyl ligand, is summarized in Scheme 3.6. We propose that the alkyne adducts rearrange to the methylene-bridged hydride products **A**, analogous to the products in the reactions of CNR, PR_3, CO and SO_2. Migratory insertion involving the alkyne and the hydride ligand would yield the substituted vinyl species **B**, as is commonly observed. A vinyl-to-methylene migration, as proposed by Maitlis,[33] would yield an allyl product, possibly having a structure such as **C**, and carbon-hydrogen bond cleavage at the *least substituted end* of the allyl group, by the adjacent metal, would yield the final vinylcarbene products (**D**). It is also possible that a direct insertion of the alkyne into the

bridging-methylene group could occur to give a bridged -CH$_2$C(R)=C(R)-moiety, followed by a 1,3 sigmatropic shift of one hydrogen, to yield the vinyl carbene products, and this possibility has not yet been discounted.

Scheme 3.6

L = RC≡CR'
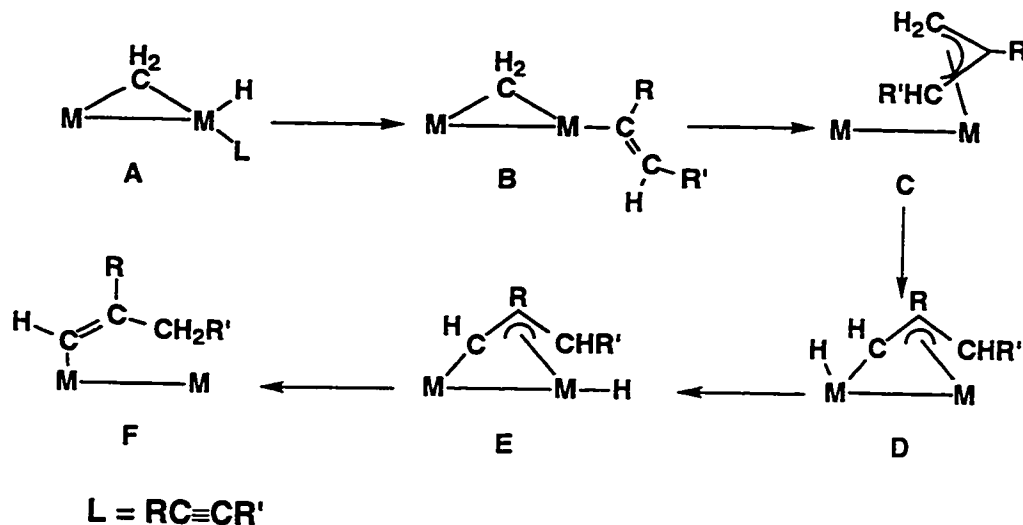
A vinyl-to-methylene migration has been proposed by Maitlis to be involved in the initiation and propagation steps of the Fischer-Tropsch reaction as outlined in Scheme 3.7.[34] One of the key transformations in the Maitlis scheme, the allyl-to-vinyl isomerization, has little literature precedent.[35] Significantly, the reaction outlined in Scheme 3.6 suggests a plausible mechanism for this isomerization in the conversion of the allyl complex C to D; this step could be followed by migration of the hydride to the adjacent metal (species E) and by subsequent transfer to the terminal carbon of the vinylcarbene moiety, yielding the vinyl complex (F). We have no direct

evidence of the last steps (**D** → **E** → **F**) in this proposed transformation and have been unable up to this point to induce such reactions.

Scheme 3.7
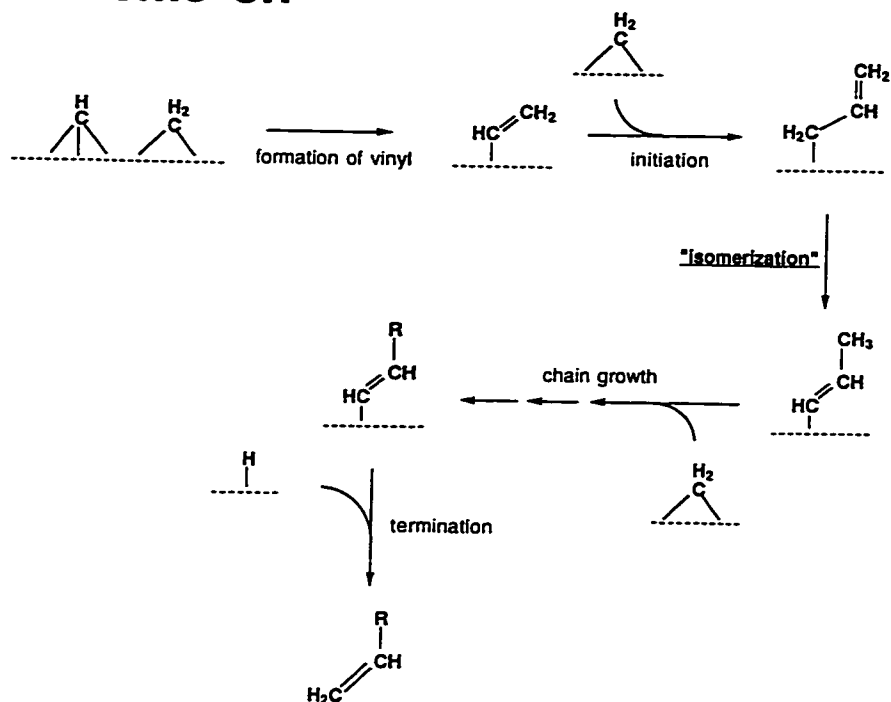
Summary

Compound **2** shows diverse reactivity with a number of different alkynes. Three basic reactivities are observed. For the alkynes with electron withdrawing substituents the alkyne moiety bridges the metals in a cis-dimetallated olefin geometry and these ligands bind strongly to the electron-rich metals and undergo no further transformations. With non-activated 1-alkynes, initial oxidative addition of the alkyne yields an acetylide-hydride species. The subsequent species, containing methyl, hydride and acetylide groups then

underwent a series of rearrangements in which either loss of methane occurred (HC≡CR reactions) or in which the methyl group ulimately ended up on the β-carbon of the acetylide group to give a methylvinylidene product. It is not clear why these two pathways are followed, but presumably subtly different factors give rise to adjacent methyl and hydride ligands leading to methane elimination for the propyne and phenyl acetylene reactions but not in the acetylene reaction.

The reaction with internal alkynes proved to be the most interesting, first proceeding through an alkyne-bridged species that slowly transforms into a vinylcarbene compound. The observation of the bridged kinetic product prior to the vinylcarbene species indicates the lability of the organic substrate in the bridging mode. We believe it is the lability of the organic substrate that provides the opportunity for the thermodynamic pathway to be followed, yielding the C-C bond formation product. The implication for this reaction in a proposed Fischer-Tropsch mechanism has been discussed.

References

1. Davidson, J. L. Reactions of Coordinated Acetylenes. In *Reactions of Coordinated Ligands*; Braterman, P. S., Eds.; Plenum Press: New York, 1986; Vol. 1, p 825.

2. Collman, J. P.; Hegedus, L. S.; Norton, J. R.; Finke, R. G. *Principles and Apllications of Organotransition Metal Chemistry*; University Science Books: Mill Valley, CA, 1987; p 156.   •

3. (a) Werner, H.; Hohn, A.; Schulz, M. *J. Chem. Soc., Dalton Trans.* **1991**, 777.   (b) Bianchini, C.; Peruzzini, M.; Vacca, A.; Zanobini, F. *Organometallics* **1991**, *10*, 3697.   (c) Holton, J.; Lappert, M. F.; Pearce, R.; Yarrow, P. I. W. *Chem. Rev.* **1983**, *83*, 135 and references cited therein.

4. (a) Bruce, M. I. *Chem. Rev.* **1991**, *91*, 197 and references cited therein. (b) Werner, H. *Angew. Chem., Int. Ed. Engl.* **1990**, *29*, 1077 and references cited therein.

5. (a) Clark, H. C.; Puddephatt, R. J. *Inorg. Chem.* **1970**, *9*, 2670.   (b) Horton, A. D.; Orpen, A. G. *Organometallics* **1992**, *11*, 8.   (c) Selnau, H. E.; Merola, J. S. *Organometallics* **1993**, *12*, 3800.   (d) Jordan, R. F.; Bradley, P. K.; Baenziger, N. C.; LaPointe, R. E. *Organometallics* **1989**, *8*, 2892.

6. Alexander, J. J. *The Chemistry of the Metal-Carbon Bond*; Hartley, F. R., Parai, S., Eds.; John Wiley & Sons Ltd.; Chichester, U. K. 1985; Vol. 2, p 339.

7. James, B. R. *Comprehensive Organometallic Chemistry*; Wilkinson, G., Stone, F. G. A., Abel, S., Eds.; Pergamon Press: Oxford, U. K., 1982; Vol. 8, Chapter 51, p 285.

8. (a) Schore, N. E. *Chem. Rev.* **1988**, *88*, 1081. (b) Finnimore, S. R.; Knox, S. A. R.; Taylor, G. E.; *J. Chem. Soc., Chem. Commun.* **1980**, 411. (c) Knox, S. A. R.; Stansfield, R. F. D.; Stone, F. G. A.; Winter, M. J.; Woodward, P. *J. Chem. Soc., Dalton Trans.* **1982**, 173. (d) Kiel, G.-Y.; Takats, J. *Organometallics* **1989**, *8*, 839. (e) Horton, A. D.; Orpen, A. G. *Organometallics* **1992**, *11*, 8. (f) Johnson, K. A.; Gladfelter, W. L. *Organometallics* **1992**, *11*, 2534. (g) Mirza, H. A.; Vittal, J. J.; Puddephatt, R. J. *Organometallics* **1994**, *13*, 3063.

9. (a) Sutherland, B. R.; Cowie, M. *Organometallics* **1985**, *4*, 1801. (b) Vaartstra, B. A.; Cowie, M. *Organometallics* **1990**, *9*, 1594. (c) Jenkins, J. A.; Cowie, M. *Organometallics* **1992**, *11*, 2767. (d) Wang, L.-S.; Cowie, M. *Can. J. Chem.* **1995**, *73*, 1058. (e) Xiao, J.; Cowie, M. *Organometallics* **1993**, *12*, 463. (f) Wang, L.-S.; Cowie, M. *Organometallics* **1995**, *14*, 2374. (g) Wang, L.-S.; Cowie, M. *Organometallics* **1995**, *14*, 3040. (h) Antwi-Nsiah, F. H.; Okemona, O. Cowie, M. *Organometallics* **1996**, *15*, 506.

10. Antwi-Nsiah, F. H. Ph.D. Thesis, University of Alberta, Edmonton, AB, 1994.

11. (a) Walker, N.; Stuart, D. *Acta Crystallogr.* **1983**, *A39*, 158–166. (b) Sheldrick, G. M. *Acta Crystallogr.* **1990**, *A46*, 467. (c) Sheldrick, G. M.

SHELXL-93. Program for crystal structure determination. University of Göttingen, Germany, 1993.

12. (a) Antwi-Nsiah, F. H.; Okemona, O. Cowie, M. *Organometallics* **1996**, *15*, 1042. (b) Sterenberg, B. T.; Hilts, R. W.; Moro, G.; McDonald, R.; Cowie, M. *J. Am. Chem. Soc.* **1995**, *117*, 245. (c) Antonelli, D. M.; Cowie, M. *Organometallics* **1991**, *10*, 2173. (d) Antonelli, D. M.; Cowie, M. *Organometallics* **1991**, *10*, 2550.

13. In dppm-bridged homo- and heterobinuclear complexes of rhodium and iridium the parallel binding mode is observed almost exclusively. Examples (a) Sutherland, B. R.; Cowie, M. *Organometallics* **1984**, *3*, 1869. (b) Cowie, M.; Southern, T. G. *J. Organomet. Chem.* **1980**, *193*, C46. (c) Cowie, M.; Southern, T. G. *Inorg. Chem.* **1982**, *21*, 246. (d) Cowie, M.; McKeer, I. R. *Inorg. Chim. Acta* **1982**, *65*, L107. (e) Cowie, M.; Dickson, R. S.; Hames, B. W. *Organometallics* **1984**, *3*, 1879. (f) Mague, J. T.; DeVries, S. H. *Inorg. Chem.* **1982**, *21*, 1632. (g) Mague, J. T. *Inorg. Chem.* **1983**, *22*, 1158. (h) see ref. 9h. (i) Vaartstra, B. A.; Xiao, J.; Jenkins, J. A.; Verhagen, R.; Cowie, M. *Organometallics* **1991**, *10*, 2708. (j) Antwi-Nsiah, F. H.; Torkelson, J. R.; Cowie, M. *Inorg. Chim. Acta.* **1997**, *259*, 213. (k) George, D. S. A.; McDonald, R.; Cowie, M. *Can. J. Chem.* **1996**, *74*, 2289. (l) Mague, J. T. *Organometallics* **1986**, *5*, 918. (m) Mague, J. T.; Klein, C. L.; Majeste, R. J.; Stevens, E. D. *Organometallics* **1984**, *3*, 1860.

14. (a) Sutherland, B. R.; Cowie, M. *Organometallics* **1985**, *4*, 1801. (b) Mague, J. T. *Inorg. Chem.* **1983**, *22*, 1158.

15. (a) Sutherland, B.; Cowie, M. *Organometallics* **1984**, *3*, 1869. (b) Cowie, M.; Dwight, S. K. *Inorg. Chem.* **1980**, *19*, 209. (c) Cowie, M.; Gibson, J. A. E. *Organometallics* **1984**, *3*, 984.

16. (a) Salah, O. M. A.; Bruce, M. I. *J. Chem. Soc., Dalton Trans.* **1975**, 2311. (b) Churchill, M. R.; Bezman, S. A. *Inorg. Chem.* **1974**, *13*, 1418. (c) Smith, W. F.; Yule, J.; Taylor, N. J.; Paik, H. N.; Carty, A. J. *Inorg. Chem.* **1977**, *16*, 1593. (d) For a review of cluster bound acetylides see: Carty, A. J. *Pure Appl. Chem.* **1982**, *54*, 113. (e) Cowie, M.; Loeb, S. J. *Organometallics* **1985**, *4*, 852. (f) Yam, V. W.; Chan, L.; Lai, T. *Organometallics* **1993**, *12*, 2197.

17. (a) Grundy, K. R.; Deraniyagala, S. P. *Organometallics* **1985**, *4*, 424. (b) Deraniyagala, S. P. Ph.D. Thesis, Dalhousie University, 1984. (c) Esteruelas, M. A.; Lahuerta, O.; Modrego, J.; Nurnberg, O.; Oro, L. A.; Rodriguez, L.; Sola, E.; Werner, H. *Organometallics* **1993**, *12*, 266.

18. George, D. S. A.; McDonald, R.; Cowie, M. *Organometallics* **1998**, *17*, 2553.

19. Further support for the proposed geometry comes from a $^{13}C\{^1H\}$ NMR experiment obtained on a sample of **20** prepared with ^{13}C-enriched CO and ^{13}C-enriched acetylene, that displays 28.3Hz coupling between a carbonyl and the α-carbon of the acetylide indicating a trans arrangement of these groups.

20. Average values for $^1J_{C-C}$ (Hz) for different hybridizations: acetylene (sp = 172), ethylene (sp^2 = 68), ethane (sp^3 = 35). From Friebolin, H. *Basic One- and Two-Dimensional NMR Spectroscopy*, VCH Publishers: New York and Weinheim, Germany, 1991; p 99.

21. Average values for $^1J_{C-H}$ (Hz) for different hybridizations: acetylene (sp = 249), ethylene (sp^2 = 156), ethane (sp^3 = 125). From Friebolin, H. *Basic One- and Two-Dimensional NMR Spectroscopy*, VCH Publishers: New York and Weinheim, Germany, 1991; p 95.

22. Collman, J. P.; Hegedus, L. S.; Norton, J. R.; Finke, R. G. *Principles and Apllications of Organotransition Metal Chemistry*, University Science Books: Mill Valley, CA, 1987; p 83.

23. Allen, F. H.; Kennard, O.; Watson, D. G.; Brammer, L.; Orpen, A. G.; Taylor, R. *J. Chem. Soc., Perkin Trans. II* **1987**, S1.

24. Example for ^{1}H NMR (a). Sumner Jr., C. E.; Collier, J. A.; Pettit, R. *Organometallics* **1982**, *1*, 1350. Examples for $^{13}C\{^1H\}$ NMR (b) Chetcuti, M. J.; McDonald, S. R.; Rath, N. P. *Organometallics* **1989**, *8*, 2077. (c) Howard, J. A. K.; Knox, S. A. R.; Terrill, N. J.; Yates, M. I. *J. Chem. Soc., Chem. Commun.* **1989**, 640. (d) Eisenstadt, A.; Efraty, A. *Organometallics* **1982**, *1*, 1100.

25. (a) Kubiak, C. P.; Woodcock, C.; Eisenberg, R. *Inorg. Chem.* **1980**, *19*, 2733. (b) Sutherland, B. R.; Cowie, M. *Organometallics* **1984**, *3*, 1869. (c) Sutherland, B. R.; Cowie, M. *Inorg. Chem.* **1984**, *23*, 2324. (d) Sutherland, B. R.; Cowie, M. *Organometallics* **1985**, *4*, 1801. (e) Xiao, J.;

Cowie, M. *Organometallics* **1993**, *12*, 463. (f) See structures for compounds **2, 3, 7, 32, 36, 40, 41, 44** this thesis.

26. (a) Wakefield, J. B.; Stryker, J. M. *Organometallics* **1990**, *9*, 2428 (supplementary material). (b) Collman, J. P.; Hegedus, L. S.; Norton, J. R.; Finke, R. G. *Principles and Apllications of Organotransition Metal Chemistry*, University Science Books: Mill Valley, CA, 1987; p 176. (c) *Comprehensive Organometallic Chemistry*, Wilkinson, G.; Stone, F. G. A.; Abel, E. W., Eds., Pergamon: New York, 1982; Vol. 6, Sections 37.6, 38.7 and 39.9. (d) Tulip, T. H.; Ibers, J. A. *J. Am. Chem. Soc.* **1978**, *100*, 3252.

27. See for example "allylidene (vinylcarbene)": (a) Dyke, A. F.; Knox, S. A. R.; Naish, P. J.; Taylor, G. E. *J. Chem. Soc., Chem. Commun.* **1980**, 803. (b) Eisenstadt, A.; Efraty, A. *Organometallics* **1982**, *1*, 1100. "metallaallyl" (c) Chetcuti, M. J.; McDonald, S. R.; Rath, N. P. *Organometallics* **1989**, *8*, 2077. (d) Muller, J.; Passon, B.; Pickardt, J. *J. Organomet. Chem.* **1982**, *236*, C11.

28. (a) Cowie, M.; Vasapollo, G.; Sutherland, B. R.; Ennett, J. P. *Inorg. Chem.* **1986**, *25*, 2648. (b) McKeer, I. R.; Sherlock, S. J.; Cowie, M. *J. Organomet. Chem.* **1988**, *352*, 205.

29. (a) Collman, J. P.; Hegedus, L. S.; Norton, J. R.; Finke, R. G. *Principles and Apllications of Organotransition Metal Chemistry*, University Science Books: Mill Valley, CA, 1987; p368. (b) Yammamoto, A. *Organotransition Metal Chemistry*, Wiley: New York, 1986; p251.

30. (a) see ref 9(e-h). (b) Berry, D. H.; Eisenberg, R. *Organometallics* **1987**, *6*, 1796. (c) Bruce, M. I. *Chem. Rev.* **1991**, *91*, 197 and references cited therein.

31. See for example: (a) Elliot, D. J.; Ferguson, G.; Holah, D. G.; Hughes, A. N.; Jennings, M. C.; Magnuson, V. R.; Potter, D.; Puddephatt, R. J. *Organometallics* **1986**, *5*, 918. (b) McDonald, R.; Cowie, M. *Inorg. Chem.* **1990**, *29*, 1564. (c) Antonelli, D. M.; Cowie, M. *Organometallics* **1990**, *9*, 1818. (d) Antonelli, D. M.; Cowie, M. *Organometallics* **1991**, *10*, 2550. (e) Antwi-Nsiah, F. H.; Torkelson, J. R.; Cowie, M. *Inorg. Chim. Acta.* **1997**, *259*, 213.

32. A similar discussion has appeared previously in ref 9(h).

33. (a) Dickson, R. S.; Greaves, B. C. *Organometallics* **1993**, *12*, 3249. (b) Carroll, W. E.; Green, M.; Orpen, A. G.; Schaverien, C. J.; Williams, I. D. Welch, A. J. *J. Chem. Soc. Dalton Trans.* **1986**, 1021. (c) Gracey, B. P.; Knox, S. A. R.; Macpherson, K. A.; Orpen, A. G.; Stobart, S. *J. Chem. Soc. Dalton Trans.* **1985**, 1935. (d) Davies, D. L.; Knox, S. A. R.; Mead, K. A.; Morris, M. J.; Woodward, P. *J. Chem. Soc. Dalton Trans.* **1984**, 2293. (e) Colborn, R. E.; Dyke, A. F.; Knox, S. A. R.; Macpherson, K. A.; Orpen, A. G. *J. Organomet. Chem.* **1982**, *239*, C15. (f) Sumner Jr., C. E.; Collier, J. A.; Pettit, R. *Organometallics* **1982**, *1*, 1350. (g) Dyke, A. F.; Guerchais, J. E.; Knox, S. A. R.; Roue, J, Short, R. L.; Taylor, G. E.; Woodward, P. *J. Chem. Soc., Chem. Commun.* **1981**, 537. (h) Levisalles, J.; Rose-Munch, F.; Rudler, H.; Daran, J-C.; Dromzee, Y.; Jeannin, Y. *J. Chem.*

Soc., Chem. Commun. **1981**, 152. (i) Jeffrey, J. C.; Moore, I.; Razay, H.; Stone, F. G. A. *J. Chem. Soc., Chem. Commun.* **1981**, 1255. (j) Barker, G. K.; Carroll, W. E., Green, M.; Welch, A. J. *J. Chem. Soc., Chem. Commun.* **1980**, 1071. (k) Dyke, A. F.; Knox, S. A. R.; Naish, P. J. *J. Organomet. Chem.* **1980**, *199*, C47. (l) Howard, J. A. K.; Knox, S. A. R.; Terrill, N. J.; Yates, M. I. *J. Chem. Soc., Chem. Commun.* **1989**, 640.

34. (a) Maitlis, P. M.; Long, H. C.; Quyoum, R.; Turner, M. L.; Wang, Z-Q. *Chem. Commun.* **1996**, 1. (b) Maitlis, P. M.; Saez, I. M.; Meanwell, N. J.; Isobe, K.; Nutton, A.; Vaquez de Miguel, A.; Bruce, D. W.; Okeya, S.; Bailey, P. M.; Andrews, D. G.; Ashton, P. R.; Johnstone, I. R. *New J. Chem.*, **1989**, *13*, 419. (c) Martinex, J. M.; Adams, H.; Bailey, N. A.; Maitlis, P. M. *J. Chem. Soc., Chem. Commun.*, **1989**, 286.

35. Two known reports are: (a) Deeming, A. J.; Shaw, B. L.; Stainbank, R. E. *J. Chem. Soc. A* **1971**, 374. (b) Wang, L. -S.; Cowie, M. *Can. J. Chem.* **1995**, *73*, 1058.

Chapter 4

C-H Activation and C-C Bond Formation

in the Reactions of

$[Ir_2(CH_3)(CO)_2(dppm)_2][CF_3SO_3]$ with Olefins.

Introduction

In an effort to extend the chemistry of the diiridium methyl system described in Chapters 2 and 3, particularly with respect to C-C bond formation, we have looked at the reaction of $[Ir_2(CH_3)(CO)(\mu\text{-}CO)(dppm)_2][CF_3SO_3]$ (2), (dppm = $Ph_2PCH_2PPh_2$) with a variety of olefins. The insertion of olefins into metal-alkyl bonds is an important step in many transition-metal catalyzed reactions, particularly olefin polymerization.[1] There are two major proposals for the C-C bond forming reactions in olefin polymerization processes. One is the Cossee mechanism (outlined below) in which the direct β-migratory insertion of a coordinated alkyl to a coordinated olefin occurs.[2] The major failing of this mechanism is the paucity of well defined cis alkyl-olefin complexes that

M———‖ ⟶ M———□ ══ ⟶ M———‖
| | |
CH₃   CH₂CH₂CH₃   CH₂CH₂CH₃
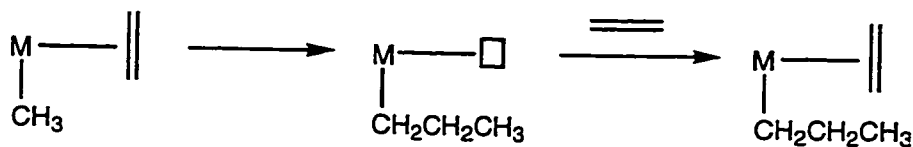
□ = open coord. site

undergo migratory insertion.[3,4] The other popular mechanism (outlined below) was proposed by Green,[5] and involves initial α-hydrogen elimination of the alkyl group to form a carbene hydride complex that then combines with the olefin, forming a metallacycle. This metallacycle then reductively eliminates with the hydride reforming an alkyl complex with an open coordination site for further olefin complexation.

$$M-CH_3 \xrightarrow{\alpha\text{-elim.}} \underset{\underset{H}{|}}{M}=CH_2 \xrightarrow{\quad} \underset{\underset{H}{|}}{M}\diamondsuit$$

$$\downarrow \text{reduc. elim.}$$

$$M-CH_2CH_2CH_3$$
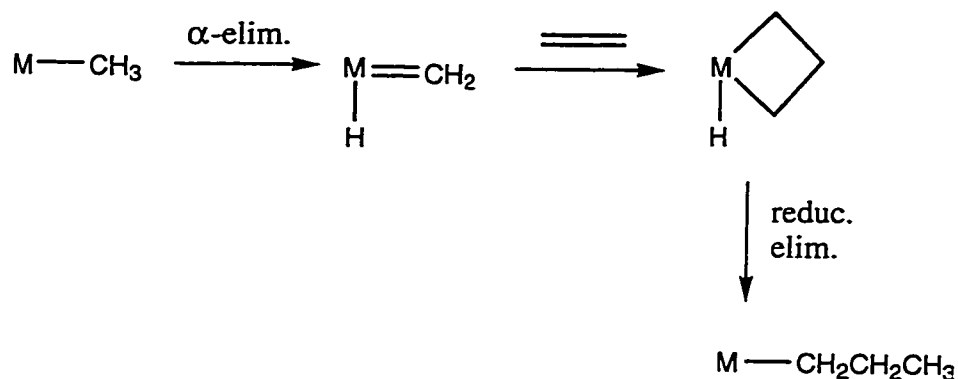
Much of the well-defined work on olefin polymerization has dealt with early metal or f-element metallocene complexes,[6,7] however more recently Brookhart[4,8] has demonstrated that *late-metal alkyl complexes* of the Ni and Co triads are also useful in the polymerization of olefins, with some Pd complexes showing cis alkyl-olefin intermediates at low temperature prior to observing polymerization.

In Chapter 2 we demonstrated that reaction of compound **2** with small molecules resulted in C-H bond cleavage of the methyl group yielding the methylene-hydride complexes $[Ir_2H(CO)_2L(\mu\text{-}CH_2)(dppm)_2][CF_3SO_3]$ (L = CO, SO_2, PR_3). This reaction is of direct relevance to the Green olefin polymerization

mechanism paralleling the α-hydrogen elimination step. In Chapter 3 the initial methyl C-H bond activation step was incorporated to explain some of the C-C bond forming reactions observed. The obvious question that then arises in the context of olefin polymerization, is whether the reaction of **2** with olefins will proceed by H elimination from the methyl group, as proposed by Green, and if so whether subsequent C-C bond formation will occur. It is also possible that direct migration of the methyl group of **2** to an olefin might occur paralleling the Cossee mechanism or the work of Brookhart.

In this chapter we present results of studies aimed at further modeling the involvement of surface-bound methyl groups, in which we demonstrate that the methyl group in the model compound (**2**), shows an interesting diversity in reactivity with olefins that is highly dependent upon the nature of the olefin.

Experimental Section

General Comments. Ethylene was obtained from Matheson, tetrafluroethylene was from PCR, allene was obtained from Canadian Liquid Air Ltd., and methylallene was from Fluka. 1,3-Butadiene, dimethylallene and all other reagents were purchased from Aldrich. NOE, HMQC and INAPT experiments were carried out on a Varian Unity 500 MHz spectrometer. The $^{31}P\{^{1}H\}$ and ^{1}H NMR and IR spectroscopic data for all compounds are given in Table 4.1 while selected $^{13}C\{^{1}H\}$ and ^{19}F NMR data are given, where appropriate, with the details on the preparation of the compounds.

Table 4.1 Spectroscopic Data for Compounds

Compound	IR cm^{-1} [a,b]	δ ^{1}H [c,e]	δ ^{31}P{^{1}H} [c,d]
[Ir$_2$(CH$_3$)(CO)$_2$(μ-C$_2$F$_4$)(dppm)$_2$][CF$_3$SO$_3$] (31)	2020 vs 2001 s	3.89 (m, 4H), 0.41 (t, 3H)	15.8 (m), 4.1 (m)
[Ir$_2$(CH$_3$)(CO)$_3$(μ-C$_2$F$_4$)(dppm)$_2$][CF$_3$SO$_3$] (32)	2062 sh 2018 b, vs	4.61 (m, 4H), 0.79 (t, 3H)	-8.7 (m), -16.4 (m)
[Ir$_2$(CH$_3$)(CO)$_2$(PMe$_3$)(μ-C$_2$F$_4$)(dppm)$_2$][CF$_3$SO$_3$] (33)	2006 vs 1990 s	5.23 (bm, 2H), 4.99 (m, 2H), 0.92 (bt, 3H), 0.80 (d, 9H)	-19.2 (m), -20.1 (m), -69.7 (t, $^3J_{P,F}$ = 55 Hz)
[Ir$_2$(CH$_3$)(CO)$_2$(H$_2$C=C=CH$_2$)(μ-C$_2$F$_4$)(dppm)$_2$][CF$_3$SO$_3$] (34)	—	6.68 (b, 1H), 6.30 (b, 1H), 4.51 (b, 4H), 1.42 (b, 2H), 0.22 (t, 3H)	-5.1 (m), -20.5 (m)
[Ir$_2$(CH$_3$)(H)(CO)$_2$(μ-H)(μ-C=C(H)C(H)=CH$_2$)(dppm)$_2$]-[CF$_3$SO$_3$] (35)	2014 sh, vs 2003 sh, vs	6.79 (d, 1H), 5.28 (ddd, $^3J_{H-H}$ = 16.5, 10, 10 Hz, 1H), 4.91 (d, 1H), 4.38 (d, 1H), 3.75 (m, 2H), 2.63 (m, 2H), -0.51 (t, 3H), -12.64 (t, $^2J_{H-P}$ = 17 Hz, 1H), -13.9 (q, 1H)	-4.9 (m), -13.1 (m)
[Ir$_2$(CH$_3$)(CO)$_2$(μ-η^1-η^3-H$_2$C=C=CH$_2$)(dppm)$_2$]-[CF$_3$SO$_3$] (36)	2003 1970	5.46 (m, 2H), 5.09 (m, 2H), 4.23 (b, 2H), 3.52 (b, 2H), 1.18 (t, 3H)	-16.7 (m)
[Ir$_2$(CH$_3$)(CO)$_2$(μ-η^1-η^3-H$_2$C=C=C(H)CH$_3$)(dppm)$_2$]-[CF$_3$SO$_3$] (37)	1994 vs	5.79 (m, 1H, PCH$_2$P), 5.38 (m, 1H, PCH$_2$P), 5.19 (m, 1H, PCH$_2$P), 5.17 (m, 1H, -C=CHH), 4.87 (m, 1H, PCH$_2$P), 4.70 (qm, $^3J_{H-H}$ = 6 Hz, 1H, C=CH(CH$_3$), 3.78 (m, 1H, -C=CHH), 1.16 (t, 3H), 1.07 (dd, $^4J_{H-P}$ = 6 Hz, 3H, C=CH(CH$_3$))	-16.0 (m)
[Ir$_2$(CH$_3$)(CO)$_2$(H$_2$C=C=C(CH$_3$)$_2$) (dppm)$_2$][CF$_3$SO$_3$] (38)	1960 w 1760 vs	3.48 (m, 2H), 3.19 (m, 2H), 1.58 (s, 2H), 1.22 (b, 3H), 1.17 (t, $^3J_{H-P}$ = 8.5 Hz, 3H), 0.98 (b, 3H)	18.3 (m), 0.2 (m)

Table 4.1 cont

Compound	IR cm^{-1} [a,b]	δ^{1}H [c-e]	δ^{31}P{^{1}H} [c,d]
[Ir$_2$(H)(CO)$_2$(μ-η^1-η^3-HCC(Me)=CH$_2$)(dppm)$_2$][CF$_3$SO$_3$] (39)	—	8.72 (m, 1H), 5.93 (m, 1H), 4.60 (m, 1H), 3.44 (m, 1H), 3.43 (m, 1H), 3.11 (m,1H), 2.89 (d, 3H), -11.38 (m, 1H)	-5.1 (m, 2P), -30.2 (m, 1P), -32.4 (m,1P)
[Ir$_2$(H)(CO)$_2$(μ-η^1-η^3-HCC(Me)=CHMe)(dppm)$_2$]-[CF$_3$SO$_3$] (25a)	—	8.79 (m, 1H), 7.12 (m, 1H), 5.83 (m, 1H), 4.60 (m, 1H), 3.78 (m, 1H), 3.29 (m, 1H), 2.72 (d, 3H), 1.42 (bm, 3H), -11.25 (m, 1H)	-5.8 (m), -6.0 (m), -34.3 (m), -37.8 (m)
[Ir$_2$(H)(CO)$_2$(μ-η^1-η^3-HCC(Me)=CHMe)(dppm)$_2$]-[CF$_3$SO$_3$] (25b)	—	8.96 (m, 1H), -11.18 (m, 1H)	-7.6 (m,2P), -30.8(m, 1P), -37.9 (m, 1P)

[a]IR abbreviations (ν(CO)) unless otherwise stated): vs = very strong, s = strong, m = medium, w = weak, sh = shoulder, b = broad. [b]Nujol mull or CH$_2$Cl$_2$ cast unless otherwise stated. [c]NMR abbreviations: s = singlet, d = doublet, t = triplet, m = multiplet, q = quintet, dm = doublet of multiplets, b = broad. [d]NMR data at 25°C in CD$_2$Cl$_2$ unless otherwise stated. [e] Chemical shifts for the phenyl hydrogens are not given in the ^{1}H NMR data.

Preparation of Compounds

(a) [Ir$_2$(CH$_3$)(CO)$_2$(C$_2$H$_4$)(dppm)$_2$][CF$_3$SO$_3$] (30). Compound **2** (20 mg, 0.015 mmol) was dissolved in an NMR tube capped with a rubber septum. Ethylene was bubbled through the solution for 2 min and then the mixture was allowed to stand for 1h. The NMR spectra showed that the product was the previously characterized [Ir$_2$(CH$_3$)(CO)$_2$(C$_2$H$_4$)(dppm)$_2$][CF$_3$SO$_3$].[9]

(b) [Ir$_2$(CH$_3$)(CO)$_2$(μ-C$_2$F$_4$)(dppm)$_2$][CF$_3$SO$_3$] (31). Compound **2** (40 mg, 0.029 mmol) was dissolved in 5 mL of CH$_2$Cl$_2$ and tetrafluoroethylene was passed over the solution for 1 min. The solution was then stirred under a static atmosphere of the gas for 18 h during which time the color changed from red to dark red-brown. The solution was evaporated to *ca.* 2 mL and a brown powder was precipitated and washed with pentane (3 × 10 mL) and dried under vacuum. Yield 93 %. Anal. Calcd for Ir$_2$SP$_4$F$_7$O$_5$C$_{56}$H$_{47}$: C, 45.65; H, 3.22. Found: C, 45.38; H, 3.02. ^{19}F NMR: δ -79.2 (m, 2F), -85.9 (m, 2F).

(c) [Ir$_2$(CH$_3$)(CO)$_3$(μ-C$_2$F$_4$)(dppm)$_2$][CF$_3$SO$_3$] (32). Compound **3 1** (30 mg, 0.020 mmol) was slurried in 5 mL of CH$_2$Cl$_2$. Carbon monoxide was then passed over the solution for 2 min causing a color change from dark red-brown to bright yellow. Compound **32** was not isolated because upon N$_2$ purge or under vacuum it lost CO, regenerating compound **31**. Its characterization was based on its spectral paramenters and crystal structure (*vide infra*). ^{19}F NMR: δ -73.0 (t, 2F), -85.9 (b, 2F).

(d) **[Ir$_2$(CH$_3$)(CO)$_2$(PMe$_3$)(μ-C$_2$F$_4$)(dppm)$_2$][CF$_3$SO$_3$]** **(33).**
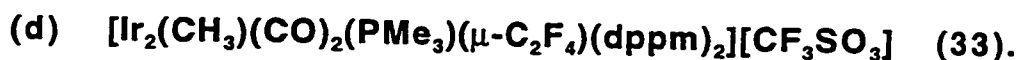
Compound **31** (30 mg, 0.020 mmol) was slurried in 5 mL of CH$_2$Cl$_2$ and one equivalent of trimethylphosphine (2.1 μL, 0.020 mmol) was added causing a color change from dark red-brown to yellow. After 10 min the solvent was evaporated to *ca.* 2 mL and a pale yellow powder was precipitated. The solid was isolated, washed with pentane (3 × 10 mL) and dried under vacuum. Yield 76 %. Anal. Calcd for Ir$_2$SP$_5$F$_7$O$_5$C$_{59}$H$_{56}$: C, 45.73; H, 3.65. Found: C, 45.70; H, 3.42. ^{19}F NMR: δ -69.6 (dt, $^3J_{F-P}$ = 55 Hz, 18 Hz, 2F), -82.8 (b, 2F).

(e) **[Ir$_2$(CH$_3$)(CO)(H$_2$C=C=CH$_2$)(μ-C$_2$F$_4$)(μ-CO)(dppm)$_2$][CF$_3$SO$_3$]**
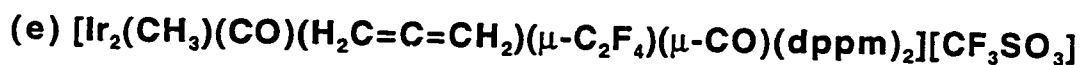
(34). Compound **31** (15 mg, 0.010 mmol) was slurried in 0.6 mL of CD$_2$Cl$_2$ in an NMR tube. Allene was bubbled through the solution for 1 min causing a color change from red-brown to orange. Compound **34** lost allene to reform compound **31** if not kept under an allene atmosphere greater than atmospheric pressure. Its characterization is based on its NMR spectral data. ^{19}F NMR: δ -76.3 (b, 2F), -83.6 (b, 2F), ^{13}C{^{1}H} NMR: δ 189.9 (b, 1CO), 177.3 (b, 1CO).

(f) **[Ir$_2$(CH$_3$)(H)(CO)$_2$(μ-H)(μ-C=C(H)C(H)=CH$_2$)(dppm)$_2$]-**
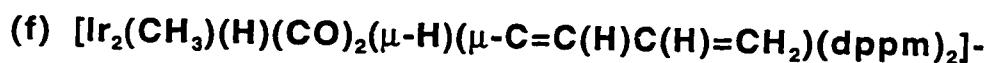
[CF$_3$SO$_3$] **(35).** Compound **2** (50 mg, 0.036 mmol) was dissolved in 10 mL of CH$_2$Cl$_2$ and 1,3-butadiene was then passed over the solution for 5 min. The solution was stirred under a static atmosphere of the gas for 48 h. The solution was then concentrated to *ca.* 2 mL and a beige powder was precipitated with addition of 15 mL of Et$_2$O. The isolated solid was washed with Et$_2$O (2 × 10 mL)

and dried under vacuum. Yield 74 %. Satisfactory elemental analysis was not obtained so the compound was characterized by NMR and IR spectroscopy. ^{13}C{^{1}H} NMR (natural abundance): δ 196.0 (q, $^2J_{C\text{-}P}$ = 9.5 Hz, (μ-C=C(H)-C(H)=CH$_2$)), 173.6 (t, $^2J_{C\text{-}P}$ = 9.8 Hz, CO), 173.2 (t, $^2J_{C\text{-}P}$ = 9.2 Hz, CO), 145.8 (s, μ-C=C(H)C(H)=CH$_2$), 112.0 (s, μ-C=C(H)C(H)=CH$_2$), -9.9 (b, CH$_3$).

(g) [Ir$_2$(CH$_3$)(CO)$_2$(μ-η^1:η^3-H$_2$C=C=CH$_2$) (dppm)$_2$][CF$_3$SO$_3$] (36). A

5 mL CH$_2$Cl$_2$ solution of compound 2 (50 mg, 0.036 mmol) was cooled to -78 °C and allene was then added causing an immediate color change from red to light yellow. The solution was stirred for 30 min at -78 °C and then warmed to room temperature and stirred for 1 h. The solvent was reduced to *ca.* 2 mL and a yellow powder was precipitated with addition of 10 mL of Et$_2$O. The isolated solid was washed with Et$_2$O (2 × 10 mL) and dried under vacuum. Yield 73 %. Anal. Calcd for Ir$_2$SP$_4$F$_3$O$_5$C$_{57}$H$_{51}$: C, 48.43; H, 3.64. Found: C, 48.23; H, 3.50. ^{13}C{^{1}H} NMR (natural abundance): δ 179.2 (t, CO), 171.2 (b, CO), 127.3 (b, μ-η^1:η^3-H$_2$C=C=CH$_2$), 61.3 (m, μ-η^1:η^3-H$_2$$C$=C=$CH_2$), -31.1 (t, $^2J_{C\text{-}P}$ = 3.3 Hz, CH$_3$).

(h) [Ir$_2$(CH$_3$)(CO)$_2$(μ-η^1:η^3-H$_2$C=C=C(H)CH$_3$)(dppm)$_2$][CF$_3$SO$_3$]

(37). A 5 mL CH$_2$Cl$_2$ solution of compound 2 (50 mg, 0.036 mmol) was cooled to 0 °C and methylallene was then bubbled through the solution for 1 min causing an immediate color change from red to light yellow. The solution was stirred for 30 min at 0 °C and then warmed to room temperature and stirred for 1 h, during which time the solution changed to bright yellow. The solvent was reduced to *ca.* 2 mL and a bright yellow powder was precipitated with addition

of 10 mL of Et$_2$O. The isolated solid was washed with Et$_2$O (2 × 10 mL) and dried under vacuum. Yield 63 %. ^{13}C{^{1}H} NMR (natural abundance): δ 179.4 (t, CO), 170.9 (b, CO), 78.7 (m, μ-η^1:η^3-H$_2$C=C=C(H)CH$_3$), 55.6 (m, μ-η^1:η^3-H$_2$$C$=C=C(H)CH$_3$), 18.6 (m, μ-η^1:η^3-H$_2$C=C=C(H)$CH_3$), -32.2 (t, CH$_3$).

(i) **[Ir$_2$(CH$_3$)(CO)$_2$(H$_2$C=C=C(CH$_3$)$_2$)(dppm)$_2$][CF$_3$SO$_3$]** **(38).**

Dimethylallene (3.2 μL, 0.033 mmol) was added to a 5 mL CH$_2$Cl$_2$ solution of compound **2** (45 mg, 0.033 mmol) at -78 °C and the solution was stirred for 10 min during which time the solution changed to bright yellow. The solution was warmed to room temperature, the solvent was reduced to *ca.* 2 mL and a bright yellow powder was precipitated with addition of 10 mL of Et$_2$O. The isolated solid was washed with Et$_2$O (2 × 10 mL) and dried under vacuum. Yield 55 %. ^{13}C{^{1}H} NMR (^{13}CO enriched): δ 206.4 (t, $^2J_{C-P}$ = 6.9 Hz,CO), 204.8 (t, $^2J_{C-P}$ = 7.0 Hz,CO)

(j) **[Ir$_2$(H)(CO)$_2$(μ-η^1:η^3-HCC(Me)=CH$_2$)(dppm)$_2$][CF$_3$SO$_3$]** **(39).**

Compound **36** (20 mg, 0.014 mmol) was dissolved in 10 mL of CH$_2$Cl$_2$ and stirred for 7 days. The solvent volume was reduced to *ca.* 2 mL and a yellow powder was obtained on addition of 10 mL of Et$_2$O. The solid was isolated, washed with Et$_2$O (2 × 10 mL) and dried under vacuum. NMR showed *ca.* 80 % conversion to compound **39**.

(k) **Production** of **[Ir$_2$(H)(CO)$_2$(μ-η^1:η^3-HCC(Me)=CHMe)-(dppm)$_2$][CF$_3$SO$_3$] (25a&b)*** from compound **37.** Cis **25(a)** and trans

25(b) isomers of compound **25** resulted from dissolving compound **37** in CH_2Cl_2 and stirring for 48 h. The product was worked up in a manner similar to that used for the isolation of compound **39**. NMR spectra showed conversion of compound **37** to compound **25(a&b)** as well as some of compound **2** and some decompositon products. The compound was never obtained pure so characterization is based on NMR spectroscopy.

*Compound **25a** was originally produced in the reaction of compound **2** with 2-butyne (see Chapter 3).

(I) **Production** **of** **[Ir$_2$(H)(CO)$_2$(μ-η^1:η^3-HCC(Me)=CHMe)-(dppm)$_2$][CF$_3$SO$_3$] (25a) from compound 38.** Compound **25a** was obtained from **38** in a manner similar to the formation of compound **39** by dissolving compound **38** in CH_2Cl_2 and stirring for 8 h. NMR showed conversion of compound **38** to compound **25a** as well as some decomposition products. Vinyl chloride (identified by ^1H and $^{13}C\{^1H\}$ NMR) was also produced in this reaction.

X-ray Data Collection. For compound **32**, crystals suitable for X-ray diffraction were grown via slow diffusion of diethyl ether into a concentrated CH_2Cl_2 solution of the compound. For compound **36**, crystals were grown by slowly diffusing diethyl ether into a concentrated 50:50 CH_2Cl_2/toluene solution of **36**. Crystals of each compound were mounted and flame-sealed in glass capillaries under solvent vapor to minimize decomposition or deterioration due to solvent loss. Data for compound **32** were collected at -60 °C on a Siemens P4RA diffractometer using graphite-monochromated Cu Kα radiation and for

compound **36** at -60 °C on a Siemens SMART CCD P4RA diffractometer using graphite monochromated Mo Kα radiation. Unit-cell parameters and space group assignments were obtained as described below. For compound **32**, three reflections were chosen as intensity standards and were remeasured every 120 min of X-ray exposure time; in no case was decay evident. Absorption corrections were applied to the data as described below. Crystal parameters and details of data collection are summarized in Table 4.2.

Unit cell parameters for compound **32** were obtained from a least-squares refinement of 50 reflections in the range 56.7°<2θ<59.2°. For compound **36**, unit cell parameters were obtained from a least squares refinement of 8192 centered reflections. For compound **32** the cell parameters and the systematic absences defined F_{dd2} as the space group, whereas for **36**, the cell parameters, the lack of absences and the diffraction symmetry suggested the space group $P1$ or $P\bar{1}$, the latter of which was established by successful refinement of the structure. Absorption corrections to **36** were applied by the method SADABS supplied through the Siemens software, while for **32** the crystal faces were indexed and measured, with absorption corrections being carried out using Gaussian integration.

Structure Solution and Refinement. For each structure, the positions of the iridium and phosphorus atoms were found using the direct-methods program *SHELXS-86*;[10a] the remaining atoms were found using a succession of least-squares and difference Fourier maps. Refinement of each structure

Table 4.2 Crystallographic Data for Compounds 32 & 36.

A. Crystal Data

compd	$[Ir_2(CH_3)(CO)_3(\mu\text{-}C_2F_4)(dppm)_2]$-$[CF_3SO_3]$ (32)•CH_2Cl_2	$[Ir_2(CH_3)(CO)_2(\mu\text{-}\eta^1\text{-}\eta^3\text{-}H_2C=C=CH_2)(dppm)_2][CF_3SO_3]$-(36)• $1/3CH_2Cl_2$
formula	$C_{58}H_{49}Cl_2F_7Ir_2O_6P_4S$	$C_{57.33}H_{51.67}Cl_{0.67}F_3Ir_2O_5P_4S$
formula wt	1586.21	1441.65
crystal dimensions (mm)	0.46 × 0.10 × 0.10	0.24 × 0.14 × 0.03
color	yellow	yellow
crystal system	orthorhombic	triclinic
space group	$Fdd2$ (No. 43)	$P\overline{1}$ (No. 2)
unit cell parameters[a,b]		
a(Å)	37.872 (2)	10.4603 (1)
b(Å)	53.711 (3)	14.2406 (1)
c(Å)	11.7901 (6)	38.7838 (4)
α(deg)	90.0	91.887 (1)
β(deg)	90.0	97.732 (1)
γ(deg)	90.0	90.281 (1)
V(Å³)	23983 (2)	5721.39 (9)
Z	16	4
ρcalcd (g cm⁻³)	1.757	1.674
μ (mm⁻¹)	11.230	4.882

B. Data Collection and Refinement Conditions

diffractometer	Siemens P4/RA[c]	Siemens SMART CCD/P4/RA[c]
radiation (λ [Å])	graphite-monochromated Cu Kα (1.54178)	graphite-monochromated Mo Kα (0.71073)
temperature (°C)	−60	−60

Table 4.2 cont

scan type	θ–2θ	mixture of ϕ rotations (0.3°) and ω scans (0.3°)
data collection 2θ limit (deg)	113.5	55.0
total data collected	8494 (-40 $\leq$ h $\leq$ 40, -58 $\leq$ k $\leq$ 58, -12 $\leq$ l $\leq$ 12)[d]	63233 (–13 $\leq$ h $\leq$ 13, –18 $\leq$ k $\leq$ 18, –50 $\leq$ l $\leq$ 50)
independent reflections	8025	23466
number of observations (NO)	7078 ($F_o^2 \geq 2\sigma(F_o^2)$)	10928 ($F_o^2 \geq 2\sigma(F_o^2)$)
structure solution method	direct methods (SHELXS–86)[e]	direct methods (SHELXS–86)[e]
refinement method	full-matrix least-squares on F^2 (SHELXL–93)[f]	full-matrix least-squares on F^2 (SHELXL–93)[f]
absorption correction method	empirical (face-indexed)	SADABS[g]
range of transmission factors	0.4347–0.2030	0.6468–0.4616
data/restraints/parameters	8025 [$F_o^2 \geq -3\sigma(F_o^2)$]/20/683	23466 [$F_o^2 \geq -3\sigma(F_o^2)$]/0/1312
extinction coefficient (x)[h]	-------	0.00027 (3)
Flack absolute structure parameter[i]	0.00 (2)	-------
largest difference peak and hole	2.137 and –1.308 e Å^{-3}	1.521 and –1.149 e Å^{-3}
final R indices[j]		
$F_o^2 > 2\sigma(F_o^2)$	R_1 = 0.0599, wR_2 = 0.1581	R_1 = 0.0867, wR_2 = 0.1392
all data	R_1 = 0.0697, wR_2 = 0.1665	R_1 = 0.2090, wR_2 = 0.1853
GOF(S)[k]	1.064	1.034

[a]For 32, obtained from least-squares refinement of 50 reflections with 56.7° < 2θ < 59.2°.

[b]For 36, obtained from least-squares refinement of 8192 centered reflections.

[c]Programs for diffractometer operation and data collection were those of the XSCANS system supplied by Siemens.

[d]Data were collected in Friedel-opposite octants with indices of the form +h +k +l and –h –k –l.

Table 4.2 cont

[e]Sheldrick, G. M. *Acta Crystallogr.* **1990**, *A46*, 467–473.

[f]Sheldrick, G. M. *SHELXL-93*. Program for crystal structure determination. University of Göttingen, Germany, 1993. Refinement on F_o^2 for all reflections (all of these having $F_o^2 \geq -3\sigma(F_o^2)$). Weighted R-factors wR_2 and all goodness of fit values S are based on F_o^2; conventional R-factors R_1 are based on F_o, with F_o set to zero for negative F_o^2. The observed criterion of $F_o^2 > 2\sigma(F_o^2)$ is used only for calculating R_1, and is not relevant to the choice of reflections for refinement. R-factors based on F_o^2 are statistically about twice as large as those based on F_o, and R-factors based on ALL data will be even larger.

[g]Programs for absorption correction were those supplied by Siemens.

[h]$F_c^* = kF_c[1 + x\{0.001F_c^2\lambda^3/\sin(2\theta)\}]^{-1/4}$ where k is the overall scale factor.

[i]Flack, H. D. *Acta Crystallogr.* **1983**, *A39*, 876–881. The Flack parameter will refine to a value near zero if the structure is in the correct configuration and will refine to a value near one for the inverted configuration.

[j]$R_1 = \Sigma||F_o| - |F_c||/\Sigma|F_o|$; $wR_2 = [\Sigma w(F_o^2 - F_c^2)^2/\Sigma w(F_o^4)]^{1/2}$.

[k]$S = [\Sigma w(F_o^2 - F_c^2)^2/(n - p)]^{1/2}$ (n = number of data; p = number of parameters varied; $w = [\sigma^2(F_o^2) + (a_0P)^2 + a_1P]^{-1}$ where $P = [\text{Max}(F_o^2, 0) + 2F_c^2]/3$). For **32** $a_0 = 0.1136$, $a_1 = 257.4679$; for **36** $a_0 = 0.0456$, $a_1 = 22.8603$

proceeded using the program *SHELXL-93*.[10b] Hydrogen atom positions were calculated by assuming idealized sp^2 or sp^3 geometries about their attached carbon atoms (as appropriate), and were given thermal parameters 120% of the equivalent isotropic displacement parameters of their attached carbons. For compound **36** there are two unique molecules per unit cell, with bond lengths and angles being comparable for both. Further details of structure refinement (other than described below) and final residual indices may be found in Table 4.2. Interatomic distances and angles have also been tabulated for each compound (Table 4.3 for **32**, Table 4.4 for **36**).

Location of all atoms in both compounds proceeded smoothly, however the triflate anion for compound **32** was not well behaved so the bond lengths were constrained to enforce an idealized geometry. The following restraints were applied to enforce an idealized geometry upon the triflate ion: $d(S-C(91))$ = 1.80(1) Å; $d(S-O(91)) = d(S-O(92)) = d(S-O(93)) = 1.45(1)$ Å; $d(F(91)-C(91))$ = $d(F(92)-C(91)) = d(F(93)-C(91)) = 1.35(1)$ Å; $d(F(91)-F(92)) = d(F(91)-F(93))$ = $d(F(92)-F(93)) = 2.20(1)$ Å; $d(O(91)-O(92)) = d(O(91)-O(93)) = d(O(92)-O(93)) = 2.37(1)$ Å; $d(F(91)-O(92)) = d(F(91)-O(93)) = d(F(92)-O(91)) =$ $d(F(92)-O(93)) = d(F(93)-O(91)) = d(F(93)-O(92)) = 3.04(1)$ Å.

Results and Characterization of Compounds

Compound **2** reacts with ethylene to yield $[Ir_2(CH_3)(CO)_2(C_2H_4)$-$(dppm)_2][CF_3SO_3]$ **(30)**, as shown in Scheme 4.1. This product was originally produced by substitution of one carbonyl by ethylene in the tricarbonyl methylene-hydride compound $[Ir_2(H)(CO)_3(\mu\text{-}CH_2)(dppm)_2][CF_3SO_3]$.[9] The previous study had established that the ethylene ligand is terminally bound to one metal with the methyl ligand bound terminally to the other. The two carbonyl ligands are bound to the same metal as the methyl ligand, interacting in a semibridging fashion with the adjacent metal.

Compound **2** also reacts with tetrafluoroethylene, producing the bridging alkene adduct $[Ir_2(CH_3)(CO)_2(\mu\text{-}C_2F_4)(dppm)_2][CF_3SO_3]$ **(31)** shown in Scheme 4.1. Compound **31** is a *rare* example of an A-frame-like compound bridged by an olefin. However, late-metal binuclear complexes with bridging tetrafluoroethylene are known.[11] The ^1H NMR spectrum of **31** shows the terminal methyl group as a triplet at δ 0.41 and a coincidental overlap for the dppm methylene signals at δ 3.89. The ^{19}F NMR spectrum shows two resonances for the olefin substituents as multiplets at δ -79.2 and -85.9, that upon ^{31}P selective decoupling are shown to be coupled to different sets of phosphorus nuclei, consistent with the bridging formulation. If compound **31** had a structure similar to the previously characterized ethylene complex **(30)** that contains a terminal ethylene and terminal methyl ligands in a symmetrical orientation (see Scheme 4.1), we would expect only one resonance for the

Scheme 4.1

Species in box has been
previously characterized.[9]
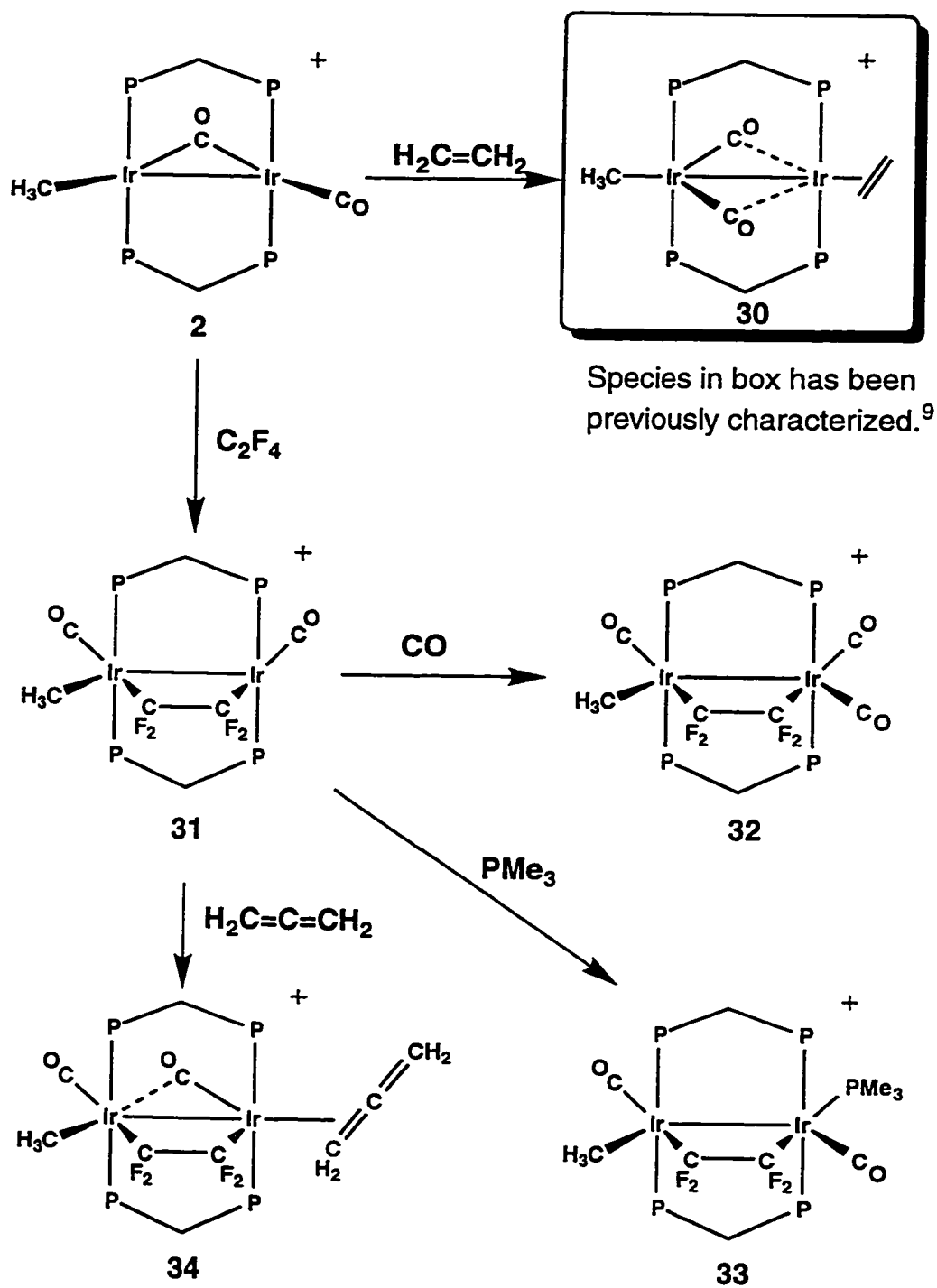
olefin fluorines, which would then be coupled to only one pair of phosphorus nuclei.

The bridging olefin can be described as a dimetallacyclobutane in which each end of the organic portion is similar to a perfluroalkyl group. It is known that perfluroalkyl transition-metal compounds typically have very strong M-C bonds and as a result migratory insertion is not well known for these types of ligands.[12]

Compound **31** was reacted with various ligands in an attempt to induce migratory insertion of the methyl ligand with either the tetrafluoroethylene ligand, a CO ligand or the added substrate (allene). Compound **31** reacts with carbon monoxide to yield the tricarbonyl compound $[Ir_2(CH_3)(CO)_3-(\mu-C_2F_4)(dppm)_2][CF_3SO_3]$ (**32**) in which the added CO has filled the vacant site at one metal (see Scheme 4.1). The ^1H NMR spectrum is similar to that observed for compound **31** showing the Ir-bound methyl proton resonance as a triplet at δ 0.79 and a coincidental overlap of the dppm methylenes at δ 4.60. In order to determine whether the olefin and methyl groups were mutually cis and therefore capable of migratory insertion without significant rearrangement, the X-ray structure of **32** was determined. A representation of the compound is shown in Figure 4.1, and a compilation of important bond lengths and angles is given in Table 4.3.

This structure confirms the bridging tetrafluoroethylene formulation and confirms that the methyl ligand is bound terminally to Ir(2) adjacent to the olefin. The structure for **32** is analogous to that seen for the alkyne-bridged
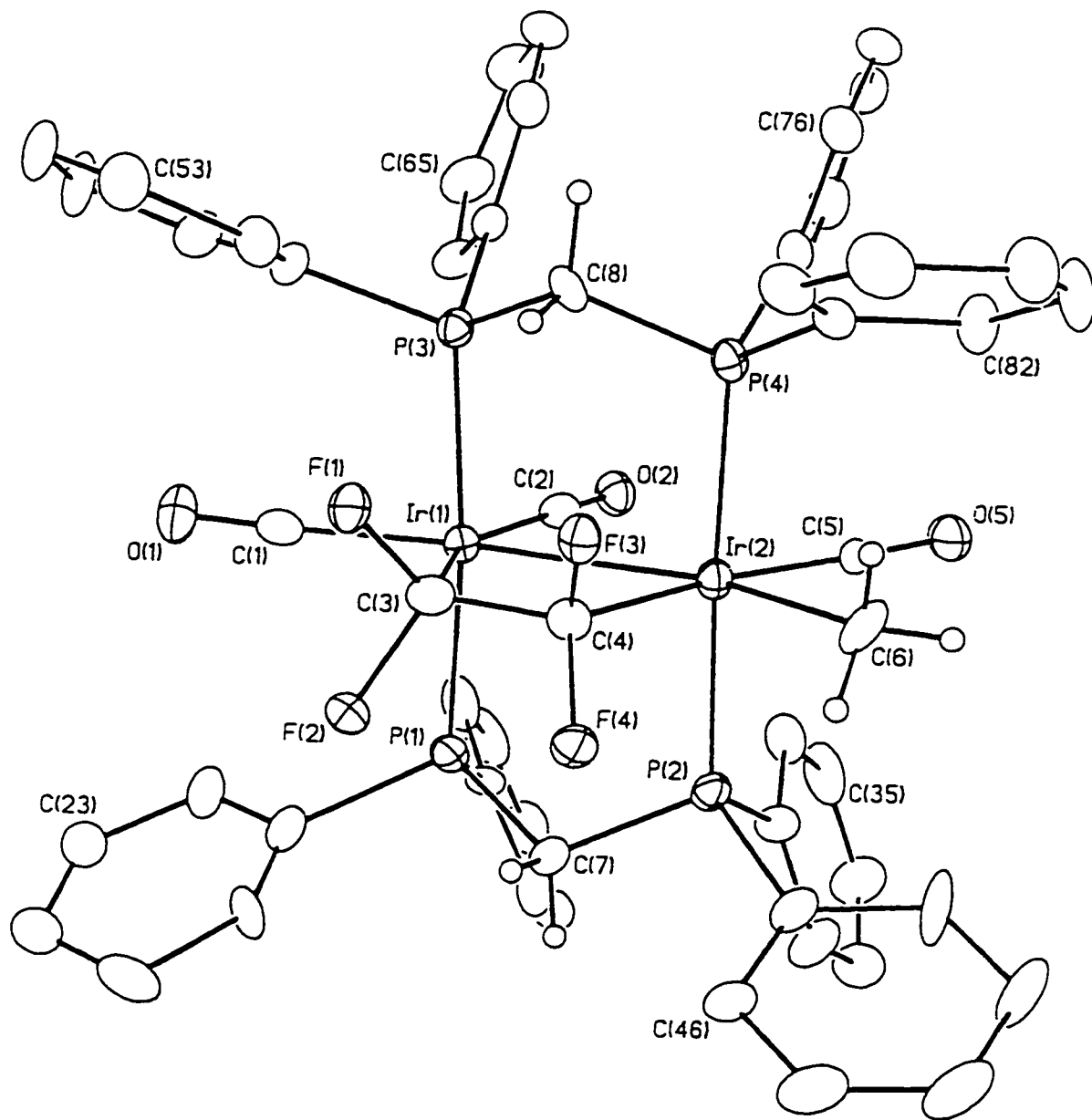
Figure 4.1 Perspective view of the [Ir$_2$(CH$_3$)(CO)$_3$(μ-C$_2$F$_4$)(dppm)$_2$]$^+$ cation of compound **32**. Thermal ellipsoids are shown at the 20% probability level except for hydrogens which are shown arbitrarily small. Phenyl hydrogens have been omitted.

Table 4.3. Selected Interatomic Distances and Angles for Compound **32**.

(a) Distances (Å)

Atom1	Atom2	Distance	Atom1	Atom2	Distance
Ir(1)	Ir(2)	2.8968(9)	Ir(2)	P(4)	2.346(5)
Ir(1)	C(1)	1.96(2)	F(1)	C(3)	1.40(2)
Ir(1)	C(2)	1.89(2)	F(2)	C(3)	1.45(2)
Ir(1)	C(3)	2.11(2)	F(3)	C(4)	1.41(2)
Ir(2)	C(4)	2.09(2)	F(4)	C(4)	1.38(2)
Ir(2)	C(5)	1.81(2)	O(1)	C(1)	1.13(2)
Ir(2)	C(6)	2.17(2)	O(2)	C(2)	1.14(2)
Ir(1)	P(1)	2.375(5)	O(5)	C(5)	1.23(2)
Ir(1)	P(3)	2.397(4)	C(3)	C(4)	1.53(3)
Ir(2)	P(2)	2.341(5)			

(b) Angles (deg)

Atom1	Atom2	Atom3	Angle	Atom1	Atom2	Atom3	Angle
Ir(2)	Ir(1)	C(1)	168.5(6)	Ir(1)	C(2)	O(2)	178.6(13)
Ir(2)	Ir(1)	C(2)	82.5(5)	Ir(1)	C(3)	F(1)	115.2(13)
Ir(2)	Ir(1)	C(3)	71.2(5)	Ir(1)	C(3)	F(2)	111.0(12)
P(1)	Ir(1)	P(3)	174.3(2)	Ir(1)	C(3)	C(4)	108.2(11)
C(1)	Ir(1)	C(2)	109.0(8)	F(1)	C(3)	F(2)	100.5(13)
C(1)	Ir(1)	C(3)	97.3(8)	F(1)	C(3)	C(4)	112.2(15)
C(2)	Ir(1)	C(3)	153.7(7)	F(2)	C(3)	C(4)	109.5(15)
Ir(1)	Ir(2)	C(4)	70.9(5)	Ir(2)	C(4)	F(3)	114.1(10)
Ir(1)	Ir(2)	C(5)	120.2(7)	Ir(2)	C(4)	F(4)	114.9(11)
Ir(1)	Ir(2)	C(6)	155.4(6)	Ir(2)	C(4)	C(3)	109.8(12)
P(2)	Ir(2)	P(4)	177.1(2)	F(3)	C(4)	F(4)	100.5(12)
C(4)	Ir(2)	C(5)	168.9(8)	F(3)	C(4)	C(3)	106.9(13)
C(4)	Ir(2)	C(6)	84.5(8)	F(4)	C(4)	C(3)	110.2(14)
C(5)	Ir(2)	C(6)	84.4(9)	Ir(2)	C(5)	O(5)	177.1(17)
Ir(1)	C(1)	O(1)	177.5(18)				

compound [Ir$_2$(CH$_3$)(CO)$_2$(PMe$_3$)(μ-DMAD)(dppm)$_2$][CF$_3$SO$_3$] (**11**) (see Chapter

3). The coordination at each metal can be described as octahedral with two

carbonyls approximately trans to the bridging tetrafluoroethylene, and the

methyl group and a carbonyl opposite the metal-metal bond. The metal-metal

separation (2.8968(9) Å) is typical (although on the long side) of an iridium-

iridium single bond[13] and the diphosphines adopt their normal trans

configuration at each metal (P(1)-Ir(1)-P(3) = 174.3(2)°, P(2)-Ir(2)-P(4) =

177.1(2)°). The carbon-carbon distance of the olefin is in the normal range for a

C-C single bond (C(3)-C(4) = 1.53(3) Å), and the angles of the substituents at

the tetrafluoroethylene carbons approach the 109.5° sp^3 hybridized value. The

corresponding metal-carbon distances (Ir(1)-C(3) = 2.11(2) Å, and Ir(2)-C(4) =

2.09(2) Å) are consistent with a single bond between iridium and the sp^3-

hybridized carbons, although slightly shorter than the the iridium-methyl

distance of 2.17(2) Å. All structural data above are consistent with

rehybridization of the olefin such that it is best described as a dimetallacyclo-
butane moiety.

Compound **31** reacts with trimethylphosphine to give the PMe$_3$ adduct,

[Ir$_2$(CH$_3$)(CO)$_2$(PMe$_3$)(μ-C$_2$F$_4$)(dppm)$_2$][CF$_3$SO$_3$] (**33**), having a structure similar to

that of **32**. The ^{31}P{^{1}H} NMR spectrum shows a broad triplet at δ -67.9 for the

PMe$_3$ ligand, displaying 55 Hz coupling to fluorine. Although we had

anticipated PMe$_3$ attack adjacent to the one end of the bridged olefin in **31**, the

large coupling between the PMe$_3$ phosphorus nuclei and two fluorines strongly

supports the geometry shown in which the PMe$_3$ ligand is trans to one end of

the tetrafluoroethylene ligand. A much smaller coupling of *ca.* 22 Hz is observed between the olefin fluorines and the dppm phosphorus nuclei that are adjacent, but in a cis orientation. The PMe_3 ligand is presumed to coordinate opposite the C_2F_4 ligand and not adjacent to it because of an unfavorable steric interaction between the PMe_3 methyl groups and the fluorines. In the ^1H NMR spectrum the terminal methyl resonance appears at δ 0.92 as a slightly broadened triplet and the PMe_3 protons appear as a doublet at δ 0.80. The lack of discernible coupling between the iridium-bound methyl group and the phosphorus nucleus of the PMe_3 ligand, indicates that they occupy positions on different metals.

Compound **31** also reacts with allene to give an allene adduct, $[Ir_2(CH_3)(CO)_2(H_2C=C=CH_2)(\mu-C_2F_4)(dppm)_2][CF_3SO_3]$ (**34**) believed to have the structure shown in Scheme 4.1. The geminal protons of the coordinated portion of the allene ligand appear in the ^1H NMR spectrum as a broad resonance at δ 1.42 with the uncoordinated olefin geminal protons showing up at δ 6.68 and 6.30. The Ir-bound methyl appears at δ 0.22 as a triplet. In the $^{13}C\{^1H\}$ NMR spectrum the carbonyls appear as broad resonances at δ 177.3 and 189.9, the latter one possibly indicating a semibridging interaction of one of the carbonyls with the adjacent metal. A similar downfield shift has been observed in compounds containing a semibridging carbonyl group.[9,14] An infrared spectrum could not be obtained on compound **34** because the allene ligand is not strongly bound and is lost if the compound is not kept under an atmosphere of allene that is at a

greater than atmospheric pressure. The structure proposed in Scheme 4.1 is based on steric considerations, placing the uncoordinated portion of the allene ligand adjacent to the semibridging carbonyl, away from the large fluorine substituents. The other possibility, with the uncoordinated portion of the allene adjacent to the tetrafluoroethylene ligand seems less likely due to unfavorable interaction between the allene and the fluorines of the tetrafluoroethylene.

Compound **2** also reacts with 1,3-butadiene under ambient conditions, however in this case a simple π-olefin adduct is not obtained. Over a 48 h period compound **2** and 1,3-butadiene react to produce a methyl-vinylvinylidene-dihydride $[Ir_2(CH_3)(H)(CO)_2(\mu\text{-}C=C(H)C(H)=CH_2)(\mu\text{-}H)(dppm)_2]$-$[CF_3SO_3]$ (**35**) that has resulted from double α-C-H activation of the butadiene substrate (see Scheme 4.2). Other examples of double C-H activation of olefins are known, but invariably harsher reaction conditions involving either high temperature or photolysis were employed.[15] Compound **35** (analogous to $[Ir_2(CH_3)(C\equiv CH)(CO)_2(\mu\text{-}H)(\mu\text{-}C=CH_2)(dppm)_2][CF_3SO_3]$ (**23**), see Chapter 3) has been extensively studied by NMR spectroscopy, and shows a downfield shift at δ 196.0 in the $^{13}C\{^1H\}$ NMR spectrum consistent with the α-carbon in a bridging vinylidene complex.[16] Two triplet resonances for the carbonyls appear at δ 173.6 and 173.2 while the IR spectrum shows stretches at 2014 and 2003 cm^{-1} consistent with terminal coordination of these groups. The vinyl portion of the vinylvinylidene ligand appears at δ 145.8 for the γ-carbon and δ 112.0 for the delta-carbon, with the Ir-bound methyl carbon appearing as a broad signal

Scheme 4.2

35: R = CH=CH$_2$
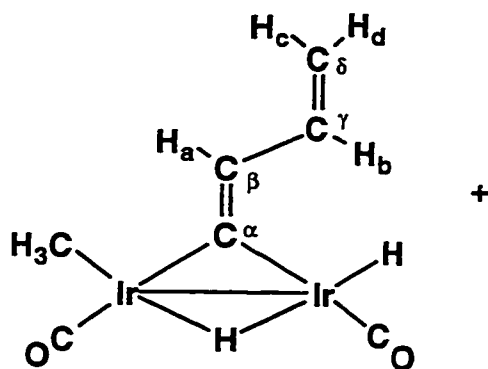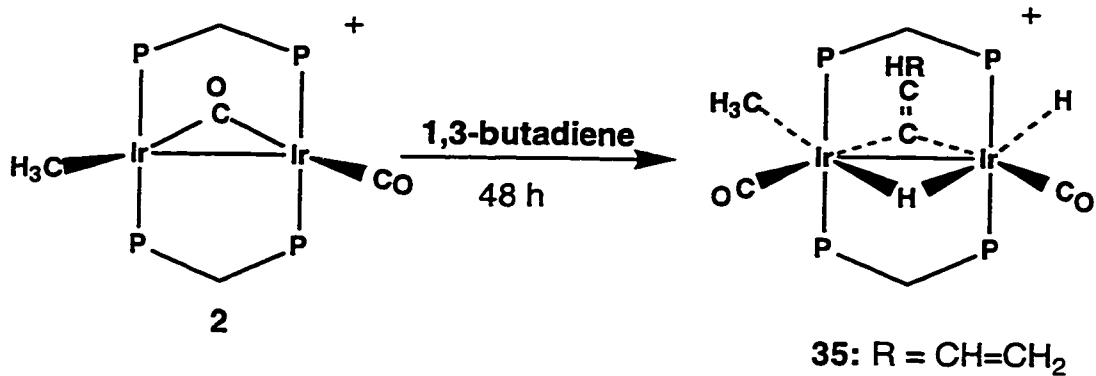
Alternate view of compound **35** in equatorial plane with phosphines omitted for clarity.

at δ -9.9. The signal for the β-carbon of the vinylidene was not observed and is thought to be obscured by the phenyl carbon resonances. In the ^{1}H NMR spectrum the vinylidene proton (labelled H_a in Scheme 4.2) appears as a doublet at δ 6.79, the vinyl β-protons (labelled H_c and H_d) appear at δ 4.91 and 4.38 and the vinyl α-proton (labelled H_b) resonance is a doublet of doublets of doublets at δ 5.79. The resonance for the Ir-bound methyl group appears as a triplet at δ -0.51 with the terminal hydride showing up as a triplet at δ -12.64 and the bridging hydride as a quintet at δ -13.9, indicating similar coupling to the two sets of differing phosphines.

When compound 2 is reacted with allene or methylallene rare examples of η^1,η^3-bridging allene adducts,[17] $[Ir_2(CH_3)(CO)_2(\mu-\eta^1,\eta^3-CH_2CC(H)R)(dppm)_2]$-$[SO_3CF_3]$ (36, R = H; 37, R = CH$_3$) (see Scheme 4.3), are initially formed. Both compounds have been extensively studied by NMR spectroscopy and assignments of the ^{1}H and ^{13}C{^{1}H} NMR chemical shifts of the $\mu-\eta^1,\eta^3$-allene were accomplished by ^{1}H, ^{1}H-COSY, HMQC, INAPT and NOE experiments. For compound 36, the ^{13}C{^{1}H} NMR spectrum shows two terminal carbonyl resonances at δ 179.2 and 171.2 , a multiplet at δ 61.3 assigned to the two equivalent α-allene carbons and a triplet at δ -31.1 for the terminal methyl group. An INAPT experiment showed the central allene carbon as a multiplet at δ 127.3. This chemical shift is consistent with a rehybridization of the central allene carbon from sp to sp^2,[18] and is in the range typically seen for the central

Scheme 4.3

39: R = R' = H
25a: R = CH₃, R' = H
25b: R = H, R' = CH₃
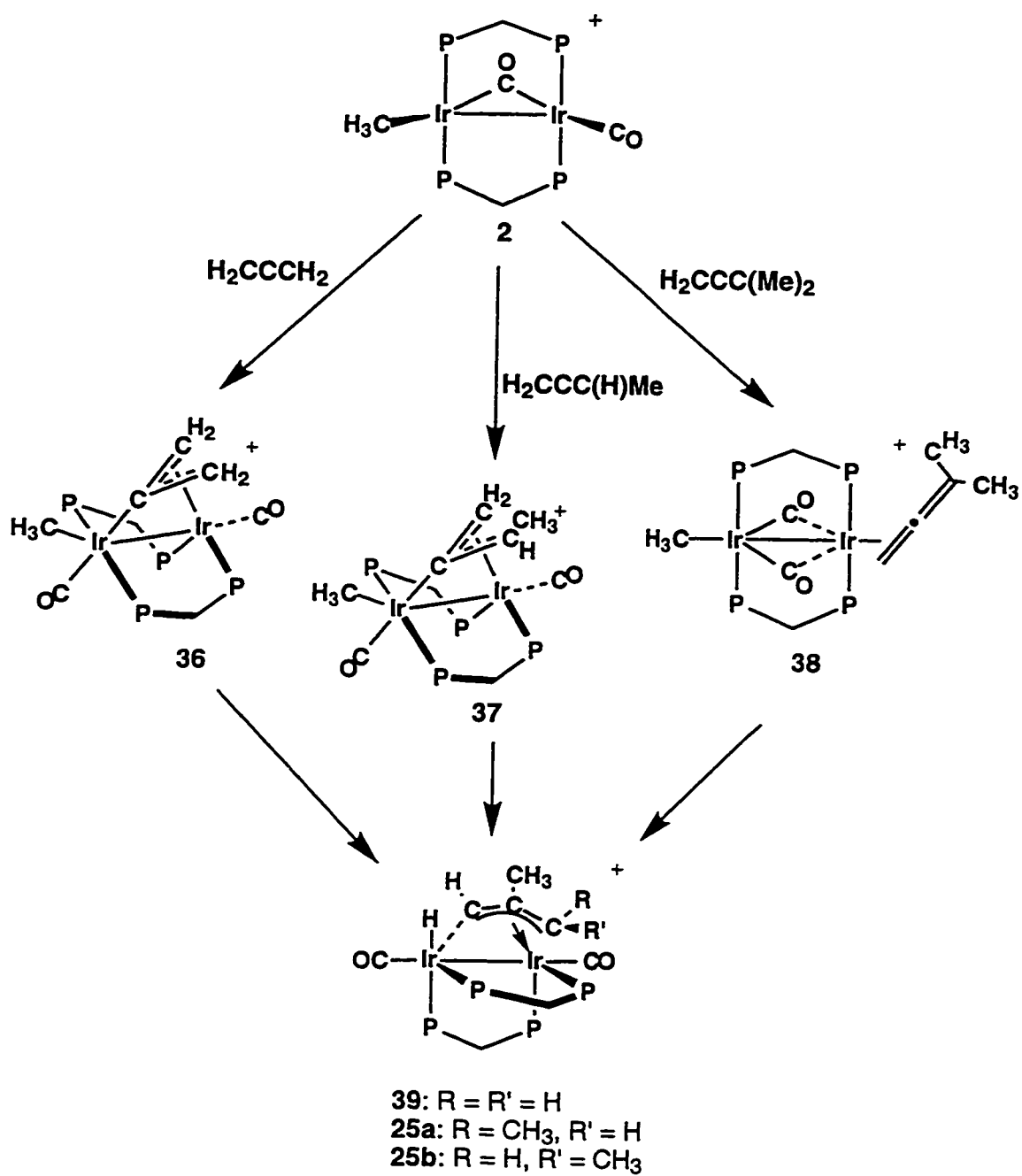
carbon of η^3-allyl groups.[19] The ^{1}H NMR spectrum shows signals for the allene protons at δ 4.23 and 3.52 arising from the anti and syn protons, respectively (as established by NOE experiments).[20] An HMQC experiment shows that both of these signals arise from protons on two carbons that are equivalent, consistent with the α-allene carbons. The resonance for the Ir-bound methyl group appears as a triplet at δ 1.18 showing coupling ($^3J_{H\text{-}P}$ = 5 Hz) consistent with being adjacent to two phosphine ligands. However, the ^{31}P$\{^1$H$\}$ NMR spectrum of **36** showed an atypical pattern consisting of one multiplet, quite different from the usual two multiplet AA'BB' pattern (see Figure 3.3 Chapter 3) observed when both sets of phosphines are trans, suggesting that there was a deviation from the trans arrangement. The proposed structure for **36** is conclusively established by the X-ray structure determination, a representation of which is shown in Figure 4.2, with an alternate view shown in Figure 4.2.1. A compilation of important bond lengths and angles is given in Table 4.4. This product is formally analogous to the alkyne- and olefin-bridged products **9** and **32** giving a cis methyl-substrate geometry at Ir(1) much like that observed in **9** and **32**, but having a cis-phosphine arrangement at Ir(2), at which η^3-binding of the iridaallyl group occurs. For bond lengths and angles the values for each crystallographically independent molecule (A and B) are given with the values for molecule B in parentheses. The allene moiety symmetrically bridges the metals; η^1-bound to Ir(1) (Ir(1)-C(4) = 2.09(2) Å (2.10(2) Å)) and η^3-bound to Ir(2) (Ir(2)-C distances: 2.20(2) (2.21(2)), 2.12(2) (2.13(2)), 2.207(15) (2.21(2)) Å).

Figure 4.2 Perspective view of the one of the two crystallographically independent $[Ir_2(CO)_2(CH_3)(\mu\text{-}\eta^1\text{:}\eta^3\text{-}C\{CH_2\}_2)(dppm)_2]^+$ cations (molecule A) of compound **36**. Thermal ellipsoids are shown at the 20% probability level except for hydrogens which are shown arbitrarily small. Phenyl hydrogens have been omitted.
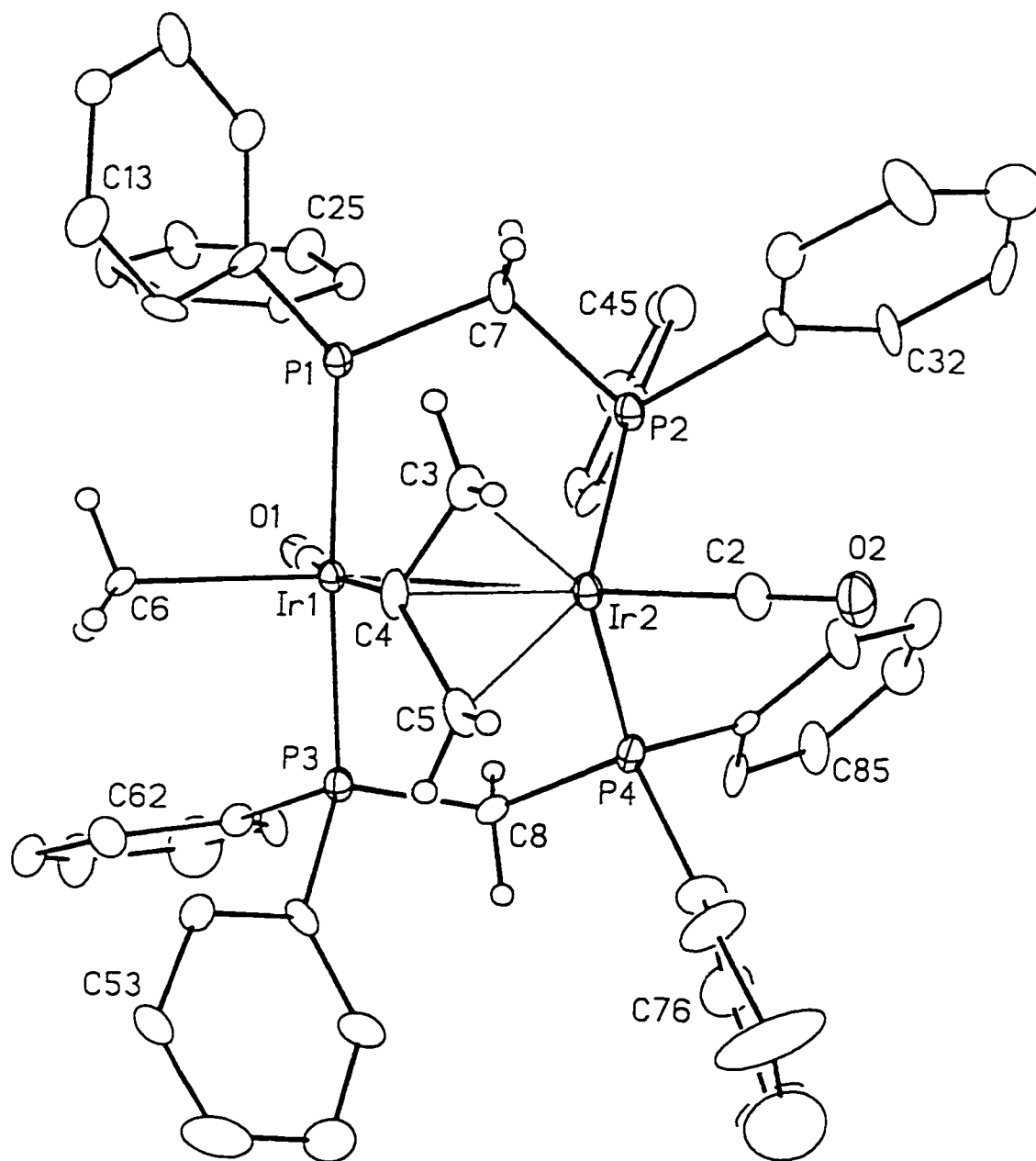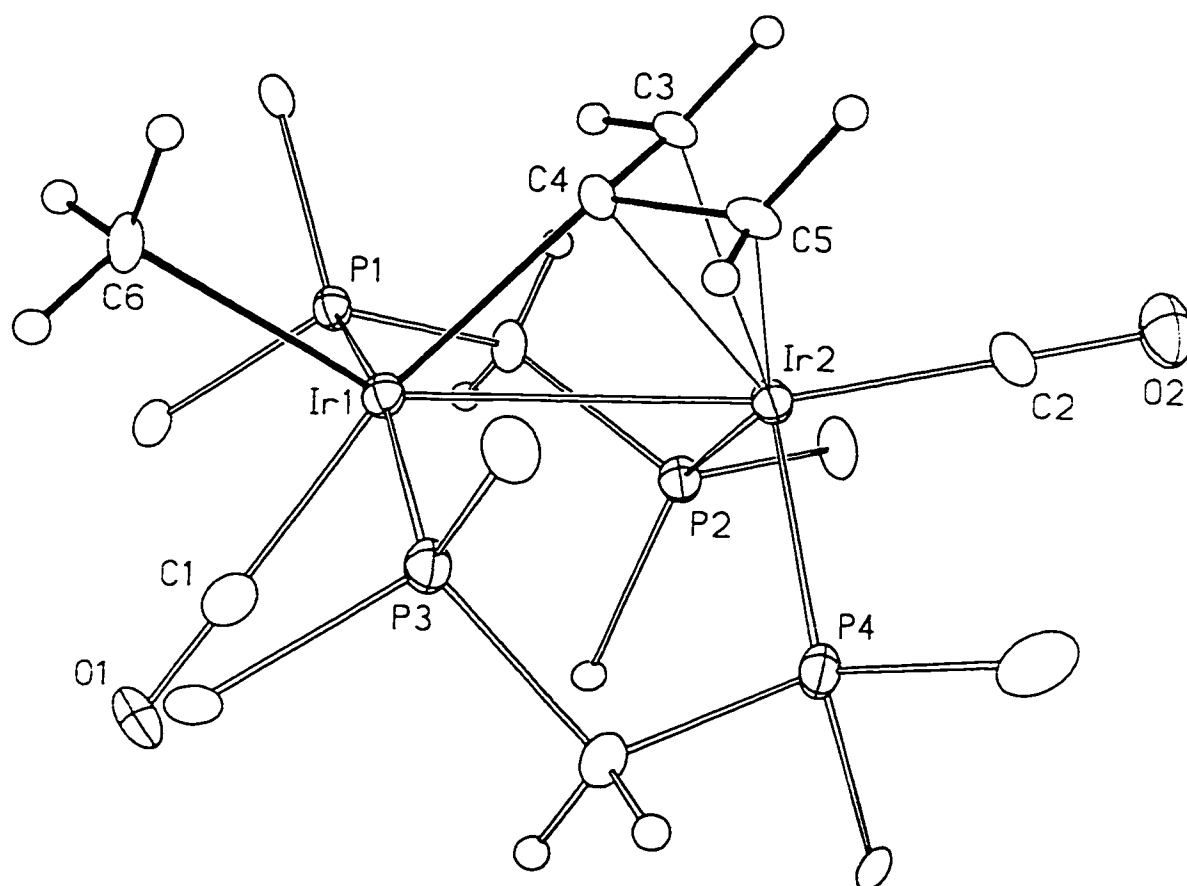
Figure 4.2.1 Alternate view of one of the two crystallographically independent [Ir$_2$(CO)$_2$(CH$_3$)(μ-η^1:η^3-C{CH$_2$}$_2$)(dppm)$_2$]$^+$ cations of compound **36**. Only the ipso carbons of the dppm phenyl rings are shown.

Table 4.4. Selected Interatomic Distances and Angles for Compound **36**.

(a) distances

Molecule A			Molecule B		
Atom1	Atom2	Distance	Atom1	Atom2	Distance
Ir(1)	Ir(2)	2.8438(10)	Ir(1)	Ir(2)	2.8353(9)
Ir(1)	P(1)	2.365(5)	Ir(1)	P(1)	2.361(5)
Ir(1)	P(3)	2.371(5)	Ir(1)	P(3)	2.335(5)
Ir(1)	C(1)	1.90(2)	Ir(1)	C(1)	1.91(2)
Ir(1)	C(4)	2.09(2)	Ir(1)	C(4)	2.100(15)
Ir(1)	C(6)	2.187(15)	Ir(1)	C(6)	2.20(2)
Ir(2)	P(2)	2.317(4)	Ir(2)	P(2)	2.341(5)
Ir(2)	P(4)	2.329(5)	Ir(2)	P(4)	2.336(5)
Ir(2)	C(2)	1.88(2)	Ir(2)	C(2)	1.90(2)
Ir(2)	C(3)	2.20(2)	Ir(2)	C(3)	2.21(2)
Ir(2)	C(4)	2.12(2)	Ir(2)	C(4)	2.13(2)
Ir(2)	C(5)	2.207(15)	Ir(2)	C(5)	2.21(2)
P(1)	C(7)	1.84(2)	P(1)	C(7)	1.83(2)
P(2)	C(7)	1.87(2)	P(2)	C(7)	1.84(2)
P(3)	C(8)	1.82(2)	P(3)	C(8)	1.87(2)
P(4)	C(8)	1.86(2)	P(4)	C(8)	1.87(2)
O(1)	C(1)	1.13(2)	O(1)	C(1)	1.14(2)
O(2)	C(2)	1.17(2)	O(2)	C(2)	1.12(2)
C(3)	C(4)	1.41(2)	C(3)	C(4)	1.45(2)
C(4)	C(5)	1.44(2)	C(4)	C(5)	1.44(2)

Table 4.4. Selected Interatomic Distances and Angles for Compound **36** (continued).

(b) angles

	Molecule A				Molecule B		
Atom1	Atom2	Atom3	Angle	Atom1	Atom2	Atom3	Angle
Ir(2)	Ir(1)	P(1)	91.41(11)	Ir(2)	Ir(1)	P(1)	91.82(11)
Ir(2)	Ir(1)	P(3)	90.24(11)	Ir(2)	Ir(1)	P(3)	92.87(11)
Ir(2)	Ir(1)	C(1)	121.1(5)	Ir(2)	Ir(1)	C(1)	117.9(5)
Ir(2)	Ir(1)	C(4)	48.0(4)	Ir(2)	Ir(1)	C(4)	48.5(5)
Ir(2)	Ir(1)	C(6)	148.6(4)	Ir(2)	Ir(1)	C(6)	151.6(5)
P(1)	Ir(1)	P(3)	167.77(15)	P(1)	Ir(1)	P(3)	173.06(15)
P(1)	Ir(1)	C(1)	86.8(6)	P(1)	Ir(1)	C(1)	87.3(6)
P(1)	Ir(1)	C(4)	93.2(6)	P(1)	Ir(1)	C(4)	93.7(5)
P(1)	Ir(1)	C(6)	92.2(5)	P(1)	Ir(1)	C(6)	89.5(5)
P(3)	Ir(1)	C(1)	82.0(6)	P(3)	Ir(1)	C(1)	86.0(6)
P(3)	Ir(1)	C(4)	96.9(6)	P(3)	Ir(1)	C(4)	93.3(5)
P(3)	Ir(1)	C(6)	92.7(5)	P(3)	Ir(1)	C(6)	88.8(5)
C(1)	Ir(1)	C(4)	169.1(7)	C(1)	Ir(1)	C(4)	166.4(7)
C(1)	Ir(1)	C(6)	90.2(7)	C(1)	Ir(1)	C(6)	90.5(7)
C(4)	Ir(1)	C(6)	100.6(6)	C(4)	Ir(1)	C(6)	103.1(7)
Ir(1)	Ir(2)	P(2)	87.20(12)	Ir(1)	Ir(2)	P(2)	87.87(11)
Ir(1)	Ir(2)	P(4)	91.12(12)	Ir(1)	Ir(2)	P(4)	89.73(11)
Ir(1)	Ir(2)	C(2)	169.0(5)	Ir(1)	Ir(2)	C(2)	167.9(5)
Ir(1)	Ir(2)	C(3)	72.6(4)	Ir(1)	Ir(2)	C(3)	74.7(4)
Ir(1)	Ir(2)	C(4)	47.0(4)	Ir(1)	Ir(2)	C(4)	47.5(4)
Ir(1)	Ir(2)	C(5)	73.6(4)	Ir(1)	Ir(2)	C(5)	73.9(4)
P(2)	Ir(2)	P(4)	108.5(2)	P(2)	Ir(2)	P(4)	114.5(2)
P(2)	Ir(2)	C(2)	97.4(5)	P(2)	Ir(2)	C(2)	96.0(5)
P(2)	Ir(2)	C(3)	91.6(5)	P(2)	Ir(2)	C(3)	91.6(5)
P(2)	Ir(2)	C(4)	113.3(5)	P(2)	Ir(2)	C(4)	113.2(4)
P(2)	Ir(2)	C(5)	151.7(5)	P(2)	Ir(2)	C(5)	151.6(5)
P(4)	Ir(2)	C(2)	96.9(7)	P(4)	Ir(2)	C(2)	99.0(5)
P(4)	Ir(2)	C(3)	153.7(5)	P(4)	Ir(2)	C(3)	149.2(5)
P(4)	Ir(2)	C(4)	116.1(6)	P(4)	Ir(2)	C(4)	111.9(5)
P(4)	Ir(2)	C(5)	92.8(5)	P(4)	Ir(2)	C(5)	87.5(5)

Table 4.4. Selected Interatomic Distances and Angles for Compound **36**. (continued)

Molecule A				Molecule B			
Atom1	Atom2	Atom3	Angle	Atom1	Atom2	Atom3	Angle
C(2)	Ir(2)	C(3)	97.1(7)	C(2)	Ir(2)	C(3)	93.7(7)
C(2)	Ir(2)	C(4)	122.1(7)	C(2)	Ir(2)	C(4)	120.8(6)
C(2)	Ir(2)	C(5)	98.4(6)	C(2)	Ir(2)	C(5)	98.0(7)
C(3)	Ir(2)	C(4)	38.1(6)	C(3)	Ir(2)	C(4)	38.9(6)
C(3)	Ir(2)	C(5)	63.2(7)	C(3)	Ir(2)	C(5)	62.9(7)
C(4)	Ir(2)	C(5)	38.7(6)	C(4)	Ir(2)	C(5)	38.8(6)
Ir(1)	P(1)	C(7)	114.3(6)	Ir(1)	P(1)	C(7)	113.5(6)
Ir(2)	P(2)	C(7)	111.1(5)	Ir(2)	P(2)	C(7)	110.5(6)
Ir(1)	P(3)	C(8)	107.4(6)	Ir(1)	P(3)	C(8)	114.2(5)
Ir(2)	P(4)	C(8)	115.2(6)	Ir(2)	P(4)	C(8)	114.4(6)
Ir(1)	C(1)	O(1)	179.8(10)	Ir(1)	C(1)	O(1)	177.6(17)
Ir(2)	C(2)	O(2)	178.7(16)	Ir(2)	C(2)	O(2)	176.1(17)
Ir(2)	C(3)	C(4)	67.9(10)	Ir(2)	C(3)	C(4)	67.6(9)
Ir(1)	C(4)	Ir(2)	84.9(5)	Ir(1)	C(4)	Ir(2)	84.1(5)
Ir(1)	C(4)	C(3)	118.8(12)	Ir(1)	C(4)	C(3)	120.7(11)
Ir(1)	C(4)	C(5)	119.8(14)	Ir(1)	C(4)	C(5)	119.1(11)
Ir(2)	C(4)	C(3)	74.1(9)	Ir(2)	C(4)	C(3)	73.5(10)
Ir(2)	C(4)	C(5)	73.8(9)	Ir(2)	C(4)	C(5)	73.2(10)
C(3)	C(4)	C(5)	108.4(15)	C(3)	C(4)	C(5)	105.8(15)
Ir(2)	C(5)	C(4)	67.5(8)	Ir(2)	C(5)	C(4)	67.9(10)
P(1)	C(7)	P(2)	112.6(10)	P(1)	C(7)	P(2)	114.9(9)
P(3)	C(8)	P(4)	114.1(9)	P(3)	C(8)	P(4)	115.7(9)

The C(3)-C(4) and C(4)-C(5) bonds of the resulting fragment (1.41(2) (1.45(2)), 1.44(2) (1.44(2)) Å) as well as the C(3)-C(4)-C(5) angle of 108.4(2) (105.8(2))° are typical of an η^3-bound allyl group.[21] Although this allene binding mode is not common, it has been observed,[17,22] and the structural parameters for **36** appear typical for such groups. The metal-metal separation of 2.8438 (10) (2.8353(9)) Å is typical for an Ir-Ir single bond[13] with the phosphines on Ir(1) showing a trans arrangement (P(1)-Ir(1)-P(3) = 167.77(15) (173.06(15))°) and the phosphines at Ir(2) showing a cis arrangement (P(2)-Ir(2)-P(4) = 108.5(2) (114.5(2))°), presumably due to the increased steric requirements needed for the η^3-metallaallyl binding mode. The methyl group has a typical iridium-carbon single bond length of 2.187(15) (2.20(2)) Å.

For compound **37** the methyl substituent on the allene moiety removes the mirror plane symmetry observed in **36**, and as a result all four ^{31}P nuclei are different, giving rise to a more complicated ABCD multiplet in the ^{31}P{^{1}H} NMR spectrum than that observed for compound **36**. Figure 4.3 shows the ^{31}P{^{1}H} NMR spectra for compounds **36** and **37**, illustrating the difference between the AA'BB' pattern observed for the cis-trans configuration of compound **36** and the ABCD pattern observed for the cis-trans configuration of compound **37**. The loss of mirror symmetry resulting from methyl substitution on one end of the allene molecule also renders the dppm methylene protons inequivalent, appearing as multiplets at δ 5.79, 5.38, 5.19 and 4.87 in the ^{1}H NMR spectrum. The two geminal methylallene protons appear as multiplets at δ 5.17 and 3.78

Compound **36**
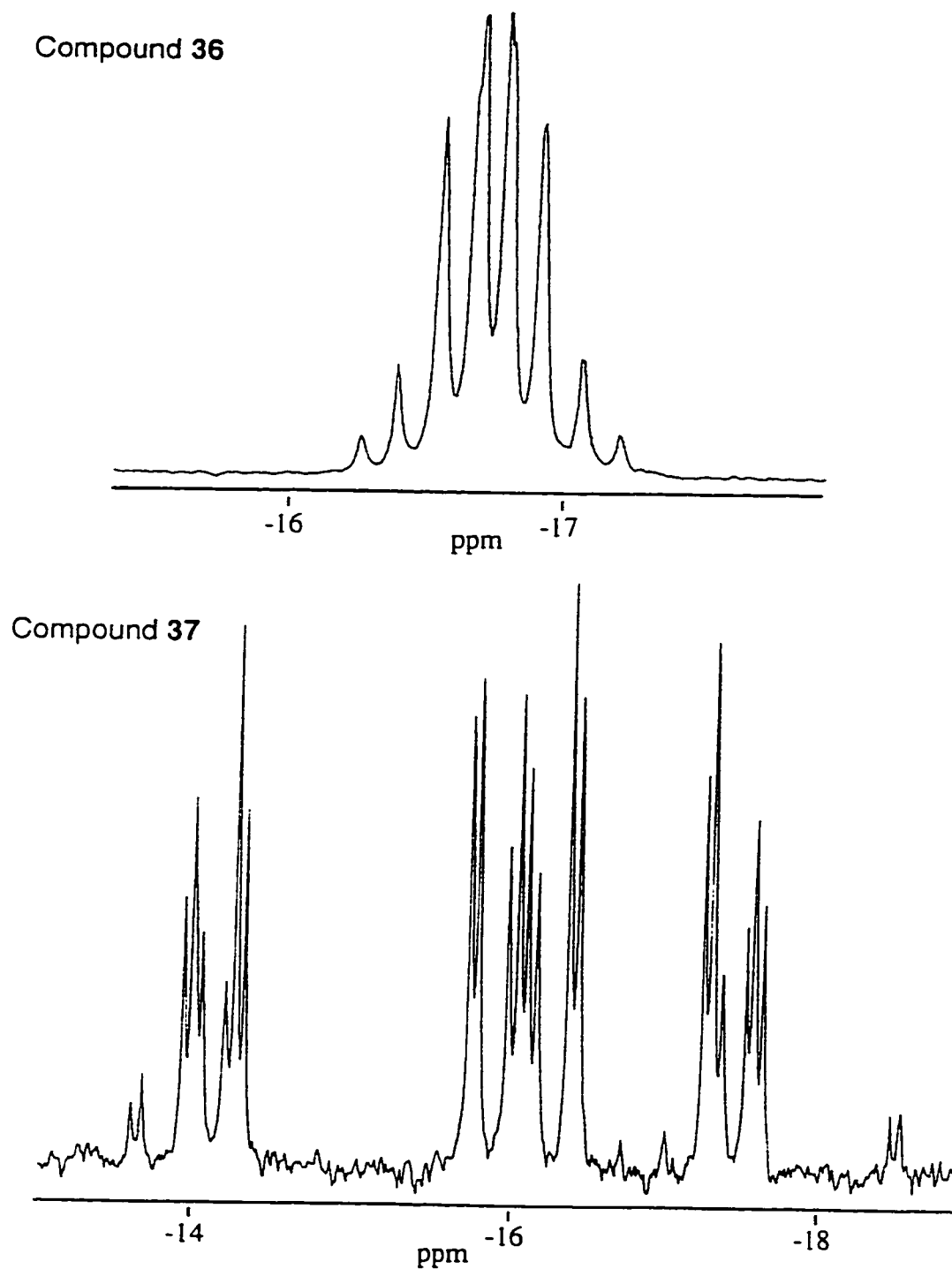
Compound **37**

Figure 4.3 ^{31}P NMR spectra for the compounds [Ir$_2$(CH$_3$)(CO)$_2$-
(μ-η_1:η_3-H$_2$C=C=CH$_2$)(dppm)$_2$][CF$_3$SO$_3$] (top) and
[Ir$_2$(CH$_3$)(CO)$_2$(μ-η^1:η^3-H$_2$C=C=C(H)CH$_3$)(dppm)$_2$][CF$_3$SO$_3$]
(bottom), illustrating the overlapped AA'BB' and ABCD
patterns, respectively.

with the other olefin proton appearing as a quartet of multiplets at δ 4.70 displaying coupling to the geminal methyl protons. The Ir-bound methyl resonance appears as a triplet at δ 1.16, and the allene methyl group shows up as a doublet of doublets at δ 1.07 displaying coupling to one phosphorus and the geminal hydrogen. For compound **37**, the $^{13}C\{^1H\}$ NMR spectrum shows two terminal carbonyl resonances, a triplet at δ 179.4 and a broad signal at δ 171.2. The inequivalent terminal-carbons of the methylallene appear as multiplets at δ 78.7 and 55.6, with the allene methyl group appearing as a multiplet at δ 18.6 and the terminal metal-bound methyl group appearing as a triplet at δ -32.2.

With dimethylallene, compound **2** reacts to form the η^2-allene adduct $[Ir_2(CH_3)(CO)_2(\eta^2\text{-}CH_2=C=C(CH_3)_2)(dppm)_2][SO_3CF_3]$ (**38**) (see Scheme 4.3), with a structure analogous to the previously characterized ethylene compound $[Ir_2(CH_3)(CO)_2(H_2C=CH_2)(dppm)_2][CF_3SO_3]$,[9] in which the methyl ligand is terminally bound to one metal with the coordinated olefin opposite the Ir-Ir bond on the adjacent metal. Both carbonyls are on the same metal as the methyl group. Presumably the difference in coordination modes for dimethylallene versus allene and methylallene is due to the higher steric demands of the more substituted substrate which presumably does not favor the η^3-binding observed for the others. The spectroscopy for compound **38** is similar to that observed for the ethylene compound (**30**), apart from the lower symmetry of **38** due to the

uncoordinated olefinic portion of the dimethylallene. The ^{1}H NMR spectrum for **38** shows the dppm methylene protons as mutiplets at δ 3.48 and 3.19, the coordinated olefin protons as a singlet at δ 1.58 and the methyl groups of the noncoordinated olefin portion as broad signals at δ 1.22 and 0.98. The signal for the terminal metal-bound methyl appears at δ 1.17 as a triplet. The ^{13}C{^{1}H} NMR spectrum shows two broad triplet carbonyl resonances at δ 206.4 and 204.8, similar to the carbonyl resonance observed for the ethylene compound (δ 204.0).[9] These are at lower field than that normally observed for terminally bound CO's in these compounds, and suggest that they may be involved in weak semibridging interactions with the adjacent metal.[9,14] ^{13}C{^{1}H} NMR experiments with selective ^{31}P decoupling show that, as in the ethylene compound, the carbonyls are weakly interacting with the phosphines on the opposite metal, supporting the proposed semibridging interaction. The infrared spectrum also supports this, showing a bridging carbonyl stretch at 1760 cm^{-1}. Unlike the ^{31}P{^{1}H} NMR spectrum observed for compounds **36** and **37**, the pattern for compound **38** is the typical AA´BB´ pattern observed when both sets of phosphines are trans.

As was observed for the products of compound **2** with internal alkynes (see Chapter 3), the allene adducts, **36** and **37** are the kinetic products. With time, compounds **36** and **37** rearrange; yielding the vinylcarbene products **3 9** and **25**, respectively. Compound **36** reacts slowly over a 7 day period converting to [Ir$_2$(H)(CO)$_2$(μ-η^1:η^3-HCC(Me)=CH$_2$)(dppm)$_2$][CF$_3$SO$_3$] (**39**) in about

80% yield as determined by $^{31}P\{^1H\}$ NMR spectroscopy. The spectroscopy for

39 is similar to the previously discussed vinylcarbene compounds **25-29** (see

Chapter 3). In the $^{31}P\{^1H\}$ NMR spectrum of **39**, an ABCD pattern is observed at

δ -5.1 (2P), -30.2 (1P), -32.4 (1P) consistent with the other vinylcarbenes of this

kind. Its ^1H NMR spectrum shows the resonance for the bridging-carbene

proton as a broad signal at δ 8.72, with the protons on the γ-carbon appearing

as broad signals at δ 3.43 and 3.11. The methyl protons of the vinylcarbene

group appear as a doublet at δ 2.79 and the terminal hydride is a second order

multiplet at δ -11.38, in the region consistent with the hydride resonances for the

other characterized vinylcarbenes (see Chapter 3). The characterization for

compounds **25a** & **b**, produced from the methylallene adduct, was straight-

forward, based on characteristic similarities in the $^{31}P\{^1H\}$ and ^1H NMR spectra

to compound **39** and a direct comparison with the spectroscopy for compound

25 produced in the 2-butyne reaction from Chapter 3 (Note: compound **25**

produced in Chapter 3 corresponds to **25a** in this chapter). However, all of the

proton resonances for compound **25b** could not be positively identified and

categorized due to the presence of the isomers, some reformation of compound

2 during the reaction and the formation of some decomposition products. The

two isomers of compound **25** are presumed to differ in the position of the methyl

group on the γ-carbon of the vinylcarbene substituent. With the methyl groups

of the vinylcarbene in a cis orientation (**25a**) the product is identical to

compound **25** formed in the reaction of compound **2** with 2-butyne, and the ^1H

and $^{31}P\{^1H\}$ NMR spectra concur. Compound **25b**, with the methyl groups of the vinylcarbene presumably in the trans orientation, shows an ABCD pattern in the $^{31}P\{^1H\}$ NMR spectrum at δ -7.6, -30.8, -37.9 and the characteristic resonances in the ^1H NMR spectrum at δ 8.96 and -11.18 for the bridging-carbene proton and terminal metal-bound hydride, respectively.

The production of compound **25a** from the extended reaction of the dimethylallene compound, **38**, was also characterized based upon only the characteristic $^{31}P\{^1H\}$ NMR spectrum that shows multiplets at δ -5.8, -6.0, -34.3 and -37.8 and the bridging-carbene proton and terminal-hydride resonances in the ^1H NMR spectrum at δ 8.65 and -11.25, respectively. In this reaction there is the *loss of one carbon-containing unit* and it was surmised from labelling studies that a radical process is occurring to promote the transformation. How this transformation occurs is not known but a labelling study carried out in CH_2Cl_2, using compound **38** that is ^{13}C-labelled in the Ir-bound methyl position, shows by $^{13}C\{^1H\}$ and ^1H NMR, the production of vinyl chloride, with no incorporation of the label into any of the vinylcarbene positions, as was observed for the reactions of **36** and **37**.

Discussion

The reaction of **2** with olefins has been found to proceed by three different routes, characterized by the nature of the added olefin. The three classes of olefins added were mono-olefins, conjugated olefins and cumulenes.

With mono-olefins such as ethylene and tetrafluroethylene reaction with **2** generates the olefin adducts **30** and **31** in which the methyl group remains terminally bound to one metal in each case. In the ethylene adduct, **30**, the olefin is terminally bound to one metal, while in **31**, the tetrafluoroethylene bridges the metals. The typical binding mode for alkynes with electron-withdrawing substituents with late-metal dppm-bridged bimetallic complexes is bridging the two metals, parallel to the metal-metal axis.[23] The parallel bridging mode is presumably observed for the alkynes because of strong Ir-C bonds. The different bonding modes for the two olefins in the final products (**30** and **31**) is undoubtedly due to a similar bond strength argument, in which tetrafluoroethylene, having the highly electronegative fluorine substituents, has stronger Ir-C bonds in the bridging rather than the terminal bonding mode (this would result from greater strain within the metallacyclopropane structure of a terminally bound olefin compared to the dimetallacyclobutane structure of a bridged geometry). Ethylene, having no electron withdrawing substituents, will be a stronger σ-donor and a weaker π-acceptor than tetrafluroethylene, so presumably the metallacyclopropane valence bond extreme is not attained meaning that the strain involving this group is less. The site of attack of the respective olefins in their reaction with **2**, adjacent to the methyl group for tetrafluoroethylene, and not adjacent to the methyl group for ethylene may also be a consequence of the difference in electronic properties.

In the only other tetrafluoroethylene-, dppm-bridged diiridium complex known, $[Ir_2(H)_2(CO)_2(\mu-H)(\mu-C_2F_4)(dppm)_2][BF_4]$,[23a] the tetrafluoroethylene ligand

is only weakly bound and is lost in the absence of excess olefin. This is not the case for compound **31** which is stable indefinitely to olefin loss. In addition, attempts to substitute the olefin ligand by hexafluorobutyne failed when compound **31** was exposed to HFB, indicating that the olefin ligand in compound **31** is strongly bound to the metals even with the large steric contribution from the fluorines of the olefin that we proposed to dictate the instability of the trihydride species $[Ir_2(H)_2(CO)_2(\mu-H)(\mu-C_2F_4)(dppm)_2][BF_4]$. The increased stability of **31** compared to the trihydride may also be a function of the lower oxidation states of the metals for **31**, making the dimetallacyclobutane structure more favorable.

The second reaction type was observed with 1,3-butadiene. When compound **2** is reacted with this conjugated olefin, double activation of one pair of geminal C-H bonds of the olefin occurs, producing a methyl-vinylvinylidene-dihydride (**35**). This species is substantially different from the products observed in the reactions of compound **2** with other olefins. We do not know why 1,3-butadiene reacts with **2** in this unusual way. There are many examples of olefin C-H activation to form vinyl-hydride compounds[24,25] but only a few instances in which further reaction is observed, leading to a second C-H activation to produce a vinylidene.[15] The reaction conditions in these rare cases invariably involve photolysis or elevated temperatures with monometallic species, or involve complexes with more than two metals that support a high degree of unsaturation and can coordinate the double bond of the resulting vinylidene.[15d,e,f] Even in multimetal systems the olefin typically undergoes only

the initial formation of the vinyl-hydride.[25] The additional C-H activation observed, yielding compound **35** is presumably due to the coordinative unsaturation displayed by both low-valent iridium centers in compound **2**. There has, to our knowledge, been no other report of a similar double C-H activation of 1,3-butadiene at ambient conditions.

Compound **35** is isoelectronic and structurally similar to the vinylidene-methyl acetylide compound (**23**) described in Chapter 3, with a hydride ligand in the place of the terminal acetylide ligand of **23**. Similar to compound **23**, compound **35** looks like a promising candidate for C-C bond formation between the vinylidene and the methyl ligand that are in a cis arrangement on the metals but this was not observed, even after refluxing in toluene for 24 h.

Attempts were made to react compound **2** with substituted butadienes (2,4-hexadiene and 1,3-hexadiene) but in each case no reaction was observed, presumably due to unfavorable steric interactions.

The third reaction type was observed with allenes. Reaction of compound **2** with allene and methylallene produced the rare η^1,η^3-bridging-allene compounds **36** and **37**. Although this unusual bridging mode was interesting in itself, the truly novel aspect of this chemistry resulted from their subsequent reactivity to produce the vinylcarbene compounds **39** and **25** analogous to the vinylcarbenes (**25-29**) observed in Chapter 3. In order to obtain mechanistic information about these novel rearrangements, and to compare to the reactivities of the alkynes with **2** as described in Chapter 3, a labelling study was carried out in which ^{13}C-methyl labelled compound **2** was

used in the reactions. In compound **39**, the ^{13}C-label was found to be incorporated (see Scheme 4.4) into the α-, 2-methyl- and γ-positions in a *ca.* 1:2:1 ratio. The incorporation of the methyl carbon into the α- and γ-sites supports a mechanism similar to that formulated for the alkyne reaction, as outlined in Scheme 4.5. We propose that the allene-bridged adduct (**36**) rearranges to the methylene-bridged hydride product **A**, analogous to the products in the reactions of CO, SO$_2$ and PR$_3$ and to the structure

Scheme 4.4

36   **39**
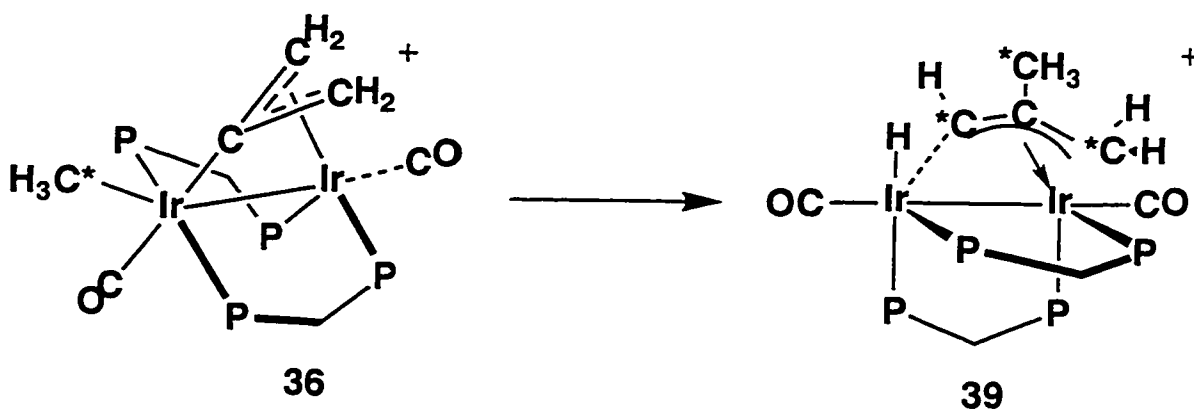
proposed for the reaction of compound **2** with nonactivated, internal alkynes (Scheme 3.4). Migratory insertion involving the allene and the hydride ligand could then yield the substituted vinyl product **B**. Although allene insertion into a metal-hydride bond has been known to yield allyl ligands,[26,27] the production of

vinyl ligands by this route has also been observed,[28] particularly with binuclear complexes.[29,30] A vinyl-to-methylene migration, as proposed by Maitlis,[31] would

Scheme 4.5
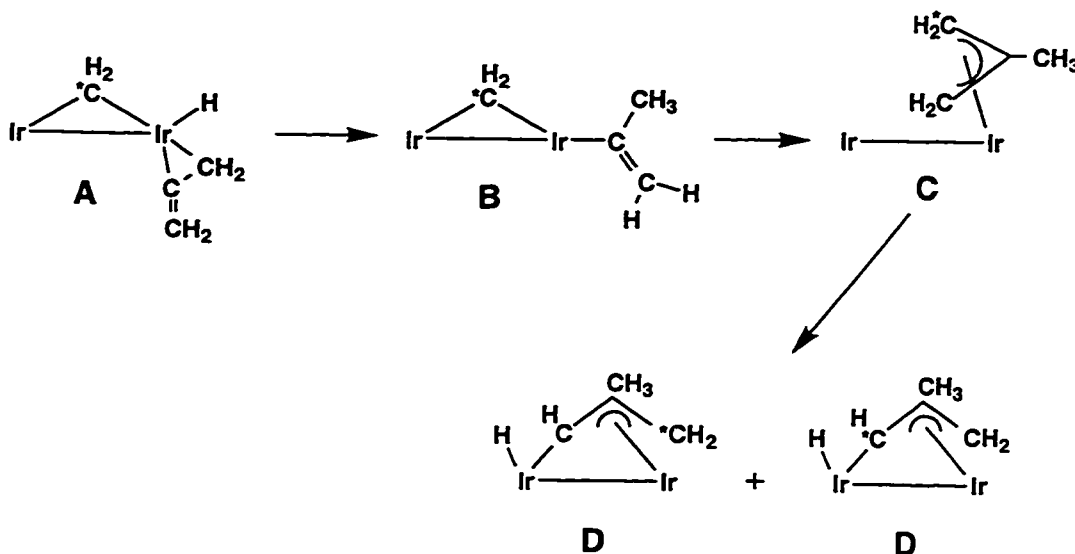
yield an allyl product, possibly having a structure such as C, and carbon-hydrogen bond cleavage by the adjacent metal, would yield the final vinylcarbene product (D). For reaction of the unsubstituted allene, C-H bond cleavage in C would be equally likely at *either* end of the symmetrical allyl ligand, scrambling the label equally between the α- and γ-sites of D, as was observed.

The incorporation of the ^{13}C-label into the 2-methyl position on the vinyl α-carbon cannot be rationalized by the above mechanism, so clearly another route must be involved. This other route, as outlined in Scheme 4.6, involves direct methyl migration to the central carbon (C(4)) of the metallallyl unit, as

suggested by the close proximity of these groups on Ir(1) in the structure of **36**, as shown on Figure 4.2. Direct methyl migration onto the central allyllic carbon in **36** could occur, yielding the 2-methyl allyl adduct, analogous to **C** in Scheme 4.5, but with the methyl group containing the ^{13}C-label. C-H bond cleavage, as

Scheme 4.6
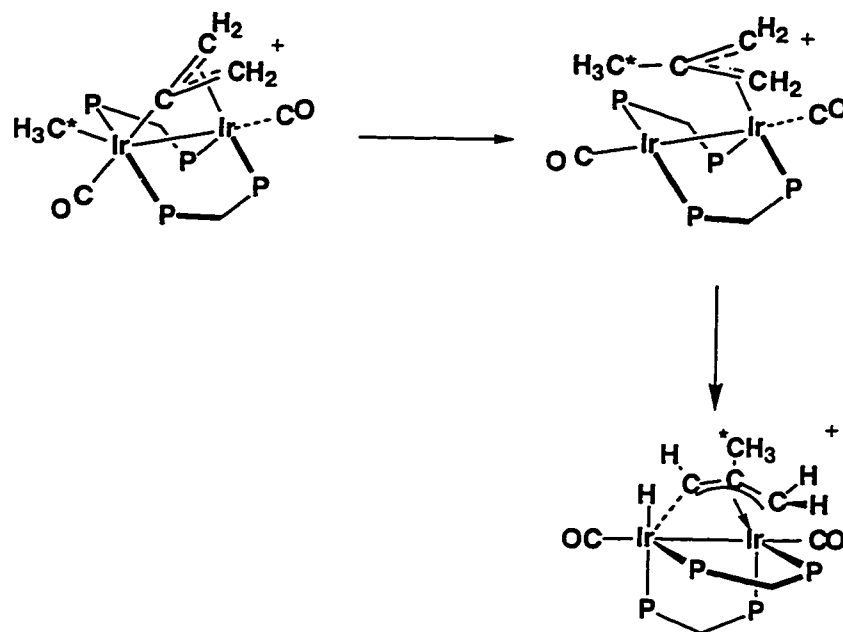
before, would occur at the terminal sites of the allyl ligand, which in this case contains no label. To our knowledge this is the first evidence of direct methyl transfer to a μ-η^1,η^3-bound allene group.

Analogous labelling studies carried out on the conversion of the methyl-allene precursor (**37**) into compounds **25a** & **b**, shows incorporation of the label into only the α- and the 2-methyl positions, supporting similar mechanisms to those outlined in Schemes 4.5 & 4.6. The lack of incorporation of the label into the γ-carbon site of the vinylcarbene is as expected based on steric

arguments, since the C-H activation of species **C** in Scheme 4.5 would occur preferentially at the least hindered end of the allyl ligand.

The dimethylallene adduct (**38**) was also found to rearrange to a vinyl-carbene compound. This reaction proved to be difficult to follow due to formation of decomposition products but ultimately it was concluded that the resulting vinylcarbene produced was **25a**. This product has resulted from a scrambling of the dimethylallene fragment with the incorporation of a hydrogen presumably from the original methyl ligand of **38**. To investigate how the vinylcarbene **25a** was being produced from **38**, a labelling study analogous to those done for the transformations of **36** and **37**, described above was performed. This study suggests a radical reaction being responsible for the transformation. In this conversion the ^{13}C-methyl label is **not** incorporated into the product but instead appears as vinyl chloride (confirmed by ^{1}H and ^{13}C{^{1}H} NMR), a byproduct of the reaction. The overall equation (in CH_2Cl_2) for the reaction is shown below. The mechanism by which compound **25a** is

$[Ir_2(^*CH_3)(CO)_2(H_2C=C=C(CH_3)_2(dppm)_2][CF_3SO_3]$ (**38**) $\xrightarrow{\quad CH_2Cl_2 \quad}$

$[Ir_2(H)(CO)_2(\mu\text{-}\eta^1:\eta^3\text{-HCC(Me)=CHMe})(dppm)_2][CF_3SO_3]$ (**25a**) + $H_2C^*=CHCl$ + other uncharacterized products
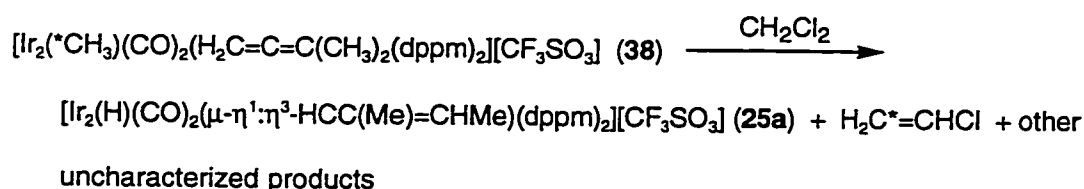
produced from compound **38** is not known but futher mechanistic work is warranted.

Conclusions

Overall we have observed three types of reactions of olefins with compound **2** that are effected by the both the steric and electronic factors inherent in the type of olefin under study. The first type of reactivity was with monoolefins. With the strongly electron-withdrawing activated olefin, tetrafluoroethylene, an olefin-bridged compound is observed with no transformation involving C-C bond formation. This is not suprising when the product is compared to the compounds formed in Chapter 3 with alkynes that have highly electron-withdrawing substituents, that bind in an analogous bridging mode. The ethylene adduct shows a terminal olefin geometry, presumably due to the dimetallacyclobutane structure not being favored.

With the conjugated olefin, 1,3-butadiene, an unprecedented reaction occurs in which the double C-H activated product **35** is observed. This compound is unique in the reactions of compound **2** with olefins.

The third reaction type is that with both allene and methylallene, generating the rare η^1,η^3-bridging allene adducts **36** and **37**, with the crystal structure for compound **36** confirming the rare binding mode. As with the alkyne adducts produced in Chapter 3, these allene-containing species are the kinetic products and react further to produce the vinylcarbene compounds described. Generation of the vinylcarbenes from both alkynes (Chapter 3) and allenes offers support for the general scheme presented (Schemes 3.6 and 4.5), in which migratory insertion, yielding a vinyl intermediate occurs in each case. The doubly substituted allene, dimethylallene, initially forms a terminally

bound species very similar to that previously characterized in the reaction of **2** with ethylene. The different binding mode observed for **38** compared to **36** and **37** is undoubtedly due to the greater steric influence of the two methyl groups in dimethylallene making the η^1,η^3-binding mode unfavorable. The rearrangement of **38** to compound **25a** in this case presumably occurs by an unexplored radical mechanism.

We have oberved three types of C-C bond forming reactions. One that involves the migratory insertion of the methyl ligand to a coordinated allene. This example can be added to the few examples of well-defined alkyl-olefin complexes that undergo insertion. The second type of C-C bond forming reaction involved the proposed initial formation of a methylene-hydride adduct by α-hydrogen elimination. The subsequent migratory insertion and C-C bond forming reaction did not follow the Green mechanism proposed for olefin polymerization, instead undergoing insertion with the hydride first. The third type of C-C bond formation involved a proposed radical reaction that warrants further investigation.

References

1. Collman, J. P.; Hegedus, L. S.; Norton, J. R.; Finke, R. G. *Principles and Apllications of Organotransition Metal Chemistry*; University Science Books: Mill Valley, CA, 1987; Chapters 6,11, and references therein.

2. (a) Cossee, P. J. *J. Catal.* **1964**, *3*, 80. (b) Arlman, E. J.; Cossee, P. J. *J. Catal.* **1964**, *3*, 99.

3. (a) Wang, L; Flood, T. C. *J. Am. Chem. Soc.* **1992**, *114*, 3169. (b) Brookhart, M.; Lincoln, D. M. *J. Am. Chem. Soc.* **1988**, *110*, 8719. (c) Ermer, S. P.; Struck, G. E.; Bitler, S. P.; Richards, R.; Bau, R.; Flood, T. C. *Organometallics* **1993**, *12*, 2634.

4. Rix, F. C.; Brookhart, M.; White, P. S. *J. Am. Chem. Soc.* **1996**, *118*, 2436 and references therein.

5. (a) Ivin, K. J.; Rooney, J. J.; Stewart, C. D.; Green, M. L. H.; Mahtab, J. R. *J. Chem.Soc., Chem. Commun.* **1978**, 604. (b) Green, M. L. H. *Pure Appl. Chem.* **1978**, *100*, 2079.

6. A few of examples are: (a) Crowther, D. J.; Baenziger, N. C.; Jordan, R. F. J. Am. Chem. Soc. 1991, 113, 1455. (b) Yang, X.; Stern, C. L.; Marks, T. J. *J. Am. Chem. Soc.* **1994**, *116*, 10015. (c) Giardello, M. A.; Eisen, M. S.; Stern, C. L.;Marks, T. J. *J. Am. Chem. Soc.* **1993**, *115*, 3326. (d) Bochman, M. *J. Chem. Soc., Dalton Trans.* **1996**, 255. (e) van der Heijden, H.; Hessen, B.; Orpen, A. G. *J. Am. Chem. Soc.* **1998**, *120*, 1112. (f) Barnhart, R. W.; Bazan, G. C.; Mourey, T. *J. Am. Chem. Soc.* **1998**, *120*, 1082.

7. A few of examples are: (a) Ewen, J. A. *J. Am. Chem. Soc.* **1984**, *106*, 6355. (b) Watson, P. L.; Parshall, G. W. *Acc. Chem. Res.* **1985**, *18*, 51. (c) Burger, B. J.; Thompson, M. E.; Cotter, W. D.; Bercaw, J. E. *J. Am. Chem. Soc.* **1990**, *112*, 1566. (d) Coughlin, E. B.; Bercaw, J. E. *J. Am. Chem. Soc.* **1992**, *114*, 7606.

8. (a) Schmidt, G. F.; Brookhart, M. *J. Am. Chem. Soc.* **1985**, *107*, 1443. (b) Brookhart, M.; Volpe, A. F.; Lincoln, D. M.; Horvath, I. T.; Millar, J. M. *J. Am. Chem. Soc.* **1990**, *112*, 5634. (c) Rix, F. C.; Brookhart, M. *J. Am. Chem. Soc.* **1995**, *117*, 1137. (d) Johnson, L. K.; Killian, C. M.; Brookhart, M. *J. Am. Chem. Soc.* **1995**, *117*, 6414.

9. (a) Antwi-Nsiah, F. H. Ph.D. Thesis, University of Alberta, Edmonton, AB, 1994. (b) Antwi-Nsiah, F.; Cowie, M. *Organometallics* **1992**, *11*, 3157.

10. (a) Sheldrick, G. M. *Acta Crystallogr.* **1990**, *A46*, 467–473. (b) Sheldrick, G. M. *SHELXL-93*. Program for crystal structure determination. University of Göttingen, Germany, 1993.

11. (a) Bonnet, J. J.; Mathieu, R.; Poilblanc, R.; Ibers, J. A. *J. Am. Chem. Soc.* **1979**, *101*, 7487. (b) Green, M.; Laguna, A.; Spencer, J. L.; Stone, F. G. A. *J. Chem. Soc., Dalton Trans.* **1977**, 1010.

12. (a) Collman, J. P.; Hegedus, L. S.; Norton, J. R.; Finke, R. G. *Principles and Apllications of Organotransition Metal Chemistry*; University Science Books: Mill Valley, CA, 1987; p368. (b) Yammamoto, A. *Organotransition Metal Chemistry*; Wiley: New York, 1986; p251.

13. (a) Kubiak, C. P.; Woodcock, C.; Eisenberg, R. *Inorg. Chem.* **1980**, *19*, 2733. (b) Sutherland, B. R.; Cowie, M. *Organometallics* **1984**, *3*, 1869. (c) Sutherland, B. R.; Cowie, M. *Inorg. Chem.* **1984**, *23*, 2324. (d) Sutherland, B. R.; Cowie, M. *Organometallics* **1985**, *4*, 1801. (e) Xiao, J.; Cowie, M. *Organometallics* **1993**, *12*, 463. (f) See structures for compounds **2, 3, 7, 23, 26, 40, 41, 44** this thesis.

14. See, for example: (a) Xiao, J.; Cowie, M. *Organometallics* **1993**, *12*, 463. (b) Antonelli, D. M.; Cowie, M. *Organometallics* **1991**, *10*, 2550. (c) Hilts, R. W.; Franchuk, R. A.; Cowie, M. *Organometallics* **1991**, *10*,1297.

15. (a) Brough, S.-A.; Hall, C.; McCamley, A.; Perutz, R. N.; Stahl, S.; Wecker, U.; Werner, H. *J. Organomet. Chem.* **1995**, *504*, 33. (b) Gibson, V. C.; Parkin, G.; Bercaw, J. E. *Organometallics* **1991**, *10*, 220. (c) Bell, T. W.; Haddleton, D. M.; McCamley, A.; Partridge, M. G.; Perutz, R. N.; Willner, H. *J. Am. Chem. Soc.* **1990**, *112*, 9212. (d) Deeming, A. J.; Hasso, S.; Underhill, M.; Canty, A. J.; Johnson, B. F. G.; Jackson, W. G.; Lewis, J.; Matheson, T. W. *J. Chem. Soc., Chem. Commun.* **1974**, 807. (e) Deeming, A. J.; Underhill, M. *J. Chem. Soc., Dalton Trans.* **1974**, 1415. (f) Deeming, A. J.; Underhill, M. *J. Chem. Soc., Chem. Commun.* **1973**, 277.

16. See for example (a) Antwi-Nsiah, F.H.; Oke, O.; Cowie, M. *Organometallics* **1996**, *15*, 506. (b) Xiao, J.; Cowie, M. *Organometallics* **1993**, *12*, 463. (c) See NMR data for compounds **21-23**, Chapter 3.

17. (a) Chacon, S. T.; Chisolm, M. H.; Folting, K.; Huffman, J. C.; Hampden-Smith, M. J. *Organometallics* **1991**, *10*, 3722. (b) Colbom, R. E.; Dyke, A. F.; Knox, S. A. R.; Mead, K. A.; Woodward, P. *J. Chem. Soc. Dalton Trans.* **1983**, 2099.

18. The allene β-carbon signal appears at *ca.* δ 212.6 in the $^{13}C\{^1H\}$ NMR spectrum compared to the ethylene carbon at δ 123.5.

19. (a) Mann, B. E.; Taylor, B. F. *^{13}C NMR Data for Organometallic Compounds*; Academic Press: London, 1981; Table 2.11. (b) Collman, J. P.; Hegedus, L. S.; Norton, J. R.; Finke, R. G. *Principles and Apllications of Organotransition Metal Chemistry*; University Science Books: Mill Valley, CA, 1987; p177.

20. These values are very close to those seen by Chacon *et al*, see ref 17a.

21. (a) Wakefield, J. B.; Stryker, J. M. *Organometallics* **1990**, *9*, 2428 (supplementary material). (b) Collman, J. P.; Hegedus, L. S.; Norton, J. R.; Finke, R. G. *Principles and Apllications of Organotransition Metal Chemistry*; University Science Books: Mill Valley, CA, 1987; p 176. (c) *Comprehensive Organometallic Chemistry*; Wilkinson, G.; Stone, F. G. A.; Abel, E. W., Eds., Pergamon: New York, 1982; Vol. 6, Sections 37.6, 38.7 and 39.9. (d) Tulip, T. H.; Ibers, J. A. *J. Am. Chem. Soc.* **1978**, *100*, 3252.

22. (a) Ben-Shoshan, R.; Pettit, R. *J. Chem. Soc., Chem. Commun.* **1968**, 247. (b) Davis, R. E. *J. Chem. Soc., Chem. Commun.* **1968**, 248. (c) Dyke, A. F.; Knox, S. A. R.; Naish, P. J. *J. Organomet. Chem.* **1980**, *199*,

C47. (d) Kuhn, A.; Burschka, Ch.; Werner, H. *Organometallics* **1982**, *1*, 496. (e) Deeming, A. J.; Arce, A. J.; De Sanctis, Y.; Bates, P. A.; Hursthouse, M. B. *J. Chem. Soc., Dalton Trans.* **1987**, 2935. (f) Gregg, M. R.; Powell, J.; Sawyer, J. F. *J. Organomet. Chem.* **1988**, *352*, 357. (g) Arce, A. J.; De Sanctis, Y.; Deeming, A. J.; Hardcastle, K. I.; Lee, R. *J. Organomet. Chem.* **1991**, *406*, 209.

23. (a) Antwi-Nsiah, F. A.; Torkelson, J. R.; Cowie, M. *Inorg. Chim. Acta* **1997**, *259*, 213. (b) Vaartstra, B. A.; Xiao, J.; Jenkins, J. A.; Verhagen, R.; Cowie, M. Organometallics 1991, 10, 2708. (c) Mague, J. T.; Klein, C. L.; Majeste, R. J.; Stevens, E. D. Organometallics 1984, 3, 1860. (d) Cowie, M.; Dickson, R. Inorg. Chem. 1981, 20, 2682. (e) Sutherland, B. R.; Cowie, M. Organometallics 1984, 3, 1869. (f) Cowie, M.; Dickson, R. S.; Hames, B. W. Organometallics 1984, 3, 1879. (g)

24. (a) Stoutland, P. O.; Bergman, R. G. *J. Am. Chem. Soc.* **1985**, *107*, 4581. (b) Ghosh, C. K.; Hoyano, J. K.; Krentz, R.; Graham. W. A. G. *J. Am. Chem. Soc.* **1989**, *111*, 5480. (c) Perez, P. J.; Poveda, M. L.; Carmona, E. *J. Chem. Soc., Chem. Commun.* **1992**, 8. (d) Bianchini, C.; Barbaro, P.; Meli, A.; Peruzzini, M.; Vacca, A.; Vizza, F. *Organometallics* **1993**, *12*, 2505. (e) Alvarado, Y.; Boutry, O.; Gutierrez, E.; Monge, A.; Nicasio, M. C.; Poveda, M. L.; Perez, P. J.; Ruiz, C.; Bianchini, C.; Carmona, E. *Chem. Eur. J.* **1997**, *3*, 860.

25. (a) Nubel, P. O.; Brown, T. L. *J. Am. Chem. Soc.* **1984**, *106*, 644. (b) Nubel, P. O.; Brown, T. L. *J. Am. Chem. Soc.* **1982**, *104*, 4955. (c)

Keister, J. B.; Shapley, J. R. *J. Organomet. Chem.* **1975**, *85*, C29. (d)

Fryzuk, M. D.; Jones, T.; Einstein, F. W. B. *Organometallics* **1984**, *3*, 185

26. Graham, T.; Cowie, M. Manuscript in preparation.

27. Lobach, M. I.; Kormer, V. A. *Russian Chemical Reviews* **1979**, *48*, 758.

28. Hills, A.; Hughes, D.L.; Jiminez-Tenorio, M.; Leigh, G.J.; McGeary, C.A.; Rowley, A.T.; Bravo, M.; McKenna, C.E.; McKenna, M.-C. *J. Chem. Soc., Chem. Commun.* **1991**, 522.

29. (a) Horton, A.D.; Mays, M.J. *J. Chem. Soc., Dalton Trans.* **1990**, 155. (b) Hogarth, G.; Lavender, M.H. *J. Chem. Soc., Dalton Trans.* **1992**, 2759.

30. Sterenberg, B. T.; McDonald, R.; Cowie, M. *Organometallics* **1997**, *16*, 2297.

31. (a) Maitlis, P. M.; Long, H. C.; Quyoum, R.; Turner, M. L.; Wang, Z-Q. *Chem. Commun.* **1996**, 1. (b) Maitlis, P. M.; Saez, I. M.; Meanwell, N. J.; Isobe, K.; Nutton, A.; Vaquez de Miguel, A.; Bruce, D. W.; Okeya, S.; Bailey, P. M.; Andrews, D. G.; Ashton, P. R.; Johnstone, I. R. *New J. Chem.*, **1989**, *13*, 419. (c) Martinex, J. M.; Adams, H.; Bailey, N. A.; Maitlis, P. M. *J. Chem. Soc., Chem. Commun.*, **1989**, 286.

Chapter 5

Methoxymethyl Complexes as Precursors to Methylene- and Methyne-bridged Species.

Introduction

The facile C-H bond activation of the methyl group that occurred upon addition of small molecules (CO, SO_2, CNR, PR_3, $RC\equiv CR'$ (R, R' = Me, Et, Ph), and allenes) to $[Ir_2(CH_3)(CO)(\mu\text{-}CO)(dppm)_2][CF_3SO_3]$ (2) was described in the previous three chapters. This transformation proved to be amazingly facile with a number of substrates, yet, suprisingly did not occur for others (eg. C_2H_4, $RC\equiv CR$ (R = CF_3, CO_2Me), and $HC\equiv CR'$ (R' = H, Me, Ph)). In order to probe this reactivity further, we sought to extend the investigation to substituted methyl groups to determine the effect on the reactivity of the C-H bond by the substituents. One obvious route to such species was the oxidative addition of substituted iodo methyl groups, ICH_2X (X = OMe, I, CN) to the formally Ir(0) complex $[Ir_2(CO)_3(dppm)_2]$, and this chemistry will be described in this chapter.

We were also interested in routes to methylene-bridged species, owing to our proposal (see Chapters 3 and 4) of their involvement in some of the observed C-C bond-forming reactions. Two promising routes to such products involved the substrates CH_2I_2 and ICH_2OCH_3. Although the first was used as a

possible route to an iridium-bound iodomethyl group, double oxidative addition into both C-I bonds, as has been observed in binuclear complexes,[1] was also possible, yielding a methylene-bridged complex. Oxidative addition of iodomethyl methyl ether to yield a methoxymethyl species provided a secondary route into methylene-bridged complexes through the propensity of the methoxy group to be removed by electrophiles.[2]

Experimental Section

General Comments. The compound $[Ir_2(CO)_3(dppm)_2]$ was prepared as previously reported.[3] The elemental analyses attempted on purified samples of most of the compounds were unsatisfactory due to some contamination by traces of the previously characterized dicarbonyl diiodo species $[Ir_2(CO)(I)_2$-$(\mu\text{-}CO)(dppm)_2]$,[4] the tricarbonyl iodide $[Ir_2(CO)_2(I)(\mu\text{-}CO)(dppm)_2][I]^4$ or other uncharacterized species which could not be removed. Characterization is primarily based on spectroscopic methods, together with the X-ray structure determination of three products. The $^{31}P\{^1H\}$ and ^1H NMR and IR spectroscopic data for all compounds are given in Table 5.1 while selected $^{13}C\{^1H\}$ NMR data are given, where appropriate, with the details on the preparation of the compounds. IR characterization for **41**, **42a** and **42b** is pending.

Preparation of Compounds

(a) $[Ir_2(CH_2OCH_3)(I)(CO)(\mu\text{-}CO)(dppm)_2]$ **(40)** The compound $[Ir_2(CO)_3(dppm)_2]$ (50 mg, 0.040 mmol) was dissolved in 10 mL of benzene and

Table 5.1 Spectroscopic Data for Compounds

Compound	IR cm^{-1}[a,b]	δ ^{1}H[c,d,g]	δ ^{31}P{^{1}H}[c,d,h]
[Ir$_2$(CH$_2$OCH$_3$)(I)(CO)(μ-CO)(dppm)$_2$] (40)	1936 vs 1732 s	4.48 (b, 4H), 3.30 (t, $^3J_{H-P}$ = 4.4 Hz, 2H), 1.95 (s, 3H)[e]	18.6 (m), -6.4 (m)
[Ir$_2$(CO)$_2$(μ-CH$_2$)(μ-I)(dppm)$_2$][CF$_3$SO$_3$] (41)		10.01 (q, $^3J_{H-P}$ = 8.3 Hz, 2H), 5.02 (m, 2H), 4.19 (m, 2H)	-7.9 (s)
anti-[Ir$_2$(CO)$_2$(I)$_2$(μ-CH$_2$)(dppm)$_2$] (42a)		6.6 (tt, $^3J_{H-P}$ = 10 Hz, 7 Hz, 2H), 5.59 (m, 2H), 4.62 (m, 2H)	-15.1 (m), -28.0 (m)
syn-[Ir$_2$(CO)$_2$(I)$_2$(μ-CH$_2$)(dppm)$_2$] (42b)		6.32 (q, $^3J_{H-P}$ = 9.5 Hz, 2H), 5.39 (m, 2H), 3.60 (m, 2H)	-25.1 (s)
[Ir$_2$(CO)$_2$(H)$_2$(μ-COCH$_3$)(dppm)$_2$][CF$_3$SO$_3$] (43)[i]	1975 vs	5.05 (s, 3H), 4.81 (m, 1H), 4.08 (m, 1H), 3.22 (m, 1H), -11.12 (m, 1H), -11.20 (m, 1H)	-2.1 (m), -4.6 (m), -14.3 (m), -16.1 (m)
[Ir$_2$(CO)$_2$(μ-I)(μ-CO)(dppm)(Ph$_2$PCHPPh$_2$)] (44)	1948 vs 1801 s	4.60 (m, 1H), 4.23 (m, 1H), 2.07 (tt, $^2J_{P-H}$ = 10 Hz, $^4J_{P-H}$ = 3.5 Hz, 1H)	-1.4 (m), -10.1 (m)

[a]IR abbreviations (v(CO): vs = very strong, s = strong, m = medium, w = weak, sh = shoulder, b = broad. [b] Nujol mull or CH$_2$Cl$_2$ cast unless otherwise stated. [c] NMR abbreviations: s = singlet, t = triplet, m = multiplet, q = quintet, b = broad. [d]NMR data at 25°C in CD$_2$Cl$_2$ unless otherwise stated. [e]NMR data at -40°C. [f]NMR data at -80°C. [g] Chemical shifts for the phenyl hydrogens are not given in the ^{1}H NMR data. [h]^{31}P{^{1}H} chemical shifts are referenced vs external 85% H$_3$PO$_4$.

CH_3OCH_2I (3.6 µL, 0.040mmol) was added by syringe. The solution was stirred for 1 h during which time the color changed from orange to yellow. The volume was reduced to *ca.* 3 mL and a bright yellow powder was precipitated with addition of pentane. The isolated solid was washed (2 × 10 mL pentane), dried under argon and then in vacuo. Yield 86%. Anal. Calcd for $Ir_2IP_4O_3C_{54}H_{49}$: C, 46.95; H, 3.58; I, 9.19. Found: C, 46.65; H, 3.34; I, 10.16.

(b) **$[Ir_2(CO)_2(\mu\text{-}CH_2)(\mu\text{-}I)(dppm)_2][CF_3SO_3]$ (41)** Compound **40** (26 mg, 0.019 mmol) was dissolved in 10 mL of benzene and $(CH_3)_3SiSO_3CF_3$ (3.4 µL, 0.019 mmol) was added causing a slight darkening of the solution. The solution was stirred for 1 h, the volume was reduced to *ca.* 3 mL and a light orange powder was obtained on addition of Et_2O. The isolated solid was washed (2 × 10 mL Et_2O), dried under argon and then in vacuo. Yield 83 %.

(c) **$[Ir_2(CO)_2(I)_2(\mu\text{-}CH_2)(dppm)_2]$ (42)** Compound **40** (30 mg, 0.022 mmol) was dissolved in 7 mL of benzene and $(CH_3)_3SiI$ (3.1 µL, 0.022 mmol) was added. The solution was stirred for 1 h, the volume was reduced to *ca.* 3 mL and a yellow powder was obtained on addition of pentane. The isolated solid was washed (2 × 10 mL pentane), dried under argon and then in vacuo. Yield 77 %.

(d) **$[Ir_2(CO)_2(H)_2(\mu\text{-}COCH_3)(dppm)_2][CF_3SO_3]$ (43)** Compound **40** (31 mg, 0.022 mmol) was dissolved in 10 mL of benzene and $CH_3SO_3CF_3$ (2.5 µL 0.022 mmol) was added causing an immediate color change from yellow to

light red. The solution was stirred for 1 h during which time the color changed to dark yellow. The solvent volume was reduced to *ca.* 3 mL and a yellow solid was obtained by addition of pentane. The isolated solid was washed (2 × 10 mL pentane), dried under argon and then in vacuo. Yield 78 %. Compound **41** was also produced in the reaction in *ca.* 10% yield as determined by $^{31}P\{^1H\}$ NMR of a reaction carried out in an NMR tube. $^{13}C\{^1H\}$ NMR (natural abundance): δ 316.6 (tt, $^2J_{C-P}$ = 55, 4 Hz,$COCH_3$), 173.6 (b, 2CO), 77.5 (t, $^4J_{C-P}$ = 10 Hz,$COCH_3$).

(e) Reaction of $[Ir_2(CH_2OCH_3)(I)(CO)(\mu\text{-}CO)(dppm)_2]$ (40) with H_2. Compound **40** (30 mg, 0.022 mmol) was dissolved in 0.6 mL of CD_2Cl_2 and H_2 gas was passed through the solution for 1 min. The solution was allowed to stand for 24 h under a static atmosphere of H_2. The excess H_2 was evacuated and ^1H and $^{31}P\{^1H\}$ NMR spectra showed the production of the previously characterized compound $[Ir_2(H)_3(CO)(\mu\text{-}H)_2(\mu\text{-}CO)(dppm)_2][I]$.[5] Dimethyl ether was observed by ^1H NMR in the reaction mixture.

(f) $[Ir_2(CO)_3(\mu\text{-}I)(dppm)(Ph_2PCHPPh_2)]$ (44) The compound $[Ir_2(CO)_3(dppm)_2]$ (30 mg, 0.024 mmol) was dissolved in 6 mL of THF and CH_2I_2 (2.0 μL, 0.025 mmol) was added. The solution changed color over 0.5 h from orange to yellow, and was stirred an additional 0.5 h. The solvent was then removed and the residue was dissolved in 2 mL of CH_2Cl_2, cooled to 0°C and a flocculent yellow precipitate was obtained upon addition of 20 mL of a 50:50 mixture of Et_2O/hexane. The precipitate was washed with the Et_2O/hexane

mixture (2 x 10 mL), dried under argon and then in vacuo. Yield 75%.

(g) Reaction of [Ir$_2$(CO)$_3$(dppm)$_2$] with ICH$_2$CN   The compound

[Ir$_2$(CO)$_3$(dppm)$_2$] (43.6 mg, 0.035 mmol) was dissolved in 7 mL of benzene and

ICH$_2$CN (2.6 µL, 0.036 mmol) was added. The solution was stirred for 10 min

during which time the color changed from orange to yellow. The solvent was

then reduced to *ca.* 2 mL and a bright yellow powder was obtained upon

addition of 10 mL of pentane. The precipitate was washed with pentane (2 x 10

mL), dried under argon and then in vacuo. NMR spectra run on the isolated

sample showed the production of compound **44**. CH$_3$CN was detected in a ^{1}H

NMR spectrum run on the crude reaction mixture.

(h) Reaction of [Ir$_2$(CH$_3$)(CO)(µ-CO)(dppm)$_2$][CF$_3$SO$_3$] (2) with

CH$_3$OCH$_2$I. Compound **2** (40 mg, 0.029 mmol) was dissolved in 10 mL of THF

and CH$_3$OCH$_2$I (2.6 µL, 0.029 mmol) was added. The solution was stirred for 3

h, the volume was reduced to *ca.* 3 mL and an orange solid was obtained upon

addition of Et$_2$O. The solid was isolated, washed (2 x 10 mL Et$_2$O), dried under

argon and then in vacuo. ^{1}H and ^{31}P{^{1}H} NMR spectra showed the production of

the previously characterized compound [Ir$_2$(C$_2$H$_4$)(CO)(µ-CO)(µ-I)(dppm)$_2$]-

[CF$_3$SO$_3$].[4]

X-ray Data Collection.   Crystals of each compound, suitable for X-ray

diffraction were grown via slow diffusion of diethyl ether into a concentrated

CH$_2$Cl$_2$ **(40, 41)** or THF**(44)** solution of the compound and were mounted and

flame-sealed in glass capillaries under solvent vapor to minimize

decomposition or deterioration due to solvent loss. Data were collected at -60°C on a Siemens P4RA diffractometer using graphite-monochromated Cu Kα radiation for compounds **40** and **41** and at -50 °C on an Enraf-Nonius CAD4 for compound **44**, using graphite monochromated Mo Kα radiation. For each compound, three reflections were chosen as intensity standards and were remeasured every 120 min of X-ray exposure time; in no case was decay evident. Crystal parameters and details of data collection are summarized in Table 5.2.

Unit cell parameters for the three compounds **40**, **41** and **44** were obtained from least-squares refinements of between 24 and 36 reflections as given in Table 5.2 For compound **40** the cell parameters and the systematic absences defined the space group as $P2_1/c$, whereas for **41** and **44** the cell parameters, the lack of absences and the diffraction symmetry suggested the space groups $P1$ or $P\bar{1}$, the latter of which was established for both compounds by successful refinement of the structures. Absorption corrections to **44** were applied by the method of Walker and Stuart,[6a] for **40** the crystal faces were indexed and measured, and an absorption correction was carried out by Gaussian integration, and for **41** ψ scans provided a semiempirical absorption correction.

Structure Solution and Refinement. For each structure, the positions of the iridium and phosphorus atoms were found using the direct-methods program *SHELXS-86*;[6b] the remaining atoms were found using a succession of

Table 5.2 Crystallographic Data for Compounds 40, 41 & 44.

A. Crystal Data

compd	[Ir$_2$(CH$_2$OCH$_3$)(I)(CO)(μ–CO)(dppm)$_2$] (40)•CH$_2$Cl$_2$ ^{a}	[Ir$_2$(CO)$_2$(μ-CH$_2$)(μ-I)(dppm)$_2$]-[CF$_3$SO$_3$] (41)•2CH$_2$Cl$_2$	[Ir$_2$(CO)$_2$(μ-CO)(μ-I)(Ph$_2$PCH$_2$PPh$_2$)-(Ph$_2$PCHPPh$_2$)] (44)•THF
formula	C$_{54.7}$H$_{50.25}$Cl$_2$I$_{1.15}$Ir$_2$O$_{2.85}$P$_4$ ^{a}	C$_{56}$H$_{50}$Cl$_4$F$_3$Ir$_2$O$_5$P$_4$S	C$_{57}$H$_{51}$IIr$_2$O$_4$P$_4$
formula wt	1478.31	1669.00	1435.16
crystal dimensions (mm)	0.34 × 0.12 × 0.06	0.44 × 0.15 × 0.11	0.42 × 0.24 × 0.03
color	yellow	yellow	yellow
crystal system	monoclinic	triclinic	triclinic
space group	P2$_1$/c (No. 14)	P$\bar{1}$ (No. 2)	P$\bar{1}$ (No. 2)
unit cell parameters^{b,c,d}			
a(Å)	20.0497 (9)	14.207 (2)	12.905 (2)
b(Å)	13.9589 (6)	14.5008 (10)	18.492 (3)
c(Å)	20.9456 (8)	17.2548 (12)	11.963 (2)
α(deg)	90.0	72.043 (7)	97.020 (14)
β(deg)	112.732 (3)	84.870 (8)	113.434 (12)
γ(deg)	90.0	63.436 (7)	78.438 (12)
V(Å^3)	5406.7 (4)	3019.7 (5)	2563.5 (7)
Z	4	2	2

Table 5.2 cont.

ρcalcd (g cm^{-3})	1.816	1.836	1.859
μ (mm^{-1})	16.89	15.832	5.960

B. Data Collection and Refinement Conditions

diffractometer	Siemens P4/RA[e]	Siemens P4/RA[e]	Enraf-Nonius CAD4[f]
radiation (λ [Å])	graphite-monochromated Cu Kα (1.54178)	graphite-monochromated Cu Kα (1.54178)	graphite-monochromated Mo Kα (0.71073)
temperature (°C)	–60	–60	–50
scan type	θ–2θ	θ–2θ	θ–2θ
data collection 2θ limit (deg)	113.5	113.5	50.0
total data collected	7450 (0 ≤ h ≤ 21, 0 ≤ k ≤ 15, -22 ≤ l ≤ 20)	8162 (0 ≤ h ≤ 14, -13 ≤ k ≤ 14, -18 ≤ l ≤ 18)	9403 (0 ≤ h ≤ 15, -21 ≤ k ≤ 21, -14 ≤ l ≤ 13)
independent reflections	7213	7775	8964
number of observations (NO)	5827 ($F_o^2 \geq 2\sigma(F_o^2)$)	6415 ($F_o^2 \geq 2\sigma(F_o^2)$)	4784 ($F_o^2 \geq 2\sigma(F_o^2)$)
structure solution method	direct methods (SHELXS–86[g])	direct methods (SHELXS–86[g])	direct methods (SHELXS–86[g])
refinement method	full-matrix least-squares on F^2 (SHELXL–93[h])	full-matrix least-squares on F^2 (SHELXL–93[h])	full-matrix least-squares on F^2 (SHELXL–93[h])
absorption correction method	Gaussian integration (face-indexed)	semiempirical (ψ scans)	DIFABS[i]

Table 5.2 cont.

range of absorption correction factors	0.4129–0.1633	0.6210–0.0966	1.255–0.844
data/restraints/parameters	7213 $[F_o^2 \geq -3\sigma(F_o^2)]$/0/613	7774 $[F_o^2 \geq -3\sigma(F_o^2)]$/5/683	8961 $[F_o^2 \geq -3\sigma(F_o^2)]$/0/563
largest difference peak and hole	2.282 and −1.976 e Å^{-3}	1.528 and −1.184 e Å^{-3}	1.782 and −1.820 e Å^{-3}
final R indices^k $F_o^2 > 2\sigma(F_o^2)$	$R_1 = 0.0552$, $wR_2 = 0.1330$	$R_1 = 0.0424$, $wR_2 = 0.0961$	$R_1 = 0.0622$, $wR_2 = 0.1270$
all data	$R_1 = 0.0725$, $wR_2 = 0.1444$	$R_1 = 0.0569$, $wR_2 = 0.1031$	$R_1 = 0.1784$, $wR_2 = 0.1646$
GOF(S)^l	1.060 $[F_o^2 \geq -3\sigma(F_o^2)]$	1.055 $[F_o^2 \geq -3\sigma(F_o^2)]$	1.015 $[F_o^2 \geq -3\sigma(F_o^2)]$

^{a} The sample crystallized as a mixture of 85% of compound **40** and 15 % [Ir$_2$I$_2$(CO)(μ-CO)(dppm)$_2$]•CH$_2$Cl$_2$

^{b} For **40**, obtained from least-squares refinement of 28 reflections with 56.9° < 2θ < 58.0°.

^{c} For **41**, obtained from least-squares refinement of 36 reflections with 53.6° < 2θ < 57.1°.

^{d} For **44**, obtained from least-squares refinement of 24 reflections with 20.1° < 2θ < 23.8°.

^{e} Programs for diffractometer operation and data collection were those of the XSCANS system supplied by Siemens.

^{f} Programs for diffractometer operation and data collection were those supplied by Enraf-Nonius.

^{g} Sheldrick, G. M. *Acta Crystallogr.* **1990**, *A46*, 467.

^{h} Sheldrick, G. M. *SHELXL-93*. Program for crystal structure determination. University of Göttingen, Germany, 1993. Refinement on F^2 for all reflections except for compound **41**, refinement on F^2 for ALL reflections except for 1 with very negative F^2. Weighted R-factors wR_2 and all goodnesses of fit S are based on F_o^2; conventional R-factors R_1 are based on F_o, with F_o set to zero for negative F_o^2. The observed

Table 5.2 cont.

criterion of $F_o^2 > 2\sigma(F_o^2)$ is used only for calculating R_1, and is not relevant to the choice of reflections for refinement. R-factors based on F_o^2 are statistically about twice as large as those based on F_o, and R-factors based on ALL data will be even larger.

[h]Walker, N.; Stuart, D. *Acta Crystallogr.* **1983**, *A39*, 158–166.

[k]$R_1 = \Sigma||F_o| - |F_c||/\Sigma|F_o|$; $wR_2 = [\Sigma w(F_o^2 - F_c^2)^2/\Sigma w(F_o^4)]^{1/2}$.

[l]$S = [\Sigma w(F_o^2 - F_c^2)^2/(n - p)]^{1/2}$ (n = number of data; p = number of parameters varied; $w = [\sigma^2(F_o^2) + (0.0839P)^2 + 35.6413P]^{-1}$ where P = [Max(F_o^2, 0) + $2F_c^2$]/3). For **40** a_0 = 0.0832, a_1 = 25.9490; for **41** a_0 = 0.0517, a_1 = 17.9707; for **44** a_0 = 0.0608, a_1 = 0.9018.

least-squares and difference Fourier maps. Refinement of each structure proceeded using the program SHELXL-93.[6c] Hydrogen atom positions were calculated by assuming idealized sp^2 or sp^3 geometries about their attached carbon atoms (as appropriate), and were given thermal parameters 120% of the equivalent isotropic displacement parameters of their attached carbons. Further details of structure refinement (other than described below) and final residual indices may be found in Table 5.2. Interatomic distances and angles have also been tabulated for each compound (Table 5.3 for **40**, Table 5.4 for **41**, and Table 5.5 for **44**).

Although all of the non-hydrogen atoms of $[Ir_2(CH_2OCH_3)(I)(CO)(\mu-CO)-(dppm)_2]$ (**40**)•CH_2Cl_2 were located, the carbon and oxygen atoms of the terminal methoxymethyl group (C(3), O(3)) did not behave well in least squares refinements. A difference Fourier map at this stage located another peak near C(3) and O(3), at approximately 2.7 Å from Ir(2). Successful refinement of the structure was achieved by placing an iodide in 15% occupancy at the peak site. The iodide ligand has apparently resulted from cocrystallization of the diiodo species $[Ir_2(I)_2(CO)(\mu-CO)(dppm)_2]$,[4] that typically can be formed as a minor impurity in the preparation of **40**. Compound **40** and $[Ir_2(I)_2(CO)(\mu-CO)(dppm)_2]$ are isomorphous, with the same space group and very similar cell parameters. The disorder was resolved and all atoms were refined anisotropically, giving the methoxy substituents (C(3), O(3), C(4)) with an occupancy of 85% and the iodide ligand (I(2)) with an occupancy of 15%. Apart from the atoms involved in the disorder, all atoms refined well, indicating that the two disordered molecules

superimpose almost exactly.

Location of all atoms in $[Ir_2(CO)_2(\mu\text{-}CH_2)(\mu\text{-}I)(dppm)_2][CF_3SO_3]$ (41)•$2CH_2Cl_2$ proceeded smoothly, however, one of the dichloromethane solvent molecules was disordered and did not behave well. The following distance restraints were applied to enforce an idealized geometry within the disordered CH_2Cl_2 molecule. $Cl(3)$–$C(93)$–$[Cl(4)/Cl(5)]$ were fixed: $d[Cl(3)$–$C(93)] = d[Cl(4)$–$C(93)] = d[Cl(5)$-$C(93)] = 1.75$ (1) Å; $d[Cl(3)$–$Cl(4)] = d[Cl(3)$–$Cl(5)] = 2.90$ (1) Å.

Location of all the atoms in compound 44 proceeded smoothly.

Dr. Bob McDonald is acknowledged for X-ray data collection and solution for compounds 40, 41 and 44.

Results and Characterization of Compounds

The compound $[Ir_2(CO)_3(dppm)_2]$ reacts with the iodomethyl methyl ether (CH_3OCH_2I) losing carbon monoxide to produce the methoxymethyl iodide compound $[Ir_2(CH_2OCH_3)(I)(CO)(\mu\text{-}CO)(dppm)_2]$ (40), as outlined in Scheme 5.1. The ^1H NMR spectrum at ambient temperature for 40 shows the methylene protons for the methoxymethyl ligand as a broad signal at δ 3.30 with the methoxy protons appearing as a singlet at δ 1.95. When the sample is cooled to -40°C the broad methylene signal sharpens into a triplet indicating terminal coordination on Ir, which is supported by selective ^{31}P decoupling experiments that show the methylene coupling to only the phosphorus nuclei that give rise to

Scheme 5.1
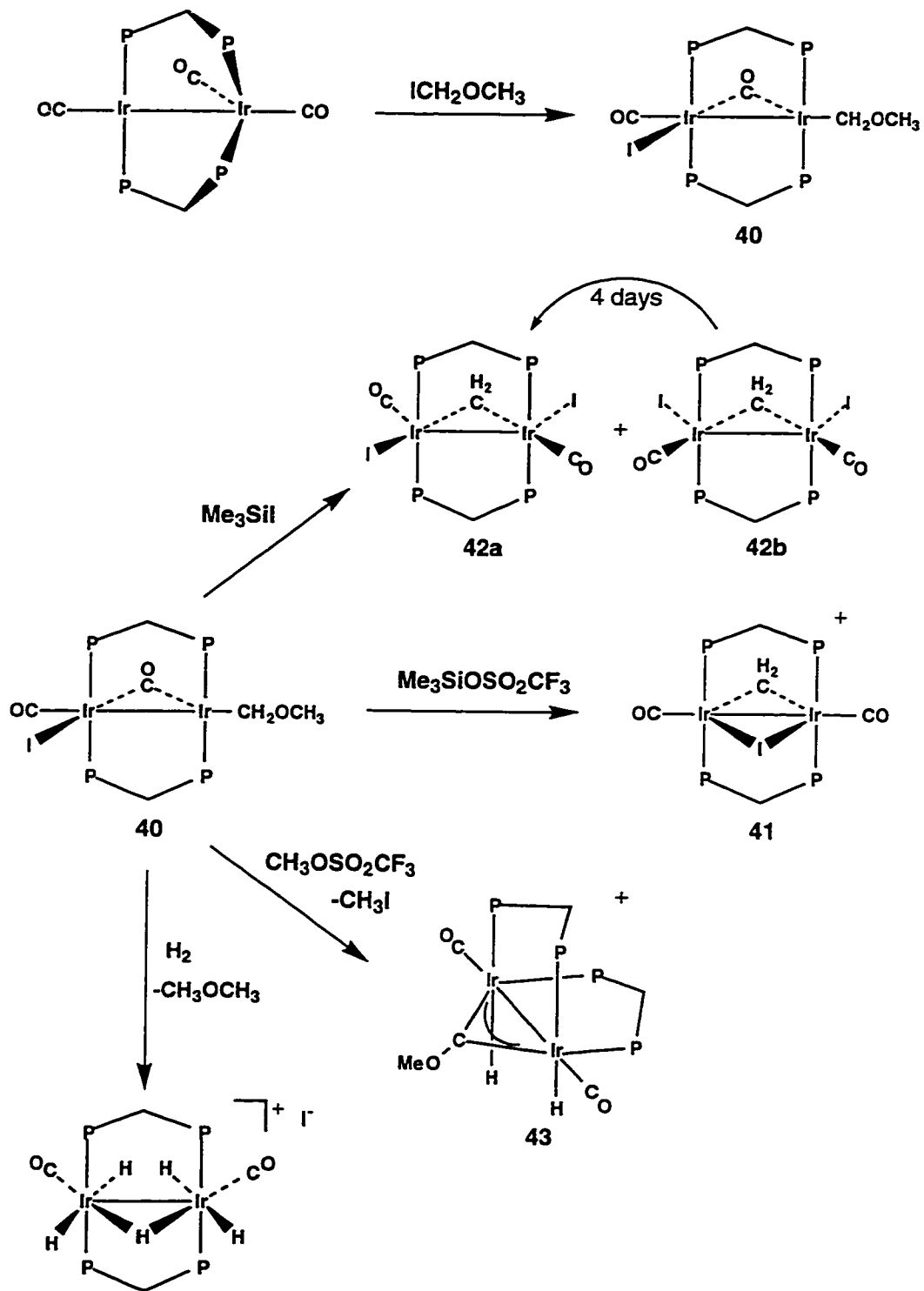
the downfield signal in the $^{31}P\{^1H\}$ NMR spectrum. The ^1H chemical shifts observed correspond well to those observed for other methoxymethyl compounds.[2] At room temperature the $^{31}P\{^1H\}$ NMR spectrum shows sharp AA'BB' signals at δ 18.6 and -6.4. The carbonyl bands in the infrared spectrum appear at 1936 cm^{-1} and 1732 cm^{-1}, suggesting a terminal and bridging orientation, which is supported by the carbonyl resonances in the $^{13}C\{^1H\}$ NMR spectrum that appear as broad signals at δ 199.8 and 175.9.[7] Confirmation of the proposed structure for **40** in the solid state comes from the X-ray structure determination, as shown in Figure 5.1, with an alternate view shown in Figure 5.1.1. Selected distances and angles are given in Table 5.3. The structure of compound **40** is essentially identical to the previously characterized diiodo compound $[Ir_2(I)_2(CO)(\mu\text{-}CO)(dppm)_2]$,[4] with one of the iodo ligands being replaced by the methoxymethyl ligand. Crystals of compound **40** are in fact contaminated with *ca.* 15% of the diiodo compound that is isomorphous with the methoxymethyl species (see Experimental section). As a result the structure is disordered, containing 85% of **40** with 15% of the superimposed diiodide. However, this disorder only affected the methoxymethyl (85%) and superimposed iodo (15%) groups and these atoms refined well. The phosphines are in a trans arrangement at each metal with angles of 173.86(10)° for P(1)-Ir(1)-P(3) and 167.54(11)° for P(2)-Ir(2)-P(4). The metal-metal separation of 2.8527(7) Å corresponds to a normal single Ir-Ir bond.[8] The carbonyls are mutually cis, with one in a terminal position almost opposite the Ir-Ir bond, and the other bridging the two metals in an unsymmetrical fashion,
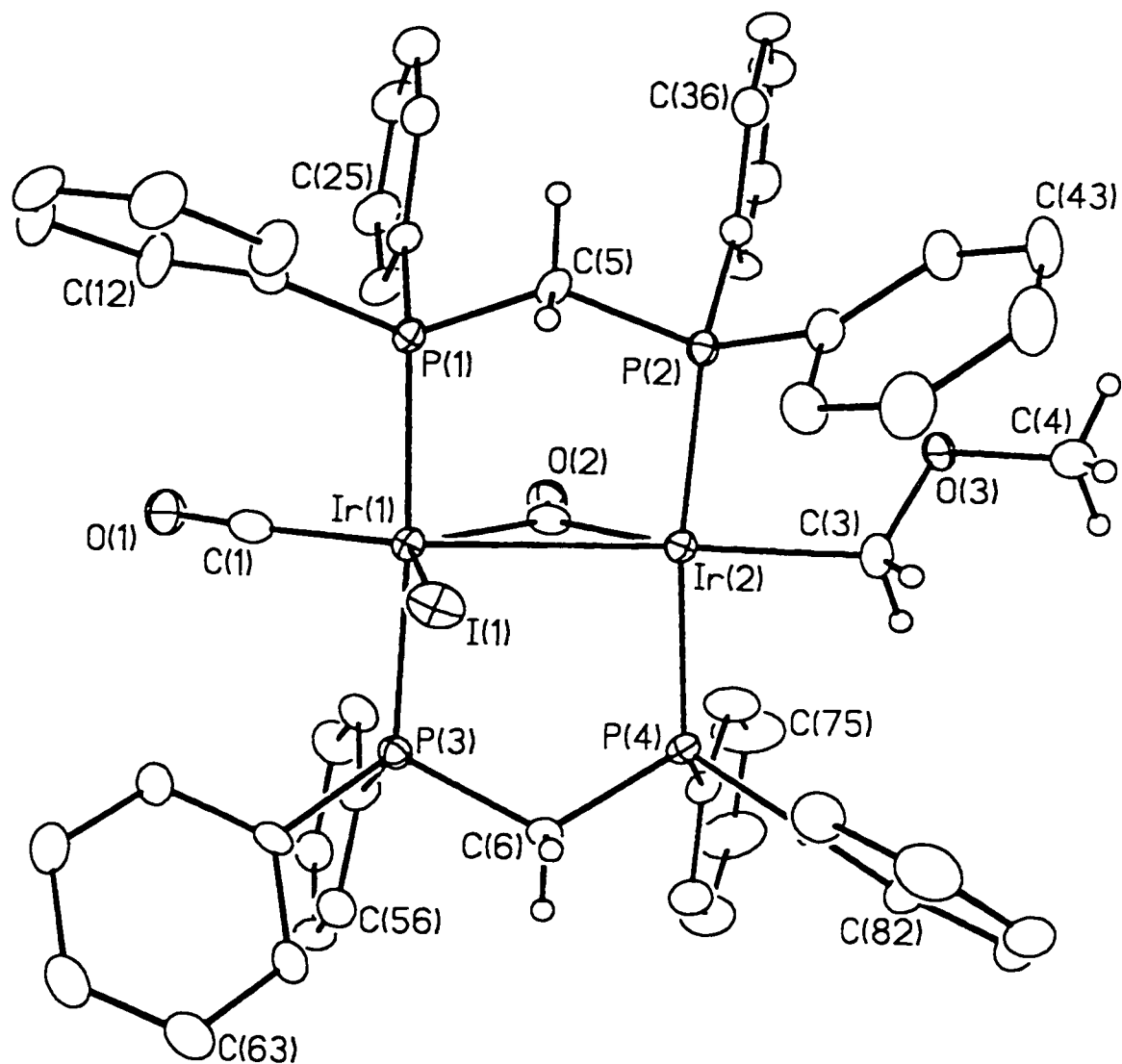
Figure 5.1 Perspective view of [Ir₂(CH₂OCH₃)(I)(CO)(μ-CO)(dppm)₂] (40). Thermal ellipsoids are shown at the 20% probability level except for hydrogens which are shown arbitrarily small. Phenyl hydrogens have been omitted.
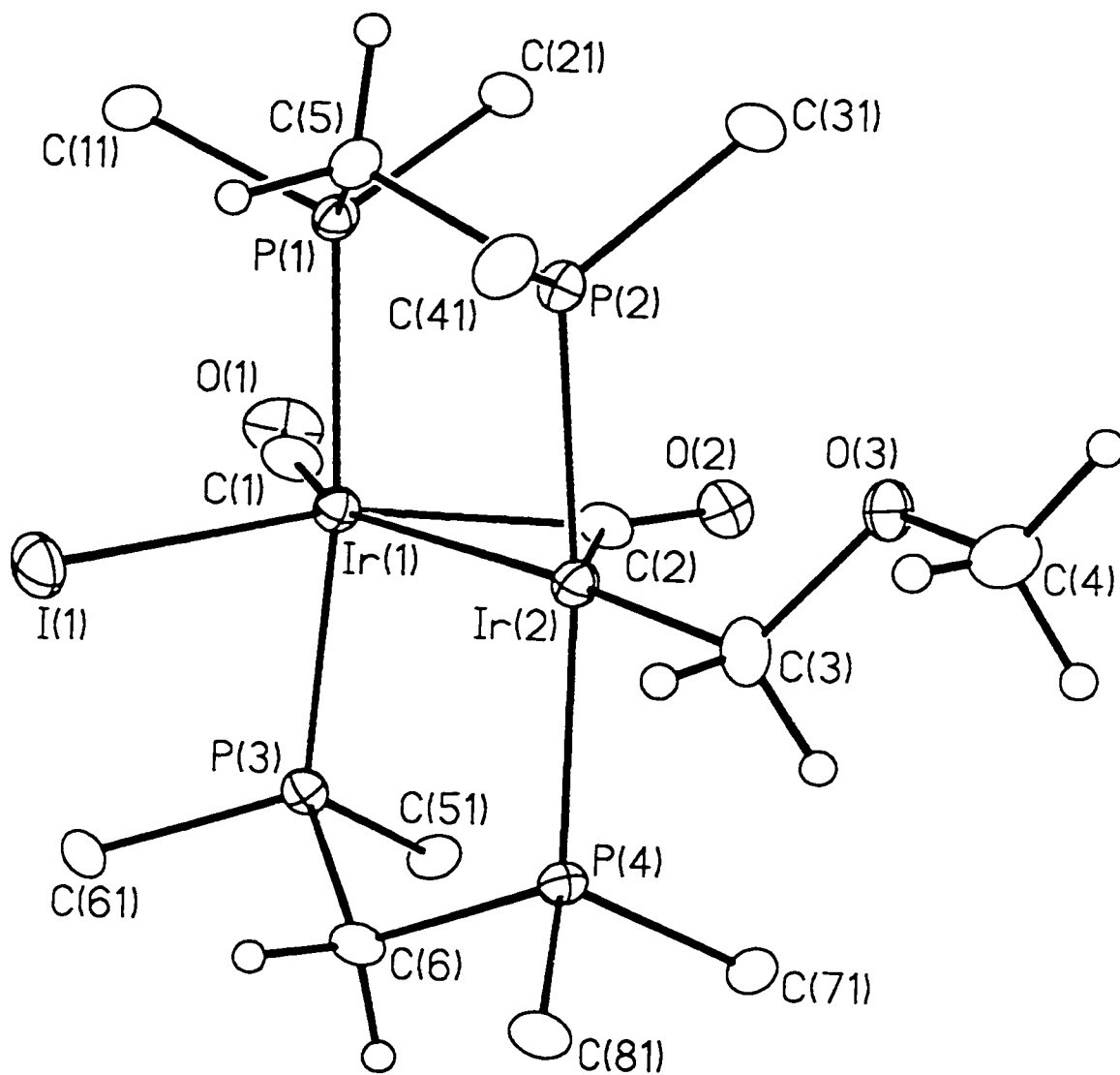
Figure 5.1.1 Alternate view of [Ir$_2$(CH$_2$OCH$_3$)(I)(CO)(μ-CO)(dppm)$_2$] (40), with only the *ipso* carbons of the dppm phenyl rings shown.

Table 5.3 Selected Interatomic Distances and Angles for Compound **40**.

(a) Distances (Å)

Atom1	Atom2	Distance		Atom1	Atom2	Distance
Ir(1)	Ir(2)	2.8527(7)		Ir(2)	P(4)	2.281(3)
Ir(1)	I(1)	2.8025(10)		Ir(2)	C(2)	1.924(12)
Ir(1)	P(1)	2.324(3)		Ir(2)	C(3)	2.08(2)
Ir(1)	P(3)	2.328(3)		O(1)	C(1)	1.13(2)
Ir(1)	C(1)	1.858(15)		O(2)	C(2)	1.185(14)
Ir(1)	C(2)	2.061(13)		O(3)	C(3)	1.39(2)
Ir(2)	I(2)	2.708(8)		O(3)	C(4)	1.37(2)
Ir(2)	P(2)	2.299(3)				

(b) Angles (deg)

Atom1	Atom2	Atom3	Angle		Atom1	Atom2	Atom3	Angle
Ir(2)	Ir(1)	I(1)	85.10(3)		I(2)	Ir(2)	C(2)	131.5(4)
Ir(2)	Ir(1)	C(1)	154.6(4)		P(2)	Ir(2)	P(4)	167.54(11)
Ir(2)	Ir(1)	C(2)	42.4(3)		C(2)	Ir(2)	C(3)	139.2(7)
I(1)	Ir(1)	C(1)	120.3(4)		C(3)	O(3)	C(4)	112.8(15)
I(1)	Ir(1)	C(2)	127.5(3)		Ir(1)	C(1)	O(1)	173.5(13)
P(1)	Ir(1)	P(3)	173.86(10)		Ir(1)	C(2)	Ir(2)	91.4(5)
Ir(1)	Ir(2)	I(2)	175.3(2)		Ir(1)	C(2)	O(2)	134.0(10)
Ir(1)	Ir(2)	C(2)	46.2(4)		Ir(2)	C(2)	O(2)	134.6(10)
Ir(1)	Ir(2)	C(3)	174.4(6)		Ir(2)	C(3)	O(3)	115.6(12)

being closer to Ir(2) than Ir(1) (1.924(12) Å vs 2.061(13) Å). The iodo ligand of compound **40** is terminally bound to the same metal as the terminal carbonyl, and is on the opposite face from the bridging carbonyl. The methoxymethyl group is the only terminal ligand on the opposite metal, falling opposite the metal-metal bond having an Ir(1)-Ir(2)-C(3) angle of 174.4(6)°, analogous to one of the iodo groups in the diiodo species mentioned above. It is interesting that the carbonyls don't assume a symmetrical arrangement with the anionic ligands on each metal as found for trans[IrCl(CO)(dppm)]$_2$,[8c] but instead adopt the unsymmetrical arrangement as observed for [Ir$_2$(I)$_2$(CO)(μ-CO)(dppm)$_2$].[4] We assume that as for the diiodo compound the bridging carbonyl is needed to remove excess electron density from the metals resulting from the good net-donor iodo groups; a bridging carbonyl is known to be a better π-acceptor than a terminal carbonyl.[9]

Compound **40** reacts with electrophiles that have both coordinating and non-coordinating anions. With trimethylsilyltriflate (Me$_3$SiO$_3$SCF$_3$) compound **40** produces the methylene- and iodo-bridged compound [Ir$_2$(CO)$_2$(μ-CH$_2$)(μ-I)-(dppm)$_2$][CF$_3$SO$_3$] (**41**), by removal of the methoxy group. The ^{31}P{^{1}H} NMR spectrum shows a singlet at δ -7.9 indicating a symmetrical structure having left-right and top-bottom symmetry, and the ^{1}H NMR spectrum shows the bridging methylene resonance as a quintet at δ 10.01 with 8.3 Hz coupling to all four chemically equivalent phosphorus nuclei. Confirmation of the symmetrical structure for **41** comes from the X-ray structure determination, a representation

of which is shown in Figure 5.2, with selected distances and angles given in Table 5.4.

Compound **41** shows approximate C_{2v} symmetry, with a terminal carbonyl on each metal opposite the Ir-Ir bond with a bridging methylene and a bridging iodo group on opposite faces of the compound. The metal-metal bond length (2.7853(5) Å) is typical of a single Ir-Ir bond.[8] The iodo ligand symmetrically bridges the metals with essentially equal Ir-I bond lengths of 2.7928(7) Å and 2.7899(7) Å. An acute Ir-I-Ir angle of 59.86(2)°, is consistent with the presence of the metal-metal bond. The methylene group also symmetrically bridges the two metals with bond lengths of 2.101(9) Å and 2.085(9) Å and an Ir-C-Ir angle of 83.4(4) that is typical for methylenes that bridge metal-metal bonds.[10]

Reaction of compound **40** with acids such as HBF_4 and triflic acid also yields compound **41** but does not proceed as cleanly as the trimethylsilyl triflate reaction, generating additional uncharacterized products.

With trimethylsilyliodide compound **40** reacts, with abstraction of the methoxy group and coordination of the iodo group, to produce two isomers of a methylene-bridged, diiodide species $[Ir_2(CO)_2(I)_2(\mu-CH_2)(dppm)_2]$ (**42 a & b**), shown in Scheme 5.1. These isomers differ in the orientation of the iodo groups as either anti (**42a**) or syn (**42b**) on adjacent metals. ^{1}H NMR experiments with selective ^{31}P decoupling of the resonaces of the anti isomer (**42a**) shows the bridging methylene resonance as a triplet of triplets at δ 6.6, showing coupling to the two sets of inequivalent phosphines of 10 and 7 Hz. The phosphines
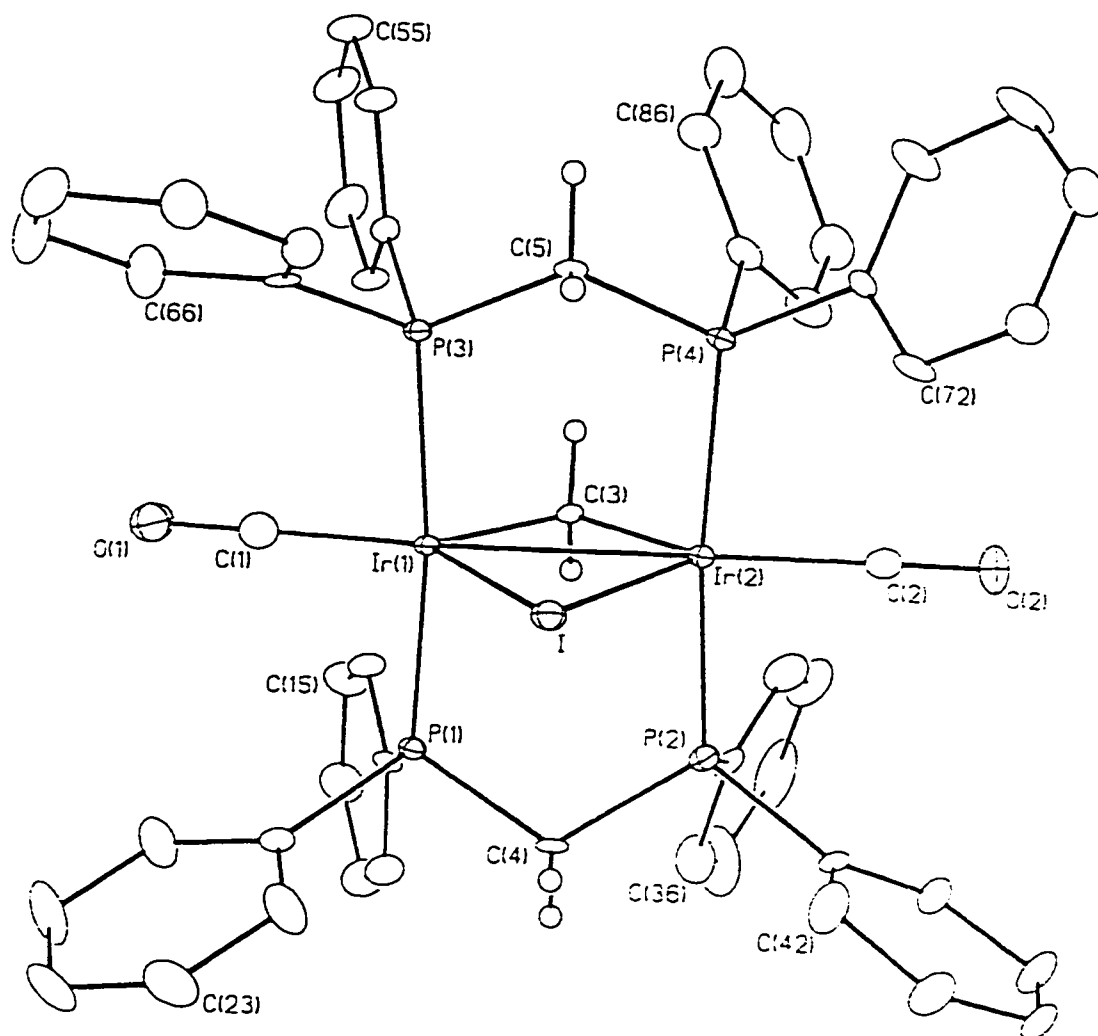
Figure 5.2 Perspective view of the [Ir₂(CO)₂(μ-CH₂)(μ-I)(dppm)₂]⁺ cation of
compound **41**. Thermal ellipsoids are shown at the 20%
probability level except for hydrogens which are shown arbitrarily
small. Phenyl hydrogens have been omitted.

Table 5.4 Selected Interatomic Distances and Angles for Compound **41**.

(a) Distances (Å)

Atom1	Atom2	Distance	Atom1	Atom2	Distance
Ir(1)	Ir(2)	2.7853(5)	Ir(2)	C(2)	1.847(11)
Ir(1)	I	2.7928(7)	Ir(2)	C(3)	2.085(9)
Ir(1)	P(1)	2.341(2)	Ir(2)	P(2)	2.343(3)
Ir(1)	P(3)	2.344(2)	Ir(2)	P(4)	2.340(2)
Ir(1)	C(1)	1.820(10)	O(1)	C(1)	1.169(12)
Ir(1)	C(3)	2.101(9)	O(2)	C(2)	1.155(12)
Ir(2)	I	2.7899(7)			

(b) Angles (deg)

Atom1	Atom2	Atom3	Angle	Atom1	Atom2	Atom3	Angle
Ir(2)	Ir(1)	I	60.02(2)	Ir(1)	Ir(2)	C(3)	48.5(3)
Ir(2)	Ir(1)	C(1)	166.7(3)	I	Ir(2)	C(2)	122.7(3)
Ir(2)	Ir(1)	C(3)	48.0(2)	I	Ir(2)	C(3)	108.6(3)
I	Ir(1)	C(1)	133.2(3)	P(2)	Ir(2)	P(4)	170.31(8)
I	Ir(1)	C(3)	108.1(2)	C(2)	Ir(2)	C(3)	128.6(4)
P(1)	Ir(1)	P(3)	173.52(8)	Ir(1)	I	Ir(2)	59.86(2)
C(1)	Ir(1)	C(3)	118.7(4)	Ir(1)	C(1)	O(1)	178.4(10)
Ir(1)	Ir(2)	I	60.12(2)	Ir(2)	C(2)	O(2)	175.6(10)
Ir(1)	Ir(2)	C(2)	177.1(3)	Ir(1)	C(3)	Ir(2)	83.4(4)

appear as two sets of multiplets in the $^{31}P\{^1H\}$ NMR spectrum at δ -15.1 and -28.0 owing to the inequivalent metal environments. In the syn isomer (42b) the bridging methylene signal appears in the ^1H NMR spectrum at δ 6.32 as a quintet showing 9.5 Hz coupling to the four equivalent phosphorus nuclei that appear as a singlet at δ -25.1 in the $^{31}P\{^1H\}$ NMR spectrum. Over a period of 4 days at room temperature the syn isomer (42b) was observed to completely transform into the anti isomer (42a), presumably because of unfavorable steric interactions in 42b between the large iodo groups on one face of the complex. Iodide dissociation and recoordination would be the most plausible process for this transformation and has been previously proposed in reactions of the diodo compounds $[Ir_2(I)_2(CO)(\mu\text{-}CO)(dppm)_2]^4$ and $[Ir_2(I)_2(CO)_2(\mu\text{-}C=CH_2)(\mu\text{-}C=CHPh)\text{-}(dppm)_2].^{11}$

A comparison of the structures of 2 (see Figure 2.2) and 40 show a remarkable similarity, apart from the presence of the iodo ligand in the latter. It therefore seemed that iodide removal from 40 would yield the methoxymethyl analogue of 2. However, attempts to remove the iodo ligand from compound 40 with the use of silver salts were not reproducible, and gave rise to mixtures of products making characterization difficult. Previous work on homobimetallic iodo complexes of Rh or Ir, by our group[11] and others[12] showed that methyl triflate addition could be effective for iodide ion removal. This worked well with compound 40 giving loss of methyl iodide (observed by ^1H and $^{13}C\{^1H\}$ NMR for the ^{13}C-labelled methyl triflate addition) upon addition of methyl triflate.

Suprisingly, iodide loss did not yield the anticipated product but instead was accompanied by a double C-H activation of the methoxymethyl ligand to give the methoxycarbyne-bridged product $[Ir_2(CO)_2(H)_2(\mu\text{-}COCH_3)(dppm)_2][CF_3SO_3]$ (43), as shown in Scheme 5.1. Methyl triflate addition also resulted in about 10% production of compound 41, as determined by $^{31}P\{^1H\}$ NMR, presumably by attack at the methoxy group. The $^{13}C\{^1H\}$ NMR spectrum of compound 43 shows the characteristic carbyne signal at low field (δ 316.6) as a pseudo triplet of triplets ($^2J_{C\text{-}P}$ = 55, 4 Hz). The signal for the carbyne carbon is at higher field than has been observed for other methoxycarbynes (δ 345 to 390),[13,14] but it falls into the range typically observed for other carbyne signals (δ 200 to 350).[15] The larger P-C coupling constant indicates that the carbyne is trans to one set of phosphines while the smaller value corresponds to cis coupling to the other pair of phosphorus nuclei. At room temperature the $^{31}P\{^1H\}$ NMR spectrum for this compound showed broad signals at δ -3.2 and -16.7 which sharpened upon cooling to -80°C, as shown in Figure 5.3. This spectrum does not have the typical AA'BB' pattern observed for a trans arrangement of the phosphines (see Figure 3.3 Chapter 3), instead showing an ABCD pattern with multiplets centered at δ -2.1, -4.6, -14.3 and -18.1. Compound 43 is believed to have a cis- phosphine orientation based on the large difference in carbon-phosphorus coupling observed for the carbyne carbon, the four multiplets observed for the phosphines and due to the inequivalence of the dppm protons that appear in the ^1H NMR spectrum as multiplets at δ 4.81, 4.08, 3.22 with the fourth signal
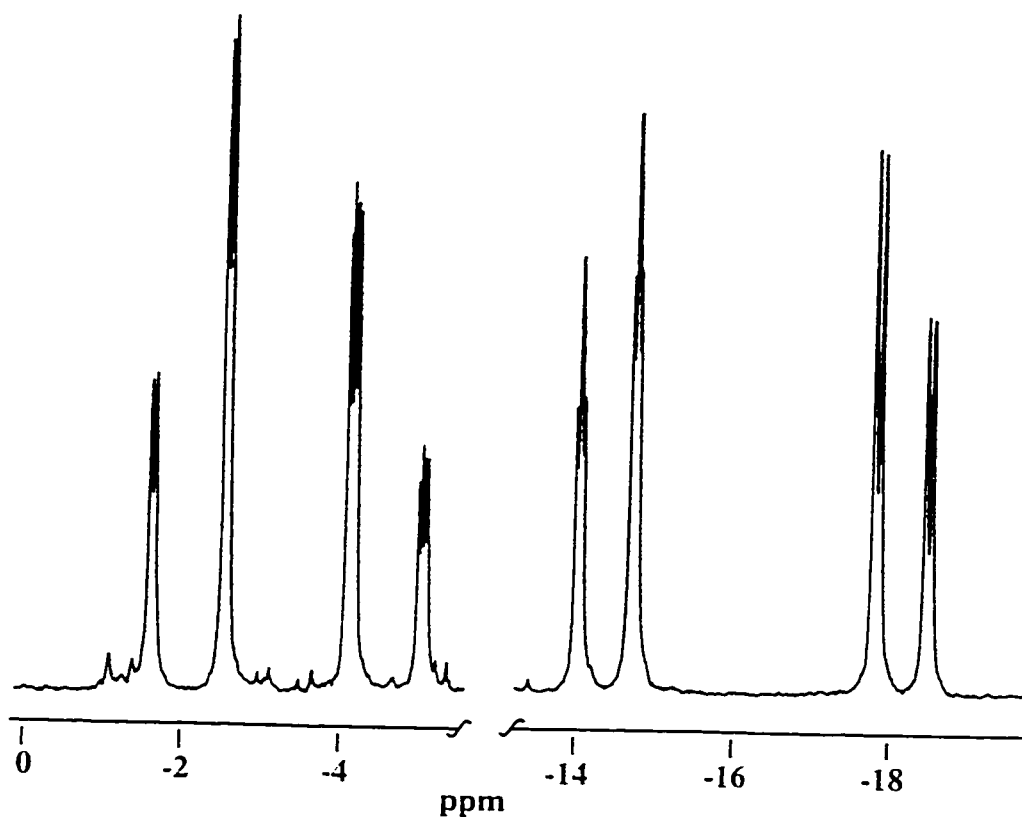
Figure 5.3 $^{31}P\{^1H\}$ NMR spectrum (-80°C) of the compound
$[Ir_2(H)_2(CO)_2(\mu\text{-}COCH_3)(dppm)_2][CF_3SO_3]$ **(43)**.

believed to be obscured by the phenyl protons. The methyl group of the methoxy substituent appears at δ 5.05 as a singlet. At room temperature the ^{1}H NMR spectrum shows the hydride signals as a broad and unresolved second order multiplet; which sharpens into a complex pattern at δ -11.16, upon cooling the sample to -80°C, as shown in Figure 5.4. Broadband ^{31}P decoupling resolves this complex pattern into two broad singlets at δ -11.12 and -11.20. ^{1}H NMR experiments with selective ^{31}P decoupling were attempted in order to elucidate the stereochemistry, however these experiments were equivocal because of the close proximity of the chemical shifts of the phosphorus AB and CD signals that did not allow full decoupling of one signal without affecting another. Decoupling the high-field phosphorus resonances had a larger effect on the hydride multiplet than decoupling the low-field resonances, indicating a larger coupling of the hydrides to the former. The two different couplings are consistent with each hydride being trans to a similar phosphorus nucleus, and therefore more strongly coupled to them, and cis to the others, to which they display a smaller coupling. Similar hydride signals had previously been observed for cis-phosphine silylene-bridged dihydride complexes, characterized in the group.[16] These species contained hydrides that had a trans-cis arrangement to the dppm phosphines and based on spectral similarities the structure shown in Scheme 5.1 is proposed for compound **43**.

The broadening of the ^{31}P{^{1}H} and ^{1}H signals upon warming suggests a fluxional process that averages the four inequivalent phosphorus nuclei into two sets. The fact that the three observed dppm methylene signals do not change
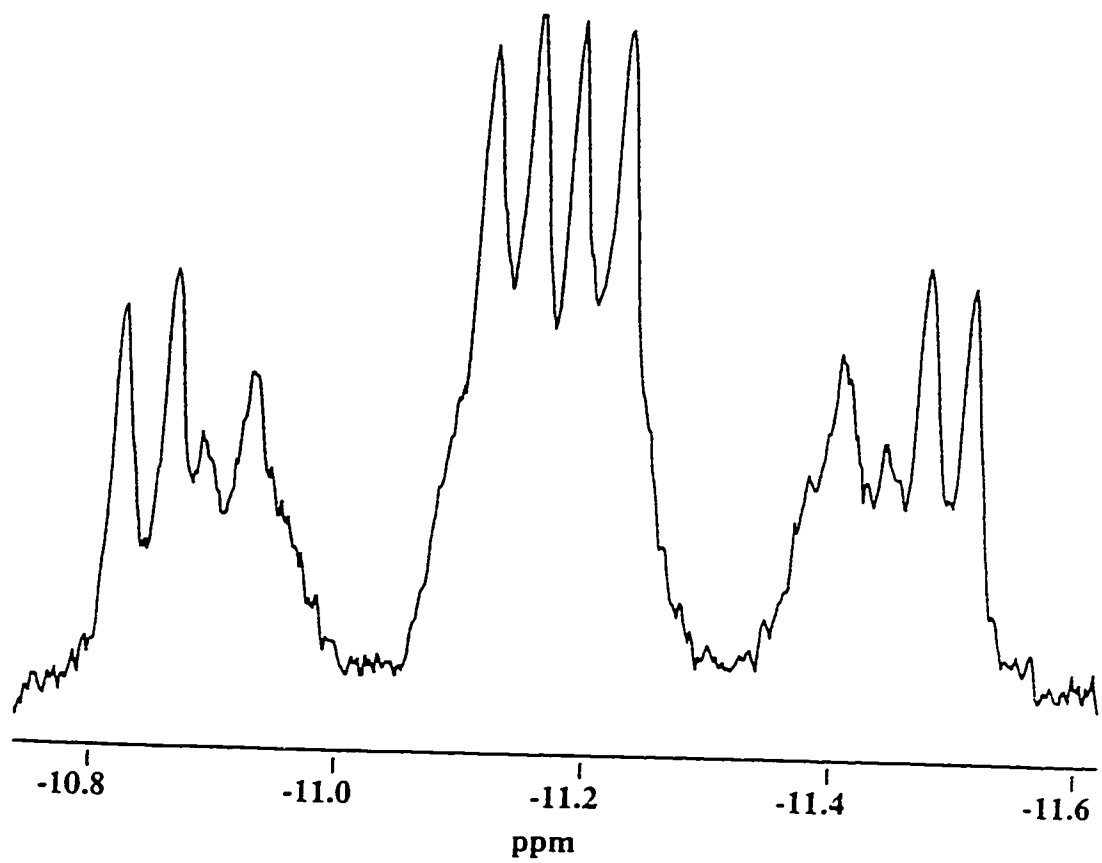
Figure 5.4   ¹H NMR spectrum (-80°C) of the hydride region of the compound [Ir₂(H)₂(CO)₂(μ-COCH₃)(dppm)₂][CF₃SO₃] (43).

upon warming indicates that this fluxional process does not average the four inequivalent methylene protons into two, further supporting the proposed structure shown in Scheme 5.1 in which the hydrides are eclipsed on adjacent metals. Such a process is easily explained by a simple rotation of the methoxy group around the C-OCH$_3$ bond (as pictured below). This rotation

43
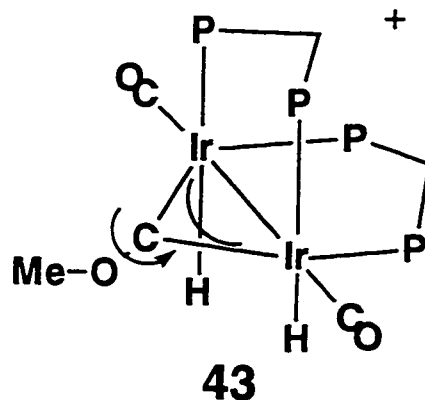
would average the ABCD phosphorus signal into an AA'BB' pattern.

The mesomeric forms, shown below, display partial π-character in the carbon-oxygen bond that is presumed to be responsible for the hindered
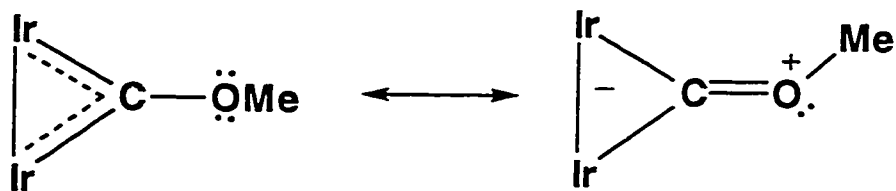
rotation of the methoxy substituent that gives rise to the limiting ^{31}P{^{1}H} and ^{1}H NMR spectra at low temperature. Note that in the resonance representation on the right the orientation of the methyl group differentiates one Ir center from the other. The partial C-O π-character is supported by crystal structures obtained on bridging-methoxycarbyne compounds, that display C-OMe bond lengths

between the carbyne carbon and methoxy oxygen between *ca.* 1.245 and 1.299 Å, intermediate between a normal single and double bond.[14a,17]

Another possible structure, shown below, with non-eclipsed terminal hydrides and a cis-phosphine orientation, similar to one of the silylene-bridged dihydride complexes previously characterized in the group,[16] can be discounted. Rotation of the methoxy group at room temperature in a complex with this geometry, would be expected to average the dppm methylenes into two signals which is not observed in this case. A high-temperature
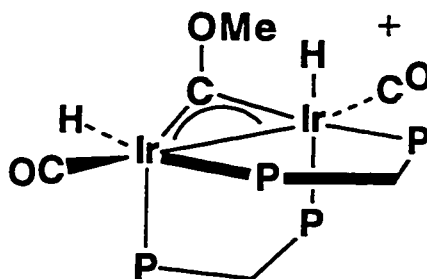
$^{31}P\{^{1}H\}$ spectrum for compound **43** is pending. If the fluxional process averaged all four phosphorus nuclei we would expect to see a coalesence of the four sharp signals at elevated temperature. The fact that at room temperature the four sharp signals have only coalesced into two broad signals centered between the AB and CD signals and they have not begun to coalesce into a single resonance argues against a process that averages all four phosphorus nuclei.

Unfortunately we have not yet been able to confirm the unusual structure proposed for **43**, by X-ray techniques owing to the failure to obtain X-ray quality crystals.

Attempts were made to react **43** with nucleophiles to generate a carbene species and also to attempt to deprotonate one of the metals by addition of base. In all cases no reaction was observed. Reaction of compound **43** with the electrophile trimethylsilyl triflate, not suprisingly, resulted in complete decomposition of the complex presumably by removal of the methoxy group of the carbyne, which would leave a highly reactive "carbide" species. Attempts at inducing reductive elimination of H_2 from the complex by refluxing in THF also left **43** unchanged.

Compound **40** was reacted with H_2 in an NMR tube yielding the known pentahydride compound $[Ir_2(H)_4(CO)_2(\mu\text{-H})(dppm)_2][I]$[5] in which three equivalents of H_2 have added to **40**, resulting in reductive elimination of CH_3OCH_3 (as observed by ^1H NMR) and loss of iodide ion. Previous reaction of the methylene hydride compound $[Ir_2H(CO)_3(\mu\text{-}CH_2)(dppm)_2][CF_3SO_3]$ with H_2 showed a dihydride, methyl intermediate prior to the reductive elimination of methane yielding the same pentahydride cation $[Ir_2(H)_4(CO)_2(\mu\text{-H})(dppm)_2]$-$[CF_3SO_3]$.[5b] Future work in the H_2 reaction with compound **40**, in attempts to deduce the initial site of H_2 attack and the intermediates leading to reductive elimination, is warranted.

The reaction of the formally Ir(0) compound, $[Ir_2(CO)_3(dppm)_2]$ with other alkyl halides was also of interest. Therefore the reaction with diiodomethane (CH_2I_2) was attempted in order to generate either an iodomethyl compound Ir-CH_2I by single oxidative addition or the methylene-bridged diodide compounds **42a** and **42b** from double oxidative addition of CH_2I_2. In addition, we attempted

to synthesize a cyanomethyl compound by the addition of iodo acetonitrile ICH_2CN. The reaction of $[Ir_2(CO)_3(dppm)_2]$ with CH_2I_2 appeared to be a more direct route to the bridging-methylene compounds (42a, 42b), rather than the route involving the methoxymethyl compound (40) as a precursor.

Suprisingly the reaction of $[Ir_2(CO)_3(dppm)_2]$ with CH_2I_2 gives neither of the products predicted but instead yields $[Ir_2(CO)_2(\mu-I)(\mu-CO)(dppm)-(Ph_2PCHPPh_2)]$ (44), as shown in Scheme 5.2, in which a hydrogen has been abstracted from one dppm ligand and an iodine atom has been transferred to the metals. Three proton resonances, consistent with the loss of one hydrogen, appear in the ^1H NMR spectrum as two multiplets at δ 4.60, 4.23 and a triplet of triplets at δ 2.07. The last signal is consistent with the methyne hydrogen of the $Ph_2PCHPPh_2$ group, showing coupling values of 10 and 3.5 Hz to phosphorus. The infrared spectrum shows terminal and bridging carbonyl bands at 1948 cm^{-1} and 1801 cm^{-1}, respectively. When the reaction is monitored by ^1H NMR spectroscopy, CH_3I is produced. Compound 44 is also produced in the reaction of iodo acetonitrile with $[Ir_2(CO)_3(dppm)_2]$; in this case acetonitrile is detected in the reaction mixture.

For compound 44 the $Ph_2PCHPPh_2$ unit can be considered an anionic ligand giving both metals a +1 oxidation state and an 18-electron configuration. The $^{31}P\{^1H\}$ NMR spectrum of compound 44 is shown together with the simulated spectrum in Figure 5.5. This spectrum differs from our usual AA'BB' spin systems due to the large coupling constants (ca. 300 Hz) between the A and B phosphorus nuclei owing to their trans alignment at the metals; usually
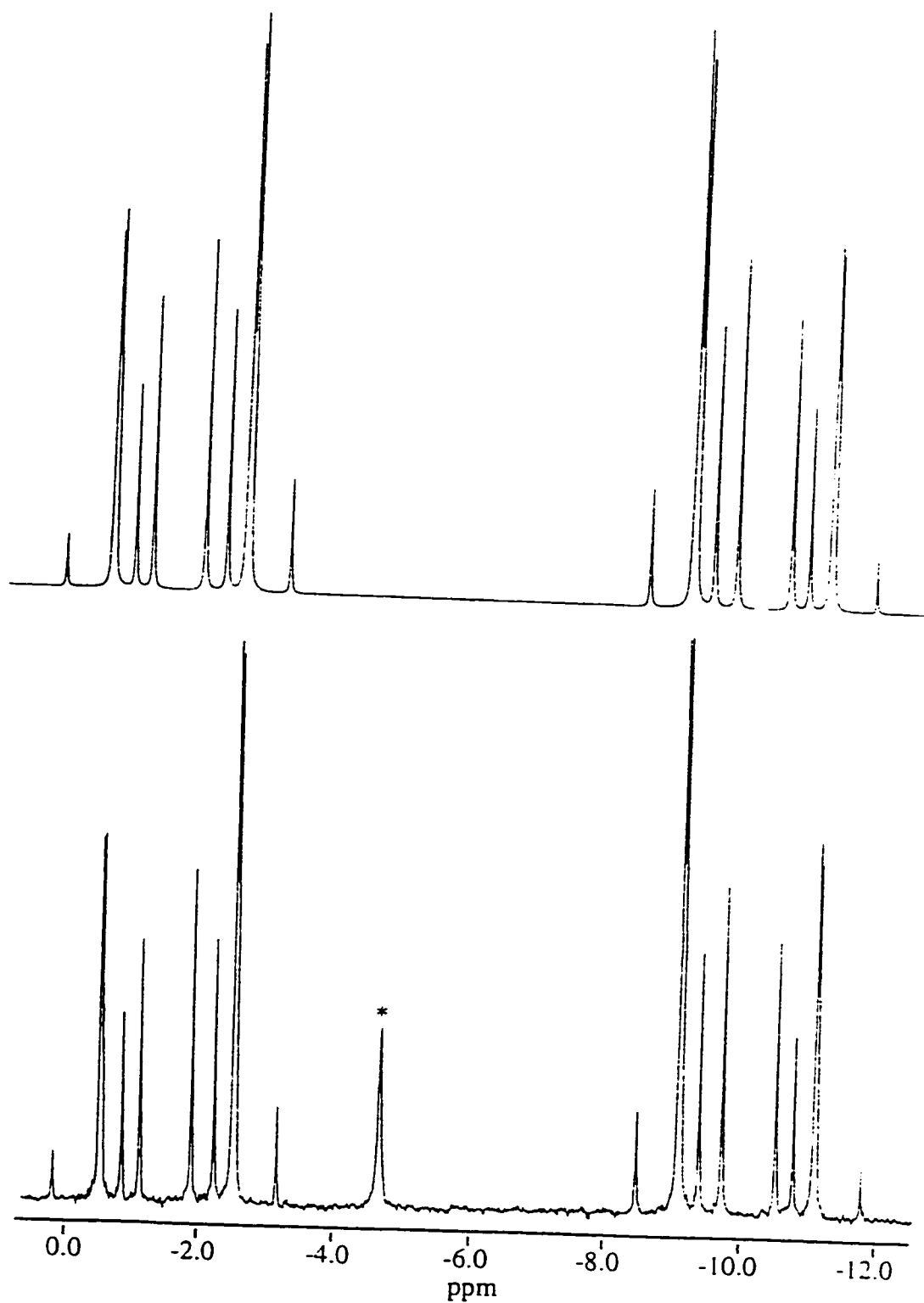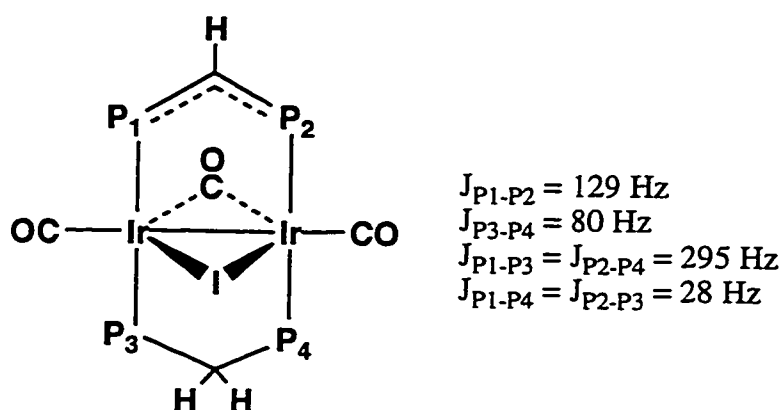
Scheme 5.2
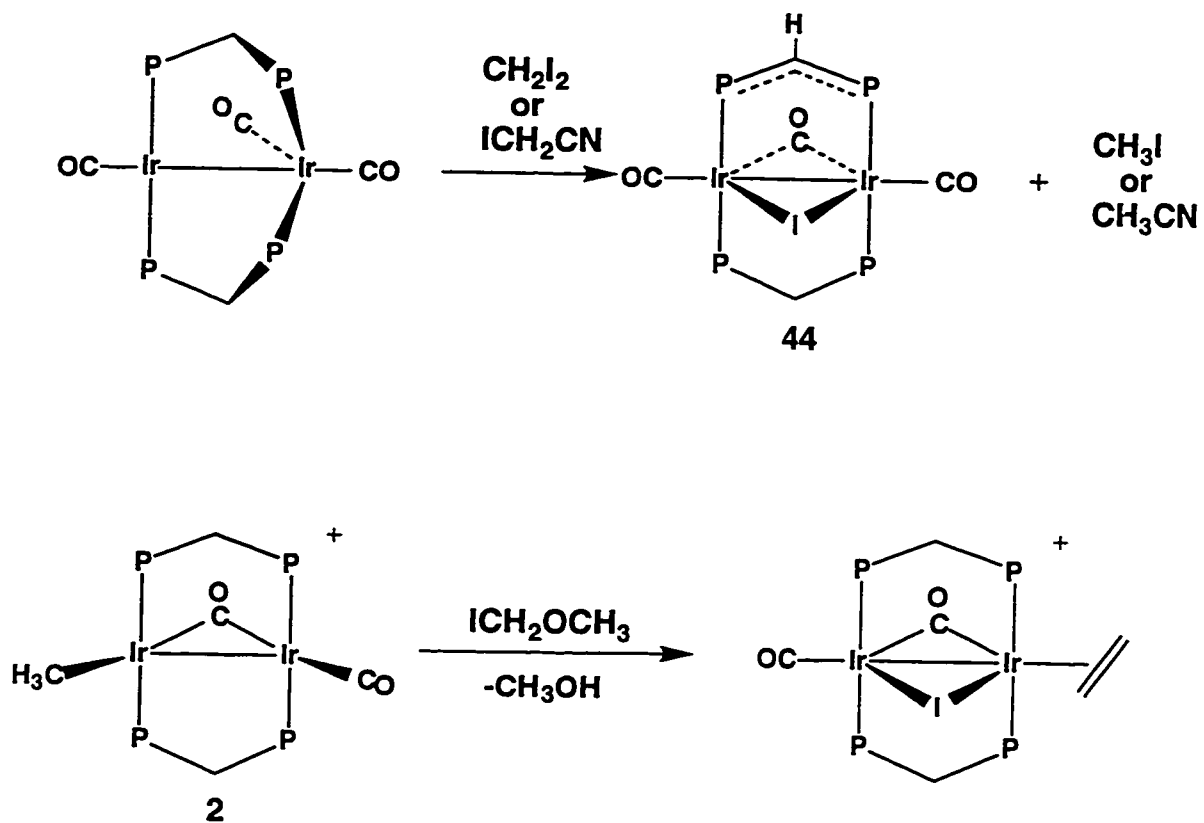
Figure 5.5 Calculated (top) and experimental (bottom) ^{31}P NMR spectrum for the compound [Ir$_2$(CO)$_2$(μ-CO)(μ-I)(Ph$_2$PCH$_2$PPh$_2$)-(Ph$_2$PCHPPh$_2$)] **(44)**. * denotes impurity.

the AB nuclei are coupled through the methylene unit with coupling constants of ca. 80 Hz. The P-C-P coupling constants, obtained from the simulation, are consistent with the formulation shown, in which the larger coupling (129 Hz vs 80 Hz) results from coupling through the sp^2 carbon of the methyne (PCHP) compared to sp^3 hybridization of the methylene carbon in the PCH_2P group. The derived coupling constants are summarized below.   Confirmation of

$$J_{P1-P2} = 129 \text{ Hz}$$
$$J_{P3-P4} = 80 \text{ Hz}$$
$$J_{P1-P3} = J_{P2-P4} = 295 \text{ Hz}$$
$$J_{P1-P4} = J_{P2-P3} = 28 \text{ Hz}$$

the proposed structure for **44** in the solid state comes from the X-ray structure determination, a representation of which is shown in Figure 5.6, with selected distances and angles given in Table 5.5. An alternate view is presented in Figure 5.6.1, which shows a symmetrical, doubly bridged structure in which there are three carbonyl ligands: two bonded terminally opposite the metal-metal bond with the third symmetrically bridging the metals (Ir-C bond lengths of 2.04(2) Å and 2.05(2) Å). The iodo group occupies the face opposite the bridging carbonyl and is symmetrically bridging (Ir(1)-I = 2.831(2) Å and Ir(2)-I = 2.835(2) Å). The metal-metal separation of 2.7828(11) Å is typical for an Ir-Ir
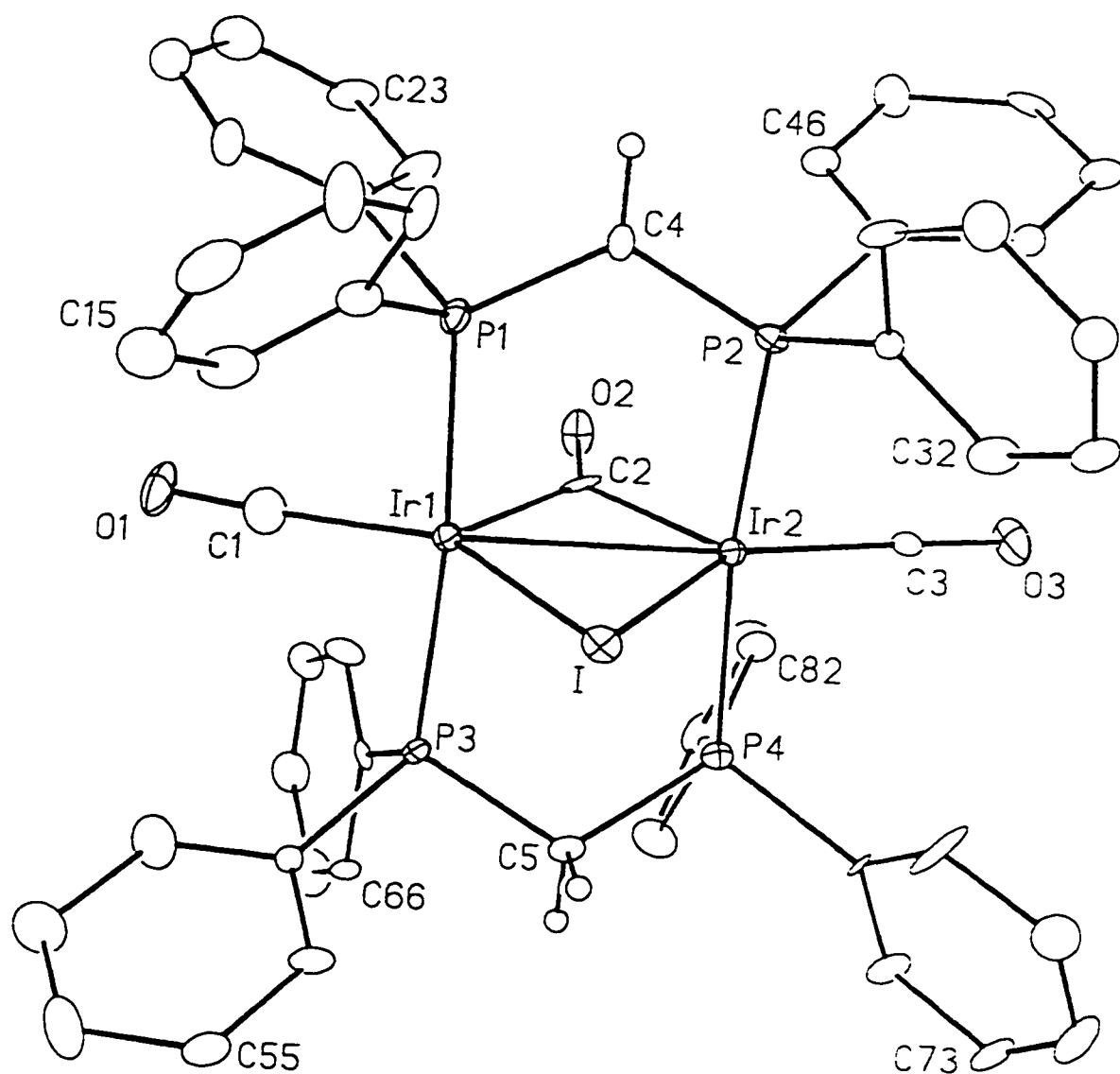
Figure 5.6 Perspective view of [Ir₂(CO)₂(μ–CO)(μ–I)(Ph₂PCH₂PPh₂)-(Ph₂PCHPPh₂)] **(44)**. Thermal ellipsoids are shown at the 20% probability level except for hydrogens which are shown arbitrarily small. Phenyl hydrogens have been omitted.
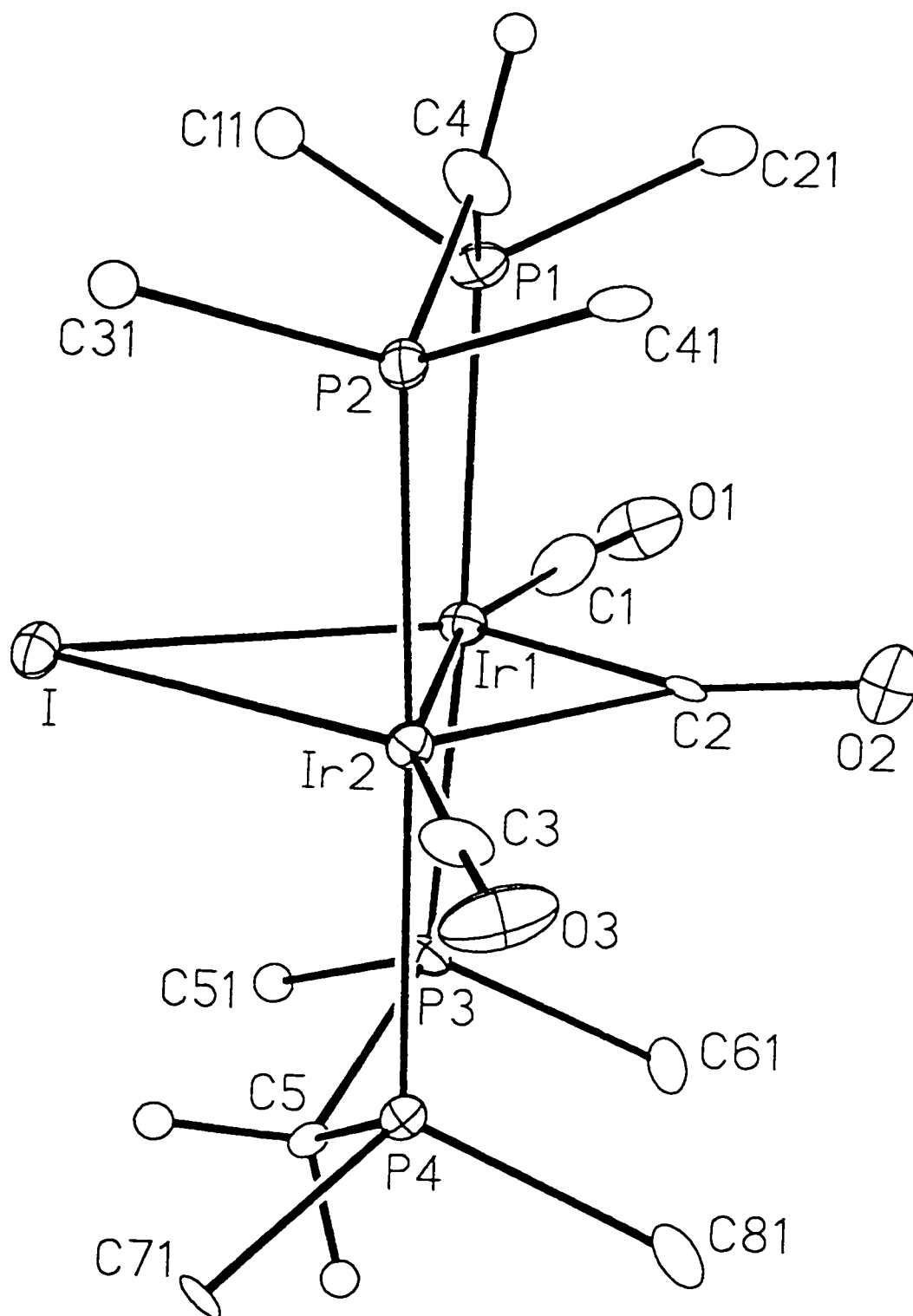
Figure 5.6.1 Alternate view of $[Ir_2(CO)_2(\mu-CO)(\mu-I)(Ph_2PCH_2PPh_2)-(Ph_2PCHPPh_2)]$ **(44)** with only the *ipso* carbons of the dppm phenyl rings shown.

Table 5.5 Selected Interatomic Distances and Angles for Compound **44**.

(a) Distances (Å)

Atom1	Atom2	Distance	Atom1	Atom2	Distance
Ir(1)	Ir(2)	2.7828(11)	Ir(2)	C(2)	2.05(2)
Ir(1)	I	2.831(2)	Ir(2)	C(3)	1.84(2)
Ir(1)	P(1)	2.352(5)	P(1)	C(4)	1.72(2)
Ir(1)	P(3)	2.341(5)	P(2)	C(4)	1.72(2)
Ir(1)	C(1)	1.85(2)	P(3)	C(5)	1.82(2)
Ir(1)	C(2)	2.04(2)	P(4)	C(5)	1.81(2)
Ir(2)	I	2.835(2)	O(1)	C(1)	1.15(2)
Ir(2)	P(2)	2.351(5)	O(2)	C(2)	1.18(2)
Ir(2)	P(4)	2.323(5)	O(3)	C(3)	1.14(2)

(b) Angles (deg)

Atom1	Atom2	Atom3	Angle	Atom1	Atom2	Atom3	Angle
Ir(2)	Ir(1)	C(1)	165.2(7)	Ir(2)	P(2)	C(4)	115.2(7)
I	Ir(1)	C(1)	134.1(7)	Ir(1)	P(3)	C(5)	112.9(6)
I	Ir(1)	C(2)	107.8(5)	Ir(2)	P(4)	C(5)	112.2(6)
P(1)	Ir(1)	P(3)	173.1(2)	Ir(1)	C(1)	O(1)	173.0(22)
C(1)	Ir(1)	C(2)	118.1(8)	Ir(1)	C(2)	Ir(2)	85.9(7)
Ir(1)	Ir(2)	C(3)	165.1(6)	Ir(1)	C(2)	O(2)	137.7(15)
P(2)	Ir(2)	P(4)	174.5(2)	Ir(2)	C(2)	O(2)	136.3(15)
C(2)	Ir(2)	C(3)	118.2(8)	Ir(2)	C(3)	O(3)	176.2(17)
Ir(1)	I	Ir(2)	58.83(3)	P(1)	C(4)	P(2)	122.2(12)
Ir(1)	P(1)	C(4)	115.4(7)	P(3)	C(5)	P(4)	112.7(10)

single bond.[8]   The structure looks remarkably like the carbonyl-bridged

A-frames [Rh$_2$(CO)$_2$(μ-Cl)(μ-CO)(dppm)$_2$][BPh$_4$],[18] [Rh$_2$(CO)$_2$(μ-H)(μ-CO)(dppm)$_2$]-

[CH$_3$C$_6$H$_4$SO$_3$],[19]   [Ir$_2$(CO)$_2$(μ-S)(μ-CO)(dppm)$_2$][20]   and   [Ir$_2$(CO)$_2$(μ-H)(μ-CO)-

(dppm)$_2$][BF$_4$][21] apart from the subtle differences resulting from formal

deprotonation of one methylene unit. A P-C-P angle of 122.2(12)° at C(4) for

the Ph$_2$PCHPPh$_2$ group compared to the non-deprotonated dppm angle of

112.7(10)° at C(5), illustrates the rehybridization of the C(4) atom from sp^3 to sp^2.

Also consistent with the difference in rehybridization, the P-C bond lengths

within the P $=$ C $=$ P unit show the π-delocalization, with a shortening of the

bonds (P(1)-C(4) = 1.72(2) Å, P(2)-C(4) = 1.72(2) Å vs. P(3)-C(5) = 1.82(2) Å,

P(4)-C(5) = 1.81(2) Å). Bond lengths and angles of the PCHP group compare

well with those observed in the dirhodium [Rh$_2$(CO)$_2$(μ-NHCH$_3$)(dppm)-

(Ph$_2$CHPPh$_2$)] complex that has a deprotonated dppm (P-C lengths of 1.738(8)

Å and 1.736(8) Å; P-C-P angle of 119.3(4)°).[22] Figure 5.6.1 clearly displays the

near planar arrangement of the Ir(1)-Ir(2)-P(2)-C(4)-P(1) ring, dictated by the sp^2

hybridization at C(4), compared to Ir(1)-Ir(2)-P(4)-C(5)-P(3) ring that shows the

sp^3 hybridized C(5) distinctly out of the plane of the other 4 atoms.

Although the reaction of methyl triflate with compound 40 was shown to

result in iodide abstraction to produce the carbyne compound (43), due

presumably to electrophilic attack at the iodide ligand, it was thought that the

reverse reaction of the methyl compound [Ir$_2$(CH$_3$)(CO)(μ-CO)(dppm)$_2$][CF$_3$SO$_3$]

(2) with ICH$_2$OCH$_3$ may give rise to a mixed dialkyl compound containing CH$_3$

and CH_2OCH_3 groups, and that C-C bond formation could be induced in such a product. In fact the reaction does not yield an identifiable dialkyl compound but instead yields the known iodide-bridged ethylene compound, $[Ir_2(C_2H_4)(CO)\text{-}(\mu\text{-}I)(\mu\text{-}CO)(dppm)_2][CF_3SO_3]$.[4] Little is presently known about the mechanism by which this species arises and it is presently under study.

Discussion

Addition of iodomethyl methyl ether to the Ir(0) compound $[Ir_2(CO)_3\text{-}(dppm)_2]$ produces the methoxymethyl compound $[Ir_2(CH_2OCH_3)(I)(CO)(\mu\text{-}CO)\text{-}(dppm)_2]$ (**40**), having a structure very similar to the analogous diiodide species $[Ir_2(I)_2(CO)(\mu\text{-}CO)(dppm)_2]$.[4] The reason the two compounds show such similar structures involving bridging carbonyls is presumed to be due to a buildup of electron density at the metals that is better alleviated through a *bridging carbonyl*. Bridging carbonyls have been shown to be better π-acceptors than terminal carbonyls.[9] This buildup of electron density is assumed to be due to the presence of the iodo ligands which are good net donors, in each species as well as the strong σ-donor alkyl group in **43**. The synthesis of this methoxymethyl species allows us the opportunity to prepare methylene complexes by reaction with electrophiles.

Bridging methylene ligands are common for late transition metals and their synthesis was of interest to us owing to their importance in the C-C chain growth step in Fischer-Tropsch chemistry.[23] Reactions of **40** with electrophiles

containing coordinating and non coordinating anions presents a convenient route into the bridging-methylene compounds **41**, **42a** and **42b**, by abstraction of the methoxy group. The subsequent reactivity of these methylene-bridged species has not yet been investigated, although several reactions are envisioned. Their reactions with unsaturated substrates such as alkynes, olefins, allenes, etc. should be followed, owing to the possibility of C-C bond formation. This may not succeed for the compounds as shown owing to their coordinative saturation, however removal of the iodide ions to generate unsaturated cationic compounds or reduction to neutral methylene-bridged carbonyls such as $[Ir_2(CO)_2(\mu-CH_2)(dppm)_2]$ is envisioned. Replacement of the iodo ligands by organic groups, which might then undergo migratory insertion is also possible.

Removal of the iodide ligand from **40**, by addition of methyl triflate was originally expected to produce a methoxymethyl species analogous to compound **2**. Instead, the reaction resulted in the *double* C-H activation of the methoxymethyl ligand producing the fluxional methoxycarbyne dihydride $[Ir_2(H)_2(CO)_2(\mu-COCH_3)(dppm)_2][CF_3SO_3]$ (**43**). A fluxional process, similar to the one described for **43**, involving the rotation of the methoxy group around the C-O bond has been observed in other bridging methoxycarbyne compounds.[14] Due to the formation of the methoxycarbyne dihydride (**43**) a direct comparison of the reactivity of the nonsubstituted methyl compound (**2**) and an analogous substituted species could not be made. Nevertheless, this reactivity certainly raises the question of why the substitution of a methyl hydrogen by a methoxy

substituent should give rise to the *double* C-H activation to form the carbyne-bridged dihydride (**43**). However, the presence of a methoxy group on the alpha carbon has previously given rise to unusual reactivity in the form of α-hydrogen elimination from a methoxymethyl ligand.[24] This α-hydrogen elimination was favored by formation of a stable Fischer carbene, so it may be that the double C-H activation of **40** upon iodide removal is favored by formation of a bridging carbyne in our case. The additional resonance stabilization imparted by the methoxy group on the methoxycarbyne moiety, as discussed in relation to the hindered rotation about the C-O bond presumably favors the carbyne moiety. The observed C-H activation in this reaction is in line with the many examples where a ligand is removed from a transition-metal complex, producing coordinative unsaturation,[25] but is *opposite* to what is observed for the unsubstituted methyl compound $[Ir_2(CH_3)(CO)(\mu\text{-}CO)(dppm)_2]$-$[CF_3SO_3]$ (**2**), which undergoes C-H activation upon *addition* of ligands, as discussed in Chapter 2.

The carbyne complex **43** was found to be remarkably unreactive. Numerous attempts to generate a methoxymethylene by addition of nucleophiles such as hydride or MeLi to the carbyne carbon, failed to yield any characterizable products. Furthermore, attempts to deprotonate **43** to yield a monohydride species also failed. Similarly complex **43** was inert to CO, HC≡CH or PMe_3 addition.

Reaction of $[Ir_2(CO)_3(dppm)_2]$ with the doubly substituted alkyl iodides CH_2I_2 and ICH_2CN appeared to be a convenient route to oxidative-addition

products. However this did not occur and instead resulted in a suprising reaction in which a dppm ligand has lost a hydrogen and an iodine atom has been transferred to the metals. Removal of a hydrogen by deprotonation of dppm ligands is not a new reaction having been observed previously in our group[26] and others.[22,27] However, the reactions observed in this case aren't simple deprotonations since first there is no strong base present, and second the hydrogen removal is accompanied by iodine atom addition and formation of CH_3I or acetonitrile. Instead we believe that a radical process is occurring. Attempts at carrying out this reaction in the presence of radical scavengers is recommended.

Conclusions

The low-valent diridium compound $[Ir_2(CO)_3(dppm)_2]$ shows a susceptibility to oxidative addition of alkyl iodides that has resulted in some interesting preliminary chemistry with regards to the substituted methyl ligand (CH_3OCH_2-), including the unprecedented formation of a methoxycarbyne by **double** C-H activation.

The ability of the methoxymethyl ligand to undergo attack by electrophiles has provided the opportunity to produce bridging-methylene compounds. Methylene species have been proposed as intermediates in some of the reactions in Chapters 3 and 4 and future reactivity studies on these methylene species toward unsaturated substrates may possibly shed some light on the mechanisms for the C-C bond forming reactions proposed in these

chapters as well as leading into further modelling studies of the Fischer-Tropsch reaction.

References

1. Jandick, P.; Schubert, U.; Schmidbaur, H. *Angew. Chem., Int. Ed. Engl.* **1982**, *21*, 73. (b) Balch, A. L.; Hunt, C. T.; Lee, C. L.; Olmstead, M. M.; Farr, J. P. *J. Am. Chem. Soc.* **1981**, *103*, 3764. (c) Theopold, K. H.; Bergman, R. G. *J. Am. Chem. Soc.* **1981**, *103*, 2489. (d) Sumner, C. E.; Riley, P. E.; Davis, R. E.; Pettit, R. *J. Am. Chem. Soc.* **1980**, *102*, 1752.

2. (a) Jolly, P. W.; Pettit, R. *J. Am. Chem. Soc.* **1966**, *88*, 5044. (b) Brookhart, M.; Nelson, G. O. *J. Am. Chem. Soc.* **1977**, *99*, 6099. (c) Brookhart, M.; Tucker, J. R.; Flood, T. C.; Jensen, J. *J. Am. Chem. Soc.* **1980**, *102*, 1203. (d) Thorn, D. L.; Tulip, T. H. *J. Am. Chem. Soc.* **1981**, *103*, 5984. (e) Thorn, D. L. *Organometallics* **1982**, 1, 879. (f) Calabrese, J. C.; Roe, D. C.; Thorn, D. L.; Tulip, T. H. *Organometallics* **1984**, *3*, 1223.

3. Sutherland, B. R.; Cowie, M. *Organometallics* **1985**, *4*, 1637.

4. Vaartstra, B. A.; Xiao, J.; Jenkins, J. A.; Verhagen, R.; Cowie, M. *Organometallics* **1991**, *10*, 2708.

5. (a) This compound was erroneously proposed to be a tetrahydride complex when reported. McDonald, R.; Sutherland, B. R.; Cowie, M. *Inorg. Chem.* **1987**, *26*, 3333. (b) Antwi-Nsiah, F. H. Ph.D. Thesis, University of Alberta, Edmonton, AB, 1994.

6. (a) Walker, N.; Stuart, D. *Acta Crystallogr.* **1983**, *A39*, 158–166. (b) Sheldrick, G. M. *Acta Crystallogr.* **1990**, *A46*, 467. (c) Sheldrick, G. M. *SHELXL-93.* Program for crystal structure determination. University of Göttingen, Germany, 1993.

7. Muritu, J.; Cowie, M. unpublished results.

8. (a) Kubiak, C. P.; Woodcock, C.; Eisenberg, R. *Inorg. Chem.* **1980**, *19*, 2733. (b) Sutherland, B. R.; Cowie, M. *Organometallics* **1984**, *3*, 1869. (c) Sutherland, B. R.; Cowie, M. *Inorg. Chem.* **1984**, *23*, 2324. (d) Sutherland, B. R.; Cowie, M. *Organometallics* **1985**, *4*, 1801. (e) Xiao, J.; Cowie, M. *Organometallics* **1993**, *12*, 463. (f) See structures for compounds **2, 3, 7, 26, 32, 36** this thesis.

9. Collman, J. P.; Hegedus, L. S.; Norton, J. R.; Finke, R. G. *Principles and Apllications of Organotransition Metal Chemistry*; University Science Books: Mill Valley, CA, 1987; p112.

10. Herrmann, W. A. *Adv. Organomet. Chem.* **1982**, *20*, 159. (b) See compound **3** Chapter 2.

11. Wang, L-S.; Cowie, M. *Organometallics* **1995**, *14*, 3040.

12. Tejel, C.; Ciriano, M. A.; Edwards, A. J.; Lahoz, F. J.; Oro, L. A. *Organometallics* **1997**, *16*, 45.

13. (a) Hodali, H. A.; Shriver, D. F. *Inorg. Chem.* **1979**, *18*, 1236. (b) Holt, E. M.; Whitmire, K. H.; Shriver, D. F. *J. Organomet. Chem.* **1981**, *213*, 125. (c) Kolis, J. W.; Basolo, F.; Shriver, D. F. *J. Am. Chem. Soc.* **1982**, *104*, 5626. (d) Fong, R. H.; Hersh, W. H. *Organometallics* **1985**, *4*, 1468.

14. (a) Johnson, B. F. G.; Lewis, J.; Orpen, A. G.; Raithby, P. R.; Suss, G. *J. Organomet. Chem.* **1979**, *173*, 187. (b) Gavens, P. D.; Mays, M. J. *J. Organomet. Chem.* **1978**, *162*, 389.

15. Collman, J. P.; Hegedus, L. S.; Norton, J. R.; Finke, R. G. *Principles and Apllications of Organotransition Metal Chemistry*; University Science Books: Mill Valley, CA, 1987; p139.

16. McDonald, R.; Cowie, M. *Organometallics* **1990**, *9*, 2468.

17. Johnson, K. A.; Gladfelter, W. L. *Organometallics* **1990**, *9*, 2101.

18. Kubiak, C. P.; Woodcock, C.; Eisenberg, R. *Inorg. Chem.* **1980**, *19*, 2733.

19. Kubiak, C.P.; Woodcock, C.; Eisenberg, R. *Inorg. Chem.* **1982**, *21*, 2119.

20. Cowie, M.; Mague, J. T.; Sanger, A. R. *J. Am. Chem. Soc.* **1978**, *100*, 3628.

21. Sutherland, B. R.; Cowie, M. *Can. J. Chem.* **1986**, *64*, 464.

22. Sharp, P.R.; Ge, Y.-W. *J. Am. Chem. Soc.* **1987**, *109*, 3796.

23. (a) Brady, R. C.; Pettit, R. J. Am. Chem. Soc. 1980, 102, 6181. (b) Maitlis, P. M.; Long, H. C.; Quyoum, R.; Turner, M. L.; Wang, Z-Q. *Chem. Commun.* **1996**, 1. (c) Maitlis, P. M.; Saez, I. M.; Meanwell, N. J.; Isobe, K.; Nutton, A.; Vaquez de Miguel, A.; Bruce, D. W.; Okeya, S.; Bailey, P. M.; Andrews, D. G.; Ashton, P. R.; Johnstone, I. R. *New J. Chem.*, **1989**, *13*, 419. (d) Martinex, J. M.; Adams, H.; Bailey, N. A.; Maitlis, P. M. *J. Chem. Soc., Chem. Commun.*, **1989**, 286.

24. Luecke, H. F.; Arndtsen, B. A.; Burger, P.; Bergman, R. G. *J. Am. Chem. Soc.* **1996**, *118*, 2517.

25. (a) Collman, J.P.; Hegedus, L.S.; Norton, J.R.; Finke, R.G. *Principles and Applications of Organotransition Metal Chemistry*; University Science Books: Mill Valley, California, 1987, p 298-300. (b) See articles in: *J.*

Organomet. Chem. **1995**, *504*, 1-155. (c) Cooper, N. J.; Green, M. H. L.; Mahtab, R. *J. Chem. Soc., Dalton Trans.* **1979**, 1557. (d) Tulip, T. H.; Thom, D. L. *J. Am. Chem. Soc.* **1981**, *103*, 2448.

26. Sterenberg, B. T.; Hilts, R. W.; Moro, G.; McDonald, R.; Cowie, M. *J. Am. Chem. Soc.* **1995**, *117*, 245.

27. (a) Puddephatt, R. J. *Chem. Soc. Rev.*, **1983**, *12*, 99. (b) Sharp, P.R.; Ge, Y.-W. *Inorg. Chem.* **1993**, *32*, 94.

Chapter 6

Conclusions

The goal of this thesis was to investigate the influence of adjacent metals on alkyl groups. We hoped to model the possible chemistry of a surface-bound methyl group specifically looking at factors that effected the reversible C-H bond cleavage/formation that occurs on metal surfaces. Using a diiridium methyl complex we were also interested in probing the factors that led to C-H activation and C-C bond formation of the methyl group or its fragments and other substrates. As an extension of the study on diiridium methyl species we were interested in studying what effect changing a substituent on the methyl group would have on its reactivity, particularly with respect to changes in the reactivity of the C-H bond. Part of this last goal also involved the utilization of the substituted methyl species as a precursor for the generation of bridging-methylene groups. Our interest in modelling surface-bound methyls and in generating bridging-methylene groups, stems from the implications of such species in heterogeneously catalyzed processes, such as Fischer-Tropsch catalysis.

The coordinatively unsaturated methyl compound $[Ir_2(CH_3)(CO)(\mu\text{-CO})$-$(dppm)_2][CF_3SO_3]$ (2) was prepared by removing a carbonyl ligand from the methylene hydride compound $[Ir_2(H)(CO)_3(\mu\text{-CH}_2)(dppm)_2][CF_3SO_3]$ (1).

Compounds like **2** (i.e. $[M_2(CH_3)(CO)_2(diphosphine)_2]^+$ (M = Rh, Ir; diphosphine = dppm, dmpm) have displayed two structure types in the solid state. Compound **2** displays a geometry similar to Eisenberg's[1] Rh_2 analogue $[Rh_2(CH_3)(CO)(\mu\text{-}CO)(dppm)_2]^+$ in which the methyl group is terminally bound to one metal. Kubiak's[2] dmpm analogue, $[Ir_2(CO)_2(\mu\text{-}CH_3)(dmpm)_2]^+$ on the other hand displays a symmetrically bridging methyl in the solid. The three species however, do not appear to differ appreciably in energy in solution, since compound **2** and the Rh_2 species are both fluxional, transferring the methyl group from metal-to-metal presumably via a methyl-bridged intermediate, analogous to the dmpm species. The solution structure and the DFT calculated structure of **2** (i.e. **2a**) also suggest that the differences observed in the solid state do not reflect electronic stabilization of the different geometries by the different phosphines, but more likely result from subtle non-bonded contacts in the solid.

The significance of reversing the C-H activation step by removing a ligand from **1** yielding **2**, suggested that ligand addition to **2** might lead to C-H bond cleavage. Although this has been realized for a number of substrates, this reactivity is not completely general as will be discussed later. Reaction of compound **2** with simple small molecules (both σ-donors and π-acceptors) has resulted in the C-H activation of the methyl ligand, generating methylene-hydride complexes $[Ir_2(H)(CO)_2L(\mu\text{-}CH_2)(dppm)_2][CF_3SO_3]$ (L = CO, SO_2, PR_3, ^tBuNC). C-H activation on addition of ligands is unprecedented for a methyl

group, and clearly demonstrates that α-hydrogen elimination of an alkyl group can be a facile process in the presence of more than one late-metal and is presumably an important process with surface-bound alkyls in heterogeneous chemistry. The very low activation energy for the exchange of the hydride and methylene hydrogens observed in the compound $[Ir_2(H)(CO)_2(\mu-CH_2)(\mu-SO_2)-(dppm)_2][CF_3SO_3]$ (7), when compared to the activation energies for similar transformations in a heterogeneous platinum system, supports our proposal that the diiridium core we have been investigating is an effective model for M-M cooperation in heterogeneous systems.

The C-H activation process occurring upon *addition of ligands*, has, to our knowledge, only been observed in one other instance,[3] in which addition of a phosphine ligand to a mononuclear ruthenium complex was proposed to increase the electron density at the metal enough to convert an agostic C-H interaction into a C-H bond-activated product, presumably by back donation from the more electron rich metal into the C-H σ* orbital. In the case of phosphines, and also for t-butyl isocyanide, which can function as a good σ-donor ligand, the addition of a basic ligand can be viewed as increasing the electron density at the metals leading to C-H bond cleavage. However, C-H activation upon addition of the superb π-acid ligands, CO or SO_2, cannot be rationalized on this basis. In addition, even for PR_3 and CNR ligands, the C-H bond activation does not occur at the metal at which these ligands bind, but instead occurs at the adjacent metal. Clearly some involvement of the adjacent

metal appears to be important. For a clue to this C-H bond reactivity, we compare the different sites of attack of SO_2 and other ligands in **2** with past studies on A-frames, for which SO_2 was again found to coordinate at a different site from most other ligands.[4] As noted earlier, compound **2** is fluxional in solution, having the methyl group moving from metal-to-metal via some methyl-bridged intermediate. One such intermediate, calculated by DeKock[5] to be only 5-6 kcal/mole above the ground state structure, is an A-frame species as shown below. If, as observed in other A-frames, SO_2 attack occurs in the pocket of the
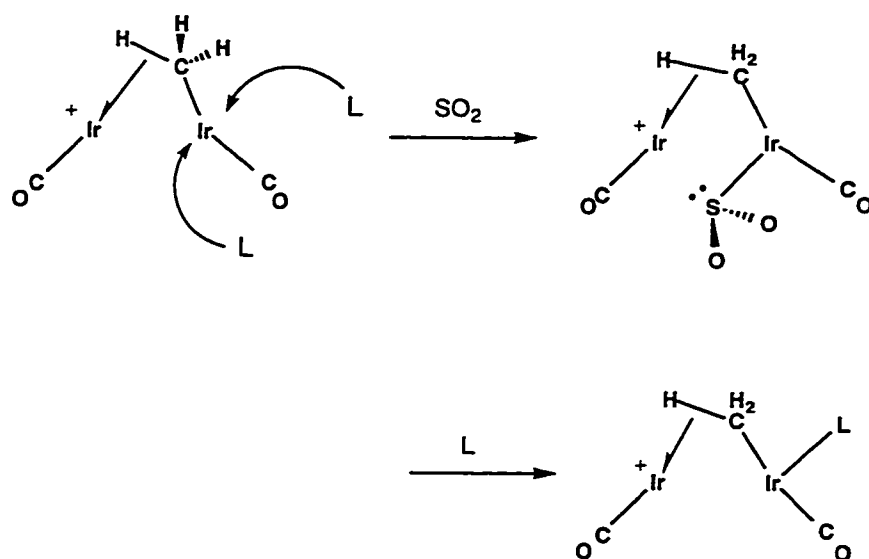
A-frame, between the metals, the species shown above would result. Again DFT calculations by DeKock[5] have identified this as a species immediately preceding C-H bond cleavage. Donation of the lone pair on the SO_2 ligand to the adjacent metal would increase the electron density at this metal leading to C-H bond cleavage. For other ligands, which attack on the outside of the A-frame, we propose that the resulting 18e Ir center can act as a donor to the adjacent metal, forming an Ir$\rightarrow$Ir dative bond, which again gives rise to the

observed C-H bond cleavage. A key point here is that in spite of the fact that π-acceptor ligands are added to one metal, the electron density at the adjacent metal can be increased by dative bond formation, either from a ligand or from the adjacent metal. In both cases the availability of the adjacent metal is pivotal in supplying electron density, either directly through a metal-metal dative bond, or indirectly through donation to SO_2, yielding a pyramidal SO_2 (formally SO_2^{2-}) which then donates to the C-H activating metal.

The same reactions of the mixed RhIr methyl compound $[RhIr(CH_3)(CO)_2(dppm)_2][CF_3SO_3]^6$ do not result in C-H bond cleavage and the observed reactivity for the homobimetallic Ir-methyl species may just be a result of a thermodynamic preference for the oxidative addition product, in which the resulting M-C and M-H bonds are stronger for Ir than for Rh. The oxidative addition is also favored by the increased basisity of Ir and its greater tendency to attain an eighteen-electron configuration compared to Rh, which prefers the sixteen-electron configuration.

Labelling of the methyl hydrogens of the SO_2-bridged methylene hydride compound (7) with deuterium has provided an opportunity to explore an IPR effect. Although this technique doesn't directly differentiate between a bridged-agostic methyl group and a methylene hydride species, the calculated ^1H chemical shifts are more in line with those expected for methylene and hydride groups, supporting the conclusion that the complex exists as a fluxional methylene hydride species in solution and not an agostic methyl complex. The structure determination of 7 although disordered, also supports this conclusion.

The barrier to exchange for the methylene hydrogens and hydride ligand in **7** was determined by line shape analysis on variable temperature ^{1}H NMR spectra. The value of $\Delta H^* = 6.11 \pm 0.33$ kcal/mole is believed to be the smallest yet observed for a homogeneous system and is more in line with the barrier to conversion between methyl and methylene fragments on a platinum metal surface.[7]

C-H activation upon addition of relatively innocent ligands such as, CO, SO_2 or PR_3 suggested that reactions with unsaturated organic substrates might lead to novel chemistry involving these substrates and either the methyl, methylene or hydride ligands. Four reaction types were observed on addition of the organic groups to compound **2**: In the first reaction type, reaction with olefins or alkynes resulted merely in coordination of the substrate in either a terminal or a bridging coordination mode. With substrates containing electron-withdrawing substituents the organic moiety was found to bridge the metals. In these cases the substrates are observed to bind parallel to the metal-metal axis, with no further isomers being observed. Although the methyl ligand in these complexes was found to be cis to the alkyne or olefin moiety, providing the correct geometry for migratory insertion, no further transformations were observed, under reflux or on addition of small molecules. Apparently, the activated substrates, when in the bridging cis dimetallated-olefin or -alkane binding mode, are strongly bound to the metals and inert to migratory insertion. With the non-activated olefins ethylene and dimethylallene, the olefins were found to bind terminally to one metal.

The second reaction type also does not result in C-H activation of the methyl group, instead giving oxidative addition of the terminal alkyne C-H bond. Reaction of **2** with 1-alkynes, such as propyne, phenyl acetylene, and acetylene, all initially form bridging-acetylide, hydride species at low temperature. These products, containing methyl, hydride and acetylide groups subsequently undergo a series of rearrangements in which either methane loss occurred (HC≡CR reactions) or in which the methyl group ultimately ended up on the β-carbon of the acetylide group to give a methylvinylidene product (HC≡CH reaction). It is not clear why these two pathways are followed, but presumably subtly different factors for the propyne and phenyl acetylene reactions give rise to adjacent methyl and hydride ligands leading to methane elimination.

The third reaction type with 1,3-butadiene is somewhat analogous to the oxidative addition of terminal alkynes, resulting in the unprecedented double C-H activation of the cumulated olefin generating a vinylvinylidene-methyl-dihydride species (**35**), analogous to the vinylidene-methyl-acetylide-hydride (**23**) produced in the reaction of **2** with excess acetylene. Both of these species appear to be good candidates for C-C bond formation with more than one organic moiety adjacent on one face of the compound, however, this was not realized. It is recommended that further attempts at inducing C-C bond formation with these complexes be examined. Typically, C-H activation of an olefin ligand yields a vinyl hydride species.[8] In only a few instances does a double C-H activation occur,[9] and these reactions usually involve harsh

reaction conditions such as photolysis or high temperatures. We do not know why 1,3-butadiene reacts in such an unusual manner.

The fourth type of reaction proved to be the most interesting, based on our interest in M-M cooperativity effects in C-H bond cleavage and C-C bond formation. When internal, non-activated alkynes, allene or methylallene were added to compound **2**, reaction results in an initial kinetic species that contains a terminal methyl group with the alkyne or allene bridging the metals. For the alkyne-bridged species, this bridging mode is unspectacular, having been well documented, however the allene adducts display the rare μ-η^1:η^3-allene coordination mode. These kinetic products, of the alkyne and allene reactions, slowly convert into vinylcarbene species over time. Labelling studies, involving $^{13}CH_3$-enriched compound **2**, suggest one route in the alkyne transformation and two routes for the allene transformations. We propose that loss of the unsaturated substrate from the bridging position and recoordination at a terminal site, as diagrammed below, yields a methylene-hydride species,
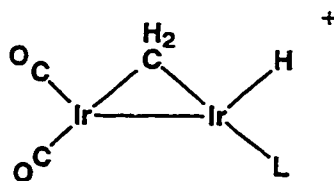
L = alkyne or allene

dppms omitted

analogous to isomers of the compounds generated upon addition of CO, PR_3, SO_2 and CNR to compound **2**. In both cases, involving the alkynes or the allenes, insertion of these groups into the metal-hydride is proposed to

generate a vinyl group that migrates to the adjacent methylene ligand yielding an allyl moiety. This allyl group then can undergo C-H bond cleavage by the adjacent metal, at the least hindered site, generating the observed vinylcarbene hydride product. With allene and methylallene another mechanism for the C-C bond forming reaction involving a direct methyl-to-allene migration was also proposed, to account for the isotopic enrichment observed in the 2-methyl position of the vinylcarbene.

Currently the mechanistic postulates are based upon ^{13}C labelling experiments. It would be ideal to carry out the reactions with deuterium labelling of the CH_3 group of **2**, however until now this has not been possible owing to facile scrambling of CD_3 in the preparation of **2**, presumably with H_2O from solvent or Me_3NO. Further work should be focused on obtaining the deuterated version of compound **2**, and verifying the proposed mechanisms for the production of the vinylcarbene products.

Synthesis of the methoxymethyl compound $[Ir_2(I)(CH_2OCH_3)(CO)\text{-}(\mu\text{-}CO)(dppm)_2]$ has opened up two important areas for further study. In the first this compound has shown highly unusual reactivity of the methylene C-H bonds upon formal substitution of a methyl hydrogen by the methoxy group, and suggests that varying the substituent on the methyl group could lead to a better understanding of the factors influencing C-H bond cleavage in these systems. Second, removal of the methoxy group by electrophiles presents a simple route into methylene-bridged species, which are of interest in C-C bond forming reactions.

The production of a bridging-carbyne by *double C-H activation* of the methoxymethyl group is unprecedented for this type of ligand. Future work on this portion of the project should be concerned with functionalization of the carbyne moiety to generate carbene functionalities as well as exploring the reactivity of the methoxycarbyne compound. The possibility arises from the double C-H activation observed with the methoxymethyl group, that a similar reaction may be occurring with the methyl group of compound **2**. Although we have no evidence for this, it could change the mechanistic proposals for the C-C bond formation reactions of Chapter 3 and 4.

The preparation of bridging methylene complexes from the methoxymethyl precursor is a straightforward transformation. The implication of methylene complexes in the C-C bond forming reactions of **2** observed with internal non-activated alkynes and allenes, deserves further study, and the methylene species produced appear to be good candidates for the initiation of this type of study. Although the subsequent reactivity of the methylene-bridged species has not yet been investigated we envision several different reactions. Their reactions with unsaturated substrates such as alkynes, olefins, allenes, etc. should be followed, owing to the possibility of C-C bond formation. Removal of the iodide ions to generate unsaturated cationic compounds or reduction to neutral methylene-bridged carbonyls such as $[Ir_2(CO)_2(\mu\text{-}CH_2)$-$(dppm)_2]$ should be pursued. Replacement of the iodo ligands by organic groups, which might then undergo migratory insertion is also possible.

Although the reactions with CH_2I_2 and ICH_2CN did not proceed according to expectation, and instead proceeded by radical H-abstraction, the desired oxidative additions should be realized by the addition of radical scavengers to inhibit the radical reaction. We envision this as a useful route to other substituted methyl groups by oxidative addition of appropriate iodo methyl substrates.

The versatility of using dppm as a bridging ligand for the diiridium core is displayed in a number of instances. The usual trans arrangement of the diphosphines is observed for many of the products. However, the trans-to-cis realignment of the diphosphines at one or both metals has been shown to occur readily, allowing coordination of sterically demanding bridging groups like vinylcarbene, and μ-η^1:η^3-allene, that would not be possible with a trans configuration of the diphosphines. Although, these diphosphine ligands are usually innocent they can become involved in the chemistry as shown in the reactions of $[Ir_2(CO)_3(dppm)_2]$ with both CH_2I_2 and ICH_2CN in which abstraction of a dppm methylene hydrogen occurred.

Overall we have shown that binuclear iridium methyl complexes can be readily prepared and display reactivity involving the methyl groups and other ligands which occur in heterogeneous catalysis, such as, α-H elimination, ligand association and dissociation, reductive elimination and oxidative addition, and insertion of CO and unsaturated substrates into the M-CH_3 bond or its fragments. The proposed α-hydrogen elimination step preceding the C-C bond forming reactions implies that methyl ligands on metal surfaces may be

good reservoirs for C_1 fragments on metal surfaces during FT synthesis. Ligand migration between metal centers was integral in the production of the vinylidene species obtained and the vinylcarbene compounds where kinetic products containing bridging alkyne and allene substituents were initially observed and transformation to terminal binding was proposed prior to the insertion steps. The adjacent metals provided a backbone for the C-H bond cleavage of the methyl and methoxymethyl groups yielding methylene-hydride and carbyne species, respectively, and also the migratory insertion of the methyl ligand of **2** was an important result of the cooperativity where the proximity of the μ-η^1:η^3 allene and the methyl ligand shown in the X-ray structure of **36** was proposed to give rise to the labelling in the methyl position of the vinylcarbene.

One important contribution to come from this thesis relates to the modelling of the Fischer-Tropsch (FT) reaction. The implication of the C-C bond forming reactions with internal, non-activated alkynes and allenes in relation to Maitlis' proposal for the FT reaction[10] was discussed in Chapters 3 and 4. Outlined below in Scheme 6.1 is the overall scheme for the reaction. Although the reactions of alkynes and allenes with compound **2** is not directly related to FT chemistry, the apparent insertion with a M-H moiety (**A**) to presumably yield a vinyl species (**B**) suggests FT-type chemistry can be modelled in our system. The resulting thermodynamic products of C-C bond formation in the alkyne and allene reactions stopped at product (**D**), however, the additional steps **D**-to-**E**-to-**F** can easily be envisioned to occur on a metal surface. This proposal provides a plausible explanation for the allyl to vinyl isomerization process put

forth in the Maitlis alkenyl mechanism which has little literature precedent.[11]

Scheme 6.1[a]
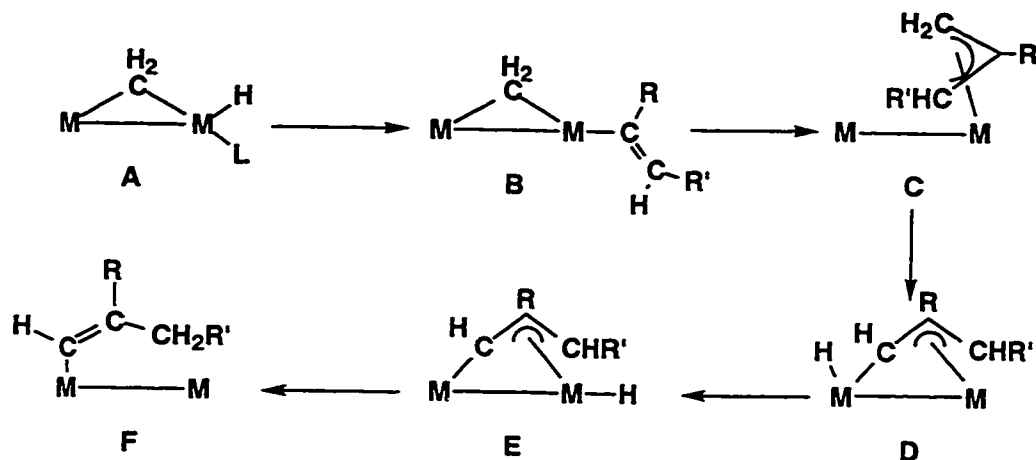
[a] L = RC≡CR'; $H_2C=C=CHR'$ (R' = H, CH_3): for allenes, R = CH_3 in scheme.

References

1. Shafiq, F.; Kramarz, K. W.; Eisenberg, R. *Inorg. Chim. Acta.* **1993**, *213*, 111.

2. Reinking, M. K.; Fanwick, P.E.; Kubiak, C.P. *Angew. Chem. Int. Ed. Engl.* **1989**, *28*, 1377.

3. Kuhlman, R.; Folting, K.; Caulton, K. G. *Organometallics* **1995**, *14*, 3188.

4. (a) Cowie, M. *Inorg. Chem.* **1979**, *18*, 286. (b) Cowie, M.; Dwight, S. K. *Inorg. Chem.* **1979**, *18*, 2700. (c) George, D. S. A.; McDonald, R.; Cowie, M. Submitted to Organometallics.

5. DeKock, R. personal communication.

6. (a) Antwi-Nsiah, F. Ph.D. Thesis, University of Alberta, Edmonton, Alberta, 1994. (b) Oke, O.; Cowie, M. unpublished results.

7. Zaera, F. *Acc. Chem. Res.* **1992**, *25*, 260.

8. (a) Stoutland, P. O.; Bergman, R. G. *J. Am. Chem. Soc.* **1985**, *107*, 4581. (b) Ghosh, C. K.; Hoyano, J. K.; Krentz, R.; Graham. W. A. G. *J. Am. Chem. Soc.* **1989**, *111*, 5480. (c) Perez, P. J.; Poveda, M. L.; Carmona, E. *J. Chem. Soc., Chem. Commun.* **1992**, 8. (d) Bianchini, C.; Barbaro, P.; Meli, A.; Peruzzini, M.; Vacca, A.; Vizza, F. *Organometallics* **1993**, *12*, 2505. (e) Alvarado, Y.; Boutry, O.; Gutierrez, E.; Monge, A.; Nicasio, M. C.; Poveda, M. L.; Perez, P. J.; Ruiz, C.; Bianchini, C.; Carmona, E. *Chem. Eur. J.* **1997**, *3*, 860. (e) Nubel, P. O.; Brown, T. L. *J. Am. Chem. Soc.* **1984**, *106*, 644. (f) Nubel, P. O.; Brown, T. L. *J. Am. Chem. Soc.* **1982**, *104*, 4955. (g) Keister, J. B.; Shapley, J. R. *J. Organomet. Chem.* **1975**,

85, C29. (h) Fryzuk, M. D.; Jones, T.; Einstein, F. W. B. *Organometallics* **1984**, *3*, 185

9. (a) Brough, S.-A.; Hall, C.; McCamley, A.; Perutz, R. N.; Stahl, S.; Wecker, U.; Werner, H. *J. Organomet. Chem.* **1995**, *504*, 33. (b) Gibson, V. C.; Parkin, G.; Bercaw, J. E. *Organometallics* **1991**, *10*, 220. (c) Bell, T. W.; Haddleton, D. M.; McCamley, A.; Partridge, M. G.; Perutz, R. N.; Willner, H. *J. Am. Chem. Soc.* **1990**, *112*, 9212. (d) Deeming, A. J.; Hasso, S.; Underhill, M.; Canty, A. J.; Johnson, B. F. G.; Jackson, W. G.; Lewis, J.; Matheson, T. W. *J. Chem. Soc., Chem. Commun.* **1974**, 807. (e) Deeming, A. J.; Underhill, M. *J. Chem. Soc., Dalton Trans.* **1974**, 1415. (f) Deeming, A. J.; Underhill, M. *J. Chem. Soc., Chem. Commun.* **1973**, 277.

10. (a) Turner, M. L.; Long, H. C.; Shenton, A.; Byers, P. K. Maitlis, P. M. *Chem. Eur. J.* **1995**, *1*, 549. (b) Maitlis, P. M.; Long, H. C.; Quyoum, R.; Turner, M. L.; Wang, Z-Q. *Chem. Commun.* **1996**, 1. (c) Maitlis, P. M.; Saez, I. M.; Meanwell, N. J.; Isobe, K.; Nutton, A.; Vaquez de Miguel, A.; Bruce, D. W.; Okeya, S.; Bailey, P. M.; Andrews, D. G.; Ashton, P. R.; Johnstone, I. R. *New J. Chem.*, **1989**, *13*, 419. (d) Maitlis, P. M. *J. Organomet. Chem.* **1995**, *500*, 239 and references therein.

11. Two known reports are: (a) Deeming, A. J.; Shaw, B. L.; Stainbank, R. E. *J. Chem. Soc. A* **1971**, 374. (b) Wang, L. -S.; Cowie, M. *Can. J. Chem.* **1995**, *73*, 1058.

IMAGE EVALUATION
TEST TARGET (QA–3)

150mm

6"
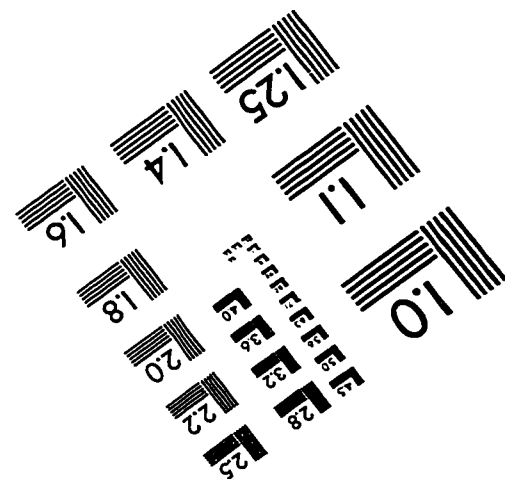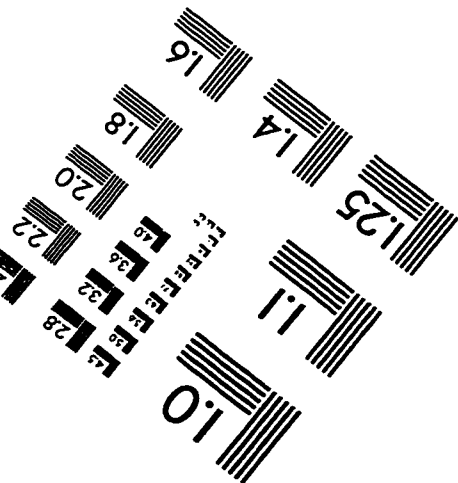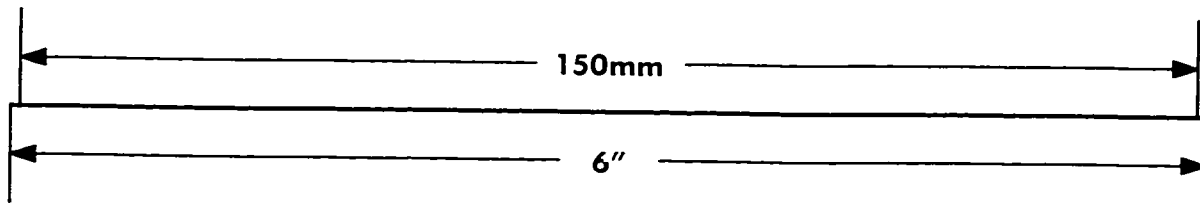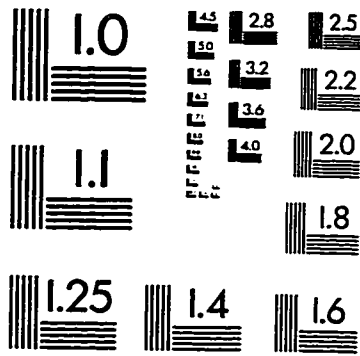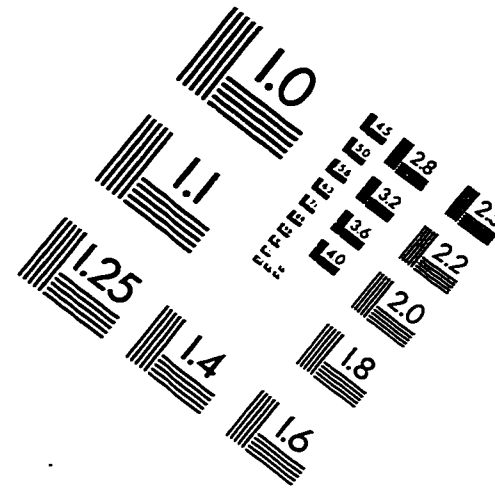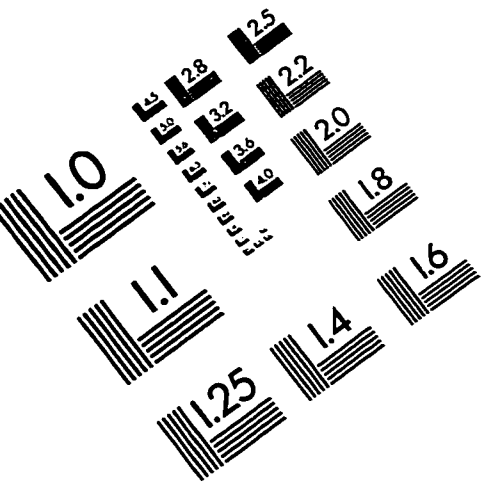
APPLIED IMAGE, Inc
1653 East Main Street
Rochester, NY 14609 USA
Phone: 716/482-0300
Fax: 716/288-5989